

University of St Andrews



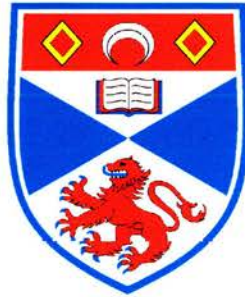
Full metadata for this thesis is available in
St Andrews Research Repository
at:

<http://research-repository.st-andrews.ac.uk/>

This thesis is protected by original copyright

Investigation of the signal model for the formation of chromatid breaks.

Thesis submitted for the degree of Doctor of Philosophy to the
University of St. Andrews



by

Margaret Rogers-Bald

School of Biology, University of St. Andrews,
St. Andrews, Fife, KY16 9TS, Scotland, UK

June 2001

I, Margaret Rogers-Bald, hereby certify that this thesis has been composed by myself, that it is a record of my own work, and that it has not been accepted in partial or complete fulfilment of any other degree or professional qualification.

Signed Margaret Rogers-Bald

Date

10-06-01

I was admitted as a research student to the Faculty of Science of the University of St. Andrews for the degree of Doctor of Philosophy in September 1998. This thesis is a record of the work carried in the University of St. Andrews between 1998 and 2001.

Signed Margaret Rogers-Bald

Date

10-06-01

I hereby certify that the above candidate has fulfilled the conditions of the Resolution and Regulations appropriate for the Degree of Doctor of Philosophy in the University of St. Andrews and that the candidate is qualified to submit this thesis in application for that degree.

Signature of Supervisor

Date

Dr. Peter E. Bryant

11/6/01.

In submitting this thesis to the University of St. Andrews I understand that I am giving permission for it to be made available for use in accordance with the regulations of the University Library for the time being in force, subject to any copyright vested in the work not being affected thereby. I also understand that the title and abstract will be published, and that a copy of the work may be made and supplied to any *bona fide* library or research worker.

Margaret Rogers-Bald

Date

10-06-01

Abstract

The main aim of this investigation was to test the assumptions and predictions of the signal model (Bryant, 1998). These predictions are that the proportion of colour switch breaks (csb) within the total chromatid breaks (Tb) formed in the G₂ phase of the cell cycle (referred to as the colour switch ratio (csr)) is independent of radiation dose, restriction endonuclease dose and sample time. The csr for any given cell type is considered to be typical of that particular type. Furthermore the chromatid breaks observed at mitosis are the result of the failure to complete a recombinogenic process initiated by a double-strand break (dsb) which is not itself directly involved in the recombination events.

The characteristics of chromatid break formation and rejoining have been investigated both theoretically and experimentally. It has been demonstrated theoretically and supported experimentally that the csr is independent of radiation dose and (log₁₀) restriction endonuclease dose at a specific sample time. This finding is in agreement with the signal model. It has however been shown that the rate of rejoining of total breaks and colour switch breaks in G₂ is not the same and thus the csr is not independent of sample time, a finding which differs from that expressed in the signal model.

It has been found, using I-SceI transfected cell lines, that a single dsb is sufficient to induce chromatid breaks and that the csr has a maximum value for a given experimental specification of I-SceI endonuclease and streptolysin (SLO) dose. The further use of this experimental model to achieve a more complete understanding of the characteristics of chromatid break is discussed.

Preliminary data presented here suggest that the csr is, within the limits of experimental error, essentially the same for all higher eukaryotic cell types and that this reflects the importance of the conserved nature of chromatin structure in the recognition and processing of DNA damage via the proposed signal model pathway.

Investigations into possible signalling molecules involved within the signal model pathway suggest that the *ATM*, *NBS*, *RAG1* and *RAG2* and possibly the *BRCA2* gene products are involved in signalling the occurrence of DNA damage in the form of dsb and are involved in the initiation of the recombinogenic process leading to the formation of both non-colour and colour switch breaks, possibly via a homologous recombination pathway.

In summary the findings presented here are in broad agreement with the signal model, with the exception of the time-independence of the csr. This hypothesis has been extended to propose a theoretical quantitative model incorporating a geometric surface which represents the chromatid breakage characteristics within the G₂ phase of the cell cycle. This quantitative model is here defined as the chromatid breakage surface model.

Acknowledgements

I would like to thank the BBSRC for funding me for the duration of my Ph.D studies under the supervision of Dr. Peter Bryant. I would also like to thank the many people within the School of Biology who have been extremely helpful, in particular Angus Gleig, Mary Wilson and John MacIntyre for technical support, the photographic department for assistance with preparation of images and understanding the intricacies of photoshop. Special thanks to Dr. Clair Peddie for generously giving her time in reading and discussing the thesis with me. I am also grateful to all those who kindly donated cell lines.

I would like to acknowledge the patience and support of my family throughout my time as a student, particularly my husband William Bald for his unfailing support, helpful discussions and suggestions, and for providing me with the theoretical proof in Appendix B.

Contents

Chapter 1. General introduction.

1. General Introduction	1
1.1. Caretakers and gatekeepers	5
1.2. Formation of double-strand break (dsb)	7
1.3. How ionising radiation damages DNA	10
1.4. Formation of dsb by restriction endonucleases	12
1.5. Mechanisms of dsb repair	14
1.5.1. Homology-dependent mechanisms of dsb repair	14
1.5.2. Conservative homology-dependent mechanisms of dsb repair	15
1.5.3. Non-conservative homology-dependent recombinational dsb repair	17
1.5.4. Homology-independent mechanisms of dsb repair	21
1.5.5. Accurate non-homologous end joining (NHEJ)	22
1.5.6. Error-prone non-homologous end joining (NHEJ)	22
1.6. Models of chromosomal aberrations	26
1.6.1. The Sax model	27
1.6.2. Revell's Exchange model	28
1.6.3. Chadwick and Leenhouts' model	31
1.6.4. The signal model	32
1.6.5. Pros and cons of the various models	35
1.7. Possible signal molecules	37
1.8. Major aims of this investigation	40

Chapter 2. Investigation of genes that affect the colour switch ratio

2.1 Introduction	43
2.2. Cell lines under investigation	45
2.2.1. Down Syndrome (trisomy 21)	46
2.2.2. Bloom Syndrome	48
2.2.3. Omenn Syndrome	50
2.2.4. Ataxia telangiectasia, Ataxia telangiectasia-like disorder and Nijmegen Breakage Syndrome	53

2.2.4.1. Ataxia telangiectasia	53
2.2.4.2. Ataxia telangiectasia-like disorder	58
2.2.4.3. Nijmegen Breakage Syndrome	59
2.2.5. BRCA1 and BRCA2	64
2.2.6. p53	67
2.3. Materials and methods	71
2.3.1. Cell culture and BrdU treatment	71
2.3.2. Irradiation and harvesting	73
2.3.3. Preparation of slides	73
2.3.4. Fluorescence plus giemsa (FPG) staining	74
2.3.5. Scoring and analysis	74
2.4. Results	75
2.4.1. A consideration of the generalised radiation damage relationship	75
2.4.2. The chromatid break-dosage relationship	76
2.4.3. Statistical analysis of chromatid breaks in lymphoblastoid cells	82
2.4.4. Control (non-irradiated) lymphoblastoid cell lines	91
2.4.5. Irradiated lymphoblastoid cell lines	91
2.4.6. Regression analysis of the data	94
2.4.7. Cell lines derived from different syndromes	97
2.4.8. Radiation damage index (rdi)	110
2.5. Discussion	117
2.5.1. Bloom Syndrome, Down Syndrome	119
2.5.2. AT and NBS cell lines	121
2.5.3. Cell lines derived from families with breast cancer	124
2.5.4. Omenn Syndrome	126
2.6. Future Work	127
Chapter 3. Rejoining characteristics of chromatid breaks.	
3.1. Introduction	130
3.1.1. Conversion of double-strand breaks into chromosomal breaks	131
3.1.2. Models of double-strand break repair and chromatid break rejoining kinetics	133

3.2. Materials and methods	
3.2.1. Cell culture and BrdU treatment	140
3.2.2. Irradiation and harvesting	140
3.2.3. Preparation of slides	141
3.2.4. Fluorescence plus giemsa (FPG) staining	141
3.2.5. Scoring and analysis	141
3.3. Results	
3.3.1. Break frequencies in normal lymphoblastoid cells	143
3.3.2. Basic theory of breakage rejoining in G ₂	147
3.3.3. Rejoining characteristics for normal lymphoblastoid cells	151
3.3.4. The chromatid breakage surface	152
3.3.5. Chromatid breakage surface for normal lymphoblastoid cells	157
3.3.6. Rejoining characteristics of AT and NBS cells	164
3.4. Discussion	179
3.4.1. Rejoining characteristics of normal lymphoblastoid cells	179
3.4.2. Rejoining characteristics of chromatid breaks in syndrome cell lines	183
3.4.3. Summary and conclusions	189
3.5. Future Work	191

Chapter 4. Induction of chromatid breaks by a single dsb

4.1. Introduction	195
4.1.1. Group I introns	196
4.1.2. The I-SceI system	199
4.1.3. The XRCC gene family	201
4.2. Materials and methods	
4.2.1. Cell culture and BrdU treatment	203
4.2.2. Cell poration and endonuclease treatment of GS1943, V79 and irs1 cells	203
4.2.3. Treatment of control cells	205
4.2.4. Irradiation of cells	205
4.2.5. Harvesting	206
4.2.6. Assay of G ₁ chromosome aberrations in GS1943 cells	206
4.2.7. Preparation of slides	206
4.2.8. Fluorescence plus giemsa (FPG) staining	207
4.2.9. Scoring and analysis	207

4.3. Results	208
4.3.1. Treatment of GS1943 cells with I-SceI endonuclease	208
4.3.2. Control treatments	217
4.3.3. Assay of G ₁ chromosome aberrations	218
4.3.4. Radiation exposure	222
4.3.5. Results of V79 and <i>irs1</i> transfected cell lines	222
4.3.6. Comparison of GS1943, V79 and <i>irs1</i> results	227
4.4. Discussion	230
4.4.1. GS1943 transfected cell line	230
4.4.2. V79 and <i>irs1</i> transfected cell lines	233
4.5. Future Work	235
4.5.1. Using the I-SceI model system to investigate translocations	235
4.5.2. Using the I-SceI model system to investigate inversion characteristics	237
Chapter 5. Determination of the colour switch ratio in different species.	
5.1. Introduction	243
5.1.1. Chromosome structure in metazoans	245
5.1.2. Chromatin remodelling	249
5.1.3. Cell lines under investigation	252
5.1.3.1. <i>Potorus tridactylus</i>	253
5.1.3.2. <i>Drosophila melanogaster</i>	254
5.1.3.3. <i>Vicia faba</i>	255
5.1.3.4. Mouse CB17 cell line	256
5.2. Materials and methods	257
5.2.1. Cell culture and BrdU treatment of CB17 and <i>Potorus</i> cells	257
5.2.2. Irradiation of cells	257
5.2.3. Harvesting	257
5.2.4. Preparation of slides	258
5.2.5. Fluorescence plus giemsa (FPG) staining	258
5.2.6. Scoring and analysis	259
5.2.7. Cell culture and BrdU treatment of <i>Drosophila melanogaster</i> cells	259
5.2.8. Harvesting, slide preparation and staining of <i>Drosophila</i> cells	260
5.2.9. Culture of <i>Vicia faba</i> seeds	260
5.2.10. Irradiation of <i>Vicia faba</i> root tips	261
5.2.11. Slide preparation and staining of <i>Vicia faba</i> root tips	261

5.3. Results	
5.3.1. Chromatid break characteristics of <i>Potorus</i> and CB17 cell lines	262
5.3.2. Comparison of species with a normal human cell line	262
5.3.3. The <i>Drosophila</i> cell line	270
5.3.4. <i>Vicia faba</i>	270
5.3.5. Breakage characteristics for V79 and GS1943 cells.	270
5.4. Discussion	274
5.5. Future Work	276
Chapter 6. Overall conclusions	
6. Overall conclusions	278
6.1. Development of a quantitative model	278
6.2. Chromatid break characteristics and type of induced damage	280
6.3. Chromatid break induction with a single dsb	281
6.4. Chromatid break rejoining characteristics	282
6.5. Constancy of csr in different cell types	283
6.6. Candidates for the signalling molecule(s)	284
6.7. Inversion frequency in chromatids	286
6.8. General conclusions	286
7. References	288
Appendix A: Summary of statistical methods used in analysing experimental data.	321
Appendix B: Proof that the time decay constant for the repair of chromatid breaks is independent of initial dose.	329

Appendix C: FISH Analysis of NC lymphoblastoid cells.	334
Appendix D: Publications	340

Nomenclature

- a, b, c, d, A, B* constants appearing in equations
- A** fraction of fragments rejoining with fast kinetics (PCC)
- ANLL** acute lymphatic leukaemia
- APRT** adenine phosphoribosyltransferase gene
- ARF** alternative reading frame
- AT** Ataxia telangiectasia
- ATAR, ATLG, ATPA** EBV-transformed lymphoblastoid cell lines derived from AT homozyote
- ATLD** Ataxia telangiectasia-like disorder
- ATM** Ataxia telangiectasia (mutated) protein
- ATP** adenosine triphosphate
- ATR** AT and Rad-3 related protein
- B** breaks; fraction of fragments rejoining with slow kinetics (PCC)
- β variable defined in Appendix B
- bp** base pairs
- B_{max}** maximum breaks
- BIAL₁** EBV-transformed lymphoblastoid cell lines derived from individual with unknown mutation
- BRCA1** breast cancer gene 1
- BRCA2** breast cancer gene 2
- BrdU** 5- bromo-deoxyuridine
- BRCT** breast cancer carboxyl terminal domain
- C** sum of chromosomes and residual fragments (PCC)
- c** intercept of linear regression line with zero value of independent variable
- cdc2** cyclin-dependent
- cdc25** cyclin-dependent

- CDK1** cyclin-dependent kinase 1
- CGH** comparative genomic hybridisation
- CHO** Chinese hamster ovary (cell line)
- Chk1** checkpoint gene 1
- Chk2** checkpoint gene 2
- CIP1** cdk interacting protein 1
- COWA₁** EBV-transformed lymphoblastoid cell lines derived from heterozygous mutant individual for *BRCA1*
- csb** colour switch breaks
- CSM** complete supplemented medium
- csr** colour switch ratio
- CT** carboxyl terminal
- CV 077, CV 105, CV 712** EBV-transformed lymphoblastoid cell lines derived from Down Syndrome individuals
- D** radiation dose
- df** degrees of freedom
- DNA** deoxyribose nucleic acid
- DNA-PK_{CS}** DNA- phospho-kinase catalytic subunit
- dsb** double-strand break
- EBV** Epstein Barr Virus
- EBNA** Epstein Barr nuclear antigen
- ELWE₁** EBV-transformed lymphoblastoid cell lines derived from heterozygous mutant individual for *p53*
- exp** exponential
- F** statistical F test
- FAP** familial adenomatous polyposis
- FAR** fraction of activity released
- FCS** Foetal calf serum
- FE2** fly extract (haemolymph) 2

- FHA fork-head-associated (domain)
- FISH Fluorescence *in situ* hybridisation
- FPG Fluorescence plus giemsa (staining)
- $g(x)$ function appearing in Woolf's statistical method (Appendix A)
- H1, H3 Histones 1, 3
- HBSS Hanks balanced salt solution
- HR homologous recombination
- hr hour
- IR ionising radiation
- IRIF ionising radiation induced foci
- ivb inversion-associated chromatid breaks
- ivr inversion ratio
- k sample time decay constant, rejoining rate constant
- K_m Michaelis constant
- IgA Immunoglobulin A
- IgE Immunoglobulin E
- IgG Immunoglobulin G
- LANY₁ EBV-transformed lymphoblastoid cell lines derived from heterozygous mutant individual for *BRCA1*
- LET linear energy transfer
- LHS left hand side (of equation)
- log logarithm to the base 10
- LOH loss of heterozygosity
- ln natural logarithm
- LSI locus-specific FISH probe
- m slope of regression lines
- μ proportion of ivb within the ncsb
- m, n numbers appearing in statistical analysis
- MEM Minimum essential medium

- min** minute
- NB1** neuroblastoma
- NBS** Nijmegen Breakage Syndrome
- NC** normal lymphoblastoid cell line
- NC AM, NC DW, NC MR, NC NC, NC SW** EBV-transformed lymphoblastoid cell lines derived from normal individuals
- ncsb** non-colour switch breaks
- ncsr** non-colour switch ratio
- NF1, NF2** neurofibromatosis
- NHEJ** non-homologous end-joining
- NPAT** nuclear protein mapped to the AT locus gene
- PEGY₁** EBV-transformed lymphoblastoid cell lines derived from heterozygous mutant individual for *p53*
- PGFE** pulsed field gel electrophoresis
- ORF** open reading frame
- PCC** premature chromosome condensation
- PHA** phytohaemagglutinin
- R** number of rejoining breaks
- r** regression coefficient
- r²** coefficient of determination
- RAG** recombination activating gene
- Rb** retinoblastoma
- RBM** Revell binary misrejoining model
- rdi** radiation damage index
- RE** restriction endonuclease
- RHS** right hand side (of equation)
- RNA** ribose nucleic acid
- RNR** ribonucleotide reductase enzyme
- rpm** revolutions pre minute

- RSS** recombination signalling sequences
- S** concentration (Michaelis-Menten)
- s, SD** standard deviation
- s²** variance
- SAR** scaffold attachment region
- SCE** sister chromatid exchange
- SCID** severe combined immunodeficiency syndrome
- SE** standard error
- SLO** streptolysin O
- SOD-1** super oxide dismutase
- SLYN₁** EBV-transformed lymphoblastoid cell lines derived from heterozygous mutant individual for *BRCA2*
- ssb** single strand break
- SSC** sodium chloride, sodium citrate solution
- SVO 09, SVO 14, SVO 20, SVO 24, SVO 26, SVO 27, SVO 28** EBV-transformed lymphoblastoid cell lines derived from normal individuals
- SV40** simian virus 40
- t** sample time, student t-test
- Tb** total breaks
- TCR β** T-cell receptor β
- TURN₁** EBV-transformed lymphoblastoid cell lines derived from individual heterozygous mutant for *BRCA2*
- UV** ultra-violet (radiation)
- V_{max}** maximum reaction rate
- V(D)J** splicing of variable, diversity and joining gene segments in generation of antibody diversity
- \bar{x}** mean value
- χ^2** Chi squared coefficient
- x, y, z** Cartesian co-ordinates

XPD xeroderma pigmentosum

XRCC X-ray repair cross-complementing gene family

Y yield of prematurely condensed chromosomes (PCC)

94P112, 94P548 EBV-transformed lymphoblastoid cell lines derived from individuals with NBS

subscripts:

- 0** zero sample time
- 1** value related to total breaks
- 2** value related to csb
- 3** value related to ncsb

Chapter 1

General Introduction

Contents	Page No.
1. General Introduction	1
1.1. Caretakers and gatekeepers	5
1.2. Formation of double-strand break (dsb)	7
1.3. How ionising radiation damages DNA	10
1.4. Formation of dsb by restriction endonucleases	12
1.5. Mechanisms of dsb repair	14
1.5.1. Homology-dependent mechanisms of dsb repair	14
1.5.2. Conservative homology-dependent mechanisms of dsb repair	15
1.5.3. Non-conservative homology-dependent recombinational dsb repair	17
1.5.4. Homology-independent mechanisms of dsb repair	21
1.5.5. Accurate non-homologous end joining (NHEJ)	22
1.5.6. Error-prone non-homologous end joining (NHEJ)	22
1.6. Models of chromosomal aberrations	26
1.6.1. The Sax model	27
1.6.2. Revell's Exchange model	28
1.6.3. Chadwick and Leenhouts' model	31
1.6.4. The signal model	32
1.6.5. Pros and cons of the various models	35
1.7. Possible signal molecules	37
1.8. Major aims of this investigation	40

1. General Introduction

A glance through old family photographs demonstrates how physical similarities are inherited from previous generations. For an individual to develop normally to healthy adulthood and pass on their genes to their children it is important to maintain genetic integrity. Such maintenance requires effective damage monitoring and repair systems at the cellular level. Throughout the evolution of life on Earth the DNA of all organisms has been damaged by endogenous (hydrolysis, methylation, oxidation) and exogenous (exposure to uv, ionising and cosmic radiation) damaging events. It is therefore not surprising that a wide range of DNA damage recognition and repair processes have evolved to deal with this problem. Subsequent damage can take a number of forms but the principle types of damage caused by ionising radiation are single and double strand breaks. Single strand breaks are formed when one strand of the DNA duplex is broken; when both strands are broken a double strand break is formed. Double-strand breaks can arise more readily in DNA with a more open chromatin structure such as when replication is occurring (Sak *et al*, 2000) and such damage must be recognised and repaired. Repair mechanisms can themselves be error-prone: lesions may escape detection and repair synthesis is not entirely error-free and repair systems may induce "repair" regions. These regions are not damaged but are "repaired" due to the extreme sensitivity of damage-sensing mechanisms which recognise subtle changes in DNA conformation (Ninio, 2000). Although such inherently error-prone repair mechanisms may be of evolutionary benefit, to the individual they represent a possible source of mutagenicity, particularly those involving recombination. Recent yeast studies however suggest that replication and recombination machinery within cells may act cooperatively to maintain genomic integrity (Marians, 2000). The quantifiable effects of radiation are the end points of a series of events initiated by the passage of the radiation through cells. Initial events occur very fast (see Figure 1.1) but the endpoint such as delayed cell death, genomic instability and carcinogenesis take longer to manifest themselves.

The genome of a eukaryotic organism is subdivided into chromosomes made up of DNA, histones and non-histones proteins which form chromatin (Alberts *et al*, 1994). The DNA exists in close association with these nuclear proteins and is highly condensed, particularly at mitosis which is the only time during the cell cycle when the individual chromosomes can be seen and identified using light microscopy. The highly conserved structure of chromatin is considered in more detail in Chapter 5, but the principle features of chromatin organisation are the looping of the duplex DNA around histone cores to form nucleosomes with spacer regions (where histone H1 is generally found). A solenoidal fibre is then formed with the nucleosomes forming a zig-zag configuration (Rydberg *et al*, 1998), this fibre is then arranged into chromatin loops. These loops are thought to be the basic unit of transcription and replication and are associated with complexes of proteins called transcription or replication factories (Iborra *et al*, 1996). The size of chromatin loops is not accurately known, estimates vary depending on the method of measurement (Laemmli *et al*, 1977; Murray and Hunt, 1993; Johnston *et al*, 1997; Ostashevsky *et al*, 1999) and whether the loops contain gene-rich or gene-poor regions of the genome (Saitoh and Laemmli, 1994; Craig *et al*, 1997).

When cells are blocked at metaphase using colcemid it is possible to fix the cells and directly observe the metaphase chromosomes by dropping the fixed cell suspension on a slide and using an appropriate stain. The resulting metaphase spreads of mitotic chromosomes can be seen using a light microscope. When chromosomes from cells exposed to ionising radiation are visualised using this method, different radiation-induced lesions are observed depending on the phase of the cell cycle in which radiation exposure occurred. Chromosome aberrations are produced when cells are irradiated prior to S phase. If the lesion is not repaired before the chromosomes undergo replication, both daughter chromatids will be damaged. Three main categories of chromosome lesion are recognisable; terminal deletions, intrachromosome exchanges (interstitial deletion, centric ring and fragment, acentric ring and pericentric inversion) and inter chromosome exchanges (dicentric, translocations, fragment and symmetrical exchange).

Chromatid aberrations are produced when cells are irradiated during G₂ and are seen as intrachromatid (gaps, breaks, fragments) or interchromatid (exchanges). As with chromosomal damage, fragments may be lost during the preparation of metaphase spreads. In practice, if non-synchronised cell populations are irradiated, cells will be present in all phases of the cell cycle and the type of aberrations observed at metaphase will depend on how long the cells are left to continue through the cell cycle before harvesting. Short incubation times in the presence of colcemid following irradiation will produce chromatid aberrations since only those cells which have entered G₂ will have proceeded to metaphase, analysis of chromosome aberrations require a longer period of incubation to enable those cells in G₁ to progress through to mitosis.

Analysis of chromatid aberrations is improved by the incorporation of bromodeoxyuridine (BrdU) over two cell cycles so that the chromatid which has incorporated BrdU in both DNA strands is weakly stained (the "light" chromatid) whereas the chromatid with only one substituted strand is more darkly stained (the "dark" chromatid). This colour distinction allows exchanges between strands to be observed. This fluorescent plus Giemsa (FPG) technique was developed by Perry and Wolff (1974) as an easier method of detecting chromatid aberrations than ³H thymidine incorporation followed by autoradiography (Taylor *et al*, 1956). The observed differential staining with Giemsa may be due to the BrdU quenching the fluorescence produced by the Hoechst staining in the BrdU-incorporated strand (Latt, 1973) but is more likely to be due to the inability of the fluorescent stain to bind to the DNA which contains the BrdU analogue. The drawback to this technique is the consequent induction of sister chromatid exchanges (SCE) in cells incubated in the presence of BrdU particularly if cells are exposed to high illumination levels during cell culture. The SCE being formed in S phase is presumably due to the replication machinery of the cell having difficulty in processing DNA and which includes the more bulky BrdU analogue (Latt, 1981; Lin and Werteleki, 1982). Generally the overall frequency of SCE does not differ significantly in

non-irradiated and irradiated BrdU-incorporated cells as the number of BrdU-induced SCE vary quite widely between individual cells and where completed chromatid exchanges are rare events.

When chromosomes are observed at mitosis, chromosomal aberrations (i.e. alterations to their normal structure) can be identified either as a result of exposure of the cells to damaging agents such as ionising radiation, or to an unknown cause, generally referred to as "spontaneous" aberrations. In G₀ or G₁ chromosomes contain a single DNA molecule whereas those in G₂ contain two following replication in S phase, so that the mitotic cell can produce two identical diploid daughter cells. Conventionally aberrations caused by damage in the G₀ or G₁ phase of the cell cycle are termed chromosome aberrations whereas those induced in S or G₂ are called chromatid aberrations. These aberrations can take several forms some of which are visible using harlequin or conventional Giemsa staining or banding techniques. Other aberrations are identifiable using fluorescence *in situ* hybridisation (FISH) techniques. A broad general classification of chromosomal aberrations are those within a single chromosome or those with rearrangements between two or more chromosomes. The first category would include terminal and interstitial deletions, inversions, gaps and breaks. The second group would include translocations and dicentrics (Pfeiffer *et al*, 2000 and references therein).

Chromosome and chromatid aberrations as described above are formed by different mechanisms. Double-strand breaks are repaired either by homologous recombination (HR) or non-homologous end-joining (NHEJ). It is now recognised that both of these mechanisms are important in the processing of DNA damage in mammalian cells, with NHEJ being the predominant pathway in G₁ and early S phase with homologous recombination used preferentially in late S and G₂ (Takata *et al* 1998). These mechanisms will be considered in more detail in section 1.6.

The formation of chromosome aberrations can be a lethal event, but non-lethal aberrations may cause oncogenic transformation or less-specifically increase genomic instability which in itself can increase the overall risk of carcinogenesis. Certain chromosomal instability syndromes, for example, Ataxia telangiectasia, Nijmegen Breakage Syndrome, (discussed in more detail in Chapter 2) are associated with both an elevated frequency of chromosome aberrations and an increased risk of cancer. Individuals with homozygous mutation of either *BRCA1* or *BRCA2* also display a significant increase in genomic instability, the accumulation of stable mutations within the genome which individually are non-lethal but cumulatively contribute to an increased risk of carcinogenesis. The different genes associated with these types of disease syndromes are associated with deficiencies in DNA repair pathways, either in the recognition or processing of damage. The importance of the abrogation of repair pathways in the maintenance of gatekeeper and caretaker functions, important in genomic instability, will be further considered below.

1.1 Caretakers and gatekeepers.

An increasing number of genes have been identified in which mutations lead to an increased disposition to develop cancer compared to the normal population. Such cancer susceptibility genes can be classified into two main groups: caretakers and gatekeepers. The concept of caretakers and gatekeepers was developed by Kinzler and Vogelstein (1996) in their studies of the multistep processes leading to colorectal cancers. The concept of requiring at least two mutations in order for tumourgenesis to occur was first elucidated by Knudson in his two-hit hypothesis for retinoblastoma. It has been proposed that mutations in both alleles of a caretaker gene, as well as mutations in both alleles of a gatekeeper gene, are necessary for a cell to be "primed" for neoplasia to take place, although additional genetic changes must also occur (Kinzler and Vogelstein, 1997).

Caretaker genes do not directly initiate tumourgenesis but maintain the overall integrity of the genome and are the group of cancer susceptibility genes most frequently associated with inherited cancer predisposition syndromes. Genes assigned to this group include *RAD51*, *RAD52* (Van Dyck *et al*, 1999) associated with resolution of dsb and recombinational repair. The nucleotide excision repair genes associated with xeroderma pigmentosum (*XPD A - F*) and the mismatch repair genes responsible for hereditary colorectal cancer are also included in this group, as is the ataxia telangiectasia gene *ATM*. Mutation of *ATM* is associated with a range of cancers including breast cancer, mutations of *BRCA1* and *BRCA2* are rarely found in sporadic cancers.

Gatekeepers control cell proliferation by inhibiting growth or promoting cell death in both tumours and healthy tissue so loss of function of one of these genes leads directly to uncontrolled cell proliferation. This group includes many of the anti-oncogenes or tumour suppresser genes associated with particular conditions described by Knudson (1993) such as Retinoblastoma (*Rb*), associated with childhood cancer of the retina, neuroblastoma (*NB1*), neurofibromatosis (*NF1* and *NF2*). Familial adenomatous polyposis (*APC*) which predisposes the carrier to colon cancer, also falls into this category.

Conditions in which inherited mutations of caretaker or gatekeeper genes are present require fewer additional mutations for the onset of neoplasia. Acquisition of a double mutation in a caretaker gene will increase genetic instability throughout the genome. Such an increase in instability, particularly in gatekeeper genes may increase the rate at which subsequent mutations occur. The particular caretaker and gatekeeper genes involved will vary depending on the tissue involved and different combinations will thus give rise to specific cancer types.

Many of the genes associated with caretaker or gatekeeper roles are mutated in disease syndromes which portray a cancer predisposition phenotype, together with an increase in the frequency of chromosomal aberrations. The dsb is the initiating lesion for the

chromosomal and chromatid aberrations associated with these conditions. The formation and subsequent repair of dsb is discussed below.

1.2. Formation of double-strand breaks (dsb).

Ionising radiation and other agents can induce the formation of dsb in cells but it is also possible for dsb to occur spontaneously in cells in all phases of the cell cycle. Some cell types can, in a controlled fashion, induce DNA dsb. For example the DNA of maturing germ cells undergo meiotic recombination during prophase of meiotic division I when non sister chromatids undergo chiasmata formation. This process is thought to be mediated by recombinational nodules; aggregations of large numbers of proteins (Alberts *et al* 1994). Although only studied in yeast systems, there is increasing evidence for the initiation of meiotic homologous recombination between maternal and paternal homologues to increase genetic variability in gametes in cell types other than yeast (Pfeiffer *et al*, 2000 and references therein).

Topoisomerases are important in controlling the degree of supercoiling in DNA during replication, recombination, transcription and chromosome segregation (Pfeiffer *et al*, 2000). Topoisomerase I induces single-stranded breaks (ssb) while topoisomerase II produces reversible dsb allowing the separation of sister chromatids during mitosis and meiosis. Both of these enzymes are associated with genome stabilisation and can promote illegitimate recombination which may give rise to chromosome aberrations (Wang, 1996). Although DNA replication is an extremely accurate process it is possible that a ssb in the parental strand of replicating DNA could be converted to a dsb upon arrest of the replication fork (Roth and Wilson, 1988). Failure to complete joining of Okazaki fragments may also lead to accumulation of dsb (Lieber, 1997a; Tishkoff *et al*, 1997). Cells lacking Rad51 have a deficient homologous recombination pathway and are inviable due to their failure to repair dsb formed in this way (Haber, 1999).

A further mechanism to increase potential genetic diversity is the splicing and recombination of immature B and T cell genes to increase the diversity in the cells of the immune system (Jeggo *et al*, 1995). In both cases it is necessary for the cell to induce dsb within the DNA to enable these events to occur. The V(D)J recombination mechanism used in this pathway is initiated by the transposases RAG1 and RAG2, and completed by a more generally used repair pathway. This process is discussed in more detail in Chapter 2 where Omenn Syndrome, a condition caused by *RAG1* and *RAG2* deficiencies is considered.

Other cellular events which can give rise to dsb include the mating type switch in yeast, where an HO endonuclease induces dsb formation followed by excision and reinsertion of transposable elements. Fragile sites such as extended micro- and mini-satellite sequences which undergo a dynamic process of expansion and deletion often associated with genetic diseases (Sutherland *et al*, 1998) are also a possible source of "spontaneous" dsb, evidence for which has been obtained in yeast studies (Debrauwere *et al*, 1999). Excision repair processes which eliminate mismatches and base damage (Tubiana *et al*, 1990) can also give rise to dsb if excision of damaged bases occurs close together on opposite strands (bases less than 10 bp apart). Although all the possible ways to induce spontaneous dsb do not individually account for the formation of many dsb, collectively they may be responsible for a small but significant number of dsb within the genome of an organism and this may have consequences for the maintenance of genomic integrity.

A variety of chemical and physical damaging agents have been used to induce chromosome aberration formation in cells. It is generally accepted that the dsb is the critical lesion for the formation of chromosome breaks (Bender *et al*, 1974; Bryant, 1984; Dikomey *et al*, 1998). Ionising radiation and restriction endonucleases can induce dsb which, if unrepaired lead to the formation of chromosome aberrations in the phase of the cell cycle within which the initiating dsb are induced. Most damage-inducing

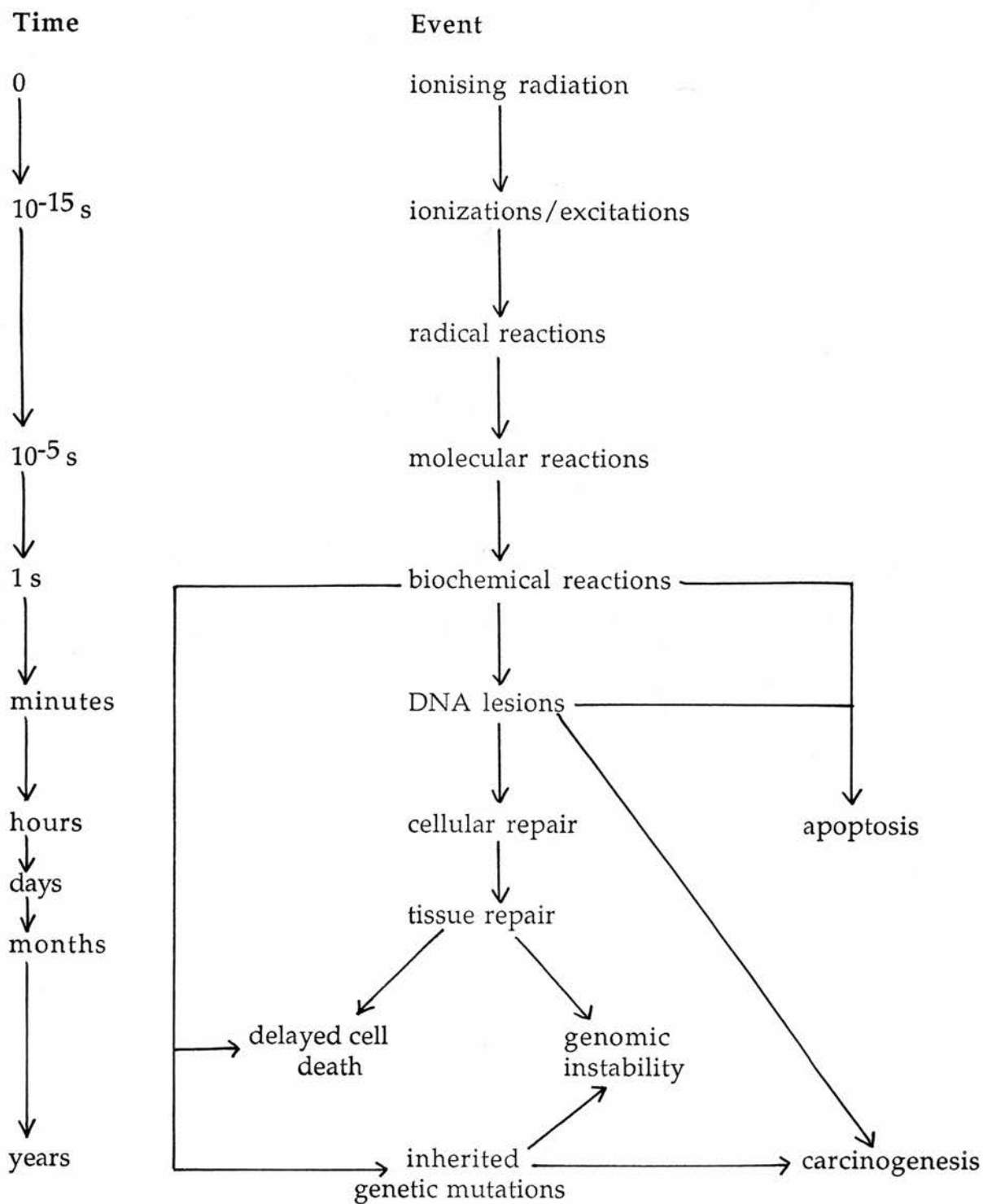


Figure 1.1. Simplified chronology of events following exposure of cells to ionising radiation (adapted from Tubiana *et al* 1990).

chemicals give rise to chromosomal aberrations only after the cell has passed through S phase (Pfeiffer *et al*, 2000) and are therefore not considered in the present study.

1.3. How ionising radiation damages DNA

Many types of DNA damage can be induced by ionising radiation (IR) (Tubiana *et al*, 1990) but the initial event is ionisation excitation of water molecules in the aqueous environment of the cell to form oxidising $\bullet\text{OH}$ and reducing $\text{H}\bullet$ radicals and aqueous electrons which are short-lived but highly reactive (Figure 1.2).

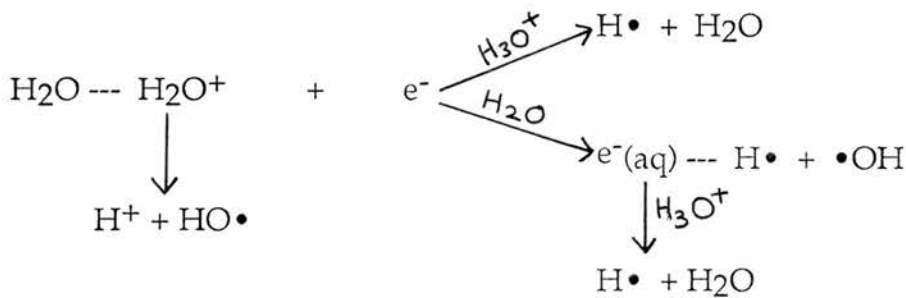


Figure 1.2. Stages in the radiolysis of water. Adapted from Tubiana *et al*, 1990.

These radicals can then diffuse away from the track and react with each other and with other molecules. The distribution of radicals along a radiation track is LET-dependent. DNA damage by radiation-induced radicals can be direct, accounting for approximately one third of sustained damage, or indirect which causes the remainder (Tubiana *et al* 1990). Direct damage is caused by the absorption of a photon by a neighbouring water molecule and the ejection of an excited electron which then interacts with the DNA to cause a break at the weakest bond which may be at the site of interaction of the DNA and the electron or the energy absorbed can migrate to break weak bonds elsewhere. The indirect effect of ionising radiation is when radiation energy is transferred to a water molecule resulting in radicals diffusing to and interacting with the DNA causing

damage. This can result in biochemical reactions, chemical alterations due to bond breakages and measurable biological effects (Figure 1.1).

Ionising radiation can cause about 100 different lesions which can be grouped into strand breaks (single and double), base alteration, sugar destruction and cross-links/dimer formation. The most frequently occurring lesion is the strand break, many of which are formed due to the indirect action of radiation. Single strand breaks (ssb) occur at a constant rate over a wide dose range (0.2 - 60,000 Gy) and are due to $\bullet\text{OH}$ action, opening up the helix allowing water in and disrupting the hydrogen bonds between the bases and changes to 3-4 nucleotides close to the break. Repair of ssb is multiphase and rapid, ssb are not thought to cause long-term damage to the genome even though they occur at a frequency of 1000 ssb/Gy. Double strand breaks (dsb) occur at a much lower frequency of 20-40 dsb/Gy and are defined as a break in both strands of the double helix due either to a single track or to the production of two ssb in complimentary strands close together due to two tracks traversing the same region of the nucleus, this however occurs very rarely. Base damage, which occurs less frequently (2-3 events per 10 ssb) (Tubiana *et al* 1990), is primarily pyrimidine damage (thymine and cytosine) as these are more radiosensitive than purines (adenine and guanine). Sugar destruction, the oxidisation and hydrolysis of the deoxyribose is even less common and leads to liberation of the base with or without breakage of the phosphodiester bond. Most types of DNA damage are rapidly repaired by activated or constitutively expressed enzymes (Carr and Hoekstra, 1995), the damage response involves a number of pathways that link DNA damage, cell cycle checkpoints and programmed cell death (Wang, 1998). There is a large degree of conservation in DNA repair mechanisms (Taylor and Lehmann, 1998). It is generally accepted that the DNA double-strand break (dsb) is the primary lesion responsible for long-term unrepaired damage in IR exposed cells (Bender *et al*, 1974; Bryant, 1984, Dikomey *et al*, 1998) which subsequently leads to changes in cellular activity and ultimately may lead to cancer. Such damage can be visualised as chromosome and chromatid aberrations which can be classified into distinct types by studying metaphase spreads. Although there is

considerable evidence supporting the idea that dsb play a major role in the formation of both chromosome and chromatid aberrations, the mechanism by which dsb are converted to visible aberrations is not understood. However the analysis of chromatid break formation (the G₂ assay) has been used to study the chromosomal radiosensitivity of tumour cells or to study individuals with cancer predisposition (Terzoudi *et al*, 2000; Parshad and Sanford, 2001). Elevated frequency of chromatid aberrations may be due to either low-penetrance predisposing genes which cause DNA repair deficiencies (Sanford *et al*, 1989, Patel *et al*, 1997, Scott *et al*, 1994, 1999) or to mutations in genes involved in cell-cycle control mechanisms such as the CDK1/cyclin B complex which is one of the regulators of the G₂/M restriction point (Terzoudi *et al*, 2000).

1.4. Formation of dsb by restriction endonucleases.

It is possible, by the use of enzymes, to induce DNA dsb in order to study the mechanisms of repair and related processes. Ionising radiation is frequently used to produce DNA damage at random throughout the genome. This mimics the type of damage that naturally occurs when cells are subjected to external sources of radiation e.g. radon and is useful for studying the mechanisms and kinetics of repair associated with particular types and intensity of radiation exposure. One of the disadvantages of using ionising radiation to induce damage is that dsb formed in this way produce "dirty ends"; the break is not always between the 3' hydroxyl and the 5' phosphate bond. Also damage around the site of radiation track interaction with the DNA can also occur leading to base or sugar damage in the vicinity of the dsb which may affect both the efficiency and fidelity of subsequent repair (Bryant, 1989).

An alternative method of inducing dsb is to use restriction endonucleases which produce "clean" breaks with cleavage always occurring at the 3' hydroxyl and 5' phosphate bonds. Restriction endonucleases originate from bacteria, where they serve as a protective mechanism against viruses by degrading viral DNA. Highly specific base sequences are

recognised by each nuclease to produce either blunt-ended or cohesive-ended breaks in the presence of magnesium ions (Winkler, 1992). Type II endonucleases have an ab formation and can bind to either the major or minor groove of the DNA (Aggarwal, 1995). The size of the recognition sequence essentially determines the frequency with which target DNA is cleaved. The advantage of this method of inducing dsb is that only one type of "end" is produced unlike radiation-induced breaks where a mixture of blunt and cohesive ends will be formed, but it is likely that mostly cohesive ends will be formed (Bryant, 1989). It is thus possible to mimic the effect of ionising radiation on cells whilst studying the processing of a particular type of break. It appears that dsb induced by restriction endonucleases are processed in the cell in a similar manner to radiation-induced breaks and can lead to similar chromosomal and chromatid aberrations and cell death (Bryant, 1984, 1985; Natarajan and Obe, 1984; Winegar *et al*, 1989; Bryant *et al*, 1987; Bryant, 1988). There has however been some disagreement as to whether both blunt- and cohesive-ended dsb are equally effective in inducing aberrations (Winegar and Preston, 1988) or whether blunt-ended dsb are more effective than the cohesive ended dsb in producing chromosomal aberrations (Bryant, 1984; Bryant and Christie, 1989). Bryant *et al*, (1984) showed that cohesive dsb were less effective than blunt breaks at producing chromosome aberrations. Cohesive-ended dsb may be less effective since the ends generated may be easily repaired due to stabilisation of hydrogen bonding at the site of the dsb (Bryant, 1984).

Recognition sites can also be inserted into genomes in order to create breaks at specific sites of known sequence in order to study inversion and recombination events (Sternberg, 1992; Bennett *et al*, 1993; Shepherd *et al*, 1994) thus making it possible to induce a single dsb within a target genome (Sargent *et al*, 1997). The use of the I-SceI system to produce a single dsb with in the cellular genome of a cell transfected with the I-SceI endonuclease recognition site is a versatile model system for investigating DNA damage recognition pathways and initiation of repair mechanisms. The background and applications of this system will be considered in more detail in Chapter 4.

1.5. Mechanisms of dsb repair

The major difference between excision repair processes and dsb repair pathways is that the former rely on the presence of an undamaged strand opposite the lesion to restore the original sequence to the damaged strand, whereas this is not possible in dsb repair pathways. Several different repair processes have evolved to deal with this problem which can be divided into two main groups: homology-dependent and homology-independent. Homology-dependent or homologous recombination repair (HRR) mechanisms require extensive regions of sequence homology (several hundred base pairs), while homology-independent or non-homologous end-joining (NHEJ) may use microhomology (1 - 10 bp) or none at all, simply pasting the broken DNA ends back together (Pfeiffer *et al*, 2000). Homology-dependent repair is thought to be the major dsb repair pathway in G₂, whereas homology-independent repair is the principle pathway in the G₁ phase of the cell cycle.

1.5.1. Homology-dependent mechanisms of dsb repair.

Homology-dependent repair is the major repair pathway in bacteria, phages and yeast and at one time was not considered to be important in metazoans. However studies of whole cells where dsb are induced in chromosomes rather than in DNA fragments, demonstrated the proficiency of vertebrate cells in repairing dsb via this pathway (Liang *et al*, 1998). In yeast this repair mechanism is dependent on RAD51 and RAD52 and homologues of these proteins have been identified in vertebrate cells indicating the highly conserved nature of this repair pathway (Pfeiffer *et al*, 2000 and references therein). The importance of RAD51 and RAD52 in relation to signalling functions for dsb processing will be considered in section 1.6. The alternative pathways for this repair process are conservative and non-conservative. Conservative homologous dsb repair

repair of the dsb by copying the sequence from the sister chromatid and can follow three distinct pathways: dsb repair; single-strand annealing or break-induced replication.

1.5.2. Conservative homology-dependent mechanisms of dsb repair.

With conservative homologous recombination repair, also called gene conversion, recombination takes place between two different alleles of the same gene, the damaged (recipient) gene being converted to the sequence of the undamaged (donor) gene (see Figure 1.3). This conversion event may affect a single gene (short track) or a series of genes (long track), or possibly the entire chromosome arm. In yeast the two main families of proteins participating in this gene conversion process are the strand transfer proteins (Rad 51p, Rad52p, Rad 54p, Rad 55p and Rad 57p) and the nucleolytic strand resection proteins (Rad 50p, Mre11p and Xrs2p). Additionally, proteins are also involved in stabilisation of DNA single strands, DNA synthesis and removal of non-homologous ends (Chen and Kolodner, 1999). The importance of this mechanism in vertebrate cells is underlined by the numerous homologues of these yeast proteins which have been identified. There are seven different Rad51 homologues (Kanaar *et al*, 1998), the functional homologue of Xrs2p is Nbs1, defective in Nijmegen Breakage Syndrome (Carney *et al*, 1998) and BRCA1 and BRCA2 have been shown to interact with Rad 50 and the Rad51/Mre11 complexes, suggesting a major role for homology-dependent recombinational repair in mammalian cells. The role of these proteins and others associated with repair processes will be further considered in Chapter 2.

The double-strand break repair model proposed by Resnick (Resnick and Martin, 1976) is an example of a homology-dependent repair mechanism. Chadwick and Leenhouts (1978) further adapted the general principles of this model to explain the formation of chromosome and chromatid aberrations as described later in section 1.6.3. The basic Resnick model (Figure 1.3), based on yeast studies, includes the following steps following dsb induction: exonuclease degradation of the damaged ends in a 5' to 3' direction,

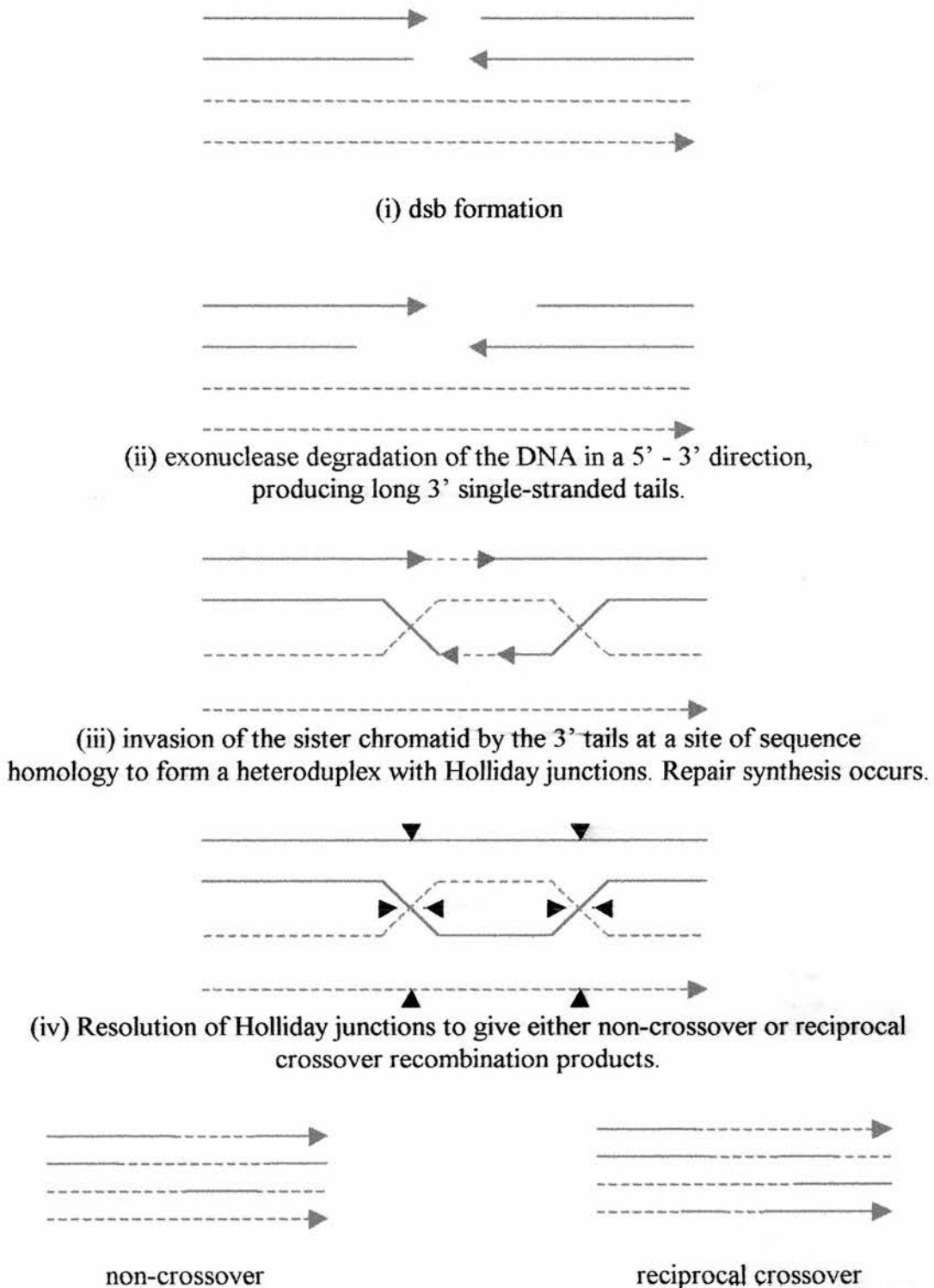


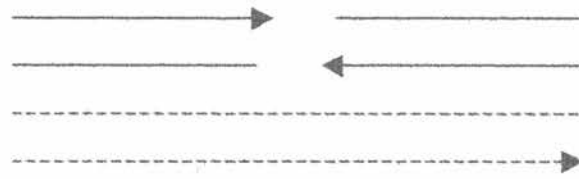
Figure 1.3. Principle steps in the homology-dependent dsb repair mechanism (Resnick model). Adapted from Pfeiffer *et al*, (2000).

producing long 3' single-stranded tails that then invade the sister chromatid (at mitosis) at a site of sequence homology. Subsequent resection may involve the Rad50/Mre11/Xrs2 complex. Strand invasion and exchange then follows, the 3' ends of the invading strands acting as primers for semi-conservative repair synthesis so that one newly-synthesised strand is present in each of the donor and recipient chromosomes. The resulting heteroduplex, bordered by regions of cross-over between chromatids called Holliday junctions, can migrate along the strands to enlarge the heteroduplex region. Resolution of the Holliday junctions can give rise to either crossover or non-crossover products.

Synthesis-dependent strand annealing (Paques and Haber, 1999) is an alternative method dsb resolution resulting in short track gene conversion (Figure 1.4). In this case the newly synthesised DNA strands are displaced from the template and returned to the broken strand, allowing the newly synthesised strands to join together so that all newly synthesis and DNA ends up on the same strand (Figure 1.4). Thus unlike the double-strand break repair model of Resnick this mechanism is conservative. If gene conversion events involve long track gene conversion then only one dsb end invades the sister chromatid and initiates both leading and lagging strand synthesis at a replication fork as observed in S phase. This break-induced replication model (Figure 1.5) can result in gene conversion to the chromosome end or can be converted into a dsb repair if a second dsb is encountered. Meselson and Radding (1975) proposed that homology-dependent recombination repair could be initiated by a ssb rather than a dsb to explain gene conversion events in fungi, but this is not a mechanism which has been considered for mammalian systems.

1.5.3. Non-conservative homology-dependent recombinational dsb repair.

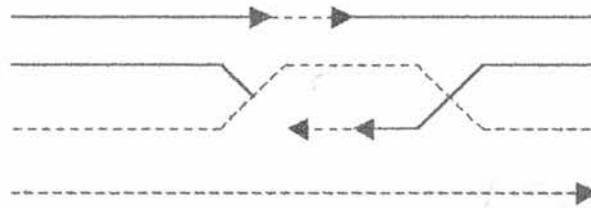
Single-strand annealing (Figure 1.6) is the repair pathway used when a dsb occurs between two flanking homologous regions. The repair mechanism begins with a 5' - 3'



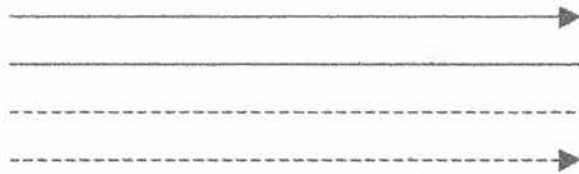
(i) dsb formation



(ii) exonuclease degradation of the DNA in a 5' - 3' direction, producing long 3' single-stranded tails.



(iii) invasion of the sister chromatid and repair synthesis



(iv) Newly synthesised strands are displaced from the template and returned to the broken strand, to yield only non-crossover recombination products.

Figure 1.4. Principle steps in homology-dependent dsb repair: synthesis-dependent strand annealing mechanism. Adapted from Pfeiffer *et al*, (2000)

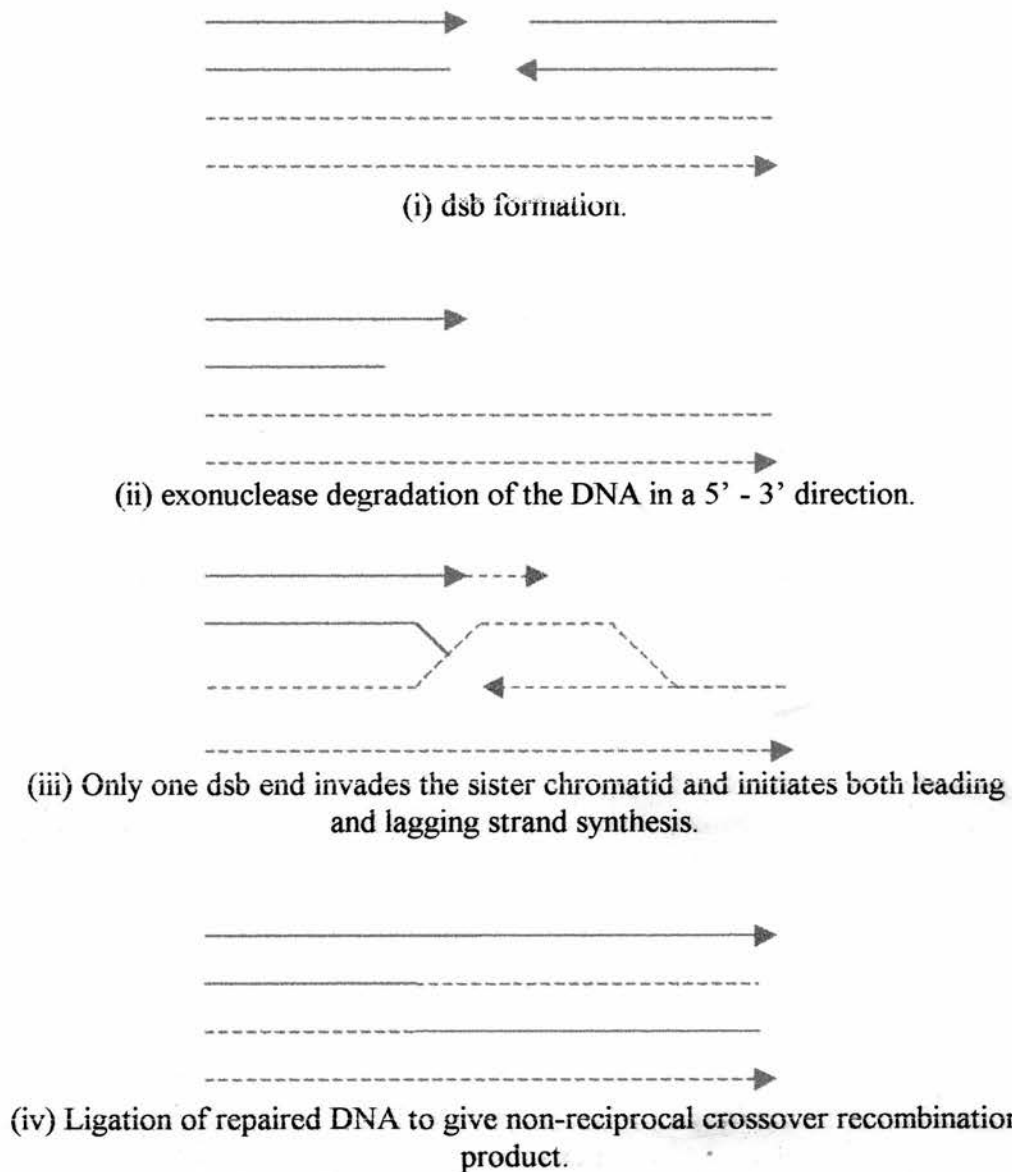
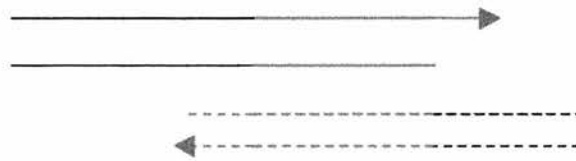
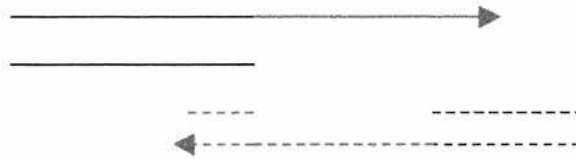


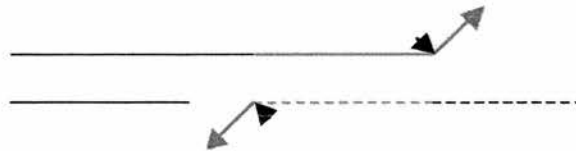
Figure 1.5. Principle steps in homology-dependent dsb repair: the break-induced replication model. Adapted from Pfeiffer *et al.*, (2000).



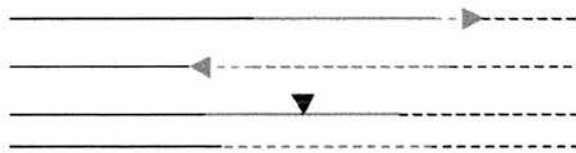
(i) dsb formation.



(ii) exonuclease degradation of the DNA in a 5' - 3' direction until substantial regions of homology are exposed on long 3' tails.



(iii) strand annealing by 3' tails and flap removal.



(iv) gap filling and ligation to yield a product which has a deletion of one copy of the repeat and the intervening sequence.

Figure 1.6. Principle steps in non-conservative homology-dependant dsb repair: the single-strand annealing mechanism. Adapted from Pfeiffer *et al*, (2000).

resection of the dsb ends (possibly mediated by the Rad50/Mre11/Xrs2 complex) until regions of homology (around 400 bp) are exposed which flank the break site on long single stranded 3' tails which undergo strand annealing (Pfeiffer *et al*, 2000). In yeast this repair pathway is Rad52-dependent but Rad51-independent.

1.5.4. Homology-independent mechanisms of dsb repair.

Homology-independent repair mechanisms or non-homologous end-joining (NHEJ) are able to join dsb ends directly and are thought to be the predominant form of dsb repair in G₀ and G₁ cells. NHEJ is able to rejoin non-complementary DNA ends irrespective of their sequence and structure and thus has mutagenic potential as the original sequence is only restored if the dsb generates two complementary or blunt ends which can be precisely ligated. Two non-matching ends must first be changed into a form which can be ligated and this enzymatic digestion of the ends can cause base pair substitutions, insertions or deletions leading to small scale mutations at the repair site. This appears to be an acceptable level of mutational change in multicellular organisms since the probability of such events occurring within an expressed gene is small and even if this occurs the intact alleles can compensate for any loss of gene function. Hamster cell lines deficient in dsb repair have been identified and these have enabled the identification of a number of genes critical for NHEJ to proceed. *XRCC4* encodes a co-factor of DNA ligase IV and *XRCC5*, *XRCC6* and *XRCC7* are the homologues of the V(D)J recombination genes coding for Ku86 (also known as Ku80), Ku70 and DNA-PK_{CS} respectively (Jeggo, 1990; Featherstone and Jackson, 1999). The Rad50/Mre11/Xrs2 complex is also thought to be involved in NHEJ as Mre11 has been found to interact with Ku70 (Goedecke *et al*, 1999). All these genes have homologues in yeast except DNA-PK_{CS} (Critchlow and Jackson, 1998) but NHEJ is not thought to be a major repair pathway in yeast as it is only detectable when the Rad52-dependent repair pathway is absent (Critchlow and Jackson, 1998). The NHEJ that does occur in yeast is of two types; a ku-dependent pathway which joins ends

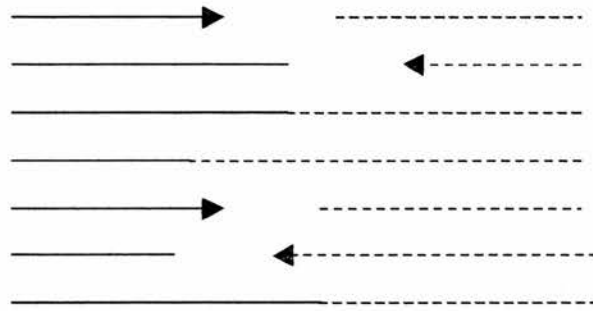
accurately and a Ku-independent pathway which forms deletions, the breaks points showing patches of microhomology.

1.5.5. Accurate non-homologous end joining (NHEJ).

The mechanism of accurate NHEJ was studied in *Xenopus* egg extracts (Pfeiffer and Vielmetter, 1988). This mechanism is able to restore the original sequence following either blunt or cohesive end dsb induced by restriction endonucleases and preserve the sequences of interacting non-complimentary DNA ends by generating either overlaps or fill-in products. Fill-in junctions typically arise during the joining of abutting ends, (i.e. blunt/5' or 3' overhang or 5'/3' overhang) while overlap junctions are formed between two overhangs of the same polarity (i.e. 3'/3' or 5'/5'). The sequences at fill-in junctions are preserved as the ends are transiently held together by non-covalent interactions while the 3' hydroxyl group of the 5' overhang is used as a primer to direct repair synthesis of the 3' overhang (Thode *et al*, 1990). In the overlap pathway single complimentary bases pair to form overlaps (Figure 1.7). It is thought an alignment factor, possibly the ku70/ku86 heterodimer maintains the DNA ends in an appropriate configuration to facilitate ligation, at the same time protecting the ends from degradation and enhancing the accuracy of NHEJ (Liang and Jasin, 1996; Critchlow and Jackson, 1998; Feldmann *et al*, 2000).

1.5.6. Error-prone non-homologous end-joining (NHEJ).

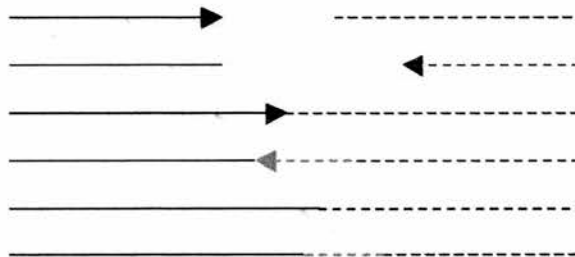
This pathway is independent of the Ku70/Ku86/DNA-PK_{CS} complex and is only detectable when Ku70/86 is not functional (Boulton and Jackson, 1996a; 1996b; Critchlow and Jackson, 1998; Feldmann *et al*, 2000). This pathway creates deletions whose break points are flanked by micro-homologies (Figure 1.8). These regions are exposed on single strands following exonucleolytic resection around the break site or helicase-driven DNA unwinding. It is similar to the single strand annealing pathway except that in this case



(i) dsb formation and cohesive ligation and overlap formation either 5'/5' or 3'/3'.

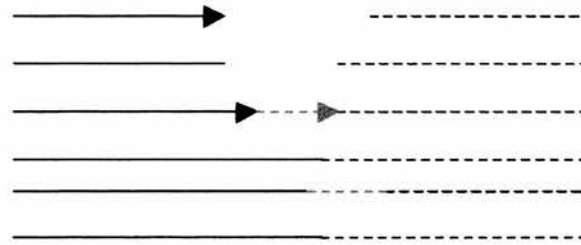


(a) blunt end ligation

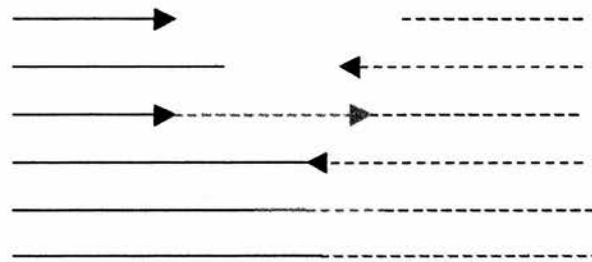


(b) blunt / 5' fill-in

Figure 1.7. Principle steps in non-homologous DNA end joining: the accurate NHEJ model. Adapted from Pfeiffer *et al*, (2000). Continued overleaf.

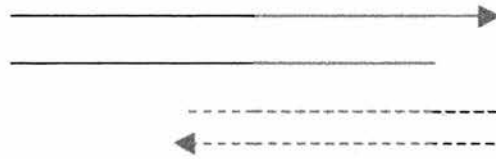


(c) blunt / 3' fill-in

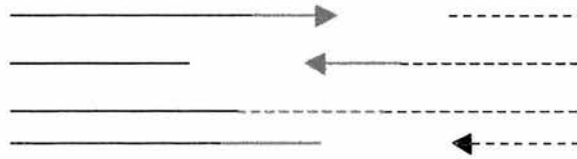


(d) 5' / 3' fill-in

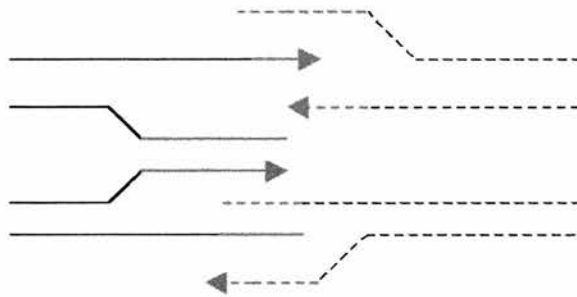
Figure 1.7 continued. Principle steps in non-homologous DNA end joining: the accurate NHEJ model. Adapted from Pfeiffer *et al*, (2000).



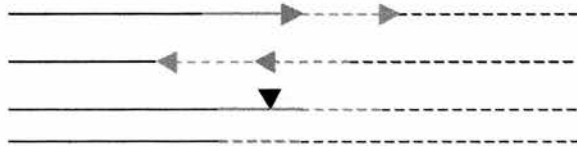
(i) microhomology driven single-strand annealing or direct repeat end-joining



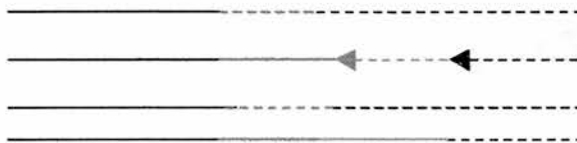
(a) terminal trimming, exposure of microhomology, annealing or



(b) duplex unwinding, exposure of microhomology, trimming and annealing.



(ii) These give rise to either microhomology priming or



(iii) microhomology ligation.

Figure 1.8. Principle steps in non-homologous DNA end joining: the error-prone NHEJ model. Adapted from Pfeiffer *et al*, (2000).

only small regions of homology are present, whereas single strand annealing requires extensive regions of homology. A patch of microhomology occurring at the tip of the 3' single strand could act as a primer for DNA fill-in synthesis; at the end of a 5' or 3' single strand it could join the recessed strand of the partner strand and be joined by microhomology ligation. In either case one strand would be quickly stabilised thereby facilitating the resolution of the second strand.

Overall, homologous-recombination repair mechanisms are most likely to restore the original DNA sequence following a dsb, though gene conversion has the potential to cause loss of heterozygosity (LOH) if the other allele carries a mutated gene. The alternatives will produce mutational changes to some degree, even the accurate NHEJ pathway leads to point mutations at repair sites if the ends are not directly ligated without further processing. Due to this dependence on sequence homology, homology-dependent mechanisms predominate in G₂ and S phases, single strand annealing and NHEJ are more likely to occur in G₁. It is also important to consider the number of dsb required to induce the formation of chromosomal aberrations and what form such aberrations may take depending on the interaction potential of dsb within the genome. Numerous models have been proposed to explain the formation of chromosomal aberrations within cells and these will now be considered.

1.6. Models of chromosomal aberrations

Radiation-induced chromosomal aberrations have been studied for many years, Muller was one of the first researchers to report structural changes in *Drosophila* chromosomes but his findings were not quantitative. Since then quantitative studies have led to the development of models to explain the mechanisms by which chromosomal aberrations are formed, the first of which was by Sax as a result of his study of *Tradescantia* pollen (Sax, 1940). His theory was later mathematically formalised by Lea (Lea, 1946). Sax's

"Breakage First" or "Breakage and Reunion" theory proposed that the primary DNA lesion was a break in the "chromonema" (Savage, 1993). A modern version of the model (Bender *et al*, 1974) suggests that most dsb which occur are repaired or restituted but some remain and can be visualised as chromosomal breaks or gaps at metaphase. In Sax's model these breaks or gaps were proposed to be the result of a single chromosome or chromatid break resulting in the observed aberrations. This model was challenged by Revell with his "Exchange Theory" in which he proposes that all open breaks observed at metaphase are the result of failed or incomplete recombination events. The primary damaging event in this theory is an unspecified lesion which interacts to form an exchange which if incomplete at metaphase results in a visible chromosome break, any visible breaks or gaps therefore being secondary not primary DNA damaging events (Revell, 1955; 1959; 1959a; 1974). Recently a new model has been proposed, the signal model (Bryant, 1998a). The signal model which has several features in common with Chadwick's model (Chadwick and Leenhouts, 1978), one of which is that both propose that the primary DNA lesion is a dsb. Chadwick and Leenhouts proposed their model as an explanation of observed aberrations but did not undertake any experimentation to support their theory which proposed that the primary dsb causes homologous recombination to occur in a manner similar to the Resnick model (Resnick and Martin, 1976). The signal model hypothesises that an initial single dsb activates a signal pathway resulting in a recombinational exchange involving a large loop of chromatin and where unfinished or incomplete recombinational exchanges appear as chromatid breaks or gaps at metaphase.

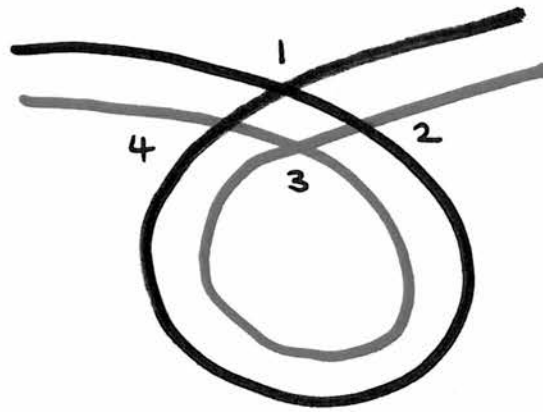
1.6.1 The Sax model

Sax proposed what is now the classical explanation for the formation of chromatid breaks based on his study of *Tradescantia* pollen. His "Breakage First" or "Breakage and Reunion" theory suggests that such breaks are formed when one or both chromatids are broken by a track of ionising (X-ray) radiation (Sax, 1940). The majority of the breaks are

rejoined or "restituted" and are thus undetectable. Misjoined breaks give rise to a chromosomal rearrangement such as sister chromatid fusion (with no acentric fragments) and ring formation while unrejoined breaks produce visible gaps or breaks at metaphase. He also showed that the rate of break restitution and/or aberration formation does not have a temperature coefficient and therefore concluded that they are not caused by a secondary chemical reaction. Sax reported that there was a linear relationship between radiation dose and chromatid break frequency but that gross chromosomal aberration frequency increased geometrically with dose rate. Based on these observations he proposed that the initial lesion is the visible chromosome or chromatid break and that the formation of an exchange-type aberration is the result of interaction between two breaks which are misjoined. Sax's hypothesis was mathematically formalised by Lea (1946). This classical model was controversially challenged by Revell who proposed an "Exchange Model"

1.6.2. Revell's Exchange Model

Revell proposed his Exchange Model based on experiments performed on the root-tip cells of *Vicia faba* (Revell, 1958). He observed that chromatid exchanges occurred between different chromosomes, a proportion of which were incomplete when visualised at metaphase. Incomplete inter- and intrachanges were postulated to give rise to four basic types of chromosome aberration dependent on the affected part of the chromosome being formed into a small loop (See Figure 1.9). In this model, the primary damaging event is caused by an ionising particle when it interacts with a chromatid causing a perturbation in the structure of the chromatid. This then decays towards a normal or undetectable state unless close to another primary damaging event with which it can interact to reach a stabilised state predisposed to chromatid exchange. Thus the primary lesions are not chromosome breaks as in the Sax model but a less definable state of chromatid instability (Revell, 1974). Such exchanges would take place where two



Incomplete exchanges at:

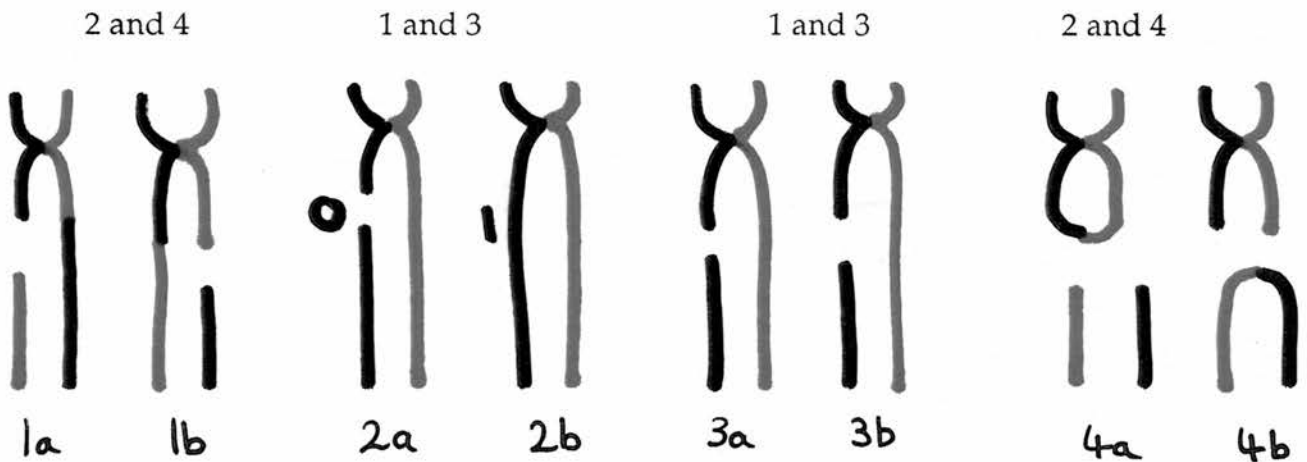


Figure 1.9. Diagram of formation of chromatid deletions using Revell's exchange hypothesis. Types 1a and 1b are visualised as colour switch breaks (csb), types 2a,2b, 3a,3b are visualised as non-colour-switch breaks (ncsb). In practice it is not always possible to distinguish the different subtypes of csb and ncsb. The proportion of deletions showing an exchange between sister chromatids is therefore 2/5 or 40%. Types 4a and 4b are isochromatid deletions and not included in the csr. Adapted from Heddle *et al* 1969.

initiating lesions occurred close enough together, that is within the same chromosome loop structure. Such "Revell Loops" were proposed as diagrammatic devices to describe the bringing of two chromosome regions into spatial proximity in order for lesion interaction to occur (Savage, 1968). Such exchanges can be either "vertical" or "horizontal" and can give rise to complete or incomplete intra- or interchromatid exchanges, producing four types of exchange aberration. Revell postulated that all four types had equal probability of occurring thus the proportion of singly incomplete chromatid deletions showing colour switches will be $2/5$ or 40% as shown in Figure 1.9. Both the Sax and Revell models have been mathematically formalised by Raiovoyevitch *et al*, (1998) in terms of repair and misrepair of dsb following high doses of ionising radiation. This analysis is however of limited value when considering chromatid aberration frequency following exposure to low radiation doses.

Revell's predictions were experimentally tested by Heddle (Heddle *et al*, 1969) who found that 38% of exchanges observed in *Potorus* cells displayed colour switches and concluded that the majority of terminal deletions were incomplete interchanges. However Heddle and Bodycote (1970) found only 15-18% of breaks were associated with a colour switch in Chinese hamster cells. Both sets of results were obtained using tritiated thymidine. The development of the use of BrdU in conjunction with FPG staining (Perry and Wolff, 1974) allowed more accurate and reliable differentiation between sister chromatids than previously possible using tritiated thymidine (Taylor *et al*, 1956). This technique was used to show that 8% of breaks also displayed colour switches. Work by Savage and Harvey (1991) suggested that all exchange types were not equally likely and that intrachromatid exchanges are more likely to occur than those between (inter) chromatids. They suggested that this is due to the chromatin actively condensing to form two spatially discrete chromatids as the cell approaches prophase making it less likely that interchromatid exchange will occur.

1.6.3. Chadwick and Leenhouts' Model

There are fundamental differences in the manner Sax and Revell account for observed chromosome and chromatid aberrations. An alternative approach was first suggested by Chadwick and Leenhouts (Chadwick and Leenhouts, 1978) when they hypothesised that aberrations were caused by a single initial radiation-induced dsb. Such a dsb would be either repaired via an enzymatically controlled recombinational exchange or partly repaired, resulting in a visible chromatid break. The recombinational exchange mechanism they proposed was based on an original idea put forward by Resnick (Resnick, 1976) (Figure 1.3). The Resnick model of homologous recombination, based on yeast studies was developed to explain the disappearance of induced dsb with time. The Chadwick and Leenhouts' model proposes that following a dsb, some exonuclease digestion of the broken ends occurs to produce single-stranded overhang regions. These then undergo recombination with either the sister chromatid of the damaged chromosome or with another chromosome. This exchange is facilitated by the formation on an endonuclease nick in the undamaged DNA strand, enabling a heteroduplex to be formed. Such a heteroduplex can follow two pathways: either DNA synthesis can occur followed by unwinding of the heteroduplex and restoration of the undamaged DNA region with the other end of the DNA dsb leading to either perfect repair or gene conversion. Alternatively the undamaged DNA can unwind to a greater extent enabling it to associate with both single stranded ends at the break site. The endonuclease-induced strand break in the undamaged DNA would then lead to reciprocal exchange of the two DNA double helices. Such a repair mechanism requires the damaged and undamaged DNA to be homologous and for both to be in close proximity.

The condition that the combining DNA helices must be homologous is fulfilled by sister chromatids in G_2 , in other phases of the cell cycle homologous recombination could only arise in regions containing repetitive sequences. Chadwick and Leenhouts proposed that such a mechanism could produce all the chromosome and chromatid aberrations

observed and classified by Revell and that chromosome break-points in exchange rearrangements (in G_1) would occur only in regions of repetitive sequences. Such a mechanism would suggest that as breaks disappeared over time, the observed numbers of sister chromatid exchanges within a cell would increase; this has not been reported.

1.6.4. The signal model

Harvey and Savage (1997) investigated the relationship between non-colour switch breaks and colour switch breaks (referred to as colour jump breaks) in various BrdU-incorporated cell lines. They reported that the proportion of colour switch breaks was constant regardless of cell type, BrdU concentration and radiation dose. They also observed that colour jump breaks occurred in cells not subjected to damage by ionising radiation. These observations, together with experimental evidence showing linearity of dsb induction with increasing radiation dose (Chadwick and Leenhouts, 1994) and linear disappearance of chromatid breaks with time (when plotted on a log scale) following exposure to low doses of ionising radiation (Macleod and Bryant, 1996) led to the development of the signal model.

The signal model proposed by Bryant (1998) is a hypothesis for the conversion of dsb into chromatid breaks in the G_2 phase of the cell cycle. The proposed model fits many of the following observations: that chromatid breaks disappear with time; that their induction is linear with dose and that the frequency of colour switch breaks as a percentage of total number of observed breaks is constant for a given cell type regardless of the magnitude or quality of radiation used. Also such breaks can occur spontaneously in control cell populations (Bryant, 1998 and references therein).

The model proposes that the induction of a dsb in one of the large chromatin domains in which the DNA helices are packaged within the nucleus (Iborra *et al*, 1996), causes a signal which activates enzymes located in these so-called transcription factories. These

factories are essentially chromatin loops associated with discrete collections of enzymatic and other proteins involved in all aspects of DNA transcription, replication and repair (Iborra *et al*, 1996). The signal model proposes that this activation process results in the excision, exchange or inversion of that part of the chromatin loop (about 5 Mbp DNA) containing the damage (Figure 1.10). It would seem logical that the part of the chromatin loop which is excised, exchanged or inverted is that part containing the initial damage but this mechanism may be a more general process which occurs in the cell. Meiotic recombination may utilise a similar mechanism in germ cells; double strand breaks are known to be induced in V(D)J recombination in B and T cell genes (Jeggo *et al*, 1995; Ramsden *et al*, 1997). In these situations the initiating event would either be an internally induced dsb (or some other event) which triggers the same signal pathway to induce recombination. If this is the case, the externally-induced damaging event which causes dsb formation is triggering not a damage repair signalling pathway but a recombinational signal pathway, though there may well be elements common to both. Such rearrangements will not normally be detectable as they are completed before the cell progresses into metaphase, incomplete rearrangements can however be visualised as breaks or gaps where the DNA has incorporated BrdU through two cell cycles (Perry and Wolff, 1974). Exchanges between sister chromatids can then be seen as colour switch breaks when the recombinational process is incomplete. Complete exchanges will be difficult to distinguish from sister chromatid exchanges except where a significant change in the lengths of the chromatids occurs leading to a "kink" in one chromatid. However there is no evidence of elevated rates of sister chromatid exchanges in irradiated G₂ cells displaying colour-switch breaks as compared to the background level of conventional sister chromatid exchange. Unlike the Sax model which proposes that aberrations are due to unrepaired chromosome and chromatid or misjoined breaks (in the case of exchanges), the signal model proposes that the conversion of dsb into chromatid breaks in G₂ is due to incomplete recombination and not an inability of the cell to repair the dsb. The rate limiting step of the mechanism producing visible chromatid breaks is therefore likely to be the final rejoining step of the recombination process.

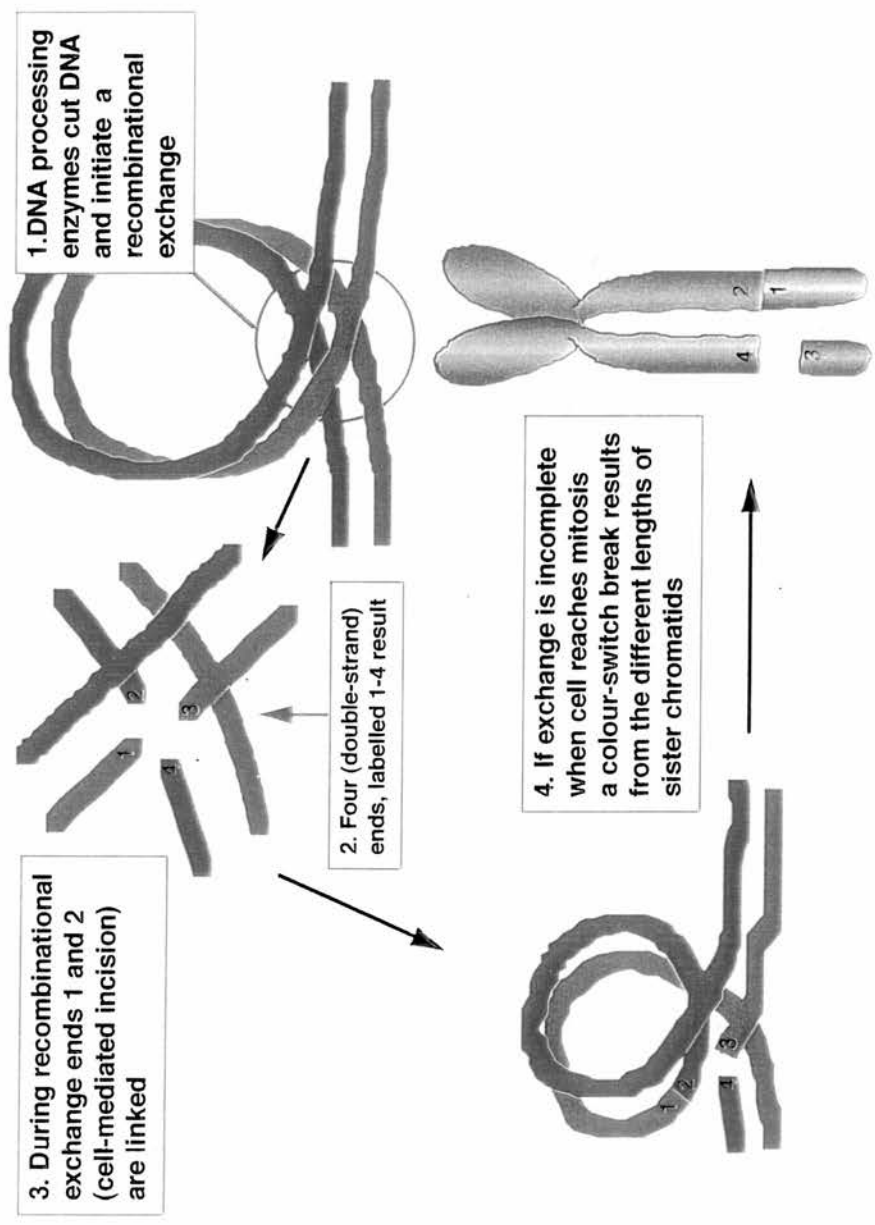


Figure 1.10. Diagram to show how a colour switch break (csb) may be formed as a result of an incomplete recombinational exchange as proposed by the signal model (Bryant 1998). The looped chromatin domain shown may be associated with a transcription factory as described by Iborra *et al* (1997) situated at the base of the loop structure. Adapted from an illustration by Bryant.

1.6.5 Pros and cons of the various models

The Oxford English Dictionary defines a model as a "representation in 3-dimensions of a proposed structure etc., a simplified description of a system etc., to assist calculations and predictions." In terms of this specific definition none of the "models" described above have been mathematically formulated to allow quantitative predictions to be made and are thus postulations or concepts. They are however possible explanations as to how DNA damage in the form of dsb gives rise to chromatid aberrations.

An argument against the Classical Breakage First (Sax) model is the very low probability of two dsb occurring within 5-40 Mbp along a chromatid, when cells are exposed to small doses (<1 Gy) of low LET radiation. Another observation that counters the classical interpretation is that chromatid breaks including a significant proportion of colour switch breaks can be observed in unirradiated cells (Harvey and Savage 1997). The linear relationship of chromatid breaks with dose although compatible with the breakage-first model would not be obtained if two independently occurring dsb are required for a visible break to occur (as argued above). The probability of two dsb occurring close enough together to produce a 5-40 Mbp break or gap of the magnitude observed is very small (Johnston *et al*, 1997; Sachs *et al*, 1998) though this probability would increase at high doses.

Because the probability of two "hits" causing dsb either from two independent tracks or from one track is extremely low, the observed deletion of a large section of a chromatid (estimated as up to a third of a chromatid arm), equivalent to the loss of about 40 Mbp (Bryant, 1998), is difficult to explain by the breakage-first hypothesis. If however there were a large amount of exonuclease digestion from the broken ends of the DNA, a phenomenon not observed in mammalian cells (though this does occur in some strains of bacteria) then the breakage first hypothesis may be valid. Also, as there is no observed increased chromatin density at the broken ends of the chromatids it is unlikely that the

size of the observed breaks can be accounted for by increased chromatin condensation away from single dsb sites.

The signal model provides an explanation for the linear relationship between chromatid breaks and radiation dose since only a single dsb is required for signalling. The signal model can also explain the observed disappearance of chromatid breaks with time. Such a disappearance would not reflect the kinetics of dsb repair but would represent the final stage of the recombinational exchange process. As such the disappearance of chromatid breaks would not be expected to follow a biphasic or continuously changing repair kinetic as has been measured by others (Dahm-Daphi and Dikomey, 1996; Foray *et al*, 1996; Glasunov *et al*, 1995; Nunez *et al*, 1995) for the repair of dsb. The constant proportion of colour-switch breaks regardless of radiation type and magnitude of radiation dose (Griffin *et al*, 1994) also supports the contention that chromatid breaks are not directly related to the kinetics of repair but represent a final recombination step.

Although the signal model is similar in some respects to the Chadwick model, being applicable principally to the G₂ phase of the cell cycle and requiring only a single initiating dsb, it differs in that it is implicit in the Chadwick model that the initiating lesion itself forms part of the recombinational event in response to DNA damage. The signal model only requires that an initiating dsb causes the signal that triggers an intra- or inter-recombinational exchange and that such events are not part of a dsb repair pathway although the observed end point i.e. a chromatid break is similar. It is not mandatory for the initiating break to be within the chromatin loop which undergoes recombinational changes, but it is an acceptable possibility. Essentially the start point and end point are similar for both the Signal and Chadwick models, the principle differences lying in the proposed intervening mechanisms. The Chadwick model has not been tested experimentally, while the signal model is presently under investigation and it is likely that study of radiosensitive cell lines may shed light on the mechanism of

induction of chromatid aberrations, in particular in identification of components of the proposed signalling pathway.

One important aspect of the formation of chromatid breaks not fully explained in any of the "models" described here is the effect of time on the chromosome or chromatid break characteristics. Although all chromosomal or chromatid aberrations are defined as occurring in G₁ or G₂ respectively, the time interval between induction of damage and harvesting of cells to determine aberration frequencies may be of importance. Generally, this has not been taken fully into account in previous models explaining the formation of chromosome and chromatid breaks. This is particularly true for chromatid aberrations as the chromatin is in a state of continual condensation as the cell approaches mitosis and this may have consequences for the types and frequency of aberration formation. As discussed in more detail in Chapter 3, the relative frequency of chromatid break subtypes can be affected by sample time.

It is of interest to compare the chromatid break frequencies and characteristics in cells deficient in different genes associated with cancer predisposition which fall into either of the caretaker or gatekeeper groups to investigate if csr and ncsr differ in these cell types compared to normal cell lines. If a significant difference in either the csr or ncsr can be detected then these gene products may perform a signalling function in response to DNA dsb, possibly activating the recombinational exchange mechanism leading to colour switch breaks.

1.7 Possible signal molecules

Candidates for the signalling molecule(s) include the DNA-PK complex which comprises of Ku70, Ku80 and p450 (Blunt *et al*, 1995; Jeggo *et al*, 1995; Weaver, 1996; Jeggo, 1997).

These proteins form a complex which associates with the ends of DNA during nonhomologous recombination during the process of V(D)J recombination (Ramsden *et*

al, 1997) and may have a structural role in DNA looping (Carey *et al*, 1997). This mechanism is defective in *scid* mice (Bosma *et al*, 1983) and it is possible that such a recombination mechanism is also responsible for meiotic recombination as well as repair of dsb that arise as a result of DNA damage (Lieber *et al*, 1997; Szostak *et al*, 1983).

It is possible that the characteristically elevated frequency of chromatid aberrations associated with sensitivity to radiation which are a feature of several conditions including Ataxia telangiectasia (Jorgensen and Shiloh, 1996), Nijmegen Breakage Syndrome (Carney *et al*, 1998; Varon *et al*, 1998), Werner's Syndrome (Fukuchi *et al*, 1989), Li Fraumeni Syndrome (Mitchell and Scott, 1997) and Bloom's Syndrome (Ellis *et al*, 1995) are due to defects in the signal pathway leading to recombination. These conditions predispose individuals to different forms of cancer (Helszouer *et al*, 1996; Scott *et al*, 1994; Bryant, 1997). Rodent cell lines have also been developed which display a range of defects in response to DNA damaging events (Jeggo, 1995, Kemp *et al*, 1984). Study of all these cell types is useful to gain an understanding of the mechanisms of DNA damage recognition and repair. It is possible that the proposed signal pathway and damage recognition and repair pathways share protein components. The ATM gene product is postulated to have a regulatory function in response to radiation damage and genomic stability (Nakamura, 1998) and may be one of a family of proteins with this role which are found in various organisms, all of which possess the PI-3 Kinase domain (Savitsky *et al*, 1995, Shiloh, 1997). It may also have a role in signalling.

Many of the early investigations were carried out on *Saccharomyces cerevisiae* mutants which display sensitivity to ionising radiation. The principle double-strand repair pathway in yeast is homologous recombination but under certain circumstances nonhomologous recombination can also occur (Kramer *et al*, 1994; Milne *et al*, 1996; Moore and Haber, 1996). Although the principle mechanism in mammals is nonhomologous recombination, homologous recombination can also occur in meiotic recombination, mitotic interchromosomal recombination and gene conversion (Roth

and Wilson, 1985). Nonhomologous recombination is the mechanism in translocations, gene amplification and V(D)J recombination. Many of the yeast genes identified which are required for repair of dsb are collectively known as the *RAD 52* epistasis group (Trujillo *et al*, 1998), mutants have defects in mitotic and meiotic recombination, both of which are initiated via induction of dsb. Homologs for many of these yeast genes have been identified in higher eukaryotes. The *RAD52* epistasis group can be further subdivided into genes associated with nucleolytic processing of dsb (*RAD50*, *Mre11*, *xrs2*); those that mediate heteroduplex formation between recombining chromosomes (*RAD51*, *52*, *54*, *55*, *57*, *RHD54*). The *RAD51* epistasis group mediates homologous recombination. *RAD 50* and *Mre11* are also required for nonhomologous recombination and telomere length maintenance and have been shown to complex with Nibrin, the protein known to be mutated in Nijmegen Breakage Syndrome (NBS) (Carney *et al*, 1998, Varon *et al*, 1998). NBS is phenotypically similar to Ataxia telangiectasia but due to mutations in different genes (Shiloh, 1997) suggesting that NBS and ATM genes are part of similar but distinct pathways in response to ionising radiation and p53 activation (Jongmans *et al*, 1997). *RAD50/MRE11* complex nuclear co-localisation is downregulated in G₁ whereas h*RAD51* nuclear focus formation is upregulated in G₂ in AT cells, suggesting that AT cells use homologous recombination instead of nonhomologous recombination due to regulatory defects arising as a result of the *ATM* gene mutation (Maser *et al*, 1997). The *RAD50/MRE11* complex is known to associate with the DNA-PK Ku complex supporting the hypothesis that the ATM protein is involved in DNA processing (Pfeiffer *et al*, 2000). The DNA-PK protein has been shown to be required for p53 activation and stabilisation and protection from MDM₂ inactivation, MDM₂ is a p53 antagonist, the *mdm2* gene being activated by p53 itself as part of a regulatory loop (Woo *et al*, 1998). The *ATM* gene is a member of the PI-3 kinase family, as is DNA-PK_{CS}, suggesting a signalling role in activating DNA damage repair pathways associated with DNA-PK (Shiloh, 1997). The *RAD50/MRE11/xrs2* complex is also associated with meiotic recombination in both yeast (Sun *et al*, 1991, Xiao and Weaver, 1997) and in humans (Dolganov *et al*, 1996).

Other candidate signalling proteins may include members of the superfamily of damage response cell checkpoint proteins which possess the BRCT domain (Bork *et al*, 1997). The XRCC4 protein interacts with DNA ligase IV and is associated with dsb repair and V(D)J recombination (Li *et al*, 1995; Critchlow *et al*, 1997; Grawunder *et al*, 1998). The XRCC9 protein is also a possible signalling molecule as it is postulated to be involved in repair (Liu *et al*, 1997). The XRCC genes include members of the Human Rad51-family, homologous to the hamster *irs* group (Liu *et al*, 1998). XRCC2 and XRCC3 participate in homologous recombination, maintenance of chromosomal stability and DNA damage repair.

The elucidation of the components of this proposed signalling pathway may also enable a better understanding of the mechanisms of increasing genetic diversity in the mammalian genome for increasing immunological diversity and maintaining a large population gene pool. It may also lead to greater insight into how chromosomal aberrations are tolerated in viable cells, a process which is believed to lead to increased genomic instability and ultimately to cancer (Marder and Morgan, 1993, Morgan *et al*, 1996).

1.8. Major aims of this investigation.

The principle goal of this investigation is to consider the predictions and assumptions of the signal model as proposed by Bryant (1998). The main areas of investigation can be summarised as follows:

- To attempt to produce a more mathematically based model to investigate the nature of chromatid break induction, which can be used to quantitatively predict and analyse the relationship between different types of chromatid (colour and

non-colour switch) breaks and the effect of DNA damaging agents on the formation and rate of rejoining of these chromatid break types with time.

- To investigate the nature of chromatid breaks in relation to radiation dose and restriction enzyme concentration. Are colour switch breaks (csb) and non-colour switch breaks (ncsb) induced in similar proportion regardless of the type of damage sustained by the DNA?
- Is the proportion of csb and ncsb (i.e. the colour switch ratio, (csr) and the non-colour switch ratio (ncsr) of the total chromatid breaks the same regardless of the type of damage sustained by the DNA?
- Is one double-strand break (dsb) sufficient to induce chromatid aberrations as predicted by the signal model? If so, are the csr and ncsr the same as those observed for damage where numerous dsb are induced either by radiation ("dirty" breaks) or by restriction endonucleases ("clean" breaks) with numerous cut sites within the DNA?
- To investigate the nature of repair of csb and ncsb to determine if the rate of repair of these break types differs by measuring the proportion of each breaks type remaining over a period of time.
- Are the csr and ncsr the same regardless of cell type, i.e. is the csr/ncsr an intrinsic property of a particular cell line or do all eukaryotic cell types produce a similar proportion of csb for the same amount of exposure to DNA damaging events such as ionising radiation?
- Is the production of csb a conserved mechanism in all eukaryote cell

types? The structure of DNA is highly conserved in eukaryotes so a similar csr in widely evolutionary diverse species may indicate that there are structural considerations in the formation of csb in the observed proportions.

- What signalling molecules may be involved in the proposed recombinogenic mechanism leading to csb? If this is a fundamental mechanism for processing dsb in the genome, it may be possible to detect a significantly different csr in cell lines derived from disease conditions known to be associated with defective dsb processing and repair and predisposition to tumourgenesis.
- Can the frequency of inversions in cells in the G₂ phase of the cell cycle be determined? The inversion of chromosomal material cannot be detected in BrdU-incorporated cells, but this may be possible using fluorescence *in situ* hybridisation (FISH). It would then be possible to determine the relative frequency of both inter-and intra-chromatid recombinational events in a cell type.

Chapter 2

Investigation of genes that affect the colour switch ratio

Contents	Page No.
2.1 Introduction	43
2.2. Cell lines under investigation	45
2.2.1. Down Syndrome (trisomy 21)	46
2.2.2. Bloom Syndrome	48
2.2.3. Omenn Syndrome	50
2.2.4. Ataxia telangiectasia, Ataxia telangiectasia-like disorder and Nijmegen Breakage Syndrome	53
2.2.4.1. Ataxia telangiectasia	53
2.2.4.2. Ataxia telangiectasia-like disorder	58
2.2.4.3. Nijmegen Breakage Syndrome	59
2.2.5. Brca1 and Brca2	64
2.2.6. p53	67
2.3. Materials and methods	71
2.3.1. Cell culture and BrdU treatment	71
2.3.2. Irradiation and harvesting	73
2.3.3. Preparation of slides	73
2.3.4. Fluorescence plus giemsa (FPG) staining	74
2.3.5. Scoring and analysis	74
2.4. Results	75
2.4.1. A consideration of the generalised radiation damage relationship	75
2.4.2. The chromatid break-dosage relationship	76
2.4.3. Statistical analysis of chromatid breaks in lymphoblastoid cells	82
2.4.4. Control (non-irradiated) lymphoblastoid cell lines	91
2.4.5. Irradiated lymphoblastoid cell lines	91
2.4.6. Regression analysis of the data	94
2.4.7. Cell lines derived from different syndromes	97
2.4.8. Radiation damage index (rdi)	110

2.5. Discussion	117
2.5.1. Bloom Syndrome, Down Syndrome	119
2.5.2. AT and NBS cell lines	121
2.5.3. Cell lines derived from families with breast cancer	124
2.5.4. Omenn Syndrome	126
2.6. Future Work	127

2.1 Introduction

A useful strategy for identifying genes involved in the recombinational rearrangements leading (or thought to lead) to chromatid breaks is to study the colour switch ratio (csr) in mutant cell lines showing elevated cellular and chromosomal radiosensitivity. A significant alteration in csr would indicate the involvement of the gene product in the rearrangement process or in its control. Thus one of the major areas of investigation proposed in the project is the determination of the proportion of colour switch breaks within the total number of chromatid breaks (i.e. the csr) of cell lines carrying different mutations. One group of such mutant cell lines are those which are derived from patients with conditions associated with predisposition to cancer such as Downs Syndrome, Nijmegen Breakage Syndrome (NBS), Ataxia telangiectasia (AT), Bloom's Syndrome, Omenn Syndrome and cell lines carrying mutations in the *BRCA1*, *BRCA2* or *p53*. genes. All these disease conditions are associated with inactivation of particular gene subsets which confer phenotypes of sensitivity to ionising radiation, increased incidence of spontaneous chromatid aberrations and, in the case of Bloom's Syndrome, very high levels of sister chromatid exchange (without breaks). It is possible that the mutant genes associated with these conditions are involved in some way with the proposed signal model recombinogenic mechanism for chromatid breaks. If this is the case it should be possible to detect significant changes in the csr. It is recognised however that the incidence of colour switch breaks may not be entirely eliminated if there are alternative pathways involving genes not directly affected by the particular syndrome.

To determine whether there is a significant difference in csr in cell lines defective in a particular subset of gene(s) as compared with controls, the following approach was adopted:

(i) The frequency distribution curve (on the assumption that the csr is variable amongst individuals) was determined for values of colour switch ratio for a group of both non-irradiated and irradiated lymphoblastoid cell lines derived from normal

individuals. It was anticipated that as for most biological systems there would be a variation in colour switch break ratio amongst normal cell lines where such a variation will take the form of a normal distribution curve. It was thus necessary to establish whether such a distribution had a broad or narrow range of values; a narrow distribution range would be required to enable detection of a small change in colour switch break frequency between mutant cell lines and normal controls. It was also necessary to establish whether there was a difference between the distributions of non-irradiated and irradiated normal control cells since the signal model predicts that the colour switch break frequency is unaffected by the absolute degree of induced damage as has been demonstrated in CHO cells (Harvey and Savage, 1996; Bryant, 1998). Thus if there is no statistically significant difference in the distribution of values for irradiated and non-irradiated cells this will in itself lend further corroborative evidence in favour of the signal model.

(ii) If it were confirmed that no significant difference occurs in the colour-switch ratio between irradiated and non-irradiated lymphoblastoid cell lines, the resulting distribution could be used as a "benchmark" to determine whether there was any observed statistical differences in colour switch break frequencies between normal lymphoblastoid lines and those from individuals associated with a particular syndrome, i.e. whether the csr for cells derived from a diseased individual fell outside the normal distribution. Any differences in frequencies observed in mutant lines may then be due to a perturbation in the proposed signalling or recombinational exchange mechanism which gives rise to such colour switch breaks.

It is recognised that the transformation of lymphocytes by the Epstein Barr virus (EBV) may have an effect on the radiation-induced response of the derived lymphoblastoid cell lines with respect to their ability to recognise and respond to primary DNA damaging events. EBV-transformed human lymphoblastoid cell lines express six virally encoded nuclear antigens EBNA-1 to 6. EBNA-5, which is required for B-cell immortalisation, can

bind both Rb and p53 (Szekely *et al*, 1993) which may impair the function of these proteins within the cell, but the effect of this is not fully understood. There is no evidence for p53 and Rb inactivation within lymphoblastoid cells such as is observed in SV40-transformed cell lines (Manfredi and Prives 1994) but the transformation of lymphocytes by EBV is thought to involve an initial, transient elevated expression of EBNA-5, p53 and Rb, with lower p53 expression in established lymphoblastoid cell lines compared to non-transformed cells (Szekely *et al*, 1995). As all the cell lines being compared in this study are lymphoblastoid cell lines they are likely to have similar p53 expression characteristics (with the exception of those lacking wild-type p53) so comparisons can be made of chromatid break characteristics within this group. There is evidence for a role for p53 in G₂ arrest (see 2.2.6) but no evidence indicating that p53 status has a direct effect on the induction of chromatid breaks. However the possible effects of transformation must be considered with direct comparison of experimental data from transformed and non-transformed cells.

2.2. Cell lines under investigation.

There are a number of human diseases characterised by defective response to DNA damaging events. A subclass of these disorders show an increase in both spontaneous and induced chromosomal breakage and include Ataxia telangiectasia (AT) (Jorgensen and Shiloh, 1996), Nijmegen breakage syndrome (NBS) (Carney *et al*, 1998), Bloom's Syndrome (Ellis *et al*, 1995), Werners Syndrome (Fukuchi *et al*, 1989), Fanconi Anaemia (Buchwald and Moustacchi, 1998; Escarceller *et al*, 1998), Down Syndrome (Sasaki and Tonomura, 1969; Porter and Paul, 1974) and Li Fraumeni Syndrome (Mitchell and Scott, 1997). All these conditions predispose individuals to different forms of cancer such as leukaemia in the case of Down Syndrome and display an elevated frequency of chromatid aberrations associated with sensitivity to radiation (Lukaszewicz *et al*, 1981; Preston, 1981; Sasaki and Tonomura, 1969; Shafik *et al*, 1988; Sanford *et al*, 1989).

Heterozygous lymphoblastoid cell lines containing mutations in the *BRCA1*, *BRCA2* or *p53* genes from families associated with familial breast cancer were investigated and the csr determined. The csr was also determined for a lymphoblastoid line derived from an individual who had been treated for sporadic breast cancer but whose genotype was wild type for all of the above genes.

2.2.1 Down Syndrome (trisomy 21)

Down Syndrome or trisomy 21 is one of the commonest congenital abnormalities known, giving rise to a wide range of developmental abnormalities including the characteristic facial expression, creased palm and heart defects. Also associated with this condition is an increased risk of developing leukaemia, estimated to be twenty times greater than for the general population (Porter and Paul, 1974). The forms of leukaemia most frequently associated with trisomy 21 are acute leukaemia (individuals are at most risk from birth to two years of age) and myeloproliferative syndrome which is clinically indistinguishable from acute non-lymphatic leukaemia or ANLL (de Alarcon *et al*, 1987). It has been postulated that the observed increase in chromosomal abnormalities and carcinogenesis associated with trisomy 21 may be due to the presence of extra chromosomal material giving rise to altered cell cycle kinetics and a delay in DNA synthesis (Porter and Paull, 1974).

The increased risk of leukaemia in trisomy 21 patients gave rise to research which investigated the increased sensitivity of their lymphocytes to ionising radiation (Lukaszewicz *et al*, 1981; Preston, 1981; Sasaki and Tonomura, 1969; Shafik *et al*, 1988). Generally it was found that trisomy 21 individuals were chromosomally more radio-sensitive to the induction of dicentric, acentric and ring aberrations, i.e. exchange aberrations which require the interaction of breaks (often on two separate chromosomes)

and that such aberrations are formed more rapidly in trisomy 21 cells due to more rapid repair increasing the probability of illegitimate rejoining (Preston, 1980). This observation was also made in trisomy 21 lymphocytes treated with bleomycin (Vijaylaxami and Evans, 1982). A decreased oxygen enhancement ratio in trisomy 21 lymphocytes has also been reported (Lukaszewicz *et al*, 1981, Kedziora *et al*, 1985), though significantly higher super oxide dismutase (SOD-1) levels prevent the formation of breaks following irradiation (Kedziora *et al*, 1985). Increased sensitivity to X-radiation and decreased repair efficiency in lymphocytes from trisomy 21 patients compared to normal patients was investigated by Countryman *et al*, (1977). They concluded that the increase in chromosomal aberrations associated with trisomy 21 was due to increased sensitivity to radiation and attenuated repair kinetics (in contrast to the conclusions of Preston, 1980). The results of Countryman *et al* suggest the probability of the interaction of two chromosome breaks forming exchange aberrations was greater in trisomy 21 lymphocytes compared with normals, the increased rejoining times allowing chromosome movement to occur leading to illegitimate rejoining. Although trisomy 21 lymphocytes were more sensitive to X-radiation damage, rejoining time of chromosome breaks in trisomy 21 (and partial trisomy 21) was reduced compared to normals. These findings could not be explained purely in terms of the classical breakage-first hypothesis, suggesting that alternative possibilities must be considered (Countryman *et al*, 1977).

One of the problems associated with using lymphocytes as a model system to study chromosomal aberrations in trisomy 21 patients is that peripheral lymphocytes are in G₀ and thus quiescent. In order to initiate cell division the lymphocytes must be treated with PHA which has an effect on cell cycle kinetics. It was found that PHA-stimulated lymphocytes from trisomy 21 patients entered S phase more quickly than those from normal patients (Leonard and Merz, 1983) and thus if the two lymphocyte populations are irradiated after a similar time post PHA-stimulation, they will not be at the same stage of the cell cycle and any results obtained will not be directly comparable. Leonard and Merz reported that normal lymphocytes irradiated eight hours after PHA

stimulation displayed frequencies of chromosomal aberrations comparable to those induced in trisomy 21 lymphocytes irradiated 30 min after PHA stimulation. When these changes in cell kinetics was taken into account, they found no difference in the frequencies of chromatid aberrations in G₂. Although these findings do not completely invalidate the observations produced by irradiating PHA-stimulated lymphocytes as described above, it does indicate that such results must be treated with caution and that cell cycle effects should be considered.

Investigations into formation of radiation-induced breaks and aberrations in transformed fibroblasts avoids the problem of differing cell cycle kinetics since these are an asynchronously dividing cell population. Studies of irradiated fibroblasts found no difference between the frequency of chromosome aberration formation in trisomy 21 and normals (Steiner and Woods, 1982, Leonard and Merz, 1997), however Kedziora *et al*, (1985) reported a decreased frequency in DNA single strand breaks in trisomy 21 fibroblasts following gamma-irradiation. It is possible that any sensitivity to irradiation or increased frequency in aberration formation may be tissue specific, which could account for the increased risk of leukaemias but not of any other forms of cancer.

In this investigation asynchronously dividing lymphoblastoid cell lines were used to determine the colour switch ratio for trisomy 21. This avoided the need for PHA stimulation and hence differing cell cycle kinetics when compared to normal lymphoblastoid cell lines.

2.2.2 Bloom Syndrome

Bloom Syndrome is one of six known syndromes caused by mutations in helicases, others include Xeroderma pigmentosa, Cockayne's syndrome, Werner's syndrome (Fukuchi *et al*, 1989; Shen and Loeb, 2000). Clinical characteristics include small size,

immunodeficiency and sun-sensitive erythema. This syndrome is also associated with an increased predisposition to cancer, in particular childhood leukaemias (Shen and Loeb, 2000) compared to the normal population, but the whole spectrum of cancers arising in Bloom Syndrome patients differs from that expected in the general population. The defective gene has been mapped to chromosome 15q 26.1 (McDaniels and Shultz, 1992) and is a member of the human equivalent of the RecQ helicase subfamily (Ellis *et al* , 1995), important in maintenance of genomic stability. RecQ is a bacterial gene the product of which has DNA-dependent ATPase and helicase activities and has the ability to translocate on single-stranded DNA in 3' to 5' direction. RecQ is associated with the RecF pathway for homologous recombination and may have a role in suppression of illegitimate recombination. RecQ homologues are proposed to have a role in recombination-mediated gap repair following replication fork stalling (Shen and Loeb, 2000).

A large number of helicase genes have been identified, 41 in *Saccharomyces cerevisiae*, 31 in humans. Most of those identified conform to the standard definition of a helicase, i.e. the ability to catalyse unwinding on duplex DNA or RNA, though not all share the defining 7 amino acid motif set in a region of 300-500 residues. Although each helicase has a subtly different target and capability as to the number of base pairs it is able to unwind, generally all have a greater affinity for single-stranded DNA than double-stranded DNA.

Bloom syndrome is characterised by increased chromosomal breakage best visualised by very high numbers of sister chromatid exchanges (SCE), a phenomenon associated with hyper-recombination. A diagnostic feature of this condition is the high frequency of exchanges between homologous chromosomes. This gives rise to an increased rate of spontaneous mutations though rates of repair are normal (as they are in Werner's Syndrome) (Ellis, 1997). DNA replication is also disturbed in Bloom Syndrome cells (Liao *et al*, 2000) where problems arise in resolving specific DNA structures generated

during replication as would be expected of a mutant in a RecQ functional homologue and the observed increase in SCEs may be visual evidence of the activation of repair processes resulting from abrogated activity of enzymes associated with replication such as topoisomerase II and DNA ligase (Runger and Kraemer, 1989). The rate of DNA chain elongation is also slowed (Gianelli *et al*, 1977; Hand and German, 1975) and cells display an abnormal distribution of replication intermediates (Lonn, 1990). Heartlein *et al*, (1987) showed that BrdU-dependent increased sister chromatid exchange (SCE) frequency in Bloom Syndrome fibroblasts was due to the ability of BrdU to inhibit topoisomerase II and this inhibition was greater in Bloom Syndrome cells than normals. This suggests that Bloom Syndrome cells have an impaired ability to resolve difficulties arising during DNA replication. Murine models of Bloom Syndrome have recently been developed (Chester *et al*, 1998), it was found that murine embryos display developmental delay, excessive apoptosis and micronucleus formation in red blood cells leading to severe anemia, dying by embryonic day 13.5.

2.2.3 Omenn Syndrome

Recombination activating gene (*RAG*) genes have been highly conserved throughout evolution and possibly originated from a bacterial mobile genetic element that was inserted into the vertebrate genome 450 million years ago (McBlane *et al*, 1995; Yu *et al*, 1999a).

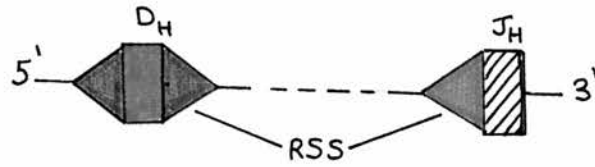
Omenn Syndrome arises due to mutations in either of the *RAG* genes, *RAG1* or *RAG2* which play an integral role in the VDJ recombination process giving rise to B and T lymphocyte receptor diversity as part of the vertebrate adaptive immune response (Bogue and Roth, 1996; Ramsden *et al*, 1997; Grawunder *et al*, 1998; Oettinger *et al*, 1990). This mechanism is shown diagrammatically in Figure 2.1. Patients with Omenn Syndrome have similar but less severe clinical features than human SCID where a

complete block of VDJ recombination occurs (Loechelt *et al*, 1995; Notarangelo *et al*, 1999), whereas Omenn Syndrome causes only a partial VDJ recombinational block. Clinical symptoms include generalised erythrodermia, failure to thrive, protracted diarrhoea, and lymphadenopathy (Notarangelo *et al*, 1999). Also there is a lack of circulating B cells (but elevated IgE) and a variable number of functionally impaired T cells with a skewed Th2 phenotype (Villa *et al*, 1998; Brooks *et al*, 1999).

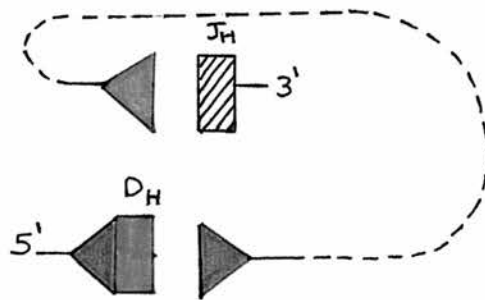
The V (variable), D (diversity) and J (joining) segments brought together during VDJ recombination are flanked by heptamer and nonamer RSS (recombination signalling sequences) elements which are recognised by the RAG gene products, the RAG protein interacting with the heptamer region, though both sequences are necessary for subsequent cleavage and dsb formation (Van Gent *et al*, 1996). Both a 12-RSS and a 23-RSS are required for the DNA to be recognised and cut by the RAG gene products, the correct recognition of these sequences ensures that the correct gene sequences are brought together in the appropriate order for production of a functional gene complex. The process requires two initiating steps (see Figure 2.1); a single strand cut at the 5' signal heptamer. The 3' end of this nick is then coupled to the phosphate in the opposite strand to create a coding end with a hairpin structure and a blunt 5' phosphorylated signal end, with RAG1 and RAG2 being required for both steps (McBlane *et al*, 1995). This hairpin structure can be opened by RAG or MRE11, enabling nucleotides to be added to the coding region via action of TdT. Finally the coding ends are joined (the VDJ recombination step), a process mediated by several proteins associated with dsb repair, such as XRCC4, ligase IV (Li *et al*, 1995; Critchlow *et al*, 1997; Kabotyanski *et al*, 1998; Bryans *et al*, 1999) and the DNA-PK complex (Jeggo *et al*, 1995; Jeggo, 1997; Lieber *et al*, 1997b). Regulation of expression of both *RAG* genes is controlled by genetic elements on the 5' side of the *RAG2* gene, this may be achieved by looping of the DNA to enable elements in this region to interact simultaneously with both *RAG1* and *RAG2* promoters (Yu *et al*, 1999). Additional restrictions on V(D)J recombination have also

The mechanism of VDJ recombination can be broken down into:

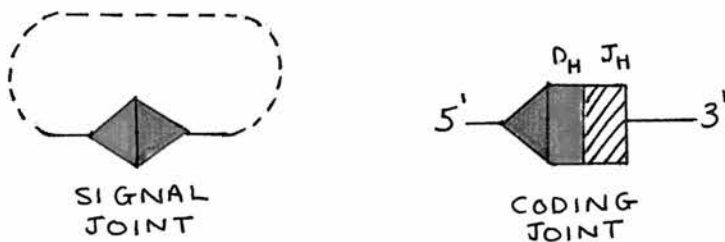
(i) Recognition of recombination signalling sequences (RSS) by RAG-1 is followed by synapsis, where the two signal sequences and adjacent coding sequences are brought into close proximity. (D_H = Diversity heavy chain segment; J_H = Joining heavy chain segment).



(ii) Cleavage then occurs at the junction of the signal and coding sequence.



(iii) Nucleotides are trimmed from the coding sequence. There may be an addition of up to 15 nucleotides (N nucleotides) at the cut ends of the V , D and J coding sequences of the heavy chain.



(iv) Repair and ligation of the coding and signal sequences.

Figure 2.1. Simplified mechanism of V(D)J recombination. Adapted from Kuby (1991).

been found in mouse embryonic stem cells with a modified T cell receptor (TCR) β locus in addition to the 12-23 rule restrictions already described (Bassing *et al*, 2000).

2.2.4 Ataxia telangiectasia , Ataxia telangiectasia-like Disorder and Nijmegen Breakage Syndrome .

Ataxia telangiectasia , Ataxia telangiectasia-like Disorder and Nijmegen Breakage Syndrome were once all thought to be variants of Ataxia telangiectasia (AT) a genetic disorder first described in 1926 by Syllaba and Henner. Subsequently those individuals displaying variations on the typical clinical and cellular presentation of AT were found to have Nijmegen Breakage Syndrome (NBS) (Shiloh, 1997), or more recently Ataxia telangiectasia-like disorder (ATLD) (Jongmans *et al*, 1997; Stewart *et al* , 1999). All three disorders share phenotypic characteristics including a radiosensitivity, radioresistant DNA synthesis and predisposition to tumourgenesis as well as other similarities in clinical presentation. The aberrant proteins associated with these conditions are part of a complex network of gene products whose interactions via site-specific phosphorylation events are triggered by ATM, to instigate repair of dsb and regulate cellular proliferation, thereby maintaining genomic integrity (Lavin *et al*, 1999; Wang, 2000). The functional interaction between ATM and NBS gene products has recently been demonstrated (Gatei *et al*, 2000b; Wu *et al*, 2000; Zhao *et al*, 2000). The three conditions will be considered separately with respect to phenotype and the genes which are thought to carry the critical mutations.

2.2.4.1 Ataxia telangiectasia

AT (reviewed Jorgensen and Shiloh, 1996, Lavin and Khanna, 1999a, Shiloh, 1997) is a multi-system disorder which occurs at a world-wide frequency of approximately 1 in

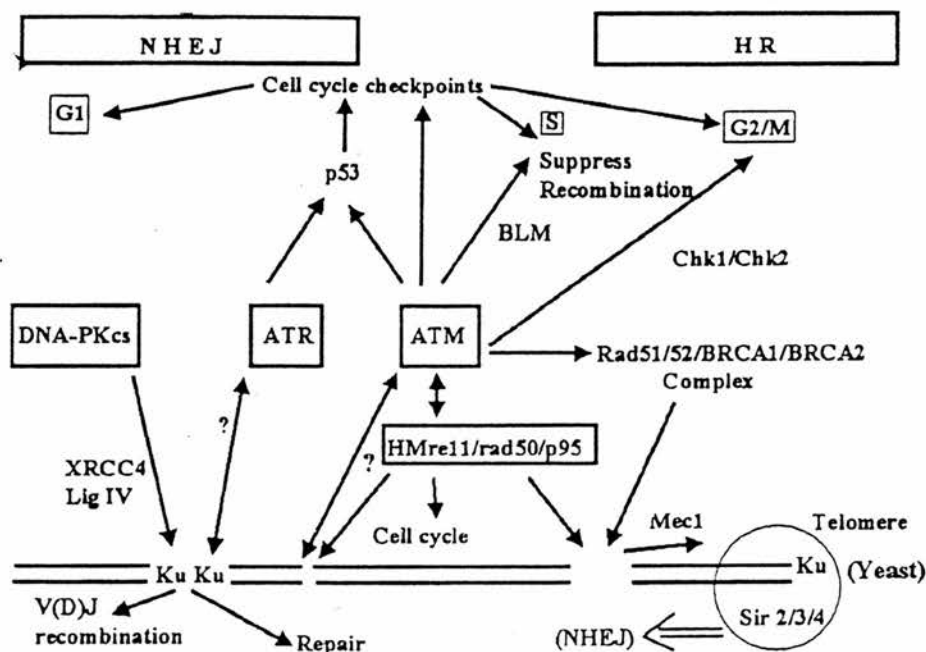


Figure 2.2(a) Interactions of ATM, ATR and DNA-PK in DNA damage recognition and repair pathways. (from Lavin *et al* 1999).
 NHEJ = non-homologous end joining, HR = homologous recombination.

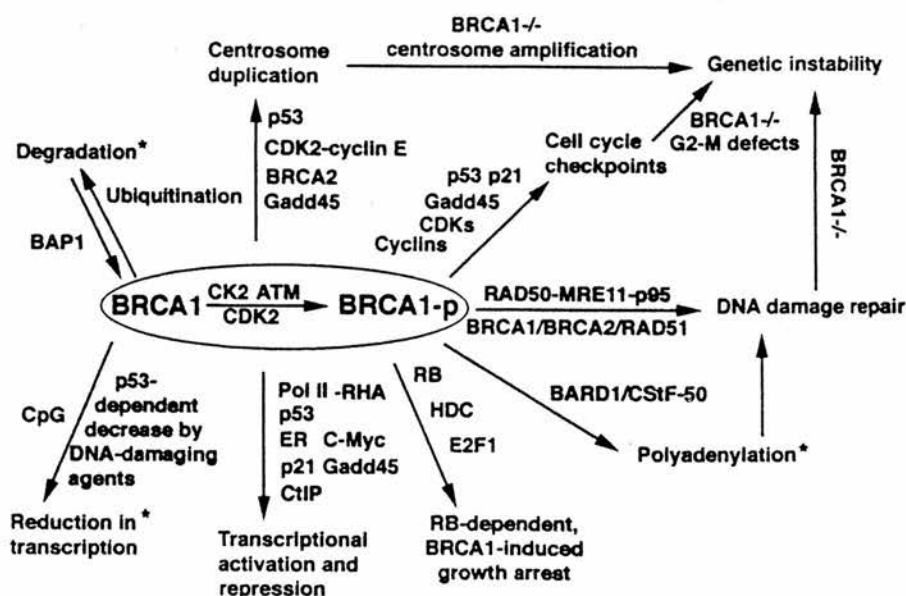


Figure 2.2(b) Diagram of the known and possible functions of Brca1 in various biological pathways (from Deng and Brodie 2000).

100,000 though a higher incidence is found in Turkey, Italy and among Moroccan Jews (Jorgensen and Shiloh, 1996). First noticed in sufferers when they are toddlers, an unsteady gait is developed (ataxia) followed by progressive neural motor degeneration and the appearance of dilated blood vessels in the conjunctivae and the face (telangiectasia). Severe immunodeficiency, growth retardation and high levels of alpha-foetoprotein are also seen. Symptoms at the cellular level include impaired ability to recognise DNA damage, absence of cell cycle arrest at the G₁ checkpoint and a shorter delay period at the G₂/M checkpoint than observed in normal cells. Clinical presentations include radiosensitivity (Thacker, 1989) and cancer predisposition (Scott, 1994) including early-onset cancer generally resulting in the death of the patient during their twenties or early thirties (Savitsky *et al*, 1995).

The *ATM* gene was localised to chromosome 11q.22.23 (Gatti *et al*, 1988) and later cloned (Savitsky *et al*, 1995). *ATM* is one of a family of genes in the PI-3 kinase superfamily, which also includes the *ATM* and *RAD3* related (*ATR*) protein kinase in vertebrates and *MEC1* and *RAD3* in yeast (Ventikaraman *et al*, 1999). The interactions of *ATM* and *ATR* gene products in DNA damage recognition pathways are shown in Figure 2.2(a). *ATM* sufferers have one of a variety of mutations including truncation of the *ATM* gene leading to absent, truncated or unstable gene products (Lakin *et al*, 1996). A correlation between the amount of *ATM* protein present in cells and the extent of radiosensitivity has been proposed (Lavin and Khanna, 1999a) and also with the extent of apoptosis in the nervous system in a mouse embryonic model system (Lee *et al*, 2000). The *ATM* protein is 350.6 kDa but being highly phosphorylated is closer to 370 kDa (Chen and Lee, 1996). The gene contains a CT domain typical of the PI3 kinase super family (Zakain, 1995, Lavin *et al*, 1995) and is associated with the radiosensitivity and radioresistant DNA synthesis and radiation-induced chromosomal breakage observed in *ATM* cells (Morgan *et al*, 1997). A high level of residual chromosomal breakage has been demonstrated in *ATM* cells using premature chromosome condensation (PCC) (Cornforth and Bedford, 1985) suggesting a possible correlation between radiosensitivity and elevated frequency of

chromosome aberrations. Repair of dsb in ATM cells is considered to be normal (Lehmann and Stevens, 1997), however dsb rejoining has also been found to be slower in ATM cells (Coquerelle *et al*, 1987). Other research has found that dsb repair is faster than normal cells over the first 16 hours and then was slower, leaving approximately 10% of dsb unrepaired 72 hours post-irradiation (Foray *et al*, 1997). A higher rate of conversion of dsb into chromosome breaks has also been observed in ATM cells (Mozdarani and Bryant, 1987,1989; Liu and Bryant, 1994; Pandita and Hittelman, 1992).

ATM (NBS and ATLD) cells show a reduced p53 response when subjected to DNA damaging events (Banin *et al*, 1998; Nakamura, 1998; Kastan *et al*, 1992; Khanna and Lavin, 1993) caused by ATM interacting with p53 in both the N and C terminal domain (Khanna *et al*, 1998). ATM undergoes autophosphorylation before phosphorylating p53 on Serine 15 and 20, both activating and stabilising p53 by preventing its degradation via MDM2. There is some disagreement as to whether phosphorylation of serine 15 or serine 20 (Lambert *et al*, 1998) acts to stabilise p53. Dephosphorylation of p53 at Serine 376 in the C terminal domain has also been shown to be ATM-dependent (Waterman *et al*, 1998), leading to an association with 14-3-3 proteins which possess sequence specific affinity for DNA. ATM cells are defective in these p53 interactions, though ATR has been shown to phosphorylate serine 15 following irradiation (Tibbetts *et al*, 1999) providing an explanation for the observation that the p53 response and hence the activity of all genes downstream of p53 such as p21 and Gadd45 is reduced but not abolished in ATM cells. ATM cells also show delayed MRE11/RAD50/p95 (nibrin) complex formation and nuclear localisation (Maser *et al*, 1997; Nelms *et al*, 1998). ATM also activates the c-abl non-receptor tyrosine kinase (reviewed in Van Etten 1999) by phosphorylating it at serine 465 in response to ionising radiation and other DNA damaging events (Baskaran *et al*, 1997) in the SH3 domain of c-abl (Shafman *et al*, 1997). The activated c-abl is then able to phosphorylate several nuclear substrates including DNAPK_{CS} (Kharbanda *et al*, 1997), RAD 51 (Yuan *et al*, 1997) and the stress-activated response associated with SAPK/JNK and p38 kinase (Lee *et al*, 1998). Activated c-abl is

also involved in damage induced apoptosis by acting to downregulate Cdk2 and G₁/S checkpoint arrest via a p53-dependent pathway (Yuan *et al*, 1997). p53-deficient cells were also shown to undergo apoptosis due to expression of c-abl, possibly by phosphorylating the p53 analogue p73, which has been found to induce apoptosis in response to cisplatin (Gong *et al*, 1999) in the absence of p53 (Agami *et al*, 1999). Exposure to ionising radiation appears to enhance the binding of p73 and the SH3 domain of c-abl. The ATM-dependent activation of the I-kappa B kinase in response to dsb formation proceeds independently of both c-abl and DNA-PK (Li *et al*, 2001).

ATM has been shown to perform a more general role in the activation of cytoplasmic signalling cascades in keeping with the pleiotropic effects of *ATM* mutation. The ATM protein is located both in the nucleus and in vesicles in the cytoplasm (Lim *et al*, 1998) and is directly involved in Ca²⁺ release from intracellular calcium stores in response to mitogenic stimuli (Famulski and Petterson, 1999) and ionising radiation which leads to the activation of intracellular signalling cascades via activation of tyrosine kinases (Khanna *et al*, 1997; Yan *et al*, 2000).

The 5' end of the *ATM* gene is close to the nuclear protein mapped to the AT locus (*NPAT*) gene and may share a bi-directional promoter (Chen *et al*, 1997; Imai *et al*, 1996). The *NPAT* gene product is a substrate for cyclin E-cdk2 and NPAT protein levels peak at the G₁/S boundary, excess amounts of this protein accelerate S phase entry (Chen *et al*, 1998b; Zhao *et al*, 1998). As *ATM*, when activated by radiation, inhibits the cyclin E-cdk2 via a p53 pathway, it has been suggested that ATM and NPAT proteins may co-ordinate the regulation G₁/S transition (Lavin and Khanna 1999b). Interestingly, *DNA-PKcs* is also expressed utilising a bi-directional promoter shared with *cdc21(MCML)* which is required for the early stages of replication in *Saccharomyces pombe* (Landenburger *et al*, 1997; Saito *et al*, 1998), again raising the possibility of co-ordinated regulation of proteins involved in DNA damage recognition and cell cycle control (Lavin and Khanna 1999b). *ATM* and *DNA-PKcs* contain few other recognisable domains which interact with other

proteins, the *ATM* gene contains a leucine zipper motif which suggests possible dimerisation (Jorgensen and Shiloh 1996). Those genes which show homology to *ATM* (*DNA-PK_{CS}*, *FRAP*, *FRP/ATR*) give rise to proteins which all act as signal transducers to downstream proteins associated with genomic stability such as cell cycle regulation, DNA repair or recombination (Jorgensen and Shiloh 1996).

Radioresistant DNA synthesis is seen in ATM cells, due an inability to inhibit cyclin A-cdk2 and cyclin B-cdc2/cdk1. ATM cells do not display an increase in cdk-associated p21, leading to a reduced delay at G₂/M compared to normal cells post-irradiation. The G₂ cell cycle restriction point is dependent on phosphorylation of Chk2 by ATM (Matsuoka *et al*, 2000; Chaturvedi *et al*, 1999). Chk2 is the mammalian homologue of the budding yeast protein RAD53 and the fusion yeast protein cds1 checkpoint kinases. Chk2 undergoes ATM-dependent phosphorylation in response to ionisation radiation-induced (but not UV-induced) damage (Matsuoka *et al*, 2000) and maintains cyclin B in an inactive phosphorylated form to maintain G₂ arrest.

ATM also has a role in meiosis; foci of ATM and ATR protein are observed at or adjacent to chiasmata (Keegan *et al*, 1996) and the gonads of AT sufferers fail to develop and mature (Xu and Baltimore 1996). Further evidence for the multi-functional nature of ATM within the cell is the recent demonstration that BRCA1 is also ATM-dependent in its response to dsb (Cortez *et al*, 1999). It has independently been shown *BRCA1* expression is diminished in ATM cells (Venkitaraman 1999). An ATM/BRCA1 complex is formed as described below in section 2.2.5

2.2.4.2 Ataxia Telangiectasia-like disorder

Recently, families have been identified which have many of the clinical features associated with ATM but lack ocular telangiectasia, this syndrome has been termed Ataxia Telangiectasia-like disorder or ATLD. It is estimated that approximately 6% of all

patients diagnosed with ATM actually have ATLD. The members of these families have wild type ATM protein but were found to possess a mutation in the *MRE11* gene leading to total loss or decreased levels of MRE11 gene product depending on the severity of the mutation present (Stewart *et al*, 1999). Although the mutant MRE11, where present, still retains a limited ability to interact with RAD50 and Nbs1 (also called p95 or nibrin), it was not possible to induce MRE11/RAD50/p95 nuclear foci following irradiation of cells. RAD50 and MRE11 have also been shown to localise in rodent spermatocyte nuclei, indicating a role in meiotic recombination events (Eijpe *et al*, 2000). The ability of ATLD cells to activate the S phase checkpoint is intermediate between the low or absent activation response observed in ATM/NBS cells and normal control cell response. However, unlike ATM, ATLD and NBS cells are able to activate the c-abl-mediated SAPKs (stress-activated protein kinases) (Shafman *et al*, 1995) also called JNKs (c-Jun N terminal kinases). Like ATM the p53 response to irradiation in ATLD cells is reduced compared to normal cells (Jongmans *et al*, 1998; Stewart *et al*, 1999) even though the p53 present is wild-type, suggesting p53/AT/MRE11 interaction may be a major response to ionising radiation damage, but other p53-independent response pathways are also active. The interactions of the MRE11/RAD50/p95 complex will be discussed more fully below.

2.2.4.3 Nijmegen Breakage Syndrome

Nijmegen Breakage Syndrome (NBS) is a rare autosomal recessive disorder, affecting approximately 70 families worldwide, mainly in Eastern Europe (Shiloh 1997; Digweed *et al*, 1999). The similarity between ATM and NBS is striking with clinical characteristics similar to those in ATM and ATLD, including microcephaly, growth retardation, immunodeficiency and predisposition to malignancy (the risk of malignancy for NBS sufferers is 10-15% higher than for ATM patients) but without telangiectasia or ataxia. Cellular characteristics include elevated frequency of chromosome breakage, radiosensitivity, radioresistant DNA synthesis, defective cell cycle checkpoints and

reduced p53 response. NBS sufferers have a deficiency in both the cellular and humoral immune systems, with deficiencies in IgA and IgG, abnormal T cell immunity and changes in normal lymphocyte ratios. B and T cell lymphomas are common in these patients, as are rhabdosarcoma, haemoblastoma and neuroblastoma. The characteristic radiosensitivity of NBS cells is a diagnostic test for this condition as is the presence of spontaneous chromosomal instability often, as in ATM, involving chromosomes 7 and 14 (Varon *et al*, 1998) which carry the immunoglobulin and T cell receptor genes. However recent studies indicate that V(D)J recombination is normal in NBS cells, suggesting that the MRE11/RAD50/p95 complex is not involved in coding end processing in V(D)J recombination (Hafst *et al*, 2000). Also in common with ATM, compromised dsb repair has been postulated (Huo *et al*, 1994, Hanawalt and Painter, 1985; Girard *et al*, 2000) however more recently dsb repair in NBS fibroblasts was found to be very similar to wild type cells when measured by pulsed-field gel electrophoresis (Kraakman-van der Zwet, *et al*, 1999).

The NBS1 gene localised to chromosome 8q21.13-q21.3 (Varon *et al*, 1998) codes for either a 85 kDa protein (Varon *et al*, 1998) or 95 kDa protein (Carney *et al*, 1998) nibrin. The ATM gene position on chromosome 11 finally disproved the possibility that NBS and ATM were two forms of the same inherited genetic condition. The majority of patients carry a 5 bp deletion of the NBS1 gene in a critical region of less than 300 kb; all NBS patients have a truncated nibrin protein. Recent reports suggest that over 90% of NBS patients carry a homozygous premature termination mutation at codon 219, the remainder possess a variant NBS1 protein produced as a result of alternative translation (Maser *et al*, 2001). The N terminal region contains a breast cancer carboxyl terminal domain (BRCT), first described in the *BRCA1* gene and a fork-head-associated (FHA) domain, both of which are involved in protein-protein interactions. Proteins containing these domains are associated with cell cycle checkpoint, DNA replication and repair functions. All truncations occur downstream of the FHA domain near the C terminal end of the BRCT motif. The C terminal end of the NBS1 gene is required for

MRE11/RAD50/p95 complex formation (Paull and Gellert, 1999). It has been suggested that the FHA domain may be involved in mediating protein interactions specifically associated with phosphorylated serine/threonine residues, making it functionally analogous to *DUN1* and *RAD53*, protein kinases found in *Saccharomyces cerevisiae* which link the S phase checkpoint to DNA damage repair. A similar kinase, *cds1* has also been identified in *Schizosaccharomyces pombe* (Varon *et al*, 1998). Biochemical analysis, suggests however that nibrin may be the mammalian functional equivalent of *XRS-2*, part of the RAD50 complex in *S. cerevisiae* (Carney *et al*, 1998).

Nibrin or p95 is part of the hMRE11/RAD50 dsb repair complex associated with non-homologous recombination, forming nuclear foci in G₁. Alternatively some cells can form a complex including RAD51. These foci, formed in G₂, are associated with non-homologous recombination (Maser *et al*, 1997). In cells with fully functional nibrin the MRE11/RAD50/p95 complex locates to the nucleus following dsb-inducing DNA damage (not following UV irradiation) and forms ionising radiation-induced foci (IRIFs). In NBS cells containing the non-functional truncated nibrin, IRIF formation does not occur (Carney *et al*, 1998). The association of hMRE11 with dsb within 30 minutes of induction of damage and focus formation followed by a return to a more uniform nuclear distribution of the protein once dsb repair was complete (Nelms *et al*, 1998) suggests a role for nibrin as a signal, leading to IRIF formation at the site of DNA damage and bringing all necessary repair complex components to the damage site. The immune system deficiencies characteristic of NBS patients, including chromosomal rearrangements associated with chromosomes 7 and 14 indicates a role for nibrin in recombination and recombinational repair. There has been no evidence to suggest defects in the V(D)J recombination mechanism in either NBS or ATM, MRE11/RAD50/p95 foci form independently of DNA-PK_{CS} and Ku proteins (Maser *et al*, 1997) but it is possible that the MRE11/RAD50/p95 complex is involved with resolution of hairpin intermediates generated in V(D)J recombination (Carney *et al*, 1998). A recent

report indicates the V(D)J recombination proceeds normally in NBS patients (Hafst *et al*, 2000).

The critical importance of the presence of p95/nibrin association to the MRE11/RAD50/p95 complex function is demonstrated in a number of recent reports. MRE11 and RAD 50 have been shown independently to be vital for normal cell proliferation in murine embryonic stem cells (Xiao and Weaver, 1997, Luo *et al*, 1999). In *S. cerevisiae* the MRE11/RAD50/Xrs2 is associated with a range of cellular functions such as dsb repair, homologous and non-homologous endjoining, telomere maintenance and checkpoint regulation in response to dsb induction. In meiotic cells the complex is required for both creation and resection of dsb (Haber 1998). The occurrence of abnormal telomeres in both ATM and NBS patients, leading in the case of NBS to characteristic telomeric fusions of chromosomes 6 and 9 (Digweed *et al*, 1999) indicates that both proteins may be involved in telomere maintenance. Both yeast and human forms of MRE11 act as a manganese (Mn^{+})- dependent 3' to 5' exonuclease on double-stranded DNA, and also as a single-stranded endonuclease (Trujillo *et al*, 1998; Usui *et al*, 1998). MRE11 also has endonuclease activity on its own but requires the presence of RAD50 for significant levels of exonuclease activity (Paull and Gellert 1998). The C terminal domain of MRE11 is required for dsb processing in mitotic cells and dsb formation in meiotic cells by acting as the binding core of the complex as it contains a consensus amino acid sequence for the cleavage of phosphodiester bonds (Tsbouchi and Ogawa 1998). The N terminal region of the protein determines the nuclease activity (Usui *et al*, 1998). MRE11 contains a consensus amino acid sequence for cleavage of phosphodiester bonds. The ability of the MRE11/RAD50/p95 complex to perform many of its functions may depend on the way the MRE11 component of the complex binds to RAD50; MRE11 has two binding sites for RAD50 and depending on how tightly the two interact may determine if it acts as an inducer of dsb or as a nuclease. The precise role of p95 or nibrin in this complex is not yet understood, however its presence is required to enable MRE11 to become hyperphosphorylated in a cell cycle-dependent manner and in

response to gamma-irradiation. This hyperphosphorylation step is a necessary precursor to IRIF formation. Nibrin or p95 may have a role in recruiting kinases to the complex, though possibly not the ATM kinase (Dong *et al*, 1999). Paull and Gellert (1999) demonstrated that the MRE11/RAD50/p95 complex is able to partially unwind the DNA duplex and cleave fully paired hairpins both activities requiring ATP and p95 to be present to proceed. ATP controls a switch in nuclease specificity that enables the complex to cleave either single or double stranded DNA. RAD 50 is required to bind ATP to the complex but ATP-dependent cleavage and duplex unwinding do not proceed in the absence of p95 as p95 acts to stabilise the DNA-MRE11/RAD50/p95 complex association. Interestingly, it also appears that Ku acts competitively with MRE11/RAD50/p95 complex to bind to DNA overhangs and thus effectively regulates complex activity. Although much of the work investigating the role of the MRE11/RAD50/Xrs2(p95) is in yeast systems, there is a growing body of evidence to suggest that the mechanisms of repair in all eukaryotic systems are very similar; dsb are repaired by both homologous and non-homologous recombination in both yeast and human cells (Kramer *et al*, 1994; Dolganov *et al*, 1996; Moore and Haber, 1996).

NBS cells have an impaired p53 response which is similar though less severe than that found in ATM (Jongmans *et al*, 1997; Matsuura *et al*, 1998; Antoccia *et al*, 1999). On exposure to gamma-irradiation, NBS cells accumulate p53 in a dose dependent manner, p53 levels reaching a maximum at 2 hours post-irradiation. This maximum value was however lower than that observed in normal cells, with the resultant decreased levels of p21 and other gene products dependent on p53 for transcriptional regulation (Matsuura *et al*, 1998). However the timescale of p53 induction in both normal and NBS cells is the same, in contrast to ATM where there is a two hour delay in p53 induction compared to normal cells. This suggests that p95/nibrin and ATM may be components of several pathways, and may act in either the same pathway or independently of each other (Matsuura *et al*, 1998). A functional link between ATM and the NBS/MRE11/RAD50 complex has been established; exposure to ionising radiation leads to the ATM-

dependent phosphorylation of serines 343 (Lim *et al*, 2000), 278 and 343 (Zhao *et al*, 2000) on the NBS protein. However investigations by Wu *et al*, (2000) found that serines 343, 397, 432, 509 and 604 in NBS are all phosphorylated in non-irradiated cells but the degree of phosphorylation is increased at these sites following radiation exposure. The loss of ATM -dependent phosphorylation of NBS at serines 278, 343, 397 and 615 (Gatei *et al*, 2000b; Lim *et al*, 2000, Wu *et al*, 2000; Zhao *et al*, 2000) has differing effects on the function of the protein; loss of serine 343 leads to inhibition of DNA synthesis (Lim *et al*, 2000; Zhao *et al*, 2000) though loss of any one of the serines above partially abrogate the ability of cells to survive exposure to radiation (Wu *et al*, 2000; Zhao *et al*, 2000).

2.2.5 BRCA1 and BRCA2

The *BRCA1* and *BRCA2* genes code for large nuclear proteins (1863 and 3418 amino acids respectively) which reach a peak level within the cell in S phase. The *BRCA1* gene on chromosome 17 contains several functional domains that interact directly or indirectly with a wide range of proteins in many biological pathways including tumour suppressors, oncogenes, repair pathways, and transcriptional regulators (for review see Deng and Brodie, 2000). This makes *BRCA1* important in cell cycle progression, growth, apoptosis, and chromatin remodelling (Bochar *et al*, 2000). These interactions are summarised in Figure 2.2(b). The *BRCA2* gene is located on chromosome 13 (Zhang *et al*, 1998).

Individuals which are heterozygous for a mutation in either gene have a predisposition to breast and ovarian cancer. Five to ten percent of all breast cancer patients carry a *BRCA1* mutation, whereas a *BRCA2* mutation, found in 45% of familial breast cancers (Wooster *et al*, 1994; Milner *et al*, 1997) is associated with male breast cancer and pancreatic cancer (Ludwig *et al*, 1996). Mutations in both *BRCA1* and *BRCA2* increase the cancer risk by 15-20 times (Zhang *et al*, 1998). Both *BRCA1* and *BRCA2* can be considered to be classic tumour suppressor genes - the loss of both alleles is necessary for cancer to occur. Individuals which are homozygous mutants for *BRCA1* display a phenotype

which includes defective cell division, chromosomal instability and hypersensitivity to genotoxins (Venkitaraman, 1999), disease characteristics similar to those of ATM sufferers. BRCA1 has been shown to form a nuclear complex with the ATM protein following gamma-irradiation, leading to phosphorylation of BRCA1 on clusters of serine/glutamine residues in the C terminal domain of BRCA1 (aas 1280-1524) containing the cdk2 phosphorylation site (Ruffner *et al*, 1999). The phosphorylation of serine 1423 and serine 1524 appear to be of particular importance. Interestingly, the ATM-dependent phosphorylation of BRCA1 is only induced following gamma-irradiation, otherwise phosphorylation is ATM-independent (Scully *et al*, 1997). This raises the possibility that BRCA1 has a signalling function in response to ionising radiation-induced dsb. BRCA1 can also be phosphorylated by ATR and possibly other kinases, suggesting that it is involved in a number of signalling pathways in response to damage. BRCA1 and BRCA2 interact with each other via both their N and C terminal domains; BRCA1 has a N terminal ring finger domain, both BRCA1 and BRCA2 have C terminal transactivating domains, though the extent of interaction is not yet fully elucidated. The BRCT (BRCA 1-C - terminal) domain is found in many DNA damage repair and cell cycle checkpoint proteins. The BRCT domain superfamily contains a functionally diverse set of proteins found in animals, plants and bacteria (for review see Huyton *et al*, 2000) and include the repair proteins XRCC1 and DNA ligases I and IV. Functional loss of this domain is associated with predisposition to breast cancer.

Both BRCA1 and BRCA2 are known to associate with RAD51 in both mitotic and meiotic cells (Scully *et al*, 1997, Bhattacharyya *et al*, 2000), mice with mutant *BRCA1* display defective G₂/M checkpoint control, genetic instability and reduced homologous recombination. The BRCA1 - RAD51 interaction is evolutionarily conserved and is possibly a selection target due to its role in maintaining genomic integrity (Huttly *et al*, 2000). BRCA1 has also been shown to associate with RAD50, part of the hRAD50/MRE11/p95 (nibrin) complex (Zhong *et al*, 1999). BRCA1 co-precipitates maximally with RAD50 in late S and G₂ when BRCA1 phosphorylation is also maximal,

via the N terminal of RAD50, suggesting the involvement of BRCA1 in DNA recombination. The BRCA1/RAD50 complex is not formed in response to DNA damage, but the complex is relocated to the nucleus indicating a possible damage-sensing function for BRCA1. Unlike BRCA1, BRCA2 has been shown to associate with RAD51 but not RAD 50. Studies of mouse cell models homozygous mutant for BRCA2 display similar characteristics to RAD51 mutant cell lines: occurrence of large numbers of chromatid breaks, triradials, quadriradials and elevated p53/p21 levels. This suggests BRCA2 may have a role in chromosomal segregation and possibly repair (Connor *et al*, 1997; Patel *et al*, 1997). BRCA2 is phosphorylated by hBubR1, a human homologue of one of a group of yeast proteins (bub1-3, Mad1-3 and Msp1) which regulate chromosome stability and segregation (Paulovich *et al*, 1997). Once phosphorylated BRCA2 is then able to fulfill its role in the G₂/M checkpoint (Futamura *et al*, 2000). Further evidence in favour of the role of BRCA2 as a tumour suppressor is provided by the occurrence of constitutive translocations and other gross chromosomal abnormalities in BRCA2-deficient cells, this provides a possible mechanism for the observed cancer predisposition in BRCA2 homozygous mutants, together with evidence that loss of RAD51 foci which are required for homology-directed repair (Yu *et al*, 2000).

The hypothesis that BRCA1 may activate repair mechanisms via homologous recombination in co-operation with BRCA2, mRAD51 and other components of the RAD52 epistasis group is supported indirectly by evidence of association of both BRCA1 and BRCA2 with mRAD 51 (Sharan *et al*, 1997; Banin *et al*, 1998; Tibbetts *et al*, 1999; Lakin *et al*, 1999) and by defective mitotic recombination in murine cells with defective BRCA1 and BRCA2. More direct evidence comes from a reduction in frequency of recombination between homologous DNA substrates inserted into the genome of BRCA1-deficient cells (Moynahan *et al*, 1997). BRCA1 and BRCA2 may have a role in G₂/M checkpoint control, BRCA1 has been shown to co-precipitate with RNA polymerase II holoenzyme and certain BRCA1 domains can induce transcription of GADD45, which mediates apoptosis and other similar genes (Chapman and Verma,

1996). Although there are similarities in the cellular location and function of BRCA1 and BRCA2; both co-localise to the nucleus of somatic cells and to synaptonemal complexes in meiotic cells (Chen *et al*, 1998b). However differences have also been reported: BRCA2 binds to mRAD51 with a higher stoichiometry through the BRC repeat region in exon 11 and the CT domain (Sharan *et al*, 1997; Wong *et al*, 1997; Scully *et al*, 1997b; Mitzuta *et al*, 1997; Chen *et al*, 1998a) and is thought to be necessary for radiation-induced assembly of RAD51 complexes (Yuan *et al*, 1998). Mutation in BRCA1 leads to a greater disruption of cell cycle checkpoints than mutations in BRCA2. It has been postulated that BRCA1 may link the repair functions of BRCA2 to damage signalling pathways via its interaction with ATM (Venkitaraman, 1999). In this investigation the type and frequency of chromatid breaks occurring in heterozygous BRCA1 and BRCA2 lymphoblastoid cell lines will be compared to normal lymphoblastoid cell lines to determine whether there is a significant difference in their response to ionising radiation.

2.2.6 p53

Since the discovery that p53 is mutated in 50% of all tumours, either due to the absence of a wild type allele or due to an alteration in the function of the p53 protein (Hollstein *et al*, 1991), p53 has been the subject of a great deal of research. p53 is a tumour suppressor gene, able to activate transcription of a large number of genes involved in cell cycle regulation, induction of apoptosis and maintenance of genomic stability (Kaelin, 1999; Carnero *et al*, 2000; Gao *et al*, 2000). Most p53 mutations found in cancers are stable missense mutations. Wild type p53 is stabilised in response to DNA damage and activates the G₁/S checkpoint by activating transcription of p21, CIP1 (cdk interacting protein 1) and 14-3-3 which inhibits Cdc25 to block the cell cycle at the G₂/M checkpoint.

p53 is one member of a larger gene family including p73 and p51 (Kaelin, 1999; Lohrum and Vousden, 2000). All three genes are found on different chromosomes, but the less well known homologues are not generally found mutated in cancers, p73-deficient mice were not found to acquire spontaneous tumours (Yang *et al*, 2000) although it has been suggested that there may be a subtle interaction between p53 and p73 and/or p51 in the cellular transformation pathway in the presence of mutant p53 (Marin *et al*, 2000).

p53 is generally a short-lived protein within the cell, being targeted for ubiquitin-mediated degradation by MDM2. Patients with sarcomas either lack a wild type p53 allele or they possess amplified copies of MDM2 (Oliner *et al*, 1992, 1993; Leach *et al*, 1993). The interaction of MDM2 and p53 may be modulated by p14^{ARF} (also known as p19^{ARF}), which is critical to the ability of p53 to respond to oncogenic stimuli. Both p14^{ARF} and p16^{INK4A} are cdk inhibitors found at the same locus and are mutated, deleted or hypermethylated in many types of cancer (Carnero *et al*, 2000). Both appear to have a role in control of cell cycle and immortality, p16^{INK4A} is thought to regulate Rb, the tumour suppressor gene product by downregulation of proteins that inhibit Rb activity (Lloyd *et al*, 2000), p19^{ARF} activates and stabilises p53 via interaction with MDM2 (Carnero *et al*, 2000). Both p19^{ARF} and p16^{INK4A} accumulate in ageing cells and may act as a form of tumour suppressor limiting the lifespan of cells.

p53 is phosphorylated by ATM following exposure to ionising radiation to activate the G₁ checkpoint and/or activate apoptotic pathways (Bell *et al*, 1999). Yeast studies have also implicated p53 in activation of the G₂ checkpoint (Weinert and Hartwell, 1988) and studies of *Saccharomyces pombe* have shown that p53-dependent activation of Chk1 and Cds1 kinases occurs, following exposure to ionising radiation and that this step is dependent on the presence of the yeast ATM homologue RAD3. Human homologues of these yeast G₂ checkpoint genes are hChk1 and Chk2. Chk1 has a G₂ checkpoint function in *Saccharomyces cerevisiae* on exposure of cells to radiation (Sanchez *et al*, 1999). Chk1 and RAD3 act together to control progression of cells through mitosis. Chk1

prevents entry into mitosis by phosphorylating Cdc25C at serine 216 leading to its cytoplasmic sequestration by 14-3-3 proteins, hence blocking entry into mitosis by preventing Cdc25C from activating Cdc2 (Peng *et al*, 1997). It also regulates the abundance of Pds1, an anaphase inhibitor while RAD3 acts via Cdc5 to prevent degradation of Pds1 and thus prevents the cell from completing mitosis. p53-activated 14-3-3 also sequesters Cdc2-cyclinB1, further supporting the position of p53 as playing a key role in G₂ checkpoint function (Chan *et al*, 1999). *hChk2*, together with *Brca1*, *Brca2* and *APC* are tumour suppressor genes which act at the G₂ checkpoint unlike other tumour suppressor genes, such as *p53* and *Rb* which act principally at the G₁ cell cycle checkpoint (Bell *et al*, 1999). *hChk2*, a homologue of the yeast proteins Cds1 and RAD3 is phosphorylated in an ATM-dependent manner in response to DNA damage and can itself phosphorylate serine 216 of Cdc25. It may represent an intermediate phosphorylation step in p53/ATM interaction. Mouse embryonic stem cells deficient in *Chk2* did not undergo G₂ arrest following exposure to gamma radiation and were also resistant to damage-induced apoptosis. They were also found to be defective in p53 stabilisation, leading to a reduction in transcription of p53-dependent genes such as p21. *Chk2* is able to phosphorylate p53 on serine 20 to prevent its interaction with MDM2 and thus avoid MDM2-mediated ubiquitination (Hirao *et al*, 2000). The correlation of inactivation of *Chk2* with the relatively rare Li Fraumeni Syndrome- associated group of cancers (Bell *et al*, 1999) suggests that inactivation or disruption of different cell cycle checkpoints may ultimately give rise to a differing spectrum of cancer endpoints.

p53 has recently been found to perform a more direct role in DNA repair (Lozano and Elledge, 2000). A p53-regulated gene *p53R2* encodes a subunit of the ribonucleotide reductase (RNR) enzyme, which catalyzes the production of dNTPs for DNA replication and repair. RNR has two subunits R1 and R2, R1 is present throughout the cell cycle while R2 is synthesised in late G₁, disappearing by late S/early G₂. *p53R2* is a p-53 inducible subunit of R2, suggesting a direct role for p53 in repair and maintenance of DNA (Tanaka *et al*, 2000). The dual loss of the *DNA-PK* and p53 genes in mouse models

suggests that p53 acts as a checkpoint regulator in early T-cell development and acts to limit the oncogenic potential of dsb generated during V(D)J recombination in pro-B cells. The high incidence of pro-B cell lymphomas in mice deficient in XRCC4 and p53 (Gao *et al*, 2000) is further evidence of the role of p53 in maintaining genomic integrity and stability and the caretaker function of the nonhomologous end-joining pathway (Guidos *et al*, 1996).

2.3 Materials and methods.

An outline of the protocol used in this investigation is shown in Figure 2.3.

2.3.1 Cell culture and BrdU treatment

Normal lymphoblastoid cell lines (codes on Tables 2.1 and 2.2) were obtained from frozen laboratory stocks and from the Cell Bank, Immunogenetics Unit, St. Mary's Hospital, Manchester. Disease lymphoblastoid cell lines investigated were 2 Bloom Syndrome (W1004 and GMB900), 2 Njimegen Breakage Syndrome (94P548 and 94P112) (from Professor Sperling), an Omenn Syndrome (OMN008), 3 homozygous Ataxia telangiectasia (ATAR, ATLG and ATPA) (from Malcolm Tylor, Birmingham) and 3 Down Syndrome (CV105, CV077 and CV712) cell lines. Cell lines derived from families associated with familial breast cancer were kindly donated by Professor Michael Steel. 2 BRCA2 heterozygous mutants (SLYN₁ and TURN₁), 2 BRCA1 heterozygous mutants (COWA₁ and LANY₁), 2 p53 mutants (ELWE₁ and PEGY₁) and a cell line from an individual who had contracted sporadic breast cancer but had no known mutations (BIAL₁)

All cell lines were grown in RPMI 1640 (Gibco BRL) + 50 IU/ml Penicillin, 50 µg/ml streptomycin (Gibco) supplemented with 2mM L-glutamine and 10% foetal calf serum (Gibco) in 25 cm³ closed vent flasks initially then transferred to 75 cm³ closed vent flasks when the cells had attained a sufficiently high density. The cells were then routinely passaged to maintain growth in a total volume of 40 ml. The cells were grown in a medium containing 33 µM 5-bromo-2'-deoxyuridine (BrdU) for two days prior to irradiation to allow the cells to incorporate the BrdU over two cell cycles. A medium containing 5 µM BrdU was used for Bloom Syndrome cells due to their sensitivity to BrdU incorporation. This concentration reduces the number of sister chromatid exchanges (SCE) per cell below the level at which there is likely to be coincidence of

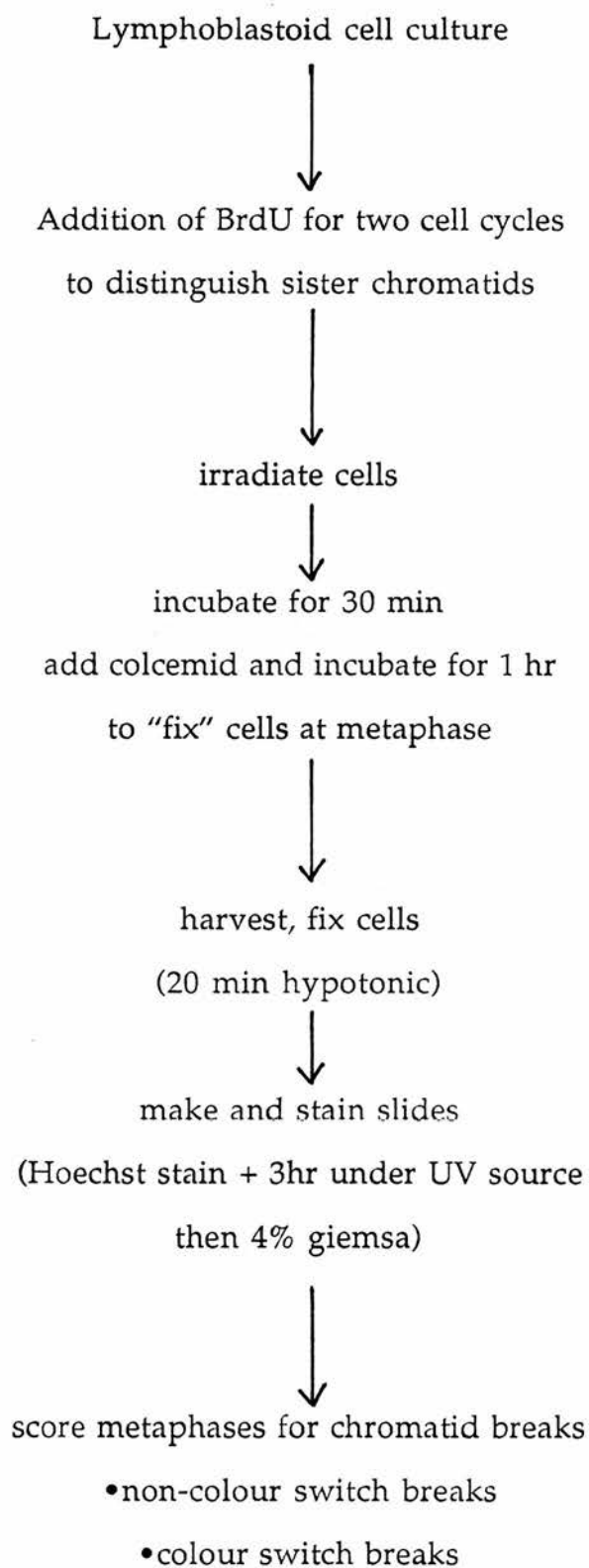


Figure 2.3 General experimental protocol.

colour switches due to BrdU incorporation and non-colour switch breaks leading to a falsely high value for colour-switch break frequency.

2.3.2. Irradiation and harvesting.

Cells were irradiated *in situ* with 0.2 Gy from a ^{137}Cs gamma source (CIS Biointernational IBL437C gamma-irradiator) at a dose rate of 7.7 cGysec^{-1} . The flasks were returned to the incubator for 30 min following irradiation before treatment with $0.1 \mu\text{g ml}^{-1}$ colcemid (Sigma) and incubated for 1 hour at 37°C . Non-irradiated (control) flasks were similarly treated with $0.1 \mu\text{g ml}^{-1}$ colcemid and incubated for 1 hour.

After incubation the cell suspension was removed to 50 ml centrifuge tubes and chilled on ice for 10 min before centrifugation at 1200 rpm ($\approx 200 \text{ g}$) for 10 min at 0°C . The medium was aspirated, the resulting cell pellet re suspended in ice-cold hypotonic solution (0.075M KCl) and held on ice for 20 minutes before centrifuging (Hereaus Laborfuge 400R) at 1200 rpm ($\sim 200 \text{ g}$). The supernatant was removed, the pellet loosened and slowly resuspended in fixative (75% methanol, 25% acetic acid v/v). The resulting cell suspension was washed at least three more times in fixative. Finally the cell pellet was resuspended in a small volume of fresh fixative and kept at 4°C .

2.3.3. Preparation of slides.

The microscope slides were first cooled in ice-cold distilled water for 30 min. The ice-cold slides were briefly wiped with the edge of a filter paper and flooded with ice-cold 50% glacial acetic acid solution before a single drop of cell suspension was placed on the slide. The slide was then dried on a warm-plate at approximately 50°C .

2.3.4. Fluorescence plus giemsa (FPG) staining

Once dry, the slides were placed in a solution of Hoechst 33258 (bis-Benzamide) solution; Sigma) at $0.2 \mu\text{gml}^{-1}$ in distilled water in the dark for 10 min and then blotted dry on filter papers. The slides were then covered with 2xSSC (0.3 M sodium chloride, 0.03 M sodium citrate, Analar) and placed under a UV-A (Philips TLD 18W/08) source for 3 hours. They were then rinsed three times in distilled water, 5 minutes each time, and blotted dry. Once dry the slides were stained in 4% Giemsa for 10 min and rinsed in distilled water containing a few drops of ammonia per litre prior to blotting dry.

2.3.5. Scoring and analysis.

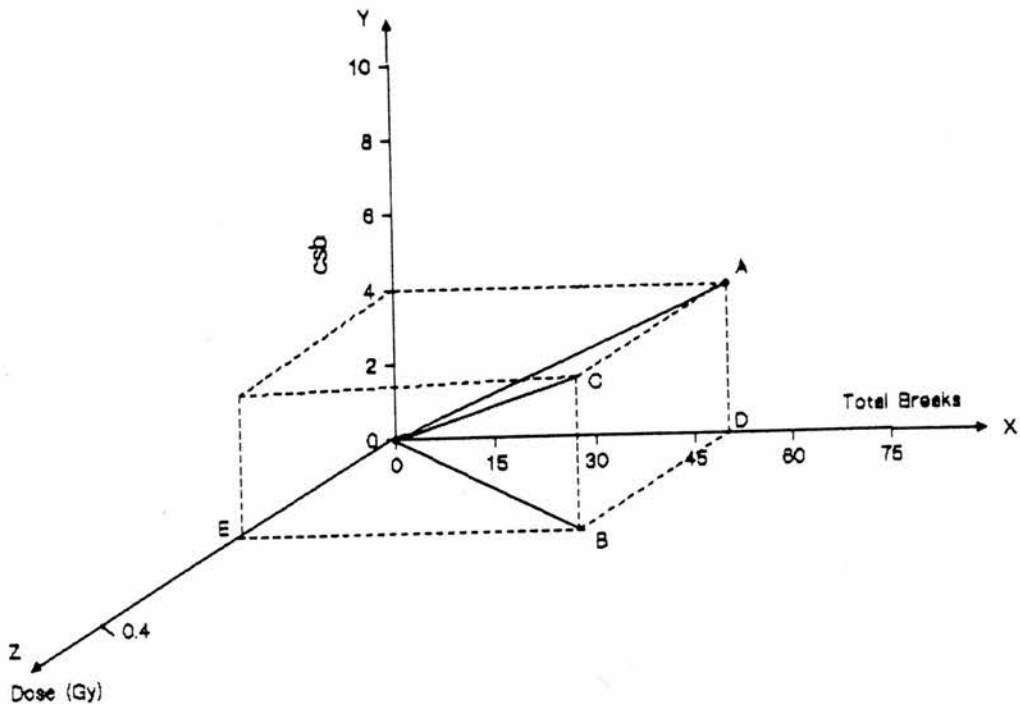
Slides were examined under a light microscope (Zeiss, with a planapochromat 1.4 aperture \times 63 objective). 400 metaphases were scored in each sample for chromatid breaks (including gaps). The frequencies of breaks occurring in the light or dark stained chromatids was noted as well as the number of breaks with associated colour-switches ("colour-switch breaks"). The colour switch ratio per 100 metaphases was determined. The sister chromatid exchange (SCE) frequency per cell was also determined using the following formula:

$$\text{SCE per cell} = \frac{\text{Frequency of SCE in 25 metaphases}}{25}$$

2.4 Results.

2.4.1 A consideration of the generalised radiation damage relationship

In this investigation of the effect of ionising radiation on the frequency of colour switch breaks and total chromatid breaks, lymphoblastoid cells are used as the standard cell type for comparison. In the most general sense the variables, namely total break frequency, colour switch break frequency and radiation dose can be plotted on a three-dimensional graph as shown below:



where the total break frequency, the radiation dose in Gy and the colour switch break frequency are plotted on the x, y and z axes respectively. It can be seen from the above 3-D graph that the point C represents a typical point in space (x,y,z) generated from the

relevant data of a specific experiment. In the idealised case a number of such experiments would produce the line vector OC shown above. Similarly the vector OA in the XOY plane represents a regression analysis of the total breaks vs. colour switch breaks data (colour switch ratio, csr) and the vector OB in the XOZ plane the total breaks vs. dosage data.

2.4.2 The chromatid break-dosage relationship

The generalised approach to the overall chromatid damage representation just described can however be simplified to a two dimensional solution by adopting the following approach.

A linear relationship between chromatid breaks and dosage for low doses of ionising radiation has been observed by various authors (Chadwick and Leenhouts, 1994, Bryant, 1998). The total number of chromatid breaks can be subdivided into colour switch and non-colour switch breaks and the results of experiments at the end of this section will show that the number of colour switch and non-colour switch breaks are also linear with dose.

Figure 2.4 shows the generalised linear relationship between radiation dose and chromatid breaks for low doses of ionising radiation. The linear expression for the number of total breaks with dose is:

$$T_b = m_1 D + c_1 \quad (2.1)$$

where T_b = total chromatid breaks, D = dose (Gy), m_1 = slope of the line (obtained by linear regression analysis of experimental data) and c_1 = the intercept on the y axis.

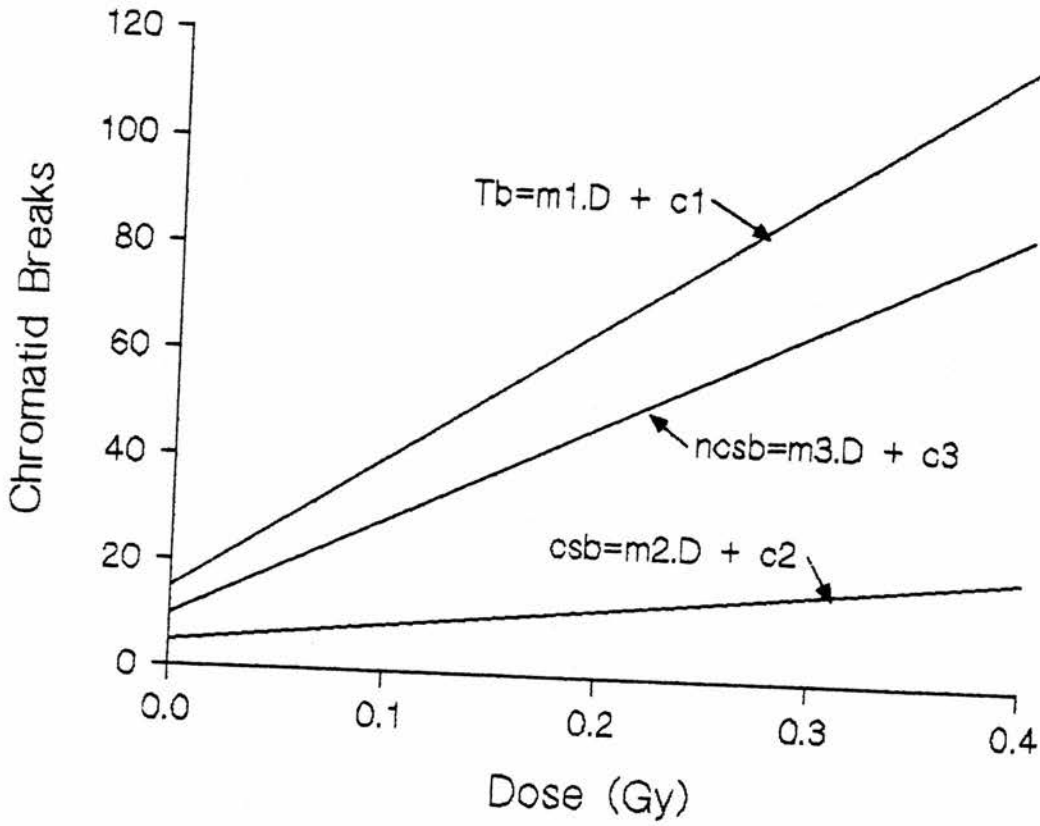


Figure 2.4 Equations representing the linear ($y = mx + c$) relationship between chromatid breaks and dose . Tb = total breaks, $ncsb$ = non-colour switch breaks, csb = colour switch breaks.

Similarly, an expression for the induction of colour switch breaks (csb) with dose (D) can be stated:

$$csb = m_2D + c_2 \quad (2.2)$$

Rearranging these expressions to make D the subject gives:

$$D = \frac{Tb - c_1}{m_1} \quad D = \frac{csb - c_2}{m_2}$$

Equating these two relationships and solving for csb gives the relationship:

$$csb = (m_2/m_1)(Tb - c_1) + c_2 \quad (2.3)$$

which is a linear relationship between csb and Tb where the csr is the slope of the line, i.e.

$$csr = m_2/m_1 = \text{CONSTANT} \quad (2.4)$$

when the intercept on the y axis (c) is zero and a good approximation when c is small. Furthermore if a linear relationship also exists between the non-colour switch breaks and dose then a similar expression can be derived for the non-colour switch ratio (ncsr) (see Figure 2.4):

$$ncsr = m_3/m_1 = \text{CONSTANT} \quad (2.5)$$

where m_3 is the slope of the line describing the linear relationship between non-colour switch breaks and dose at low doses of ionising radiation as obtained by linear regression analysis of experimental data. Since for any dose

$$Tb = csb + ncsb$$

then:

$$1 = \frac{csb}{Tb} + \frac{ncsb}{Tb}$$

i.e.

$$1 = csr + ncsr$$

thus

$$1 = m_2/m_1 + m_3/m_1$$

or:

$$m_1 = m_2 + m_3 \quad (2.6)$$

i.e. the slope of the total breaks vs. dosage line for a given cell line is the sum of the slopes of the component break lines.

A sample lymphoblastoid cell line was subjected to 0.2 and 0.4 Gy of ionising radiation as described in section 2.3.2 and the resulting chromatid breaks per 100 metaphases scored and compared with the non-irradiated control. The results of this experiment are shown in Figure 2.5 where the slopes of the least squares fit lines are also indicated. The experimental values for m_1 , m_2 and m_3 confirm both equation (2.6) and the linear theory just discussed. This data also shows that for this particular lymphoblastoid cell line the $csr = m_2/m_1 = 0.183$ and the $ncsr = m_3/m_1 = 0.817$ at a sample time of 1.5 hr. The relevant equations representing the linear regression analysis of Figure 2.5 are therefore:

$$Tb = 269.25 D + 10 \quad (2.7)$$

$$csb = 49.25 D + 0.083 \quad (2.8)$$

$$ncsb = 220.0 D + 8.6 \quad (2.9)$$

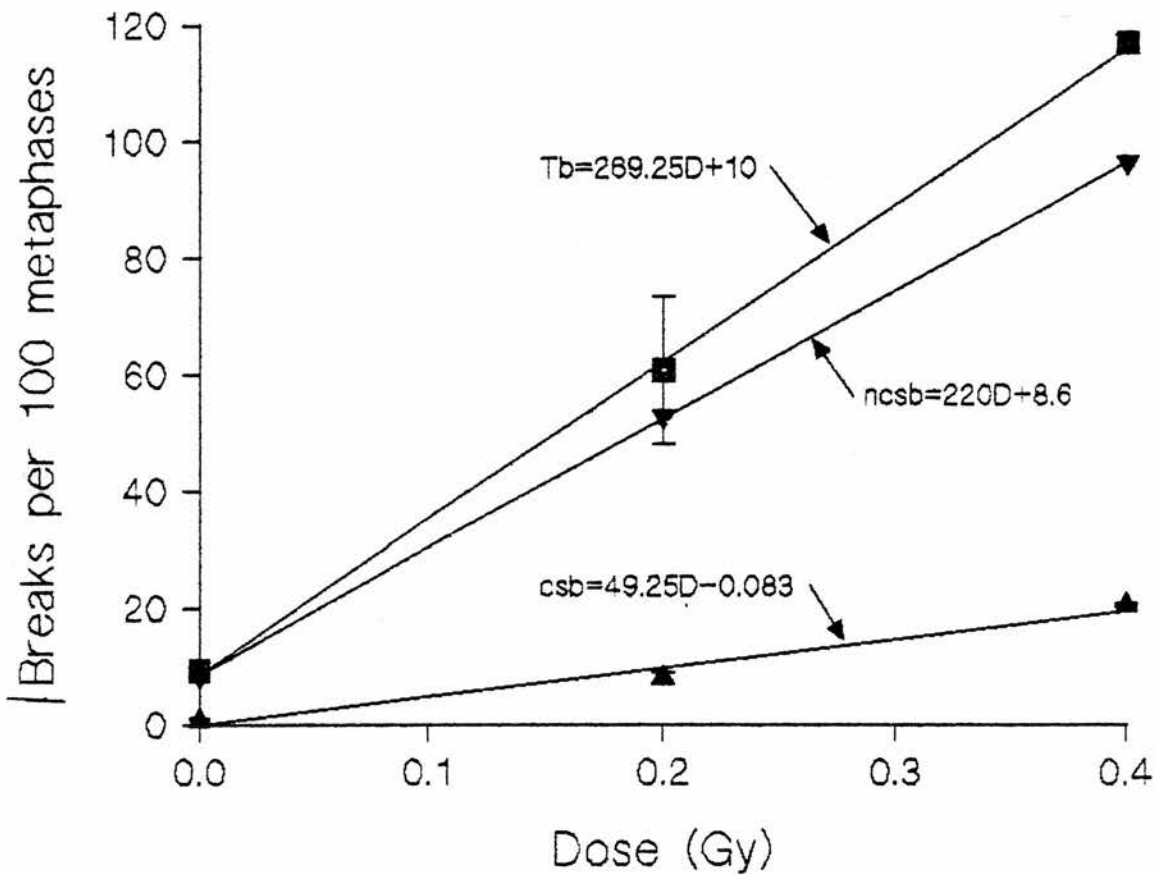


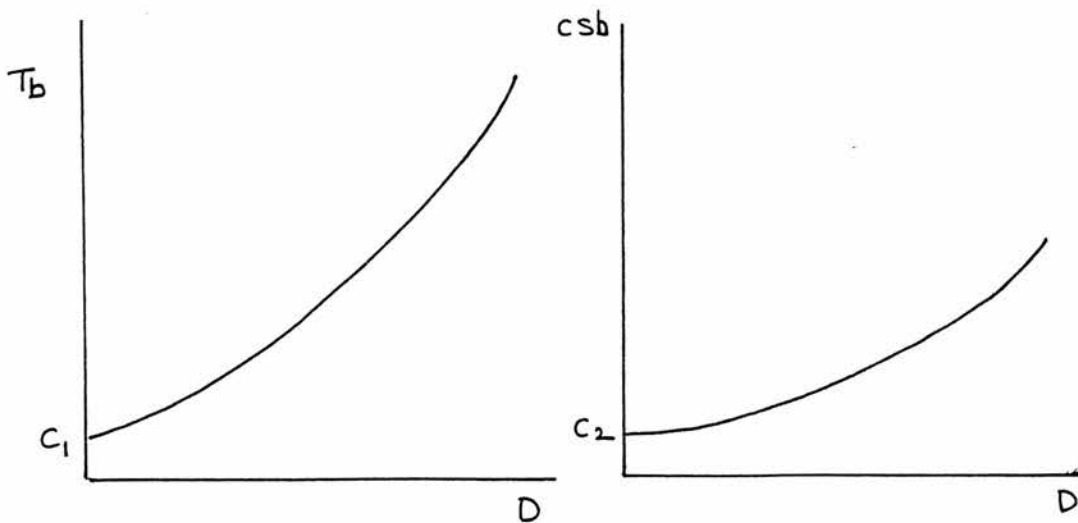
Figure 2.5 Graph showing experimental results of chromatid breaks per 100 metaphases vs dose to verify relationship between chromatid breaks and dose in Figure 2.4. A single normal lymphoblastoid cell line was used and 400 metaphases scored per point. Data obtained from at least two independent experiments. Error bars represent standard error of the mean. $r^2(Tb) = 99.9\%$, $r^2(ncsb) = 97.6\%$, $r^2(csb) = 99.9\%$.

A basic algebraic relationship thus exists when cells are subjected to low doses of ionising radiation. If a linear relationship exists between total breaks (T_b) and radiation dose and some different linear relationship exists between colour switch breaks (csb) and dose then the ratio csb/T_b known as the colour switch ratio (csr) must be constant and equal to m_2/m_1 where m_2 is the slope of the csb line and m_1 is the slope of the T_b line. Furthermore this basic relationship must also exist for the non-colour switch breaks ($ncsb$).

It can therefore be concluded from the above statement that the observations stated in the signal model described in Chapter 1, namely that the csr is constant is in fact a consequence of the linear breaks-dose relationship and not a separate observation or phenomenon.

It can be shown that the csr (and $ncsr$) is still constant for higher doses of ionising radiation when a linear relationship between total breaks and dose no longer exists.

Consider for example the situation where a quadratic relationship occurs for total and colour switch breaks as shown below:



$$T_b = AD^2 + c_1$$

$$csb = BD^2 + c_2$$

The above relationships satisfy the condition at $D = 0$, of $Tb = c_1$ and $csb = c_2$ and where A and B are constants, then:

$$D^2 = \frac{Tb - c_1}{A} = \frac{csb - c_2}{B}$$

re-arranging gives:

$$csb = \frac{B}{A} \cdot Tb + c_2 - \frac{B}{A} \cdot c_1 \quad (2.10)$$

which again is a linear relationship between csb and Tb where the slope is again equal to the csr :

$$\text{i.e.} \quad csr = B/A = \text{CONSTANT} \quad (2.11)$$

2.4.3 Statistical analysis of chromatid breaks in lymphoblastoid cells

The normal procedure for displaying the results of chromatid break information in this field is simply to provide the relevant experimental data in tabular form. It can therefore be difficult to visualise trends and differences among the measured values and assign the relative importance to individual quantities. To overcome this shortcoming, the experimental data will be analysed in two separate but inter-related approaches; namely the histogram-student t test approach and the regression relationships discussed in the previous two sections.

Tables 2.1 and 2.2 show the results of measuring chromatid breaks in normal and irradiated lymphoblastoid cells for 12 different sample cell lines. This was considered to be the minimum number of sample cell lines which might show a significant statistical

Table 2.1. Frequencies of chromatid breaks per 100 metaphases in normal lymphoblastoid cells. 400 cells scored per sample. Mean $\text{csr} = 17.6$, $\text{SD} = 4.1$. Results obtained from at least two independent experiments.

Cell line	No. damaged cells	Breaks in light strand*	Breaks in dark strand*	Colour-switch breaks	Total breaks	Colour switch ratio (%)
NC NC	9.5	3.0	5.5	0.8	9.3	8.6
DW NC	11.8	3.8	5.5	2.8	12.1	23.1
MR NC	9.5	3.8	4.0	2.0	9.8	20.4
AM NC	13.8	6.0	6.3	3.3	15.6	21.1
SW NC	13.8	6.3	6.5	2.8	15.6	17.9
SVO 09	18.8	8.0	9.5	2.8	20.3	13.8
SVO 14	14.0	5.5	6.5	2.8	14.8	18.9
SVO 20	7.8	2.5	4.0	1.8	8.3	21.7
SVO 24	7.0	2.5	3.8	1.5	7.8	19.2
SVO 26	16.8	4.8	9.5	3.0	17.3	17.3
SVO 27	11.8	4.5	5.8	2.0	12.3	16.3
SVO 28	8.8	3.3	4.8	1.3	9.4	13.8

*non-colour switch breaks are the sum of the light and dark strand breaks.

Table 2.2. Frequencies of chromatid breaks per 100 cells in normal lymphoblastoid cells subjected to 0.2 Gy irradiation. 400 metaphases scored per sample. Mean colour switch ratio = 15.6, standard deviation = 2.6. Results obtained from at least two independent experiments.

Cell line	No. damaged cells	Breaks in light strand*	Breaks in dark strand*	Colour-switch breaks	Total breaks	colour switch ratio (%)
NC NC	40.8	20.8	32.0	8.0	60.8	13.1
DW NC	43.5	30.3	30.3	9.8	70.4	13.9
MR NC	30.5	18.3	22.3	7.5	48.1	15.6
AM NC	47.5	25.5	26.8	12.5	64.8	19.3
SW NC	38.0	20.3	21.5	7.0	48.8	14.3
SVO 09	41.3	20.3	24.0	9.8	54.1	18.1
SVO 14	31.0	20.0	15.5	6.0	41.5	14.4
SVO 20	35.0	20.5	19.3	6.8	46.6	14.6
SVO 24	34.3	19.8	21.8	6.5	48.1	13.5
SVO 26	36.8	20.8	21.5	8.3	50.6	16.4
SVO 27	35.0	17.0	22.3	5.8	45.1	12.8
SVO 28	40.8	20.8	21.3	11.3	53.4	21.1

*non-colour switch breaks are the sum of the light and dark strand breaks.

trend and a means of comparing the frequency of breaks between normal and irradiated cells. In addition a major objective of the research project was aimed at confirming or otherwise the postulation of the signal model that csr is not affected by the amounts of radiation-induced damage.

Taking the values of colour switch breaks in Tables 2.1 and 2.2 the mean (\bar{x}) for controls is 2.24 (SD = 0.784) and 8.275 (SD = 2.14) for cells subjected to 0.2 Gy irradiation. Also from the tables, 75% of the colour switch breaks in control cells and 66.7% of colour switch breaks in irradiated cells fall within the interval $\bar{x} \pm SD$ which is a requirement for the normal distribution of the data. However, the F test shows that the ratio of the variances for colour switch breaks is $F = 7.45$ which is much greater than the statistically tabulated value of $F = 3.48$ for a significance level of 0.05 and $12 - 1 = 1$ df. Thus the null hypothesis is rejected that the colour switch break values of Tables 2.1 and 2.2 are not normally distributed and the tabulated data are therefore non-parametric. Non-parametric tests are a less powerful means of data analysis than parametric tests. The same argument as discussed above for the colour switch break values can also be shown to apply to both the total breaks and the number of damaged cells listed in Tables 2.1 and 2.2, i.e. the data is non-parametric.

A convenient statistical way around this problem is to normalise the values for the control and irradiated lymphoblastoid cell lines by dividing the colour switch break frequency by either the number of damaged cells or by the total breaks. Figures 2.6 and 2.7 show the colour switch break frequency values of tables 2.1 and 2.2 plotted against the number of damaged cells and total breaks respectively. The straight lines representing a regression analysis fit of the plotted data is also shown. In Figure 2.6, the slope of the lines through the data points represents the ratio of the colour switch breaks to the number of damaged cells for both the control and irradiated lymphoblastoid cells and is here referred to as the damaged cell ratio (dcr). Similarly, the slopes of the lines in Figure

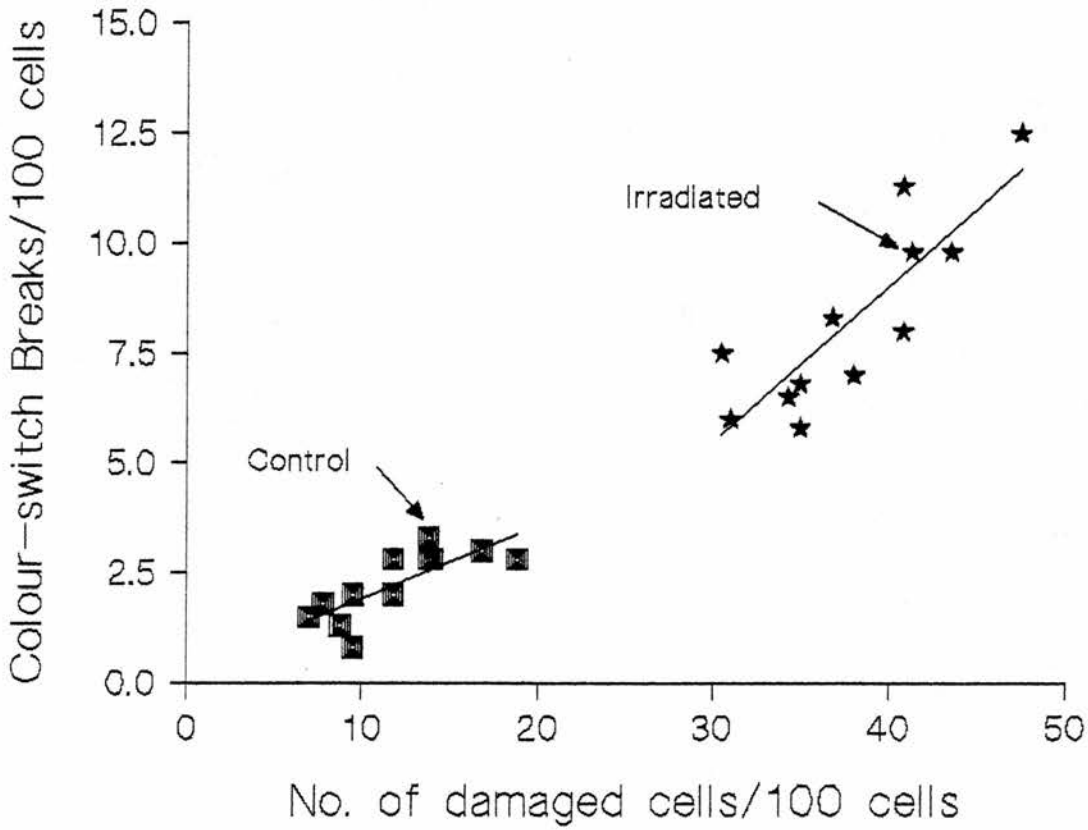


Figure 2.6. Graph of number of damaged cells vs. colour switch break frequency for non-irradiated and irradiated lymphoblastoid cells per 100 cells. A total of 12 cell lines were investigated and 400 metaphases per cell line were scored in total. Data obtained from at least two independent experiments. The slopes of the lines represent the damaged cell ratio (dcr) and have values of 0.166 and 0.355 for the control and irradiated values respectively. $r^2(\text{control}) = 59.5\%$, $r^2(\text{irradiated}) = (71.2\%)$.

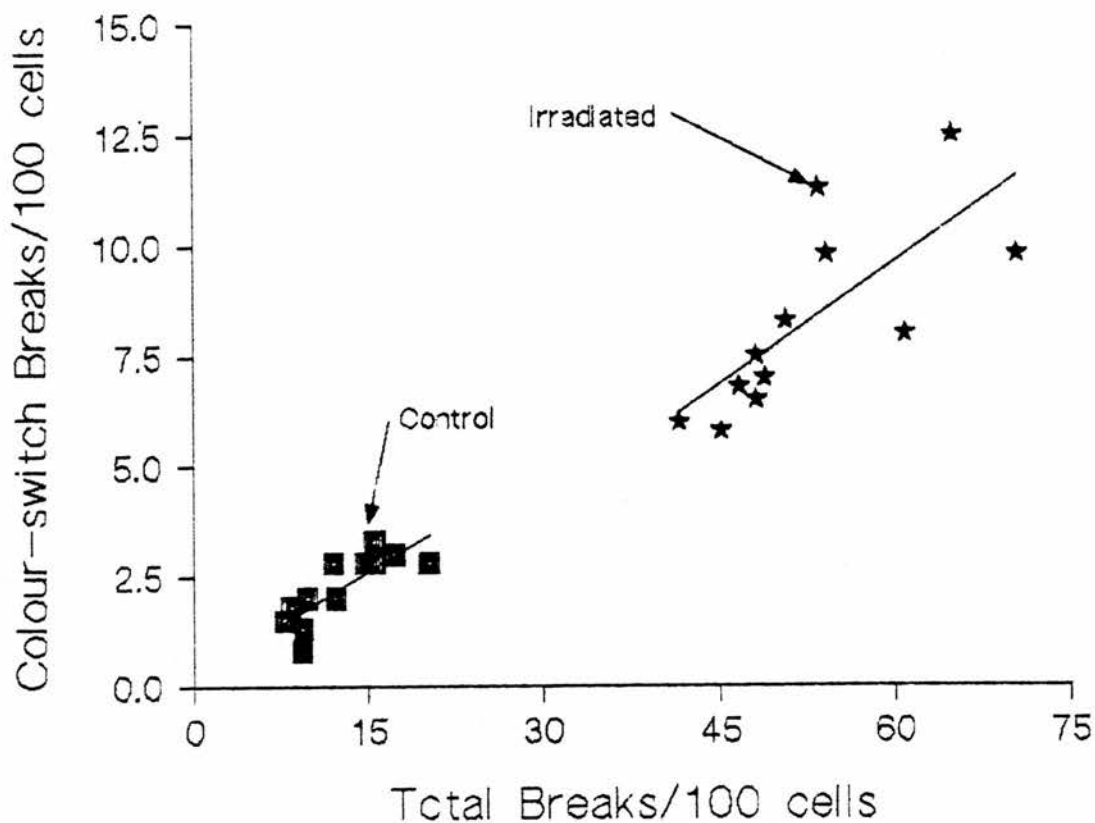


Figure 2.7 Graph of total chromatid breaks vs. colour switch breaks for non-irradiated and irradiated lymphoblastoid cells per 100 cells. A total of 12 cell lines were investigated and 400 metaphases per cell line were scored in total. Data obtained from at least two independent experiments. The slopes of the lines represent the colour switch ratio (csr) and have values of 0.158 and 0.185 for the control and irradiated values respectively. $r^2(\text{control}) = 64.5\%$, $r^2(\text{irradiated}) = 55.0\%$.

2.7 represents the ratio of colour switch breaks to total breaks, i.e the colour switch ratio (csr) for both the control and irradiated lymphoblastoid cells. Comparing Figures 2.6 and 2.7 shows clearly that the slopes of the two lines for csr are much closer than for the dcr which would suggest that the normalisation ratio of Figure 2.7 will produce the least difference between the control and irradiated cells values, which is in line with the recombination mechanism predicted by the signal model (Bryant, 1998). The correlation of the data points for csb and Tb in Tables 2.1 and 2.2 can be tested by determining the Product Moment Correlation Coefficient for this data. This analysis gives a value of $r = 0.952$ which suggests a strong positive correlation between csb and Tb.

As described by Fowler and Cohen (1990) and fully discussed in Appendix A, it is not strictly correct to apply the method of linear regression analysis to obtain a best-fit line of the data in Figures 2.6 and 2.7. This is because the csb and total breaks are both random experimental variables whereas in section 2.4.2 and Figure 2.5 the dose is not a random variable and consequently linear regression analysis is valid in this latter application. Figure 2.8 therefore shows the line representing a reduced major axis regression analysis of both the control and irradiated data for the lymphoblastoid cells and where the slope of the line is the $csr = 0.161$ and where the correlation coefficient indicates that 93.1% of the data points is represented by this line. The analysis of section 2.4.2 also justifies plotting control and irradiated data on the same two-dimensional graph because this linear analysis shows that the Tb vs. csb line is independent of dose. Normalisation of the experimental data of Tables 2.1 and 2.2 therefore shows that the csr value is a convenient quantity for comparing the overall results for lymphoblastoid cells. This quantity will therefore be used to see if the data of Tables 2.1 and 2.2 produce a normal distribution with parametric properties and where the means of the two distributions can then be compared using a t test to show if the control and irradiated cell populations are significantly different (see Appendix A).

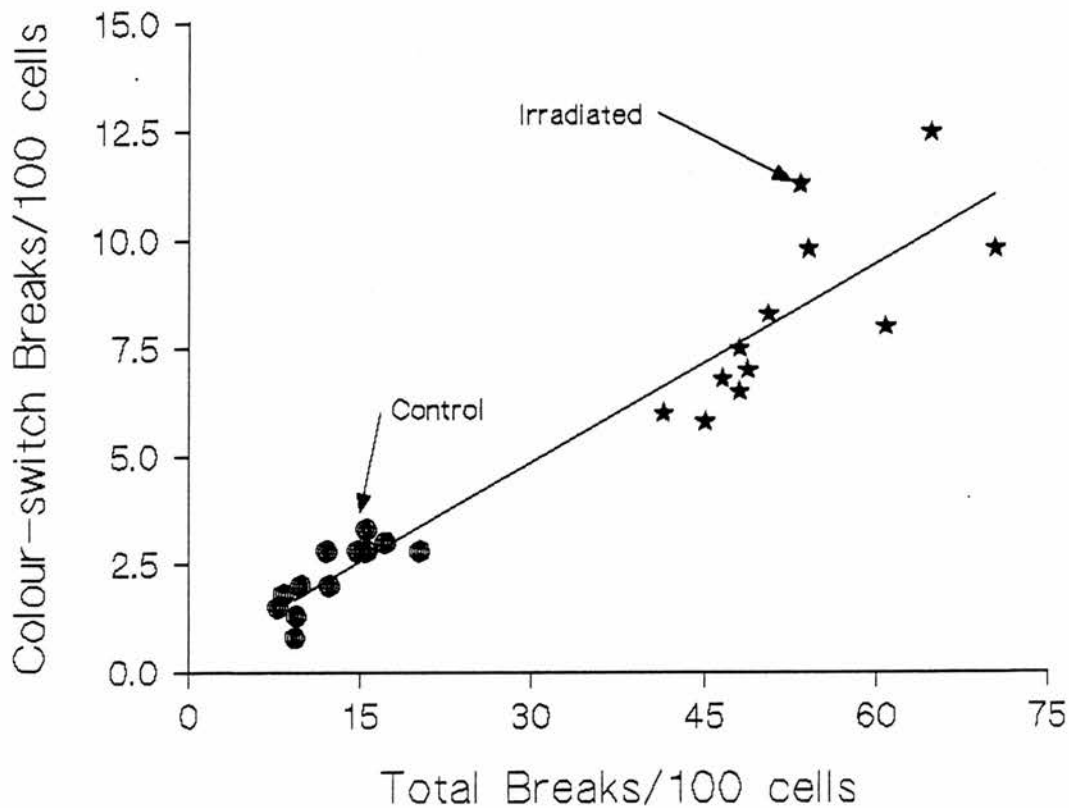


Figure 2.8. Graph of total chromatid breaks vs. colour switch breaks for both non-irradiated and irradiated lymphoblastoid cells per 100 cells. A total of 12 cell lines were investigated and 400 metaphases per cell line were scored in total. Data obtained from at least two independent experiments. The line represents a reduced major axis regression analysis for both control and irradiated data, the slope of the line represents the colour switch ratio (csr) and has a value of 0.161. $r^2 = 93.1\%$.

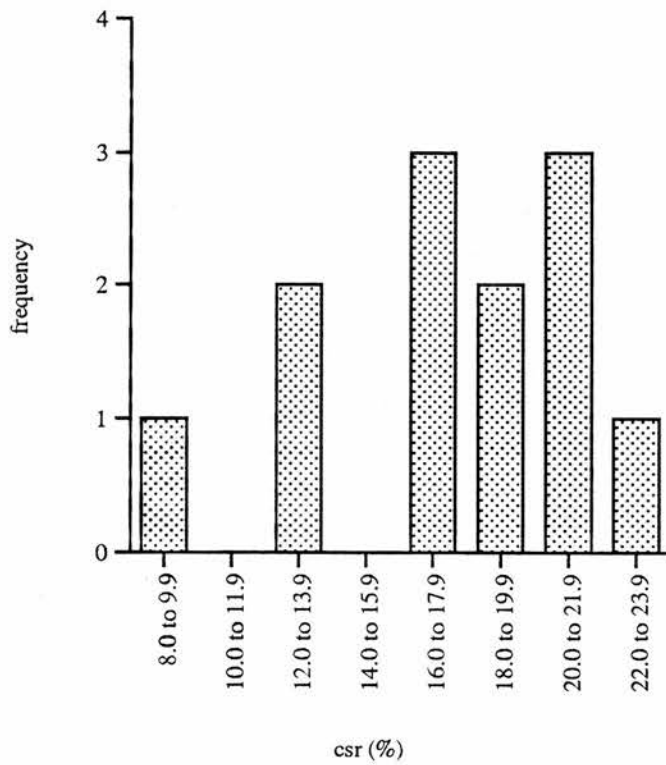


Figure 2.9 Histogram of distribution of colour switch ratios per 100 metaphases for non-irradiated normal lymphoblastoid cell lines from results in Table 2.1. The distribution approximates to a normal distribution with a mean csr value of 17.6 and standard deviation of 4.1.

2.4.4 Control (non-irradiated) lymphoblastoid cell lines.

Frequencies of the colour switch ratio (csr) values in twelve normal (non-irradiated) lymphoblastoid cell lines are shown in Table 2.1 and Figure 2.9. A total of 400 metaphases were scored (4×100 metaphases) per cell line to attempt to obtain a sufficiently high number of colour-switch breaks to enable the csr to be calculated. Generally there was only 1 break or gap in any damaged cell. The mean csr for these lines was calculated as 17.6 % (SD = 4.1). As described in detail in Appendix A, 83% of the csr values lie within one standard deviation on either side of the mean value. The frequency distribution of csr (Figure 2.9) is therefore approximately normal, which would further improve with a larger sample size producing a significantly smaller standard deviation in accordance with statistical theory.

2.4.5 Irradiated lymphoblastoid cell lines

Results for the frequencies of csr values in lymphoblastoid cells exposed to 0.2 Gy are shown in Table 2.2 and Figure 2.10. As with the control (non-irradiated) cells, 400 metaphases (4×100) per cell line were scored to ensure a sufficiently high frequency of colour-switch breaks. The mean colour switch ratio for these cell lines is 15.6 % (SD = 2.6). Again 83% of the csr values lie within one standard deviation on either side of the mean and therefore the frequency distribution of csr for irradiated lymphoblastoid cell lines (Figure 2.10) is also approximately normal and similar to that obtained for control (unirradiated) lines as shown in Figure 2.9. Those cells which had frequently sustained damage had more than one gap or break, the number of cells in metaphase observed was also lower in the irradiated cells than control cells. The variances for the control and irradiated lymphoblastoid cell lines of Figs. 2.9 and 2.10 were calculated and found to be close using the F-test described in Appendix A to justify further statistical analysis. The F value for this (2.58) was well within the tabulated value for a 0.05 level of significance

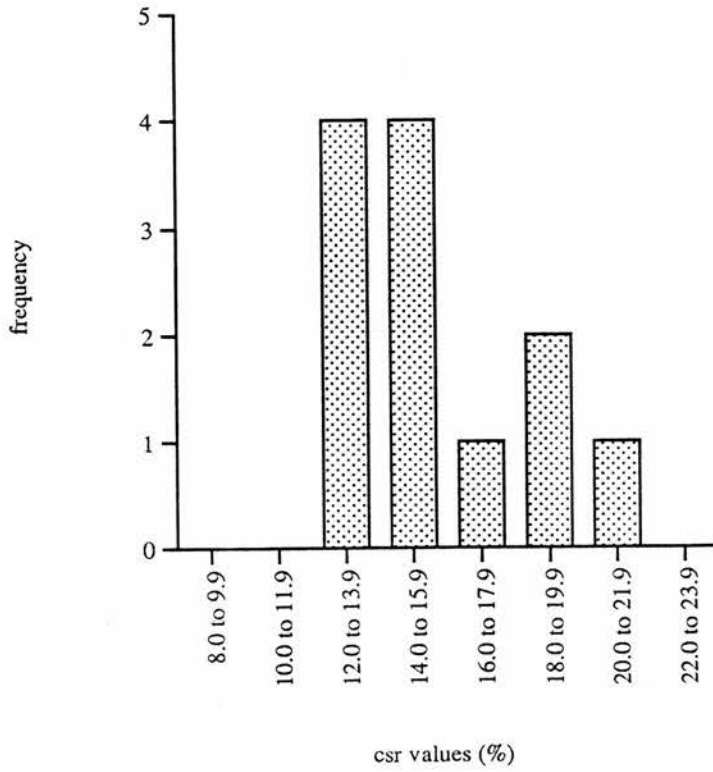


Figure 2.10 Histogram of distribution of colour switch ratios per 100 metaphases for normal lymphoblastoid cell lines subjected to 0.2 Gy radiation, from results in Table 2.2. The distribution approximates to a normal distribution with a mean csr value of 15.6 and standard deviation of 2.6

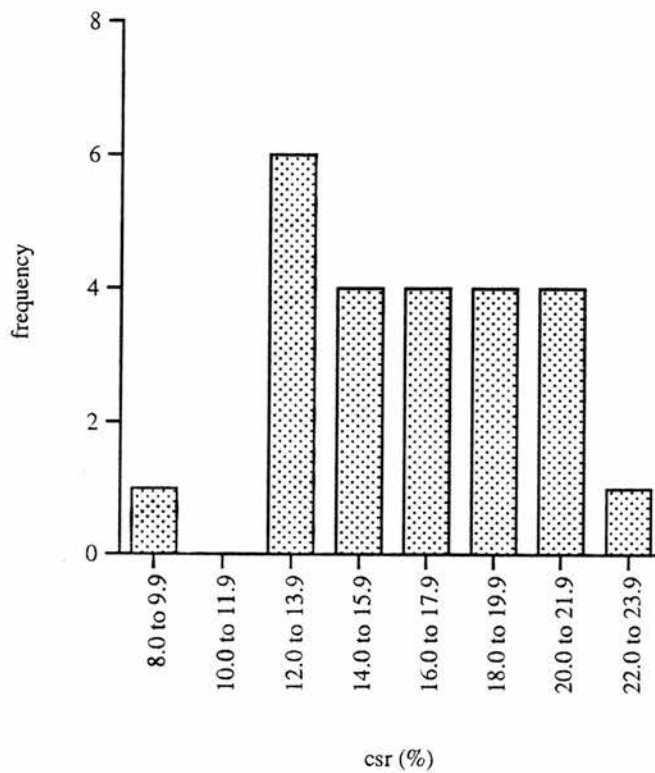


Figure 2.11 Histogram of distribution of combined colour switch ratios per 100 metaphases for both non-irradiated and irradiated normal lymphoblastoid cell lines from results in Tables 2.1 and 2.2. The distribution approximates to a normal distribution with a mean csr value of 16.63 and standard deviation of 3.52.

(see Appendix A). A t-test was therefore justifiable to compare the two distributions (Figures 2.9 and 2.10) which showed that the means of the two sample populations were not significantly different ($t_{0.05} = 1.43$, $df = 22$). The csr values of Tables 2.1 and 2.2 were also compared using the t-test for matched pairs which gave a calculated value of $t_{0.05} = 2.201$, $df = 11$, indicating that there is no significant difference between the means of the data. These results therefore support the postulate (Bryant, 1998) that the recombinogenic mechanism giving rise to colour switch breaks is unaffected by the absolute degree of radiation damage sustained by the cell. The combined csr distribution for control and lymphoblastoid cell lines is shown in Figure

2.11. The combined distribution has a mean of 16.63 % (SD = 3.52). However it was decided not to combine the results for control and irradiated lymphoblastoid cell lines when comparing the mean csr with that obtained in the next section for disease cell lines as the spread of values differed in the two distributions (Figs 2.9 and 2.10). This is probably due to sampling error as the absolute number of damaged cells scored in the control experiment is small compared to the absolute number of damaged irradiated cells scored. The mean number of damaged cells in the control procedure was 11.95 (SD = 3.63) compared to a mean of 37.88 (SD = 5.09) for the irradiated cell lines. Thus it was decided to compare "like with like" when considering the csr for disease cell lines. The mean frequency of sister chromatid exchanges (SCE) per cell for both non-irradiated and irradiated normal lymphoblastoid cell lines are shown in Table 2.3. There was no overall increase in SCE frequency with radiation, though the SCE values are lower than the generally values of 5-6 per cell.

2.4.6 Regression analysis of the data

In section 2.4.3, Figure 2.8 has already illustrated and discussed the method of regression analysis to obtain the best-fit line for the lymphoblastoid cell lines of Tables 2.1 and 2.2 and where the slope of the straight line represents the mean csr for all the data. The slope of this line gives a csr = 0.161 (16.1%) and where the correlation coefficient shows

Table 2.3. Frequencies of sister chromatid exchanges (SCE) per cell in normal lymphoblastoid cell lines. The BrdU concentration during two cell cycles was 33 μ M. 25 metaphases scored per sample.

Cell type	SCE/cell
NC NC: non-irradiated	1.11
irradiated	1.52
DW NC: non-irradiated	1.20
irradiated	1.50
MR NC: non-irradiated	1.12
irradiated	1.20
AM NC: non-irradiated	1.70
irradiated	1.56
SW NC: non-irradiated	0.96
irradiated	1.48
SVO 09: non-irradiated	1.28
irradiated	0.50
SVO 14: non-irradiated	0.64
irradiated	0.92
SVO 20: non-irradiated	1.58
irradiated	0.96
SVO 24: non-irradiated	1.22
irradiated	0.76
SVO 26: non-irradiated	0.68
irradiated	0.72
SVO 27: non-irradiated	0.72
irradiated	1.22
SVO 28: non-irradiated	1.80
irradiated	0.70

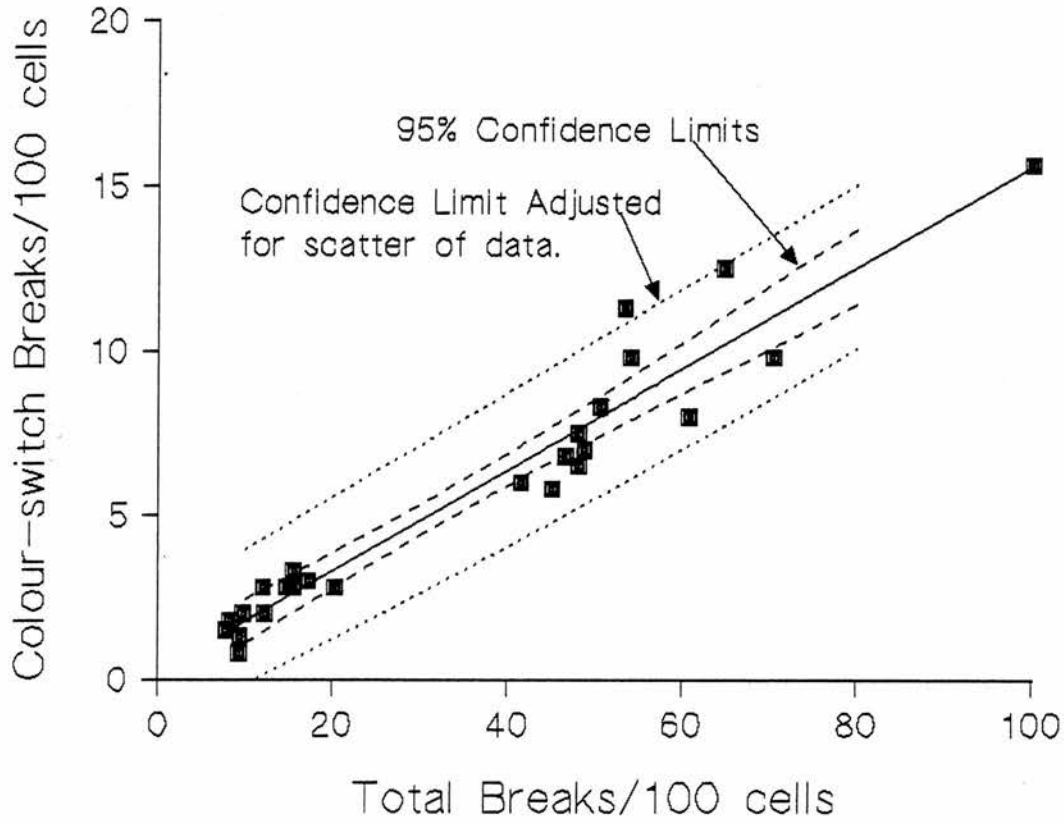


Figure 2.12 Graph of total chromatid breaks vs. colour switch breaks for non-irradiated and irradiated normal lymphoblastoid cells per 100 cells showing 95% confidence limits (dashed line) and confidence limit adjusted for scatter of data (dotted line). A total of 12 cell lines were investigated and 400 metaphases per cell line were scored in total. Data obtained from at least two independent experiments. $r^2 = 93.1\%$.

that the line represents 93.1% of the data. This figure shows clearly the expected scatter of experimental data points and where the value 0.161 should be compared with the histogram values illustrated in sections 2.4.4 and 2.4.5.

To allow for the scatter of experimental data and to account for the error in the resulting regression line, 95% confidence limits can be calculated by the methods described by Fowler and Cohen, (1990). Using their approach a second confidence zone can be determined as shown in Figure 2.12 for the lymphoblastoid results. This is the zone for normal healthy cells which will be compared with the disease cells of the next section.

2.4.7 Cell lines derived from different syndromes.

Table 2.4 shows the results of measuring the frequency of chromatid breaks in different syndrome cell lines where 400 metaphases (4×100) per cell line were scored. Examples of metaphases of some typical breaks are shown in Figure 2.13. The mean csr for each diseased cell line of Table 2.4 was calculated for both the non-irradiated and irradiated cells and compared with the appropriate mean and standard deviation of Tables 2.1 and 2.2. using the t-score (Appendix A).

One of the advantages of normalising the lymphoblastoid cell line data using the csr values is that a direct comparison between these distributions and specific values for syndrome cells can be made using a t score (Appendix A). Table 2.4 therefore includes the t score for each disease cell line sample. In any specific case where the t score > 2.2 this would indicate that these cells are significantly different from the normal lymphoblastoid cells. Like the normal lymphoblastoid cell lines, the sister chromatid exchange (SCE) frequency (Table 2.5) does not show any particular trend in changes in SCE frequency with radiation damage, though the observed SCE frequency was low.

Table 2.4. Frequencies of chromatid breaks in disease syndrome lymphoblastoid cell lines per 100 metaphases in disease cell lines. 400 cells scored per sample. 0.2 Gy irradiation was used. Results obtained were pooled from at least two independent experiments.

Cell line	No. damaged cells	Breaks in light strand*	Breaks in dark strand*	Colour-switch breaks	Total breaks	Colour switch ratio (%)	t score (2.2)
Nijmegen Breakage Syndrome:							
94P548 non-irradiated	13.5	4.0	8.5	1.3	13.8	9.4	2.0
94P112 non-irradiated	9.5	3.0	7.8	0.3	11.1	2.7	3.6
94P548 irradiated	58.0	28.5	64.0	5.0	97.5	5.1	4.04
94P112 irradiated	75.3	33.5	109.8	3.3	146.6	2.2	5.1
Bloom Syndrome:							
W1004 non-irradiated	2.0	1.5	1.5	0	3.0	0	-
GMB900 non-irradiated	2.0	1.3	0.5	0.3	2.1	14.3	0.8
W1004 irradiated	39.0	21.3	25.0	6.3	52.6	12.0	1.38
GMB900 irradiated	39.8	26.5	37.0	11.8	75.3	15.7	0.04
Omenns Syndrome:							
OMN 008 non-irradiated	19.5	6.3	14.5	3.3	24.1	13.7	0.95
OMN 008 irradiated	50.0	31.3	40.0	4.8	76.1	6.3	3.6

*non-colour switch breaks are the sum of the light and dark strand breaks.

Table 2.4 continued. Frequencies of chromatid breaks per 100 metaphases in disease syndrome cell lines. 400 cells scored per sample. 0.2 Gy irradiation was used. Results obtained were pooled from at least two independent experiments.

Cell line	No. damaged cells	Breaks in light strand*	Breaks in dark strand*	Colour-switch breaks	Total breaks	Colour switch ratio (%)	t score (2.2)
Ataxia telangiectasia:							
ATAR non-irradiated:	35.0	15.5	24.0	7.5	47.0	16.0	0.27
ATLG non-irradiated:	23.3	8.8	15.0	2.3	26.1	8.8	2.18
ATPA non-irradiated:	31.8	18.5	16.8	4.3	39.6	10.8	1.67
ATAR irradiated	78.8	63.5	76.5	13.3	153.3	8.6	2.68
ATLG irradiated:	71.5	53.0	69.5	8.8	131.3	6.7	3.44
ATPA irradiated:	67.8	49.8	60.8	10.0	120.6	8.3	2.80
Down Syndrome:							
CV 105 non-irradiated:	13.5	4.5	8.5	1.5	14.5	10.4	1.75
CV077 non-irradiated:	24.8	10.3	14.0	3.0	27.3	11.0	1.6
CV712 non-irradiated:	25.8	8.3	14.3	3.3	25.9	12.7	1.2
CV105 irradiated	50.3	18.8	46.0	4.3	69.1	6.2	3.6
CV077 irradiated	35.7	13.0	19.3	5.8	38.1	15.2	0.15
CV712 irradiated	56.3	35.8	44.0	13.0	92.8	14.0	0.61

*non-colour switch breaks are the sum of the light and dark strand breaks.

Table 2.4 continued. Frequencies of chromatid breaks per 100 metaphases in disease syndrome cell lines. 400 cells scored per sample. 0.2 Gy irradiation was used. Results obtained were pooled from at least two independent experiments.

Cell line	No. damaged cells	Breaks in light strand*	Breaks in dark strand*	Colour-switch breaks	Total breaks	Colour switch ratio (%)	t score (2.2)
Unknown mutation Cell Lines:							
BIAL1 non-irradiated	16	5.3	9.3	1.5	16.1	9.32	2.02
BIAL1 irradiated	58.5	36.5	46.5	9.0	92.0	9.78	2.24
p53 mutant cell lines:							
PEGY1 non-irradiated	22.3	11.3	11.5	3.0	25.8	11.63	1.46
PEGY1 irradiated	58.0	42.0	59.0	7.5	108.5	6.91	3.34
ELWE1 non-irradiated	17.5	6.5	9.8	2.5	18.8	13.30	1.05
ELWE1 irradiated	50.5	36.0	41.5	5.5	83.0	6.63	3.45

*non-colour switch breaks are the sum of the light and dark strand breaks.

Table 2.4 continued. Frequencies of chromatid breaks per 100 metaphases in disease cell lines. 400 cells scored per sample. 0.2 Gy irradiation was used. Results obtained were pooled from at least two independent experiments.

Cell line	No. damaged cells	Breaks in light strand*	Breaks in dark strand*	Colour-switch breaks	Total breaks	Colour switch ratio (%)	t score (2.2)
Brca2 mutant cell line (heterozygous)							
SLYN1 non-irradiated	21.8	8.3	13.8	2.3	24.4	9.43	1.99
SLYN1 irradiated	60.3	41.8	48.3	10.1	100.2	10.1	2.11
TURN1 non-irradiated	19.3	9.0	11.0	2.8	22.8	13.46	1.01
TURN1 irradiated	60.0	43.5	42.0	9.5	95.0	10.0	2.15
Brca1 mutant cell lines (heterozygous):							
COWA1 non-irradiated	25.5	14.5	12.5	4.0	31.0	12.90	1.15
COWA1 irradiated	55.3	35.8	38.5	11.0	85.3	12.90	1.04
LANY1 non-irradiated	18.3	9.3	8.3	2.8	20.4	13.73	0.94
LANY1 irradiated	57.3	33.8	38.8	11.5	84.1	13.67	0.74

*non-colour switch breaks are the sum of the light and dark strand breaks.

Table 2.5. Frequencies of sister chromatid exchanges (SCE) per cell in disease syndrome and mutant lymphoblastoid cell lines. The BrdU concentration during two cell cycles was 33 μM (except for Bloom's Syndrome where a concentration of 5.0 μM was used). 25 metaphases scored per sample.

Cell type	SCE/cell
Nijmegen Breakage Syndrome:	
94P548 non-irradiated	1.36
94P548 irradiated	1.88
94P112 non-irradiated	2.20
94P112 irradiated	2.48
Bloom Syndrome:	
W1004 non-irradiated	27.1
W1004 irradiated	16.6
GMB900 non-irradiated	14.9
GMB900 irradiated	13.68
Omenns Syndrome:	
OMN 008 non-irradiated	1.36
OMN 008 irradiated	0.88
Down Syndrome:	
CV 105 non-irradiated	0.76
CV105 irradiated	0.88
CV077 non-irradiated	0.96
CV077 irradiated	2.02

Table 2.5 continued. Frequencies of sister chromatid exchanges (SCE) per cell in disease syndrome and mutant lymphoblastoid cell lines. The BrdU concentration during two cell cycles was 33 μ M. 25 metaphases scored per sample.

Cell type	SCE/cell
Brca2 mutant cell line:	
SLYN ₁ non-irradiated	2.28
SLYN ₁ irradiated	1.92
TURN ₁ non-irradiated	0.96
TURN ₁ irradiated	0.60
Brca1 mutant cell lines:	
COWA1 non-irradiated	3.96
COWA1 irradiated	3.60
LANY1 non-irradiated	3.80
LANY1 irradiated	4.44
p53 mutant cell lines:	
ELWE1 non-irradiated	0.76
ELWE1 irradiated	1.52
PEGY1 non-irradiated	1.08
PEGY1 irradiated	0.48
Unkown mutation cell line:	
BIAL1 non-irradiated	0.72
BIAL irradiated	0.76

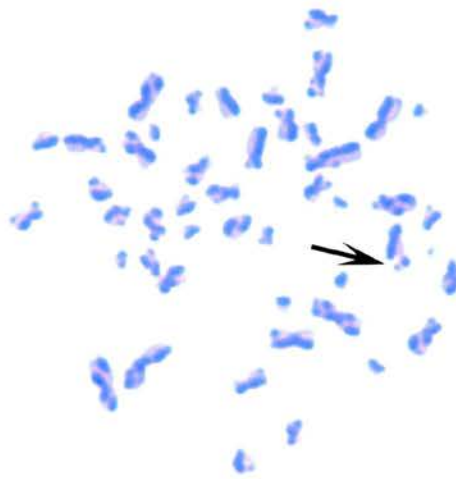


Figure 2.13 (a) Typical metaphase spread of a Bloom Syndrome lymphoblastoid cell irradiated with 0.2 Gy showing a colour switch break (arrow) and numerous sister chromatid exchanges.

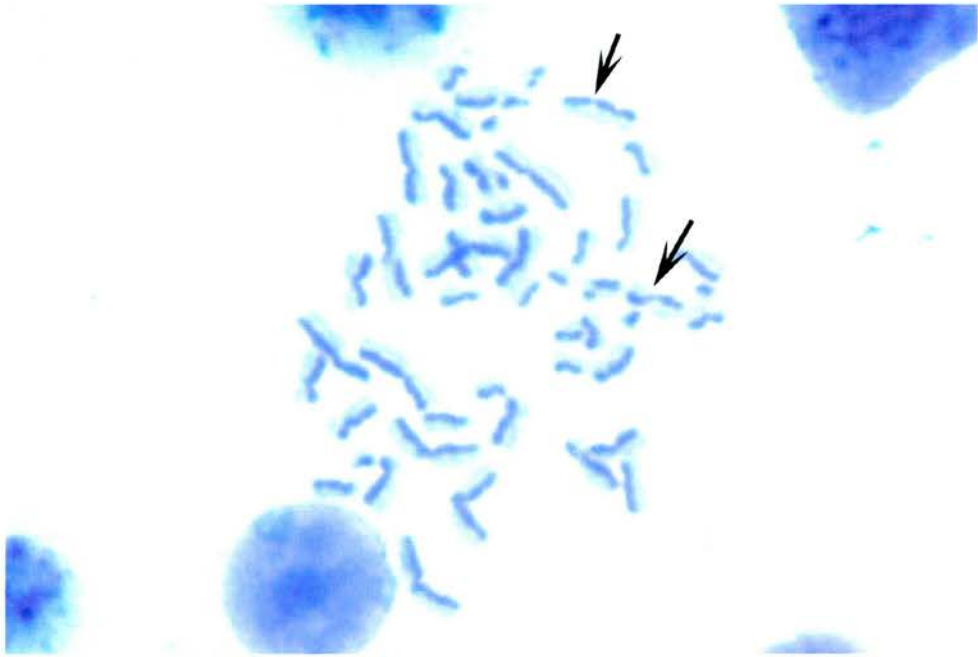


Figure 2.13 (b) Typical metaphase spread of an Omenn Syndrome lymphoblastoid cell irradiated with 0.2 Gy showing light and dark strand breaks.

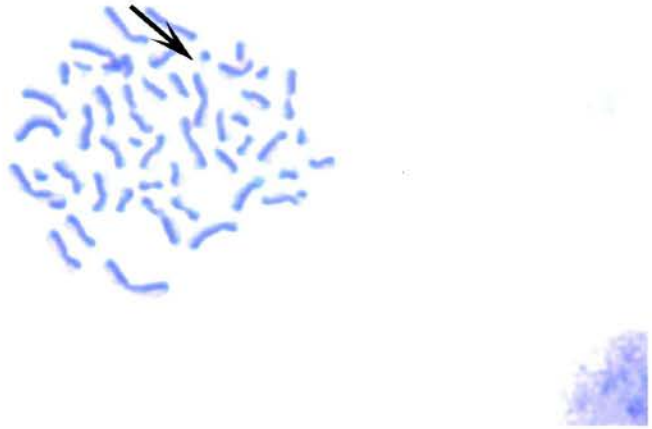


Figure 2.13 (c) Typical metaphase spread of an ATM (ATAR) lymphoblastoid cell irradiated with 0.2 Gy showing a dark strand break.

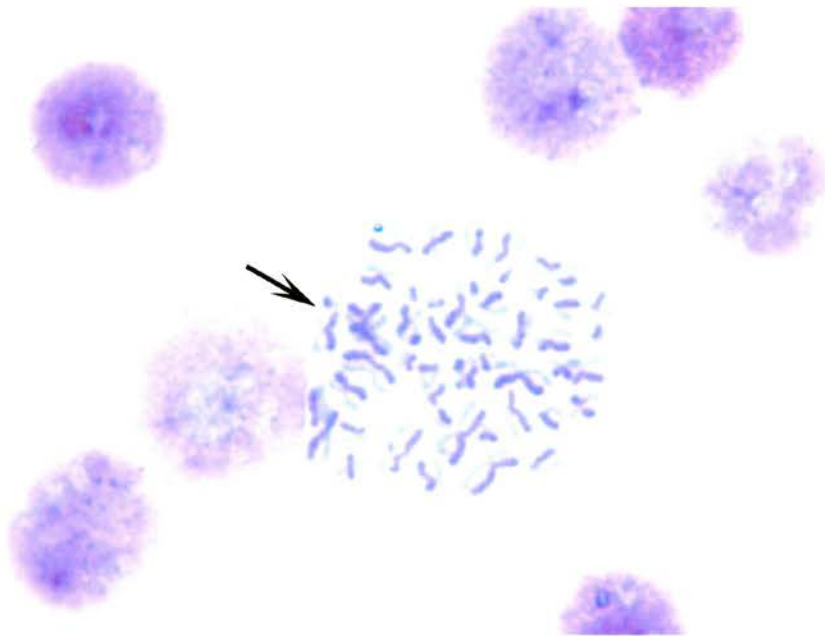


Figure 2.13 (d) Typical metaphase spread of a heterozygous *Brcal* mutant (COWA1) lymphoblastoid cell showing a colour switch break.

The t scores indicate that the csr values for NBS cell lines are all significantly different from both control and irradiated csr lymphoblastoid values (one value, 94P548 non-irradiated, is borderline significant). The t scores for ATM, Omenn, p53 cell lines are indicative of significantly different csr in irradiated but not non-irradiated cells. ATM and Omenn cell lines both show an approximately 2.5-fold increase in absolute numbers of damaged cells following irradiation. NBS show a mean 6-fold increase in numbers of damaged cells following irradiation. A number of possible terminal translocations were observed in the ATM irradiated cell lines, but not in the non-irradiated experiments. These were both light strand to dark strand translocations and vice-versa, occurring at a frequency of approximately 5.3 per 100 cells scored. These were investigated by Predrag Sljepcevic (personal communication) using FISH analysis but the negative results suggest that these are terminal SCE. BRCA2, BRCA1 and p53 cell lines all displayed a 2 to 3 fold increase in numbers of damaged cells on exposure to irradiation.

The comparison of single syndrome cell lines with a normal lymphoblastoid cell population is more rigorous than a comparison of a single normal cell line with a single syndrome cell line. However the results are still ambiguous since many of the syndrome cell lines showing significantly lower csr ($t > 2.2$) when irradiated have t scores for non-irradiated samples which fall below the critical threshold value of 2.2 (Table 2.4). A much clearer illustration than the t score value that a specific disease cell line is very different from normal lymphoblastoid cells can very conveniently be seen using Figure 2.14 where the data for disease cells are shown in relation to the confidence zone described in the previous section. Any data points lying outwith these confidence limits represent cell lines with significantly different csr characteristics compared with normal lymphoblastoid cell lines. The cell lines represented by these outlying data points are shown in the key on Figure 2.14. It is of interest to note that all the outlying data points are csr values from irradiated cell samples and include one of the Down Syndrome lines (CV055), the Omenn Syndrome line (OMN008), both the NBS lines (94P548 and 94P112)

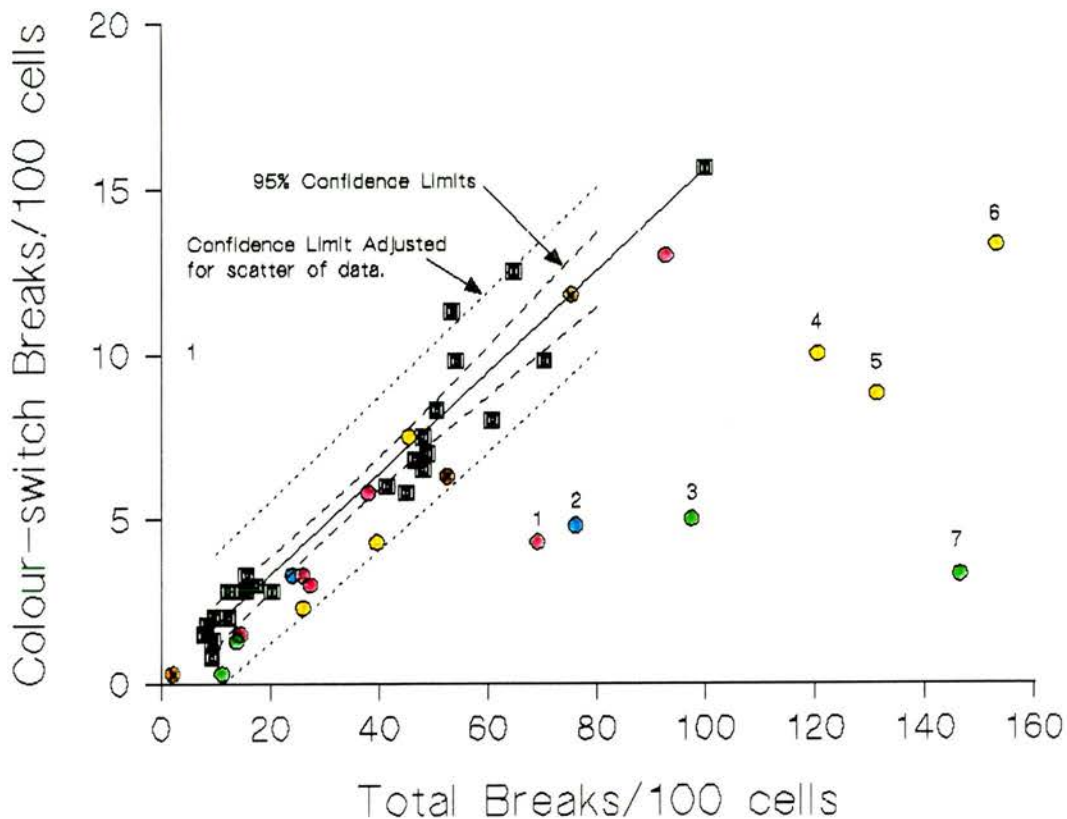


Figure 2.14 Graph of total chromatid breaks vs. colour switch breaks for non-irradiated and irradiated normal lymphoblastoid cells per 100 cells showing 95% confidence limits (dashed line) and confidence limit adjusted for scatter of data (dotted line) from Figure 2.12. Data points represented by squares are the values for control and irradiated normal lymphoblastoid cell lines; those represented by coloured circles are values for disease syndrome cell lines (see also Table 2.4 for corresponding t scores).

Key for the disease syndrome cell lines and numbered data points which lie outside the 95% confidence limits:

- Bloom's Syndrome.
- Down Syndrome (1. Down Syndrome CV105, irradiated).
- Omenn Syndrome (2. Omenn Syndrome OMN008, irradiated).
- Nijmegen Breakage Syndrome (3. Nijmegen Breakage Syndrome 94P548, irradiated;
7. Nijmegen Breakage Syndrome 94P112, irradiated).
- Ataxia telangiectasia (4. Ataxia telangiectasia ATPA, irradiated;
5. Ataxia telangiectasia; ATLG, irradiated; 6. Ataxia telangiectasia ATAR, irradiated).

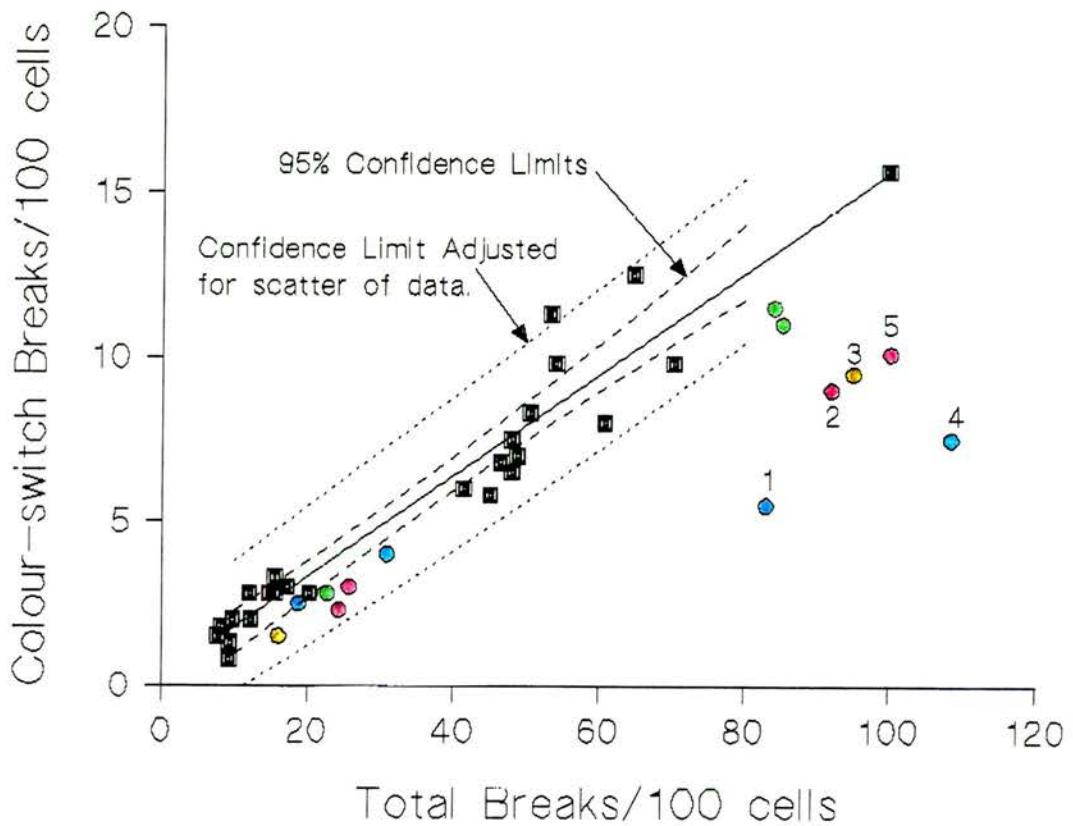


Figure 2.15 Graph of total chromatid breaks vs. colour switch breaks for non-irradiated and irradiated normal lymphoblastoid cells per 100 cells showing 95% confidence limits (dashed line) and confidence limit adjusted for scatter of data (dotted line) from Figure 2.12. Data points represented by squares are the values for control and irradiated normal lymphoblastoid cell lines; those represented by coloured circles are values for disease cell lines (see also Table 2.4 for corresponding t scores).

Key for the mutant cell lines and numbered data points which lie outside the 95% confidence limits:

- p53 mutation (1. ELWE₁ irradiated,; 4. PEGY₁ irradiated,)
- BRCA1 mutation (COWA₁; LANY₁)
- BRCA2 mutation (2. BIAL₁ irradiated; 5. SLYN₁ irradiated)
- Unknown mutation (3. TURN₁ irradiated)

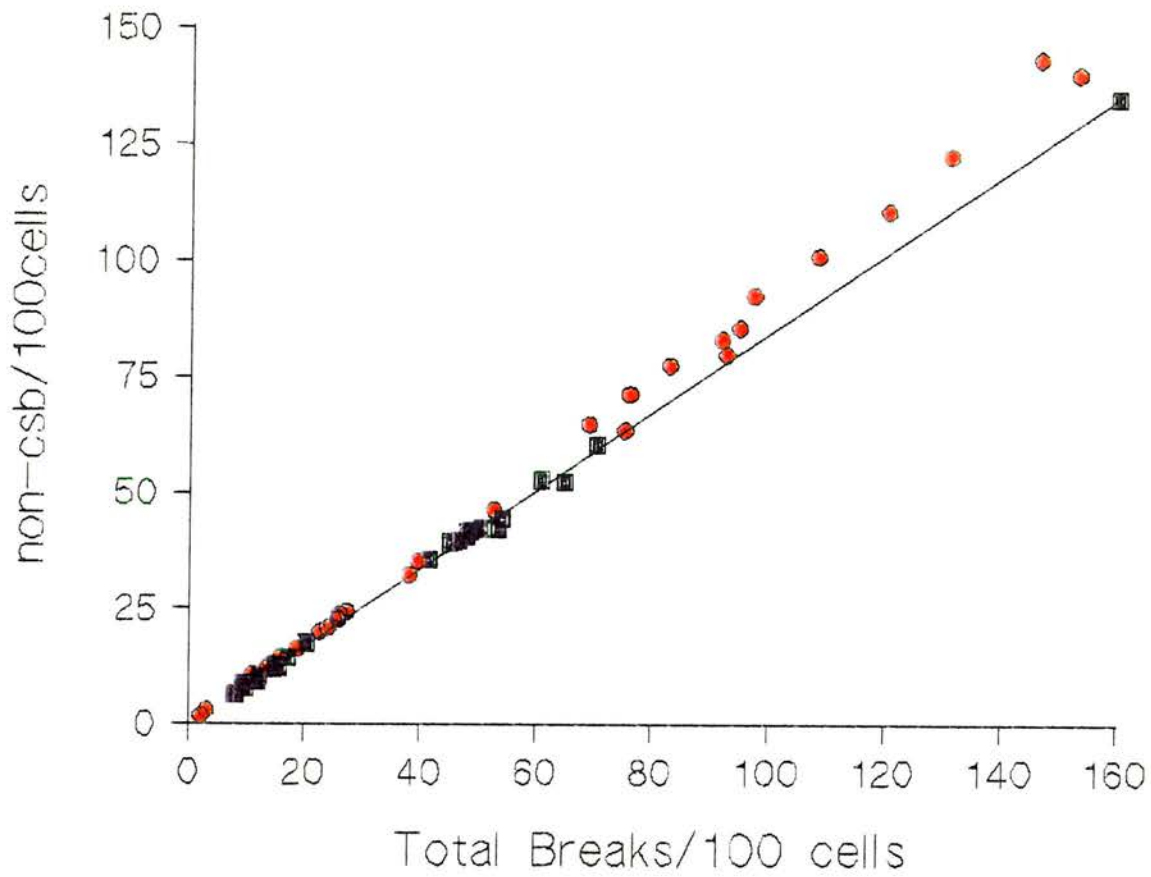


Figure 2.16 Linear regression analysis of total chromatid breaks vs. non-colour switch breaks for non-irradiated and irradiated normal lymphoblastoid cells per 100 metaphases and comparison with data values for disease syndrome and mutation cell lines. Confidence limits are not included as the data points are close to the reduced major axis regression line. A total of 12 cell lines were investigated and 400 cells per cell line were scored in total. Results obtained from at least two independent experiments. Data points represented by squares are the values for control and irradiated normal lymphoblastoid cell lines; those represented by red circles are values for disease cell lines.

and all three ATM cell lines (ATLG, ATPA, ATAR). None of the csr values for Bloom Syndrome cell lines (W1004 and GMB900) fall outside the 95% confidence limits for normal lymphoblastoid cells.

Results for cell lines derived from families of patients with familial breast cancer with either p53 mutations (PEGY₁ and ELWE₁) or unknown mutations (BIAL₁) were similarly compared to the csr for normal lymphoblastoid cells in Figure 2.15. The outlying data points for BIAL₁, EIWE₁, TURN₁, SLYN₁ and PEGY₁ are all irradiated values, non-irradiated values lying within the adjusted confidence limits for normal lymphoblastoid lines. All data points for the heterozygous BRCA1 (COWA₁ and LANY₁) mutants lie well within the 95% confidence limits for normal lymphoblastoid cell lines (Figure 2.15 and Table 2.4).

The ncsr for normal lymphoblastoid cell lines was determined using the method described in 2.4.2, using regression analysis to obtain a value for the slope of the line (Figure 2.16). As the scatter of the experimental data was so much less than that obtained for total breaks vs. colour switch breaks (Figure 2.12) it was not considered necessary to calculate 95% confidence limits. All data point for disease cell lines were very close to the reduced major axis regression line, indicating none of the cell lines investigated had a significantly different ncsr even if the csr was significantly different (Figures 2.14 and 2.15).

2.4.8 Radiation Damage Index (rdi)

Another parameter which can be used to compare normal and diseased cell lines is to compare the radiation sensitivity of normal lymphoblastoid cell lines to that of disease cells. A measure of this factor is the ratio of the total breaks divided by the number of damaged cells, which is here defined as the Radiation damage index (rdi). The use of this

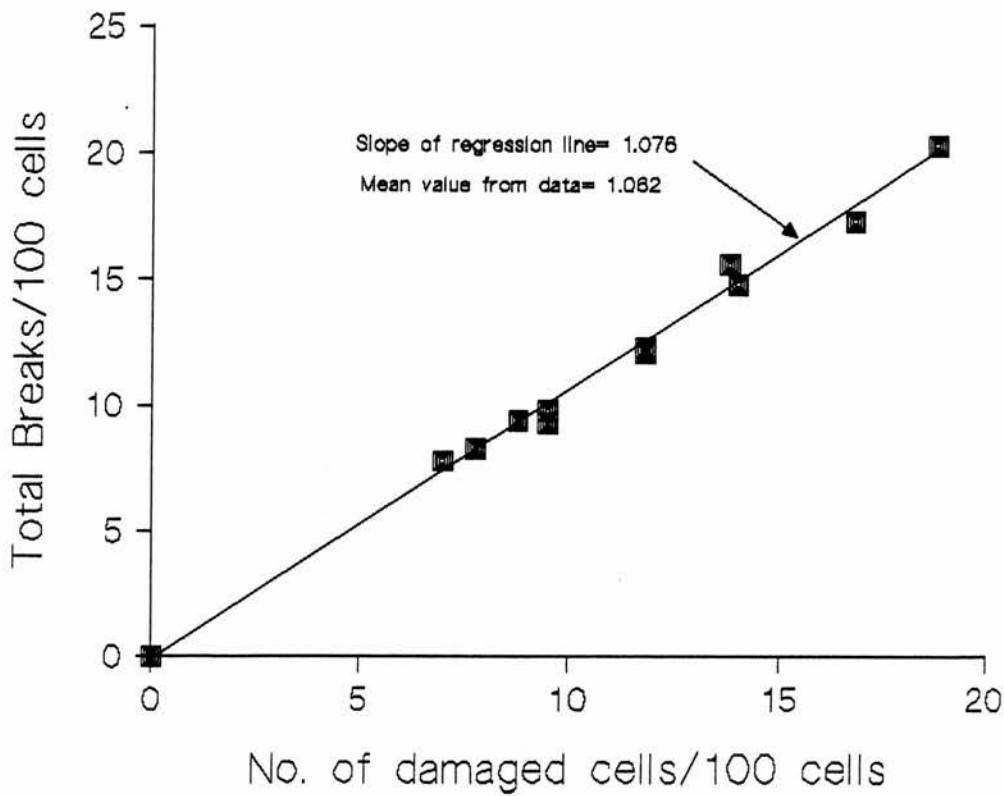


Figure 2.17 Graph of number of damage cells vs. total breaks per 100 cells for non-irradiated normal lymphoblastoid cell lines. A total of 12 cell lines were investigated and 400 metaphases scored in total. Results obtained from at least two independent experiments. The slope of the line represents the reduced major axis regression analysis for these data points and has a value of 1.076 and a correlation coefficient of 98.2%.

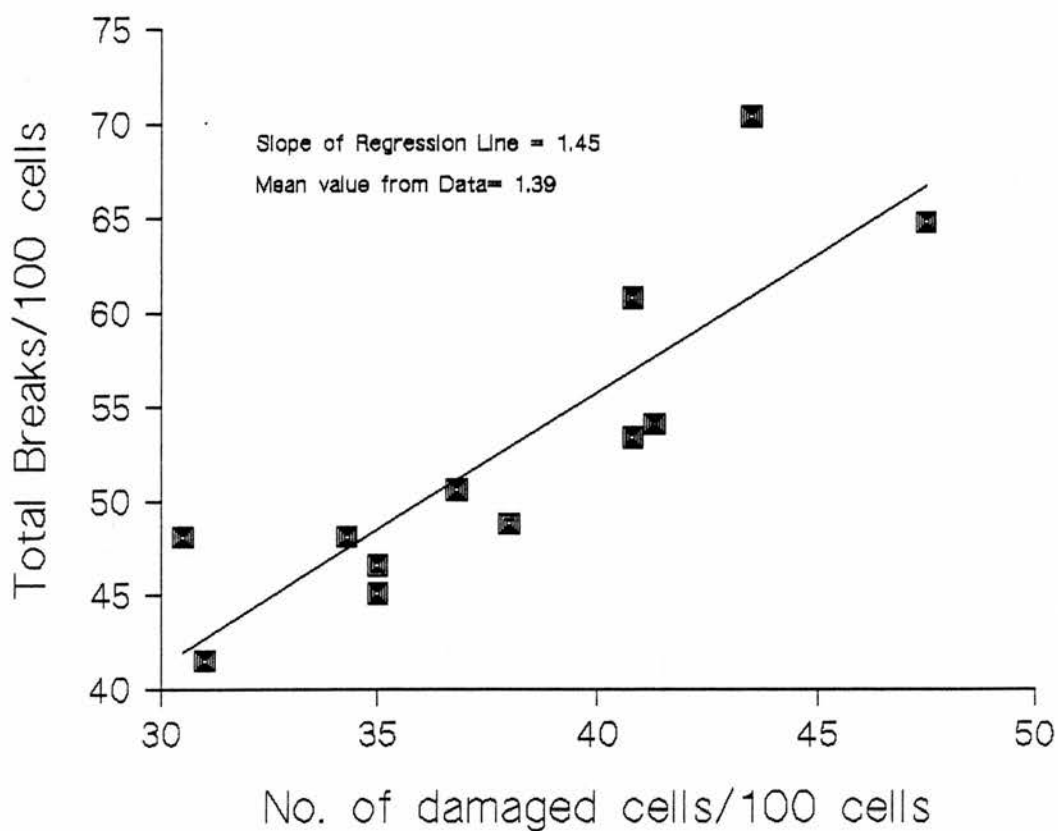


Figure 2.18 Graph of number of damage cells vs. total breaks per 100 cells for irradiated normal lymphoblastoid cell lines. A total of 12 cell lines were investigated and 400 metaphases scored in total. Results obtained from at least two independent experiments. The slope of the line represents the reduced major axis regression analysis for these data points and has a value of 1.68. $r^2 = 74.5\%$. The mean value for the data from Table 2.2 is 1.39.

ratio to compare relative sensitivity to radiation is based on the assumption that when break frequencies in non-irradiated cells or those subjected to low levels of ionising radiation (in this case 0.2 Gy), one break per cell would be expected, based on probability. For the non-irradiated values of Table 2.1 the mean value for rdi is $\bar{x} = 1.062$, $s = 0.045$. Alternatively Figure 2.17 shows a plot of the control values from Table 2.1 where the slope of the line is the rdi for normal non-irradiated lymphoblastoid cell lines. As the probability of "spontaneous" or non-induced damage is small and thus it is unlikely that an individual cell would sustain more than one "spontaneous" damage event, it may be predicted that the rdi would be near unity. Figure 2.17 shows that the non-irradiated cells have a rdi value slightly greater than unity at 1.076 from the regression analysis compared to a value of 1.062, the mean of the calculated ratios from Table 2.1.

Using the values from Table 2.2 the mean rdi value for the irradiated lymphoblastoid cells is $\bar{x} = 1.39$, $SD = 0.11$. Figure 2.18 shows the plotted irradiated values for lymphoblastoid cell lines where in this case the slope of the line representing the rdi determined by reduced major axis regression analysis, gives a value of 1.68 with a correlation coefficient of determination of 74.5%. This value for r^2 represents a poor correlation of the data of Figure 2.18 and Table 2.2 and consequently the mean rdi value from Table 2.2 will be used for comparison with the disease cell lines.

It is now possible to compare the radiation sensitivity of the various disease cell lines with the foregoing irradiated value for normal lymphoblastoid cells. This comparison is illustrated in Figures 2.19 and 2.20 using the arbitrary baseline of unity as described above and a sensitivity level 1.39 from the tabulated values (Table 2.2). With the exception of a Bloom Syndrome and two of the Down Syndrome cell lines, all show increased sensitivity to radiation-induced damage to some degree. The greatest increases in radiation sensitivity are seen in the ATM lines, one of the NBS lines and one of the p53 mutant cell lines PEGY1.

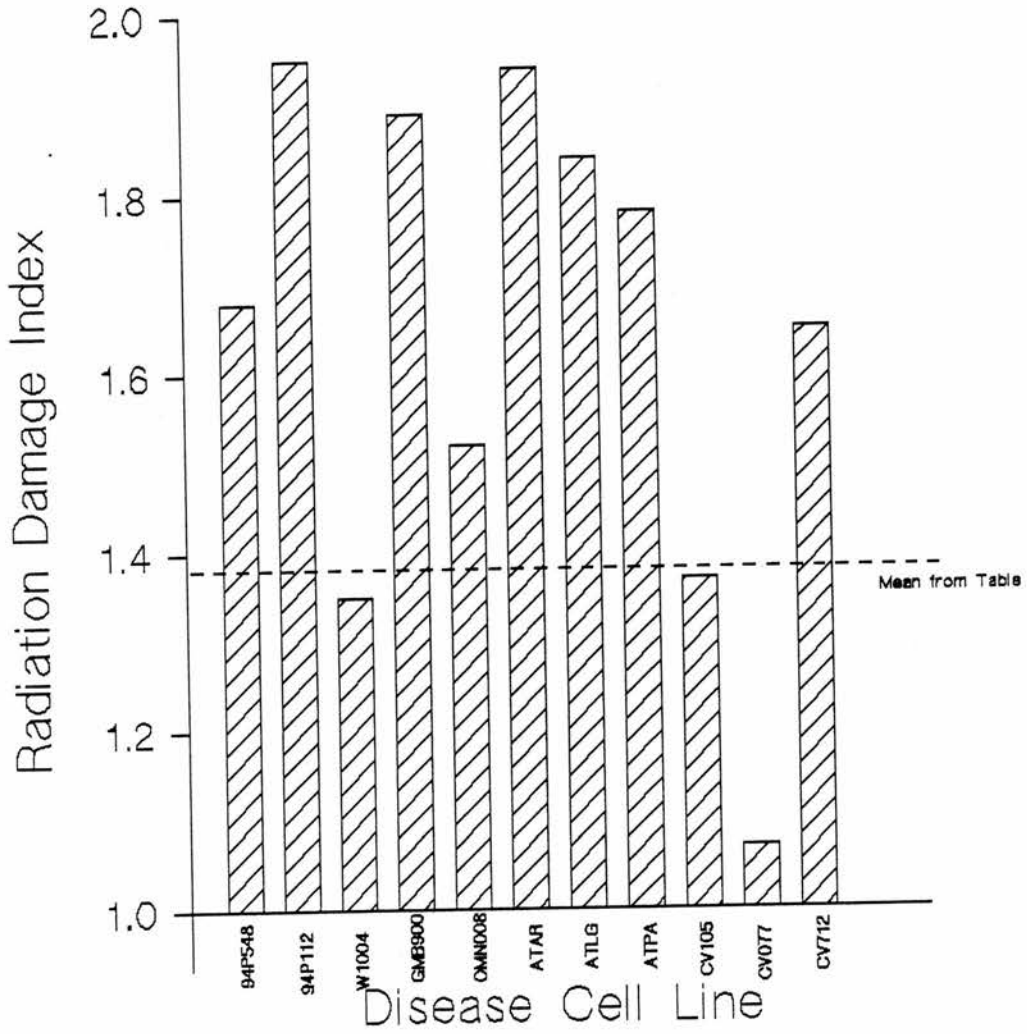


Figure 2.19. Histogram of rdi values for mutant cell lines compared to the rdi value for irradiated normal lymphoblastoid cell lines using the mean value for the data from Table 2.2. An arbitrary baseline of 1 is used, as explained in the text and a sensitivity level of 1.39 derived from the mean tabulated value.

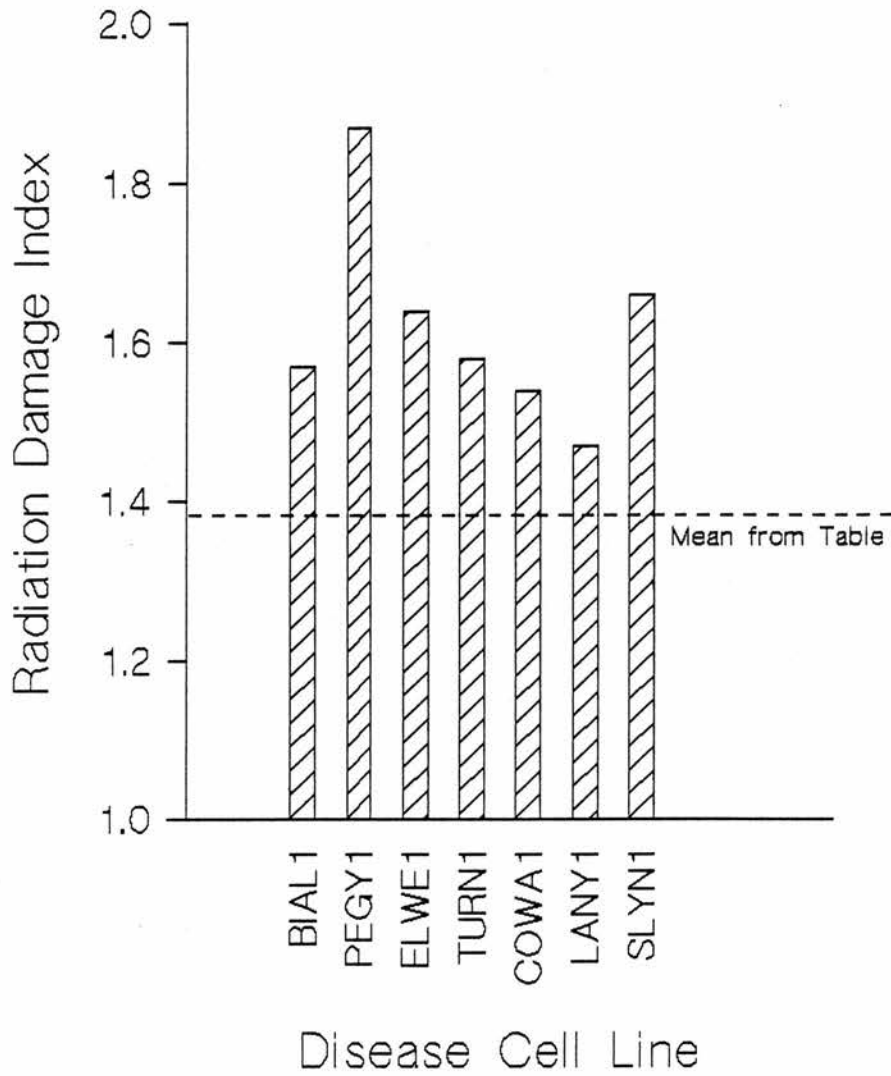


Figure 2.20. Histogram of rdi values for *BRCA1*, *BRCA2* and *p53* mutant cell lines compared to the rdi value for irradiated normal lymphoblastoid cell lines using the mean value or the data from Table 2.2. An arbitrary baseline of 1 is used, as explained in the text and a sensitivity level of 1.39 derived from the mean tabulated value.

Most of the cell lines investigated show increased sensitivity to ionising radiation also displaying a high frequency of damaged cells in non-irradiated samples (see Table 2.4) and high radiation damage index (rdi) values compared to normal lymphoblastoid cells (Figures 2.19 and 2.20). Bloom cell lines, though radiosensitive as shown by an increase in rdi (see Figure 2.19) do not have a significantly different csr in either control (non-irradiated) or irradiated conditions (Table 2.4). Similarly Down Syndrome cell lines (with one exception, CV105 irradiated) have mean rdi values not significantly different from normal lymphoblastoid lines, but the csr values indicate that one Down Syndrome cell line (CV712) is more sensitive, two (CV077 and CV105) are less sensitive to radiation-induced damage compared to normal lymphoblastoid cell lines. Although the csr values for the BRCA1 mutant cell lines (COWA₁ and LANY₁) lie well within the confidence limits for normal lymphoblastoid cell lines and like the other cell lines derived from members of families associated with familial breast cancer they show an increase in radiation sensitivity (Figure 2.20), intermediate in magnitude between the NBS (94P548 and 94P112), ATM (ATLG, ATPA, ATAR), the BRCA2 heterozygous mutants (SLYN₁ and TURN₁), p53 mutant lines (ELWE₁ and PEGY₁) and the normal lymphoblastoid lines.

2.5 Discussion

The basic chromatid breakage relationship in sections 2.4.1 and 2.4.2 show that if the total breaks, *csb* and *ncsb* vary linearly with dosage then for a specific sample time within G₂ the *csr* for that particular cell type must be constant. Therefore the invariance of the *csr* reported by various authors (e.g. Harvey and Savage, 1997, Bryant, 1998) is in fact a consequence of the linear breaks-dosage relationship for the two types of breaks observed by the same authors.

The most accurate and convenient method for displaying the linear relationship between *csb* and total chromatid breaks, is to apply reduced major axis regression analysis to the experimental data points where the slope of the resultant line represents the *csr* (Figure 2.12). The reduced major axis regression line obtained for normal lymphoblastoid cells together with 95% confidence limits on either side of this line can be used to compare this population of normal cell lines with the data points representing disease cell lines (Figures 2.14 and 2.15). It is important to note that all these data were obtained at the same sample time (1.5 hr) within the G₂ phase of the cell cycle.

It has been shown that the *csr* data obtained is normally distributed for both control and irradiated samples allowing more rigorous parametric statistics to be used when analysing the data. It has thus been possible to compare single disease cell lines to a population of normal cell lines by both calculation of *t* scores (Table 2.4) and by direct graphical comparison (Figures 2.14 and 2.15). This approach provides a much more rigorous comparison than the normal approach of comparing chromatid break frequencies in single disease cell lines with single normal cell lines (for example Antoccia *et al*, 1997) as it avoids the problem of whether or not the individual lymphoblastoid cell line used for comparative purposes is a typical "normal" line. It would be expected, as shown here, that there is some variation within a given cell line population for inherent traits and that, in the absence of any information on the spread of values for a given

characteristic under investigation, it is not possible to determine where any specific cell line falls within this distribution. The csr is in itself a convenient method of normalising the data presented and thus does not necessarily represent a biological phenomenon. It may however, be indicative of an underlying cellular mechanism occurring in the G₂ phase of the cell cycle.

When comparing disease syndrome or mutant cell lines with normals it can be seen from Table 2.4 that the t scores alone do not provide conclusive evidence of a significant departure from the csr for a normal lymphoblastoid cell population. In many cases the t score for non-irradiated cell samples is below the critical threshold value of 2.2 (see Appendix A) but the t score for irradiated cells is well above. However, comparing csr using the reduced major axis regression analysis approach (Figures 2.14 and 2.15) those cell lines with significantly different csr values can be easily identified. It would be possible, with more data from a larger number of disease cell lines to generate a reduced major axis regression line and hence the csr for all the specific disease syndrome and mutant cell populations. This approach also circumvents the problem of low absolute numbers of csb, particularly in non-irradiated cells, a problem which would normally be addressed by scoring a very large number of metaphases.

It is interesting that the ncsr is near normal for all disease cells even when the csr is significantly lower (Figures 2.16). This is due partly to the large proportion of ncsb making up the total breaks, but it also suggests the possibility that ncsb and csb are formed by different mechanisms. Although there is a wide range of radiation sensitivity, measured as the rdi (section 2.4.8 and Figures 2.19 and 2.20), generally there is a correlation between a high rdi and low csr value for ATM, NBS and p53 cell lines which is interesting since all these have been postulated to act together in damage recognition and response pathways (Zhou and Elledge, 2000). The csr and rdi of the various disease cell lines will be discussed in more detail.

There appears to be no overall correlation between sister chromatid exchanges (SCE) formation and either csr or rdi, which is in line with the accepted mechanism of SCE formation taking place in S phase, not G₂ (Lin and Wertlecki, 1982).

The regression analysis approach could also be used for analysis of peripheral lymphocyte populations to determine either total chromatid break or csr values (or any other measurable traits which show linearity). Subgroups of the population could then be identified which may carry gene mutations conferring predisposition to conditions such as breast cancer. This approach would allow a quick comparison with a normal population to be made for diagnostic purposes.

2.5.1. Bloom Syndrome, Down Syndrome

The Bloom Syndrome and Down Syndrome cell lines investigated here do not show significantly different csr to those obtained for the normal lymphoblastoid cell lines (Table 2.4). This suggests that in the case of Bloom Syndrome that either the defective helicase is not involved in the recombinogenic mechanism that gives rise to colour switch breaks or that there is an equally effective alternative pathway operating which allows these types of breaks to occur at the same frequency as when the gene implicated in the Bloom Syndrome condition is fully operational. As the defective gene in this case is a member of the human equivalent of the RecQ helicase family (Ellis *et al*, 1995), all of which have a greater affinity for single-stranded rather than double-stranded DNA, it is perhaps not surprising that the processing of double-strand breaks associated with recombinogenic mechanisms such as the postulated signal model do not appear to be dependent on the activity of these types of gene products. Further supportive evidence for the lack of involvement of this gene product in the putative signal model pathway is the absence of any trend towards an increase in sister chromatid exchanges (SCE) with damage in the Bloom Syndrome cell lines investigated. A diagnostic feature of this

condition is a very high rate of SCE so it may be expected that the greater the amount of induced damage in the cells, the greater the SCE formation. The lack of any overall increase in SCE with damage in any of the cell lines investigated supports the generally accepted view that SCE formation occurs at S phase as a result of the replication machinery encountering breaks in the replicating DNA strand rather than as a result of exchanges between sister chromatids after recombinational repair in G₂. One Bloom Syndrome cell line (GMB900) does however display a greater radiation sensitivity than normal cells which confirms previous observations (Ellis *et al*, 1995). Ionising radiation is responsible for producing a wide range of damage types within a target cell, the vast majority of which are single strand breaks (ssb), so that the increased sensitivity of these cells to induced radiation damage may be due to unrepaired single-strand DNA breaks.

Down Syndrome is classically associated with Leukaemia and an increase in chromosomal abnormalities due to the extra chromosomal material present within the cells (Porter and Paull, 1974). The severity of clinical presentation of individual Down Syndrome patients varies a great deal and thus it may be expected that the cellular characteristics may also show variation (Table 2.4). The results presented here support this since the csr for irradiated cells varies more within these cell lines than within other disease cell lines. Also the degree of radiation sensitivity varies, with Down Syndrome lines displaying both radiosensitivity and radioresistance (Figure 2.19). Such differences may be due to changes in cell cycle kinetics or to changes in the kinetics of pathways involved in damage sensing and/or repair leading to an overall increase in genomic instability caused by the presence of an extra chromosome. Down Syndrome cell lines (CV077 and CV105) have rdi values below the threshold levels and hence normal radiation sensitivity (Figure 2.19). One Down Syndrome line (CV105) has a t score for irradiated cells of 3.6, showing a significantly lower csr value while another (CV077) has a t score of 1.6 for irradiated cells, well below the threshold value of 2.2 (Table 2.4), indicative of a csr value similar to that obtained for the normal lymphoblastoid cell population. The remaining Down Syndrome cell line (CV 712) displays elevated

sensitivity to ionising radiation (Figure 2.19) yet has a normal csr value (Table 2.4). Thus there does not seem to be any relationship between the csr value and the degree of radiosensitivity displayed by these cell lines.

2.5.2 ATM and NBS cell lines

The ATM and NBS lymphoblastoid cell lines investigated here all show csr which are significantly different from the normal lymphoblastoid cell lines (Table 2.4 and Figure 2.14). These findings support the hypothesis that ATM and the MRE11/RAD50/nibrin complex are involved in a damage processing pathway which involves inter- and intra-chromatid recombinational events. If incomplete at mitosis, this mechanism would give rise to both intra- and inter- (colour switch) chromatid breaks. Although all the ATM non-irradiated samples have t scores below the critical value for significance, the irradiated values are significantly different from the normal population (Table 2.4). This is clearly illustrated when comparing the individual data points with the csr obtained by reduced major axis regression analysis of the normal lymphoblastoid cell lines (Figure 2.14). There are insufficient data to calculate a reduced major axis regression line to give a csr value for the ATM population as a whole (see section 2.4.2). However it can be seen that given more data it would be possible to produce such a value and that the data available suggests that this csr would be lower than that obtained for the normal lymphoblastoid cell population. Similarly, the values obtained for NBS cell lines are significantly different from both the non-irradiated and irradiated lymphoblastoid cell lines investigated (Table 2.4 and Figure 2.14). As with ATM cells, if a greater number of cell lines were available for analysis, it would also be possible to calculate a csr value for the NBS lymphoblastoid cell population using reduced major axis regression analysis. The results currently available indicate a significantly lower csr than either the ATM or the normal cell lines, since both non-irradiated and irradiated values are significantly lower than those obtained for the normal population.

The wide-ranging interactions of ATM and NBS (section 2.4.4.1) involving both homologous and non-homologous recombination repair pathways mean that it is impossible to determine from the results presented here whether the reduced csr is due to an abrogation in the RAD51-dependent homologous recombination (HR) pathway or the RAD50-dependent non-homologous end-joining (NHEJ) pathway, or both. However, HR has been postulated to be the major repair pathway in G₂ so it is likely that it is this ATM-dependent route that is most affected by the loss of wild type *ATM*. It is however not possible to determine from these studies which homologous recombination pathway(s) (section 1.5) may be *ATM*-dependent and thus produce a low csr. This postulate is further supported by the correlation between rdi and csr observed for *ATM*, NBS and p53 cell lines, suggesting that these proteins may be involved in the same pathway, the loss or reduction of which leads to increased chromosomal (and hence genomic) instability and decreased ability to form csb which are formed via a recombinational pathway.

The increased radiosensitivity of both NBS and *ATM* cell lines (Figure 2.19) is in agreement with previously published work (e.g. Liu and Bryant, 1994, Morgan *et al*, 1997, Pandita and Hittelman, 1992, Thacker, 1989; Varon *et al*, 1998; Digweed *et al*, 1999) and is indicative of a deficiency in either the ability of the cell to recognise DNA damage or to act on such information. An alternative possibility, that csb induction in *ATM* and NBS cells is normal but rejoining rates of csb are faster than those observed in normal cells, which would give rise a lower csr endpoint. This explanation is contrary to previous observations on the formation and repair of damage in *ATM* cells and also to experimental evidence presented in Chapter 3.

The *ATM* and NBS gene products are believed to be components of a network of proteins responsible for repair of dsb and regulation of cellular proliferation (Lavin *et al*, 1999; Wang, 2000), with *ATM* playing a central role in these events. The increase in the

absolute number of breaks per cell compared to normal lymphoblastoid cell lines supports the view that in ATM (and NBS) cells there is a higher rate of conversion of dsb to chromosome breaks (Liu and Bryant, 1994). This higher conversion rate is indicative of an increase in genomic instability which leads to the characteristic early-onset cancers in patients with these conditions (Savitsky *et al*, 1995; Shiloh, 1997; Digweed *et al*, 1999). It has been shown that ATM, ATLD and NBS cells all display a reduced p53 response when subjected to DNA damaging events (Banin *et al*, 1998; Nakaurama *et al*, 1998; Kastan *et al*, 1992; Khanna and Lavin, 1993), with ATM interacting with both p53 (Khanna *et al*, 1998) and NBS (Gatei *et al*, 2000b; Lim *et al*, 2000; Wu *et al*, 2000; Zhao *et al*, 2000) to inhibit cell cycle progression and DNA synthesis in damaged cells. The reduced csr obtained for p53 mutant cell lines (Table 2.4 and Figure 2.15) is also supportive of the idea that ATM and p53 are both required for the functioning of this processing pathway.

Nibrin, the protein mutated in NBS (Carney *et al*, 1998; Varon *et al*, 1998) has been shown to complex with hRAD50 and hMRE11 which are required for both non-homologous recombination and heteroduplex formation between recombining chromosomes. The hRAD50/hMRE11 complex, which has been shown to form discrete nuclear foci in response to dsb-inducing agents (Maser *et al*, 1997) is also known to associate with the DNA-PK/Ku complex, suggesting that non homologous recombination may be an alternative mechanism occurring in response to a damage signal.

The loss of this pathway by mutation of the *ATM* or *NBS* genes in these cells has reduced, but has not abolished the ability of the cells to undergo recombinational repair leading to csb where this process has failed to go to completion before the cell enters mitosis (Bryant,1998). Evidence from other experimental data suggesting that the MRE11/RAD51/p95 complex is principally associated with homologous recombination (HR) (Maser *et al*, 1997) and the MRE11/RAD50/p95 complex with non-homologous

recombination (NHEJ), makes it impossible to determine whether HR or NHEJ is the principle pathway leading to the formation of *csb*, but the favoured pathway is likely to be HR in G₂.

2.5.3. Cell lines derived from families with breast cancer.

The BRCA1 heterozygous mutant cell lines have *csr* values not significantly different from the normal lymphoblastoid cell population (Table 2.4) and well within the 95% confidence limits for normal lymphoblastoid cells (Figure 2.15). As BRCA1 is considered to be a classic tumour suppresser gene, like the retinoblastoma (*Rb*) gene first described by Knudson in the formulation of his two-hit hypothesis for cancer formation; it displays a normal phenotype if a normal copy of the gene is present. However, the higher radiation sensitivity observed for these cells, though not as extreme as that observed for the ATM, NBS or p53 mutant cell lines, nevertheless suggests that there is an increase in genomic instability in these lines. This is detectable by an increased occurrence of damage events per cell compared to normal lymphoblastoid cells, following exposure to ionising radiation (Figure 2.20). This observation is in agreement with the recently published theory on the association of a BRCA1^{+/-} genotype with cancer predisposition and/or onset if the individual is haplo-insufficient, (i.e. if a precursor cell had sustained a germline mutation at a critical locus such as p53) and thus has an impaired ability to maintain genomic integrity (Scully and Livingston, 2000). BRCA1, like ATM and the NBS/MRE11/p95 complex has been shown to interact with both RAD51 (Lakin *et al*, 1996; Sharan *et al*, 1997; Banin *et al*, 1998; Tibbetts *et al*, 1999) and RAD50 (Zhong *et al*, 1999), suggesting it may play a role in regulation of both homologous and non-homologous recombination. The presence of a single functional copy of the BRCA1 gene may also affect the levels of protein expression within the cell, or the kinetics of interaction with its cellular targets. The precise role of BRCA1 in *csb* formation cannot be determined at present since viable BRCA1 homozygous mutant cells have not been

available, although breast-specific *BRCA1* inactivation has now been achieved (Cortez *et al*, 1999).

The *BRCA2* mutant cell line investigated here has a significantly lower *csr* than the normal population and a significantly elevated *rdi* (Figure 2.20). The *csr* result suggests that heterozygous mutants of *BRCA2* may also display increased genomic instability due to haplo-insufficiency as described for *BRCA1*. Enhanced radiosensitivity of both *BRCA1* and *BRCA2* heterozygote cells has been previously reported using clonogenic and micronucleus assays as endpoints, but the G₂-specific response of these cell types was not addressed (Foray *et al*, 1999a). This difference in results from *BRCA1* and *BRCA2* is interesting since *BRCA2* (in contrast to *BRCA1*) interacts only with RAD51 which regulates homologous recombination repair pathways and not RAD50, associated with non-homologous end-joining (Scully and Livingston, 2000). This is further support for the postulate that the principle pathway for the formation of *csb* is that of the homologous recombination repair pathway.

The correlation of low *csr* and high *rdi* displayed by the p53 mutant cell lines indicates the importance of p53 in damage recognition and signalling to maintain the genomic integrity of cells but is inconclusive as to which recombinational pathway is the principle mechanism for formation of *csb*. Although p53 is known to interact with ATM (Lavin and Khanna, 1999), *BRCA1*, *BRCA2* (Scully and Livingston, 2000) and the NBS protein (Jongmans *et al*, 1997; Matsuura *et al*, 1998 and Antoccia *et al*, 1999), the wide-ranging cellular interactions of p53 make it impossible to single out a single effect with this type of experimental approach.

The lymphoblastoid cell lines with unknown mutations investigated here derived from families with breast cancer show both significantly different *csr* (Table 2.4 and Figure 2.15) and enhanced radiation sensitivity (Figure 2.20) compared with normal lymphoblastoid cell lines. Although it is not possible to speculate on the causes of these differences, they

do suggest that these family members may have an elevated level of genomic instability. They may carry mutations which alter but do not abolish the function of gene products associated with recognition, repair of DNA damage and/or cell cycle checkpoints. Such subtle changes in gene function are harder to detect and quantify than complete or partial abolition of gene function, but they may "potentiate" the affected cells, rendering them vulnerable to transformation if subjected to further damaging events.

2.5.4. Omenn Syndrome

The low csr reported here for the Omenn Syndrome cell line suggests that a significant number of csb formed in normal lymphoblastoid cell lines are produced via a non-homologous end-joining (NHEJ) mechanism. The *RAG* genes mutated in this syndrome are responsible for a wide range of clinical symptoms associated with defective B and T cell formation due to defective VDJ recombination in developing lymphocytes (Van Gent *et al*, 1996). The results presented here suggest that this recombinogenic mechanism is used in B cells throughout their lifetime and may be a common pathway for repair within cells. The lack of any increase in radiation sensitivity (Figure 2.19) suggests that this cell line is not deficient in the damage recognition pathways normally employed by cells in G₂. These observations suggest that the formation of colour switch breaks (csb) is possible via at least two recombinogenic pathways, one of which utilises a *RAG* -dependent pathway involving NHEJ.

2.6 Future Work

The principle analytical approach adopted here is the linear or reduced major axis regression analysis of normal lymphoblastoid lines to obtain a csr value for a normal population. This allows the comparison of single (or populations) of syndrome cell lines to be easily and directly compared with a normal population to determine if they are significantly different. This approach is one that can be adapted for any cell population and any trait, providing it is possible to perform a regression analysis on the data. The advantage of this approach is that the value assumed for a normal population is based on a large experimental sample which once established can be used repeatedly to assess individuals for normality. It could thus be suitable for a wide range of diagnostic applications.

There is evidence for HR being the principle pathway leading to the formation of csb, and for the involvement of ATM, the NBS protein (and thus the MRE11/RAD51/p95 complex), BRCA2 and p53 in this pathway. Although results supporting the involvement of BRCA1 in this pathway are inconclusive, new developments in generating viable cell lines lacking functional BRCA1 (Cortez *et al*, 1999) would enable the importance of this gene product to be elucidated. Of particular interest is the possible role of BRCA1 and BRCA2 in chromatin remodelling. It has been postulated that formation of a dsb, which itself causes active chromatin remodelling in the vicinity of the break (cited in Paul *et al*, 2000), may trigger the release of BRCA1 for recruitment to the break region, where it interacts with recombinational repair proteins like RAD51 (Scully and Livingston, 2000 and references therein). The hamster mutant cell lines of complementation group XRCC8 displays phenotypic characteristics similar to those observed in ATM and NBS cells and the defective gene in this line is thought to be the hamster homologue of ATM in humans ((Johnson *et al*, 2000). It would therefore be of interest to determine if the chromatid break characteristics and csr for this cell type are similar to those observed for ATM and NBS lymphoblastoid cell lines.

Although a principle pathway probably exists, there are alternative pathways giving the same endpoint and hence a degree of redundancy in the system. Further information is required to obtain a csr value for these syndrome cell populations before the relative importance of these gene products within repair pathways can be considered. It would also be of interest to investigate lymphoblastoid cell lines which are deficient in combinations of genes implicated in the proposed recombinogenic pathway to investigate how the csr is affected, particularly if the two genes targeted are suspected of acting in parallel but distinct recombinational pathways. An interesting combination (if possible) would be a double mutant cell line lacking wild type *ATM* and *RAD50* and to compare the csr and rdi characteristics of these cells with an *ATM* and *RAD51* double mutant cell line as well as with a normal cell population. This may provide good evidence in support of a principle pathway for the formation of csb within G₂. An alternative approach could be to use site-directed mutagenesis to produce cell lines with particular regions of these key genes missing or inactivated and compare break characteristics with cells containing wild type genotypes.

An interesting strategy might be to unravel the numerous interactions in which ATM is involved within the cell and their relative role in csb formation. It would be interesting to investigate whether DNA damage sensors like ATM and BRCA1 only recognise a particular type of dsb. It may then be possible to categorise dsb subtypes in terms of how the chromatin around the dsb is remodelled and other structural factors influencing its three-dimensional presentation to such sensor proteins. This may then lead to the recruitment of different repair complexes to initiate repair that may be recombinational and give rise to different types of chromatid aberration at metaphase if incomplete when the cell enters mitosis. Not only must a cell be able to sense and react to DNA damage but it must also be aware of when repair is complete and successful so that the cell cycle can proceed. The role of DNA damage sensors such as ATM, BRCA1/2, p53 and also DNA-PK in monitoring this whole process from damage recognition to completed repair

and resumption of normal cell cycle function needs to be addressed. It is possible that the breakdown in these feedback mechanisms promotes an increase in genomic instability and thus increases the chances of tumourgenesis. The role of telomeric complexes, which include ATM, in these genomic surveillance mechanisms also needs to be further explored.

Chapter 3

Rejoining characteristics of chromatid breaks

Contents	Page No.
3.1. Introduction	130
3.1.1. Conversion of double-strand breaks into chromosomal breaks	131
3.1.2. Models of double-strand break repair and chromatid break rejoining kinetics	133
3.2. Materials and methods	
3.2.1. Cell culture and BrdU treatment	140
3.2.2. Irradiation and harvesting	140
3.2.3. Preparation of slides	141
3.2.4. Fluorescence plus giemsa (FPG) staining	141
3.2.5. Scoring and analysis	141
3.3. Results	
3.3.1. Break frequencies in normal lymphoblastoid cells	143
3.3.2. Basic theory of breakage rejoining in G ₂	147
3.3.3. Rejoining characteristics for normal lymphoblastoid cells	151
3.3.4. The chromatid breakage surface	152
3.3.5. Chromatid breakage surface for normal lymphoblastoid cells	157
3.3.6. Rejoining characteristics of ATM and NBS cells	164
3.4. Discussion	179
3.4.1. Rejoining characteristics of normal lymphoblastoid cells	179
3.4.2. Rejoining characteristics of chromatid breaks in syndrome cell lines	183
3.4.3. Summary and conclusions	189
3.5. Future Work	191

3.1. Introduction

The importance of functional DNA repair mechanisms within the cell to prevent the accumulation of genomic damage cannot be overstressed. Many heritable syndromes are associated with genetic and chromosomal instability which has been shown to confer a cancer-predisposition phenotype (Parshad *et al*, 1996; Sanford *et al*, 1989; Scott *et al*, 1994; 1996; 1999). The chromatid break characteristics of some of these heritable syndromes are considered in Chapter 2. The DNA double strand break (dsb) is considered to be the major lethal lesion induced by ionising radiation in cells, these give rise to chromosomal aberrations (Bryant, 1984; 1997; Natarajan and Obe, 1984, Frankenberg-Schwager and Frankenberg, 1990). The possible mechanisms of dsb repair are described in Chapter 1 and will not be considered here. However it is important to consider the critical role such repair pathways fulfil in the maintenance of genomic integrity.

Studies of mammalian cell lines investigating the possibility of a correlation between dsb induction and radiation sensitivity are not all in agreement. Some studies indicate a correlation between initial dsb induction and cellular radiosensitivity (Macmillan and Peacock, 1994; Ruiz de Almodovar *et al*, 1994), whereas other research has not found any correlation (Smeets *et al*, 1993). It has been estimated using pulse field gel electrophoresis (PGFE) that 1.2% of dsb remain unrepaired (Dahm-Daphi *et al*, 1996) and that it is these residual dsb that determine the radiosensitivity of a particular cell line. It is therefore important to understand the mechanisms by which a dsb gives rise to a chromosome or chromatid aberration since it is this endpoint which is frequently used to assess the extent of damage to a cell population following exposure to ionising radiation (or restriction endonucleases).

3.1.1. Conversion of double-strand breaks into chromosomal aberrations.

The frequencies of chromosomal breaks in mutant (xrs) rodent cell lines deficient in repair of double-strand breaks (dsb) and the wild type CHO parental cell lines have been investigated (Kemp *et al*, 1984; Bryant *et al*, 1986; Illiakis *et al*, 1988; Macleod and Bryant, 1992). Both xrs5 and CHO cell lines displayed equal frequencies of double-strand breaks are induced by a given radiation dose (Illiakis *et al*, 1988). However the xrs cells display a higher degree of radiosensitivity and increased frequency of chromosomal aberrations than the wild type CHO cells (Kemp *et al*, 1984). Thus it appears from this work that it is not the initial rate of dsb induction but the efficient repair mechanism and the relatively large number of residual dsb that is the important factor in whether a cell population has a radiosensitive phenotype, although this does not appear to be the reason for the observed elevated frequency of chromatid breaks in xrs5 cells. The rate of dsb rejoining in these cells has been found to be more rapid in G₂ than in the G₁ phase of the cell cycle (Mateos *et al*, 1994).

Cornforth and Bedford (1983) used the premature condensed chromosome (PCC) method to investigate the conversion of dsb into chromosome breaks (i.e. breaks formed in G₁ chromosomes). This technique, in which G₁ or G₀ chromosomes are fused with mitotic cells allows visualisation of interphase chromosomes, therefore making it possible to measure radiation-induced damage nearer to the exposure event (~20 min post-irradiation) than would be possible using cytogenetic analysis as an end point (~1 hr). Cornforth and Bedford refined the PCC method devised by Johnson and Rao (1970) by using BrdU-substituted mitotic cells to allow easier differentiation between mitotic and G₁ chromosomes. The disappearance of fragments, which was assumed to equate with the rejoining of dsb, displayed first-order kinetics. ATM cell lines

(see Chapter 2 for ATM characteristics), have the same initial numbers of PCC fragments as wild type cells but a higher frequency of PCC fragments persists in ATM cells over time.

The situation is more complicated when considering the G₂ phase of the cell cycle. When PCC is performed on cells in G₂ there is a difference in the initial frequencies of observed fragments between ATM and wild type cells (Pandita and Hittelman, 1992; Mozdarani and Bryant, 1987). This, together with the reported increased frequencies of chromatid breaks between one and one and a half hours post-irradiation, suggests that the conversion of dsb into chromatid breaks is more immediate and not purely the result of the continued presence of residual dsb within the genome. This hypothesis is supported by display of normal repair characteristics by ATM cells (Lehmann and Stevens, 1977; Foray *et al*, 1997). In addition the rejoining of chromatid breaks observed in both ATM and wild type cells can be blocked by treatment of cells with 9- β -D-arabinofuranosyladenine (ara A) which is an inhibitor of dsb repair in Ehrlich ascites tumour cells (Bryant and Blocher, 1982). However the absolute frequencies of chromatid breaks remained higher in ATM cells compared to wild type (Mozdarani and Bryant, 1987; 1989; Bryant 1997). A similar comparison can be made between wild type CHO and X-ray sensitive (xrs) cell lines, the latter of which show an overall deficiency in dsb repair (Kemp *et al*, 1984). Short intervals after irradiation in G₂, where dsb repair in both cell lines is considered to be normal, absolute frequencies of chromatid breaks in xrs5 cells are higher than those in CHO cells (Bryant and Slijepcevic, 1992; Mateos *et al*, 1994).

Thus it would appear that dsb repair may play a more direct role in the production of chromosome breaks in G₁, but the relationship between dsb repair and chromatid break frequency in G₂ is more complex. In order to

achieve a better understanding of both the importance and characteristics of dsb repair it is useful to develop quantitative models which can be applied both as a useful analytical tool to assess measured data and also to predict repair kinetics and test such hypotheses experimentally.

3.1.2. Models of double-strand break repair and chromatid break rejoining kinetics.

The use of various forms of mathematical model to study the break frequencies and potential lethality of high doses of ionising and other forms of radiation is well established (Tubiana *et al*, 1990; Reddy *et al*, 1995; Lange *et al*, 1997). Such models are useful in developing effective radiotherapy treatments (Ostashevsky, 1992; Brenner *et al*, 1998) and predicting the physical consequences of high levels of radiation exposure. Radioyevitch *et al*, (1998) used data obtained using pulsed-field gel electrophoresis to investigate the types of double-strand breaks (dsb) produced by high doses (80-160 Gy) of X-rays. They fitted their data to three models; the Revell binary misrejoining (RBM) model, the Sax subset (SS) model and the Revell subset (RS) model. The RBM model assumes that dsb can either form complete exchanges with other dsb or be repaired. The SS model assumes two types of dsb, those that can be repaired and are considered inactive and those which will be misjoined and are therefore active. The RS model is based on a Revell-type misrejoining mechanism and assumes all dsb are essentially the same but all have the potential to misjoin or repair and hence there are effectively two dsb subsets depending on how a dsb is resolved. Their analysis supported the hypothesis that at least two types of dsb are formed at high doses of radiation and thus their findings did not support the RBM model. However they were unable to distinguish between the latter two models (SS and RS) using the available data.

Studies have also been published suggesting that residual levels of damage remain following dsb repair in cells exposed to radiation levels in the range 10 - 80 Gy (Foray *et al*, 1999). In these investigations, DNA damage was measured as a fraction of activity released (FAR) by pulsed-field gel electrophoresis (PFGE). Using this technique, cells with ^3H -thymidine incorporated in the DNA of the nucleus are irradiated and the measured fraction of activity released when the cells are run out on a gel can be equated to the number of dsb present within the sample using the formula devised by Blocher (1990). The presence of residual DNA damage following dsb repair suggests that, within the dose range considered, dsb repair is never complete, i.e. some residual dsb always remain, albeit after a dose of some 30 Gy.

These and other similar findings and their analysis in terms of the models described above are informative as to the repair of DNA subjected to lethal levels of radiation damage. However these same models are not directly applicable to damage induced in cells at low LET sub-lethal dose exposures, where the absolute numbers of dsb induced are much lower and where the long-term consequences of radiation exposure history is of principle interest.

The kinetics of double-strand break (dsb) repair at low radiation doses can be measured using a range of techniques including neutral elution and premature chromosome condensation (PCC). The PCC technique was used to compare the repair kinetics of damage induced by alpha particles (2.7 Gy) and X-rays (6 Gy) by applying first and second order kinetic models (Loucas and Geard, 1994). The first order kinetic model can be further subdivided into one with a single repair component or with two components. The equation describing the single component model is:

$$Y = Ae^{-kt} + C \quad (3.1)$$

where Y = yield of prematurely condensed chromosomes and fragments at time t ; A = fraction of fragments which eventually rejoin, C = sum of chromosomes and residual fragments and k = rejoining rate constant (Loucas and Geard, 1994).

The two component model equation is:

$$Y = Ae^{-k_1t} + Be^{-k_{ij}t} + C \quad (3.2)$$

where A = the fraction of fragments which rejoin with fast kinetics; B = the fraction of fragments which rejoin with slow kinetics; k_1 = rejoining rate constant of the fast component; k_{ij} = rejoining rate constant of the slow component and Y , C and t are the same as for the single component model (3.1).

A second order kinetic model predicts that higher numbers of induced breaks will result if faster rates of rejoining occur. Second order kinetics can be described by the equation:

$$Y = [A/(1 + Akt)] + C \quad (3.3)$$

where A = fraction of breaks capable of rejoining; k = rejoining rate constant and Y , C and t are the same as for (3.1) (Loucas and Geard, 1994). Using this approach it is possible to calculate the number of dsb at time zero, ($t = 0$) without the need to either attempt to directly measure this or graphically extrapolate back data points. Both first order kinetic models fitted the data presented by Loucas and Geard (1994) with similar rejoining rates for both high LET (alpha particles) and low LET (X-rays) but with a greater number of excess

fragments remaining in the X-ray treated samples. The half time ($t_{1/2}$), which is the time taken for the measured yield of chromosome fragments to halve was 1.7 hr for the simple first order model (equation 3.1) and is agreement with the $t_{1/2}$ reported by Cornforth and Bedford (1983). A half time of a few minutes for the fast component of the two component first order model and a $t_{1/2}$ value of 1 - 4 hr for the slow two component first order kinetic model (equation 3.2) was determined. The data did not fit the second order model (equation 3.3). A slightly different approach was adopted by Foray *et al*, (1996) in interpreting dsb repair as biphasic, i.e. the repair half time is continuously changing with time, possibly reflecting a continuous spectrum of ability to repair damage or different modes of dsb repair (Pfeiffer *et al*, 2000). Studies investigating the kinetics of recombinational repair of plasmid DNA dsb and gaps of different sizes in the *Saccharomyces cerevisiae* mutant *rad54-3* indicated that small DNA double strand gaps and breaks (up to 400 bp) are repaired with different kinetics compared to large (~1.4 kbp) (Glasunov *et al*, 1995). Small gaps and breaks followed a first order two component repair model with the two phases separated by a plateau. They found that larger breaks have repair kinetics which only followed the second phase of repair. The first rapid phase of repair is performed by constitutively expressed enzymes whereas in the second slower phase repair is carried out by inducible enzymes.

The postulate that dsb rejoining kinetics following the two component first order model is further supported by an investigation of dsb rejoining in *xrs5* cells which are associated with a deficiency in dsb rejoining detectable by elevated break frequencies (Mateos *et al*, 1994). The filter elution technique was used to determine $t_{1/2}$ values of 9 min and 3.6 hr for the fast and slow components respectively. It must be borne in mind when comparing repair half times that dsb rejoining kinetics is cell cycle dependent. Double strand breaks rejoin more rapidly in G₂ than G₁; measured $t_{1/2}$ values are 15 min and

8.8 hr for G₁ compared to 9 min and 3.6 hr for G₂ (Mateos *et al*, 1994). These observations suggest that there is no deficiency in dsb repair in *xrs5* cells in G₂ and is dependent on the assumption that similar repair pathways with similar kinetics operate in both G₁ and G₂ phases of the cell cycle.

The two component first order kinetics of double-strand break repair cannot be completely investigated using metaphase analysis as an end point even when solely investigating the G₂ phase of the cell cycle. This is because the rejoining of dsb in the first phase of the two component model proceeds too rapidly compared with the time scale of allowing cells to proceed to mitosis (Bryant and Slijepcevic, 1993). Measurement of chromatid break rejoining kinetics is still possible but relating this to the repair kinetics of the dsb which give rise to such chromatid breaks is more difficult suggesting a possible dissociation between dsb and chromatid breaks. For example studies of the rejoining kinetics of chromatid breaks in mouse CB17 and SCID cells (Bryant *et al*, 1998) showed similar rejoining kinetics for both cell types ($t_{1/2} = 1.5$ hr) but an elevated frequency of chromatid breaks. This similarity in "rejoining" of chromatid breaks occurred even though SCID cells are deficient in their ability to rejoin dsb suggesting a higher rate of conversion of dsb into chromatid breaks in SCID cells. This and another study looking at the effects of adenine arabinoside (ara A) on chromatid break rejoining kinetics (MacLeod and Bryant, 1992) did not distinguish between chromatid break subtypes or apply first order repair kinetic models to the data. The conclusion drawn from the work of both Bryant *et al*, (1998) and Macleod and Bryant, (1992) is that the measured rate of rejoining of chromatid breaks cannot be related to dsb rejoining kinetics.

More recently the PCC technique has been used in conjunction with fluorescence *in situ* hybridisation (FISH) to investigate the kinetics of

chromatid break rejoining in lymphocytes following low-LET irradiation (Sipi *et al*, 2000). Although a rejoining time $t_{1/2} = 1$ hr was measured it was not possible to make a direct comparison between results from the G₂-PCC and the cytogenetic analysis of G₂ metaphases due to the 30 min incubation period prior to colcemid treatment giving a total incubation time of 1.5 hr.

A different study has however successfully attempted to quantify radiation-induced chromatid break rejoining kinetics with initial dsb formation and subsequent repair (Gotoh *et al*, 1999) allowing comparison with experimental results. The approach adopted was to use a modified premature chromosome condensation (PCC) technique using calyculin A (a specific inhibitor of protein phosphatases type 1 and 2A) to induce precipitation of chromosomes. This faster technique allows break frequencies to be measured more rapidly as condensation occurs within 5 min following the addition of calyculin A, compared to a minimum time of 20 min for the method used by Cornforth and Bedford (1983). A range of 0 - 4 Gy gamma irradiation was used together with a rejoining time of up to 8 hr. The initial linear chromatid break-dose relationship was characterised and kinetics of PCC rejoining investigated. Their results conform to a two-component first-order kinetic model (equation 3.2) for chromatid breaks as described by Loucas and Geard (1994), but not for exchanges. The half times for the fast and slow components were $t_{1/2} = 5$ min and 90 min respectively and more significantly, the rejoining rate constant (k) was found to be constant within the radiation dose range used. Their findings support the hypothesis of different rejoining kinetics for G₁ and G₂ which is indicative of different rejoining mechanisms operating in these cell cycle phases, possibly non-homologous end joining (NHEJ) in G₁ - early S phase and recombinational repair in the late S - G₂ phase of the cell cycle.

In the present investigation the rejoining of chromatid breaks induced by a low

dose of ionising radiation was measured for a normal lymphoblastoid cell line (NC). A dose of 0.4 Gy was used for this investigation rather than the higher irradiation dose used by Macleod and Bryant, (1992) of approximately 0.8 Gy in lymphocytes to ensure sufficient numbers of metaphases were available for scoring. Relative numbers of non-colour switch breaks (ncsb) and colour switch breaks (csb) were determined to examine whether the csr is constant with time as assumed by the signal model (Bryant, 1998) and other published research investigating colour switch break frequencies (Harvey and Savage, 1997). The analysis carried out in 3.3.5 enabled predictions to be made regarding the chromatid break frequencies already measured at 0.2 Gy and discussed in Chapter 2 (Table 3.2). These predictions were then further tested experimentally at $t = 3$ hr.

Chromatid break rejoining characteristics were then determined for a homozygous ATM (ATAR) and an NBS (94P112) lymphoblastoid cell line. It was shown in Chapter 2 that these ATM and NBS cell lines had a significantly lower csr than that obtained for a population of normal lymphoblastoid cell lines (Figure 2.14). It would therefore be of interest to determine if the chromatid break rejoining characteristics of these cell lines also differed from that of normal lymphoblastoid cell lines.

Results were analysed to determine if they fit the two component first order kinetics model used previously (Loucas and Geard, 1994; Gotoh *et al*, 1999). The possibility of development of a quantitative model linking the three variables in this experimental system (i.e. dose, chromatid breaks and time) is fully discussed resulting in a proposed three-dimensional breakage surface model representing the G₂ phase of the cell cycle.

3.2. Materials and Methods

3.2.1 Cell culture and BrdU treatment

The normal lymphoblastoid cell line (NC), the ATM (ATAR) and NBS (94P112) cells lines were those used in Chapter 2. The cell lines were grown in RPMI 1640 (Gibco BRL) + 50 IU ml⁻¹ Penicillin, 50 µg ml⁻¹ streptomycin (Gibco) supplemented with 2mM L-glutamine and 10% foetal calf serum (Gibco) initially in 25 cm³ closed vent flasks then transferred to 75 cm³ closed vent flasks when the cells had attained a sufficiently high density. The cells were then routinely passaged to maintain growth in 40 ml media. For two days prior to irradiation the cells were grown in a medium containing 33 µM 5-bromo-2'-deoxyuridine (BrdU) to allow the cells to incorporate the BrdU over two cell cycles.

3.2.2. Irradiation and harvesting.

Cells were irradiated with 0.2 or 0.4 Gy from a ¹³⁷Cs gamma source (CIS Biointernational IBL437C gamma-irradiator) at a dose rate of 7.7 cGysec⁻¹. One set of three flasks was immediately treated with 0.1 µg ml⁻¹ colcemid (Sigma) before being returned to the incubator for one hour at 37°C. The remaining flasks were returned to the incubator for two, three or four hours prior to harvesting. Each set of three flasks was treated with 0.1 µg ml⁻¹ colcemid 1 hour prior to harvesting and returned to the incubator.

After incubation the cell suspension was removed and placed in 50 ml centrifuge tubes and chilled on ice for 10 min before centrifugation (Hereaus Laborfuge 400R) at 1200 rpm (~200 g) for 10 min at 0°C. The medium was aspirated, the resulting cell pellet resuspended in ice-cold hypotonic solution

(0.075M KCl) and held on ice for 20 minutes before centrifuging at 1200 rpm. The supernatant was removed, the pellet loosened and slowly resuspended in fixative (75% methanol, 25% acetic acid v/v). The resulting cell suspension was washed in fixative at least three more times. Finally the cell pellet was resuspended in a small volume of fresh fixative and kept at 4°C.

3.2.3. Preparation of slides.

The microscope slides were first cooled in ice-cold distilled water for 30 min. The ice-cold slides were briefly wiped with the edge of a filter paper and flooded with ice-cold 50% glacial acetic acid solution before a single drop of cell suspension was placed on the slide. The slide was then dried on a warm-plate at approximately 50°C.

3.2.4. Fluorescence plus giemsa (FPG) staining

Once dry, the slides were placed in a solution of Hoechst 33258 (bis-Benzamide solution; Sigma) at $0.2 \mu\text{gml}^{-1}$ in distilled water in the dark for 10 min and then blotted dry on filter papers. The slides were then covered with 2xSSC (0.3 M sodium chloride, 0.03 M sodium citrate, Analar) and placed under a UV-A (Philips TLD 18W/08) source for 3 hours. They were then rinsed three times in distilled water, 5 minutes each time, and blotted dry. Once dry the slides were stained in 4% Giemsa for 10 min and rinsed in distilled water containing a few drops of ammonia per litre prior to blotting dry.

3.2.5. Scoring and analysis.

Slides were examined under a light microscope (Zeiss, with a planapochromat 1.4 aperture \times 63 objective). 200 metaphases were scored in each sample and

examined for chromatid breaks (including gaps). A scorable chromatid was determined to be where there was clear discontinuity in the chromatid material either in the light or dark strand or in both. The frequencies of breaks occurring in the light or dark stained chromatids was noted as well as the number of breaks with associated colour-switches ("colour-switch breaks"). The colour switch ratio per 100 metaphases was determined. The sister chromatid exchange (SCE) frequency per cell was also determined by scoring the SCE frequency in 25 cells and using the following formula:

$$\text{SCE per cell} = \frac{\text{Frequency of SCE in 25 metaphases}}{25}$$

3.3 Results

3.3.1 Break frequencies in normal lymphoblastoid cells

Table 3.1 shows the time variation in frequencies of total chromatid breaks, non-colour switch breaks (ncsb) and colour switch breaks (csb) at different times in normal lymphoblastoid (NC) cells subjected to 0.4 Gy irradiation. Cells were incubated for between one and four hours, inclusive of one hour in the presence of colcemid. Sister chromatid exchange (SCE) frequencies were similar to those presented in Table 2.3 for this cell line (NC). Table 3.1 also shows chromatid break frequencies for normal lymphoblastoid (NC) cells subjected to 0.2 Gy irradiation at $t = 1.5$ hr (from Table 2.2) and $t = 3$ hr.

As will be made clear later in section 3.3.5, it was decided to experimentally produce a complete rejoining curve at 0.4 Gy radiation so that chromatid breaks occurring at lower radiation doses could be interpolated more accurately. This would avoid having to extrapolate to higher D values as would be the case if a complete rejoining curve was produced at 0.2 Gy. Consequently the measured chromatid break frequencies listed in Table 3.1 (b) at 0.2 Gy were used to check the accuracy of the theoretically predicted values.

The data in Table 3.1 for 0.4 Gy irradiation dose can be graphically represented by plotting either the exponential decay curve (Figure 3.1) or alternatively on a log scale (Figure 3.2) which linearises the relationship between time and break frequency. The latter approach (Figure 3.2) tends to obscure differences in break frequencies, also it is necessary to apply a correction factor ($\log_{10}e$) to obtain accurate decay time constants on a \log_{10} scale. Non-linear regression analysis now available on computer software means that the best-fit curve representing the experimental data can now be readily achieved as shown in

Table 3.1(a). Frequencies of chromatid breaks in normal irradiated lymphoblastoid cells showing frequencies of chromatid breaks per 100 cells in normal lymphoblastoid cells subjected to 0.4 Gy ionising radiation and incubated for up to 4 hours, inclusive of 1 hour in the presence of colcemid. 200 metaphases scored per sample.

Time after irradiation (hr)	Total no. damaged cells	Breaks in dark strand*	Breaks in light strand*	Colour switch breaks	Total breaks	Colour switch ratio (%)
1	129.9	50.7	57.3	20.8	128.8	16.15
2	61.9	40.9	50.0	15.2	106.1	14.33
3	40.0	26.0	25.3	6.2	57.5	10.78
4	36.5	21.5	27.0	6.0	54.5	11.01

Table 3.1(b) Frequencies of chromatid breaks in normal irradiated lymphoblastoid cells per 100 cells subjected to 0.2 Gy ionising radiation and incubated for 1.5 or 3 hours, inclusive of 1 hour in the presence of colcemid. 400 metaphases scored for the 1.5 hr and 200 metaphases scored for the 3 hr sample time.

Time after irradiation (hr)	Total no. damaged cells	Breaks in dark strand*	Breaks in light strand*	Colour switch breaks	Total breaks	Colour switch ratio (%)
1.5	40.8	32.0	20.8	8.0	60.8	13.1
3	28.6	18.5	15.2	4.0	37.7	10.6

*Non-colour switch breaks are the sum of the dark and light strand breaks.

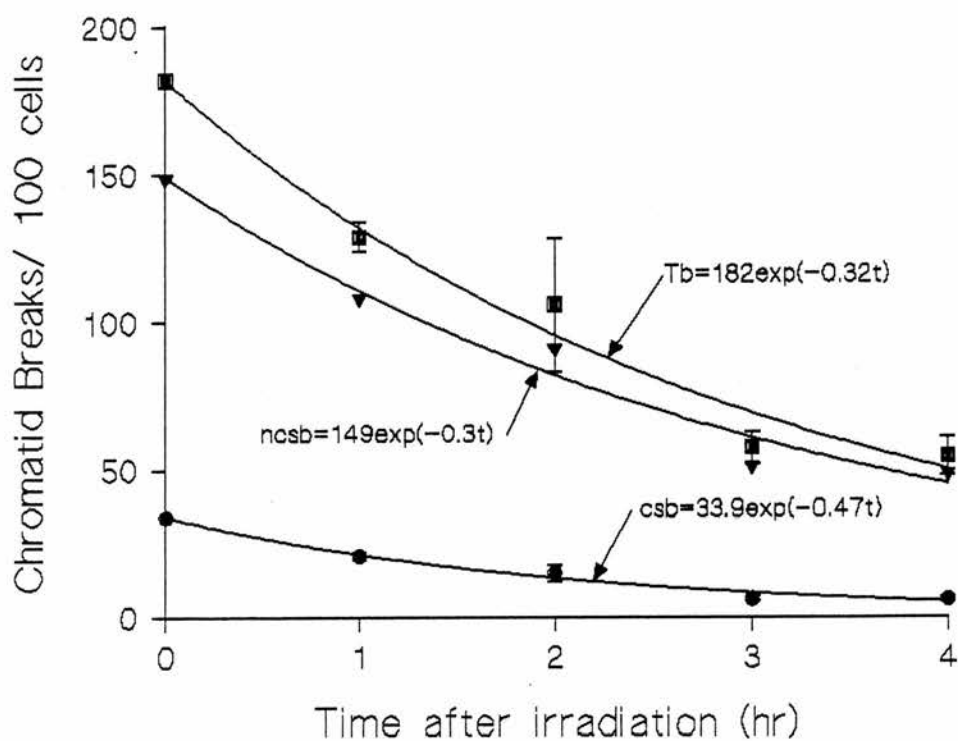


Figure 3.1. Graph of time after irradiation (0.4 Gy) vs. exponential decay in the frequency of chromatid breaks per 100 cells for normal lymphoblastoid cells from Table 3.1. 200 metaphases were scored in total and results obtained from three independent experiments. Best fit curves were obtained using non-linear regression analysis. Equations describing the exponential decay of total chromatid break (Tb), non-colour switch break (ncsb) and colour switch break (csb) frequencies are shown. Zero time data points show the predicted values at start of slow phase. Error bars represent standard error of the mean. $r^2(Tb) = 97.5\%$; $r^2(csb) = 98.5\%$; $r^2(ncsb) = 97.3\%$.

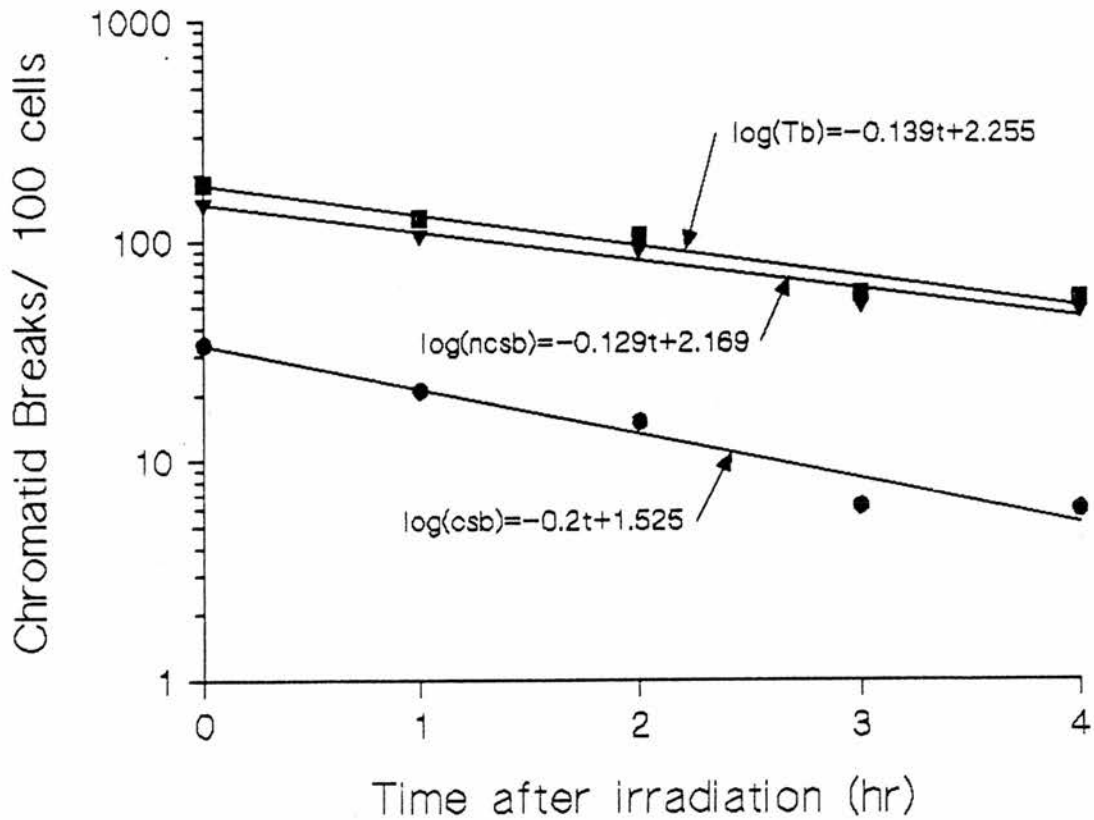


Figure 3.2. Graph of time after irradiation (0.4 Gy) vs. log of frequency of chromatid breaks per 100 cells for normal lymphoblastoid cells, using the same data as in Figure 3.1. 200 metaphases were scored in total and results obtained from three independent experiments. Best fit curves were obtained using linear regression analysis. Equations describing the decline in the total chromatid break (Tb), non-colour switch break (ncsb) and colour switch break (csb) frequencies are shown. Error bars represent standard error of the mean. $r^2(Tb) = 95.1\%$; $r^2(csb) = 94.7\%$; $r^2(ncsb) = 95.0\%$.

Figure 3.1. The data points shown in Figures 3.1 and 3.2 at initial time zero (start of the slow phase of rejoining) have been extrapolated back from the best-fit regression curve obtained from the measured data at times 1, 2, 3 and 4 hours.

3.3.2. Basic theory of breakage rejoining in G₂.

A number of papers have been published in the past which show that for cells subjected to relatively high doses of radiation, the rejoining characteristics are bi-phasic showing both a fast and slow phase of the DNA repair or rejoining curve.

In the present investigation where cells have been subjected to low doses of radiation only the slow phase of the rejoining phenomenon is being considered. Thus when a given cell line is subjected to a known low radiation dose, the repair or rejoining of chromatid breaks can be represented by a mono-exponential type equation which, for the case of total chromatid breaks (Tb) would be:

$$Tb = Tb_0 \exp \{-k_1(t - t_0)\} \quad (3.4)$$

where the time $t = t_0$ represents the start of the slow phase of rejoining and where $Tb = Tb_0$ is the number of chromatid breaks at the start of the slow phase. k_1 in equation (3.4) is the decay time constant for a specific cell type.

In the following discussion of the present investigation it will be assumed for simplicity that $t_0 = 0$ and where time zero in Figure 3.1 etc represents the start of the slow phase of chromatid breakage rejoining.

Thus equation (3.4) using $t_0 = 0$ simplifies to:

$$Tb = Tb_0 \exp(-k_1 t) \quad (3.5)$$

The rejoining of the colour switch breaks (csb) and non-colour switch breaks (ncsb) can be similarly represented by the expressions:

$$csb = csb_0 \exp(-k_2 t) \quad (3.6)$$

$$ncsb = ncsb_0 \exp(-k_3 t) \quad (3.7)$$

From equations (3.5) and (3.6) the colour switch ratio can therefore be expressed as:

$$csr = csb/Tb = \frac{csb_0 \exp(-k_2 t)}{Tb_0 \exp(-k_1 t)}$$

which can be simplified to:

$$csr = csr_0 \exp((k_1 - k_2) t) \quad (3.8)$$

where csr_0 represents the colour switch ratio at time $t = 0$ at the start of the slow phase of rejoining.

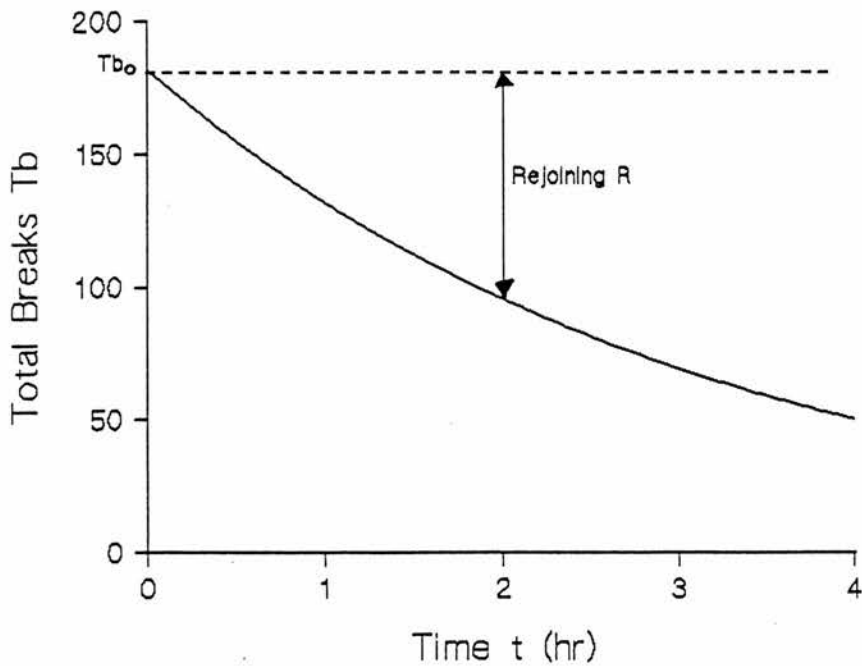
Equation (3.8) shows that the csr will only remain constant during the G₂ phase rejoining if $k_1 = k_2$.

Much of the literature which presents the repair or rejoining characteristics of dsb quantifies the rejoining using the time $t_{1/2}$ which is the time required to reduce the number of chromatid breaks from their initial value (Tb_0) to half

this value (e.g. Macleod and Bryant, 1992; Mateos *et al*, 1994) (i.e. $T_b = 1/2 T_{b0}$ in equation (3.5)). Thus using this value in equation (3.5) shows that $t_{1/2} = 0.693/k_1$ and further that $t_{1/2} = 0.693/k_2$ for the csb from equation (3.6).

It can therefore be concluded that the half time for rejoining of T_b and csb will only be the same value provided $k_1 = k_2$.

As the frequency of breaks shown in Figure 3.1 decreases with time, then conversely, the repair or rejoining of the chromatid breaks, increases as defined in the diagram below:



The rejoining (R_1) of the total chromatid breaks is therefore given by :

$$R_1 = Tb_0 (1 - \exp(-k_1t)) \quad (3.9)$$

and similarly the rejoining of csb (R_2) and ncsb (R_3) are given by:

$$R_2 = csb_0 (1 - \exp(-k_2t)) \quad (3.10)$$

$$R_3 = ncsb_0 (1 - \exp(-k_3t)) \quad (3.11)$$

The rate of rejoining of total chromatid breaks, csb and ncsb can be found by differentiating the above equations (3.9) - (3.11). Thus the rate of rejoining of total breaks is given by:

$$dR_1/dt = k_1Tb_0 \exp(-k_1t) = k_1Tb \quad (3.12)$$

Similarly the rate of rejoining of csb is given by:

$$dR_2/dt = k_2 csb \quad (3.13)$$

and the rate of rejoining of ncsb:

$$dR_3/dt = k_3 ncsb \quad (3.14)$$

The foregoing equations show that if $k_1 = k_2 = k_3$ then the rate of rejoining would be greatest for the total breaks. However as will be shown later this equality is unlikely to be the case for any cell type.

Using equations (3.13) and (3.14) the ratio of the rate of rejoining of csb to ncsb

(R*) is given by:

$$R^* = k_2 (csb)/k_3 (ncsb) = k_2 (csb)/k_3 (Tb - csb)$$

i.e. $R^* = k_2 (csr)/k_3 (1 - csr)$ (3.15)

where the csr is given by equation (3.8).

3.3.3. Rejoining characteristics for normal lymphoblastoid cells.

The regression analysis best fit rejoining curves of Figure 3.1 for normal lymphoblastoid cells subjected to 0.4 Gy irradiation show that the basic experimental values defined by equations (3.5), (3.6) and (3.7) are:

$$\begin{array}{lll} T_{b0} = 182 & csb_0 = 33.9 & ncsb_0 = 149 \\ k_1 = 0.32 & k_2 = 0.47 & k_3 = 0.3 \end{array}$$

These data values show that $k_1 \neq k_2$ and consequently in accordance with equation (3.8) the csr is not constant but decays exponentially with time given by the equation:

$$csr = (33.9/182) \exp ((0.32 - 0.47) t)$$

i.e. $csr = 0.19 \exp (-0.15t)$ (3.16)

This value of csr is plotted in Figure 3.3 and is in disagreement with previous assumptions of a constant csr during the G₂ phase of the cell cycle.

From the above values for Tb_0 and csb_0 at the start of the slow phase of rejoining ($t = 0$), and using the appropriate values for k_1 and k_2 , the half time $t_{1/2} = 2.16$ hr for total breaks (Tb) and $t_{1/2} = 1.47$ hr for colour switch breaks (csb). This illustrates the significant difference in half time values between Tb and csb due to the different values for the decay constants k_1 and k_2 .

The rejoining of breaks R_1 , R_2 and R_3 represented by equations (3.9) - (3.11) are shown graphically in Figure 3.4 for normal lymphoblastoid cells subjected to 0.4 Gy irradiation. The rate of rejoining of csb and $ncsb$ as defined by equations (3.13) and (3.14) are shown in Figure 3.5.

The expression for the ratio of the rate of rejoining of csb to $ncsb$ is found by using equation (3.16) in equation (3.15) to give:

$$R^* = 0.47(0.19 \exp(-0.15t))/0.3(1 - 0.19 \exp(-0.15t))$$

which simplifies to:

$$R^* = 0.3 \exp(-0.15t)/(1 - 0.19 \exp(-0.15t)) \quad (3.17)$$

Expression (3.17) for normal lymphoblastoid cells is plotted in Figure 3.6 and shows that the ratio $csb:ncsb$ is decreasing. The rate of rejoining of $ncsb$ is obviously much greater than the rate of csb rejoining as illustrated by Figure 3.5.

3.3.4. The chromatid breakage surface.

The foregoing results and analysis show that at a specific initial radiation dose the number of observed chromatid breaks decay exponentially with time. In Chapter 2, a linear relationship was demonstrated between chromatid breaks

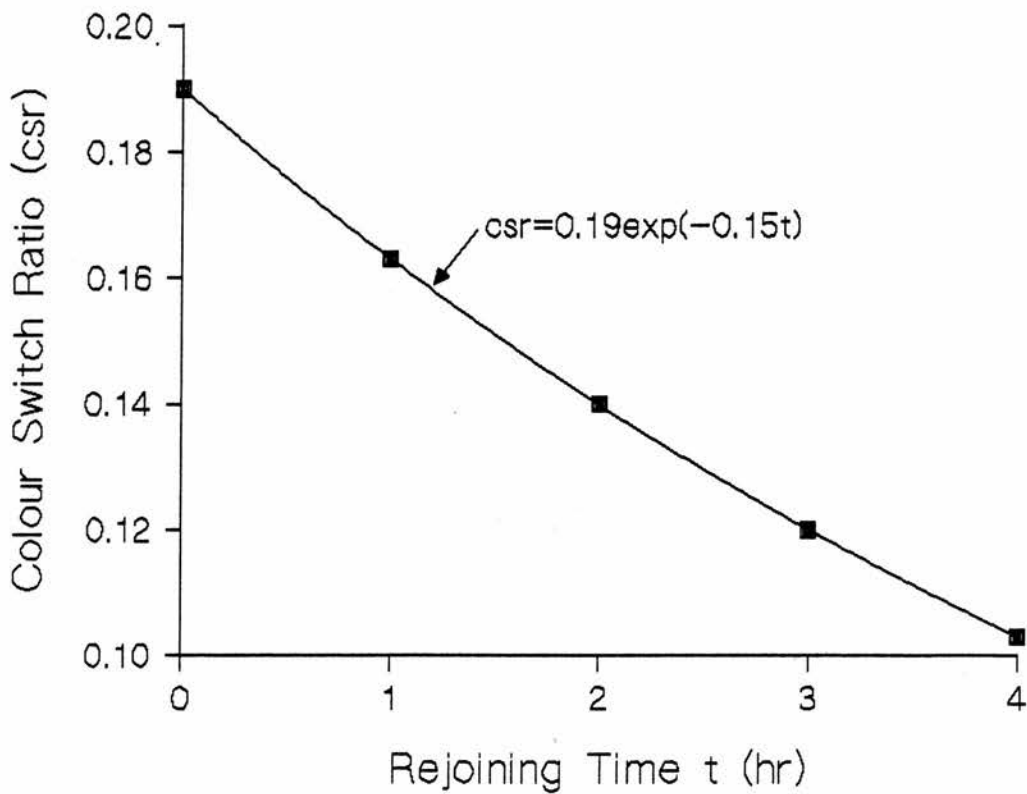


Figure 3.3. Graph of rejoining time for chromatid breaks per 100 cells vs. colour switch ratio (csr) value for normal lymphoblastoid cells subjected to 0.4 Gy irradiation. The csr values are obtained using equation (3.16). The curve shows a decline in csr with rejoining time.

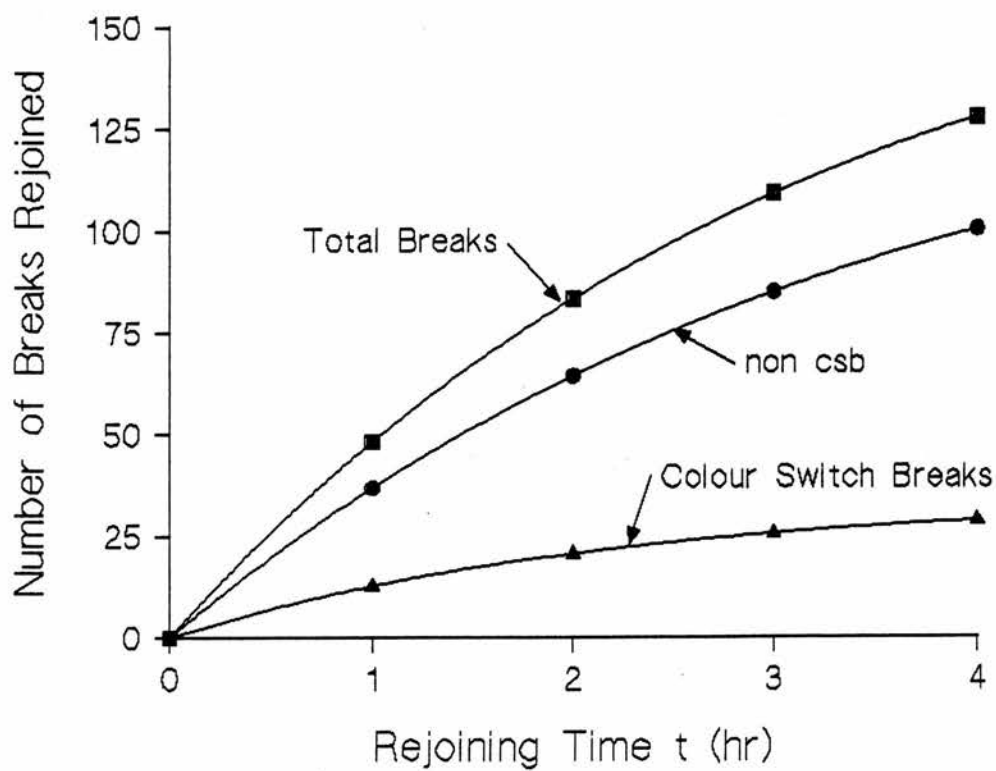


Figure 3.4. Graph of rejoining time vs. number of chromatid breaks rejoined per 100 cells for normal lymphoblastoid cells subjected to 0.4 Gy irradiation. The curves were obtained using equation (3.9), (3.10) and (3.11).

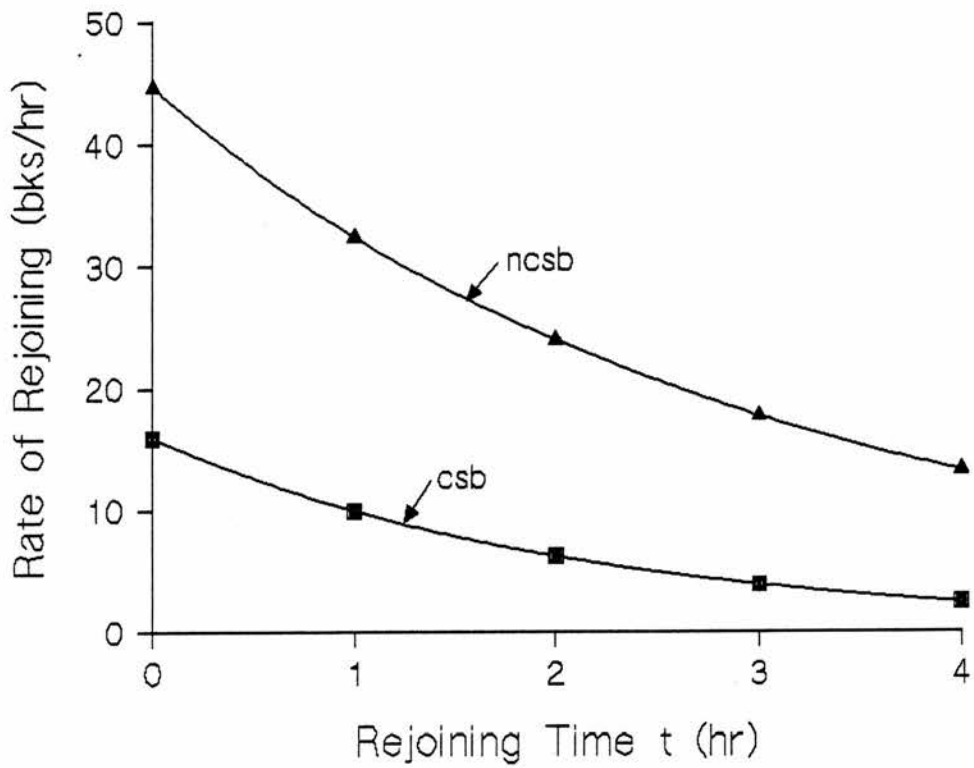


Figure 3.5. Graph of rejoining time vs. rate of rejoining of chromatid breaks per 100 cells for normal lymphoblastoid cells subjected to 0.4 Gy irradiation. Rates of rejoining are shown for non-colour switch breaks (ncsb) and colour switch breaks (csb). The curves were obtained using equations (3.13) - (3.14).

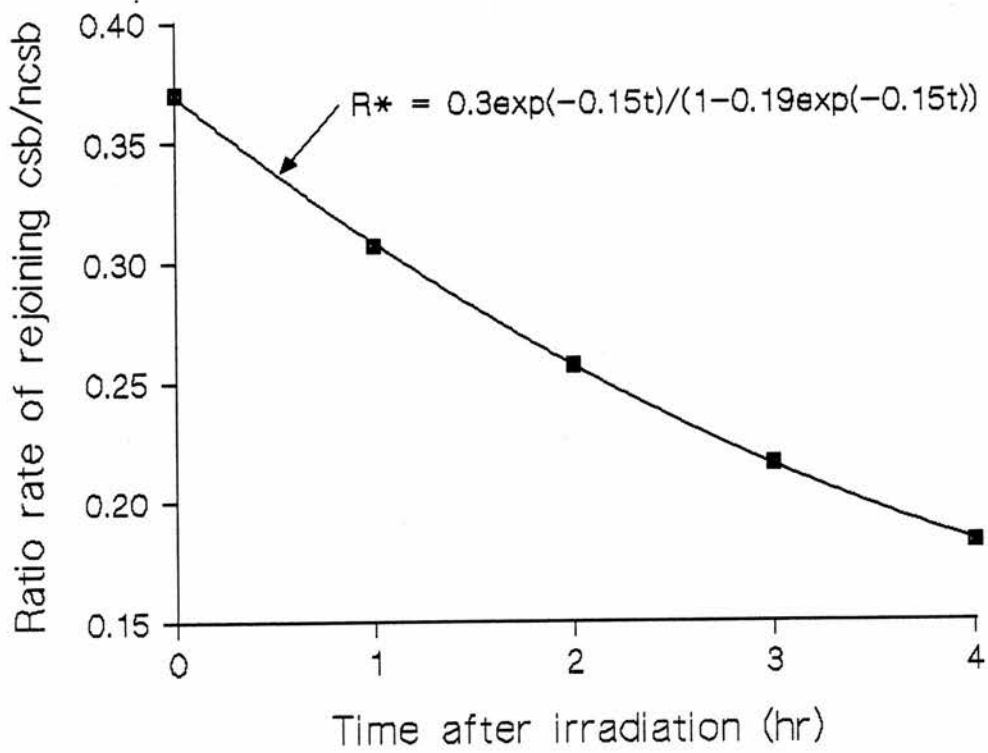


Figure 3.6. Graph of time after irradiation vs. ratio of rate of rejoining of colour switch breaks (csb) to non-colour switch breaks (ncsb) for normal lymphoblastoid cells subjected to 0.4 Gy irradiation. The data points were calculated using equation (3.17).

and dose at a specific sample time (1.5 hr). These relationships for normal lymphoblastoid cells are represented by equations (2.7) - (2.9) and Figure 2.5 for T_b , $ncsb$ and csb .

In studying radiation-induced DNA damage, the experiments discussed in this chapter and in Chapter 2 suggest that three variables are involved in the damage - break rejoining phenomenon; radiation dose, sample time and chromatid breaks. The obvious way to illustrate the relationship amongst these three variables for a given cell type is therefore to construct a breakage surface subtended above the dose-time horizontal plane where any point on this surface would represent the expected number of chromatid breaks for a specified radiation dose and sample time during G_2 . A different surface would obviously arise for any cell type for total chromatid breaks, csb and $ncsb$.

3.3.5. Chromatid breakage surface for normal lymphoblastoid cells.

As an example of the technique for generating a chromatid-breakage surface the total breaks (T_b) - Dose (D) relationship of Figure 2.5 measured at a sample time $t = 1.5$ hr together with the time decay of T_b shown in Figure 3.1, for a radiation dose $D = 0.4$ Gy will be used as the starting point.

The following diagram shows the resulting three-dimensional relationships suspended above the Dose-sample time horizontal plane representing $T_b = 0$.

$$Tb = 269.25 \times 0.2 + 10$$

$$Tb = 64$$

Remembering that $k_1 = 0.32$ and using the above value for Tb in equation (3.5) for $t = 1.5$ hr then

$$64 = Tb_0 \exp(-0.32 \times 1.5)$$

$$Tb_0 = 103 \text{ at } D = 0.2 \text{ Gy} \quad (\text{point C in diagram})$$

also from figure 3.1:

$$Tb_0 = 182 \text{ at } D = 0.4 \text{ Gy} \quad (\text{point A in diagram})$$

From these two total break values at 0.2 and 0.4 Gy the slope of the straight line at $t = 0$ is:

$$m_{10} = (182-103)/(0.4-0.2) = 395$$

The linear relationship for the total breaks at time zero in the D - Tb plane can be written in general terms as:

$$Tb_0 = m_{10} D + c_{10} \quad (3.18)$$

where m_{10} and c_{10} are the slope and intercept respectively at time $t = 0$ of the G_2 phase.

Using this equation at $D = 0.4$ Gy:

$$182 = 395 \times 0.4 + c_{10}$$

$$c_{10} = 24$$

Hence the linear relationship for the total breaks for normal lymphoblastoid cells at the start of the G₂ phase, $t = 0$ (line AB in diagram) is:

$$Tb_0 = 395 D + 24 \quad (3.19)$$

Remembering that $k_1 = 0.32$ is constant at different radiation doses the general relationship for the total chromatid breakage surface for normal lymphoblastoid cells can be written using equations (3.5) and (3.19) as:

$$Tb = (395 D + 24) \exp(-0.32t) \quad (3.20)$$

Figure 3.7 shows the 3-D plot of the breakage surface represented by equation (3.20) generated using the Microsoft Excel software package.

Adopting the same approach as described above, the breakage surface for csb for normal lymphoblastoid cells is given by the equation:

$$csb = (69 D + 6.3) \exp(-0.47t) \quad (3.21)$$

which is represented by the 3-D plot of Figure 3.8.

It was demonstrated in Chapter 2 that the csr was constant at a specific sample time but as expressed by equation (3.16) however decays exponentially with time. These two factors enable the complete csr surface to be generated for normal lymphoblastoid cells as shown in Figure 3.9.

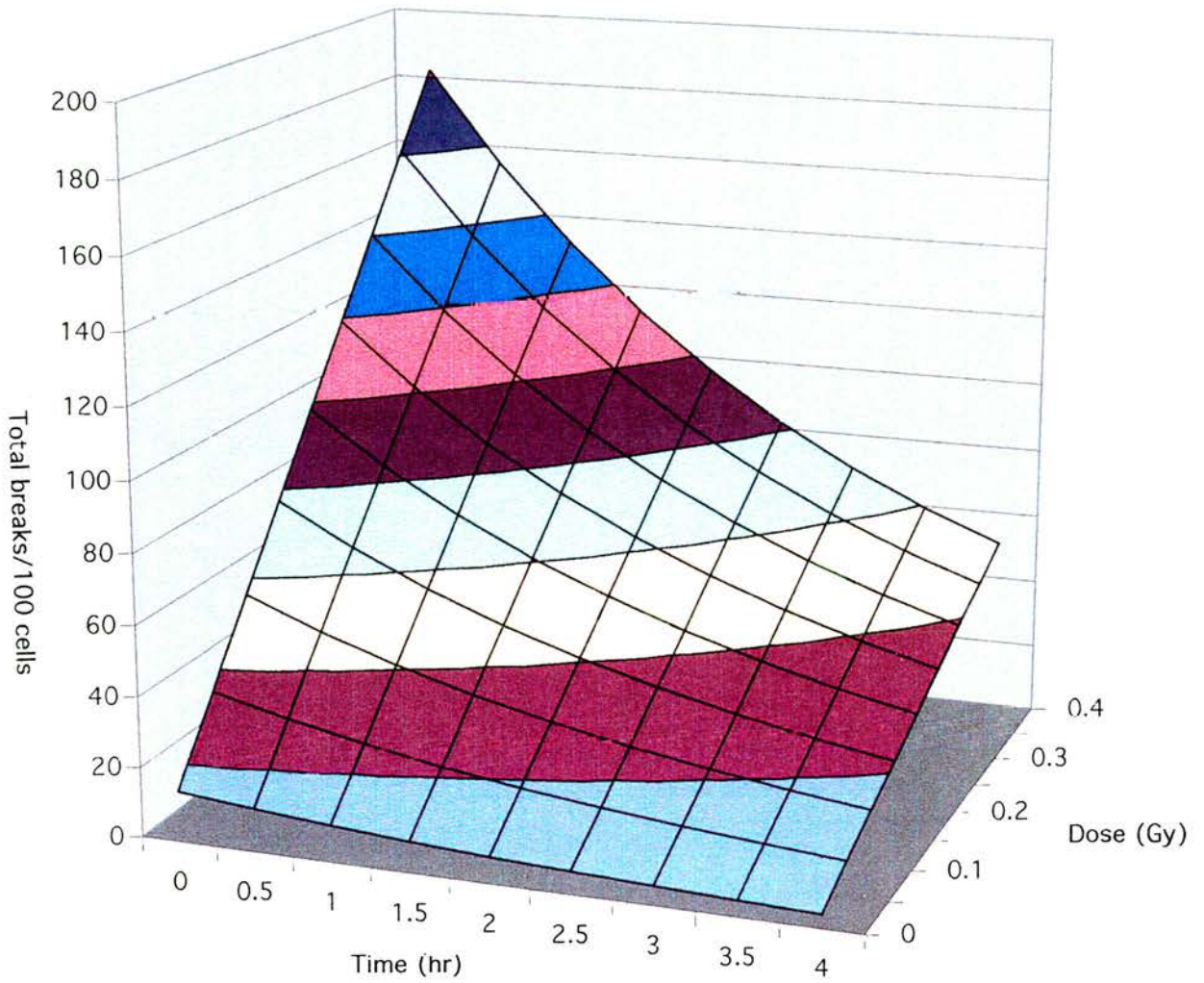


Figure 3.7. Three-dimensional plot of total chromatid break surface for the G₂ phase of the cell cycle (4 hr) showing time vs. dose vs. total chromatid breaks per 100 cells for a normal lymphoblastoid cell line. Data points were calculated using equation (3.20) as described in the text.

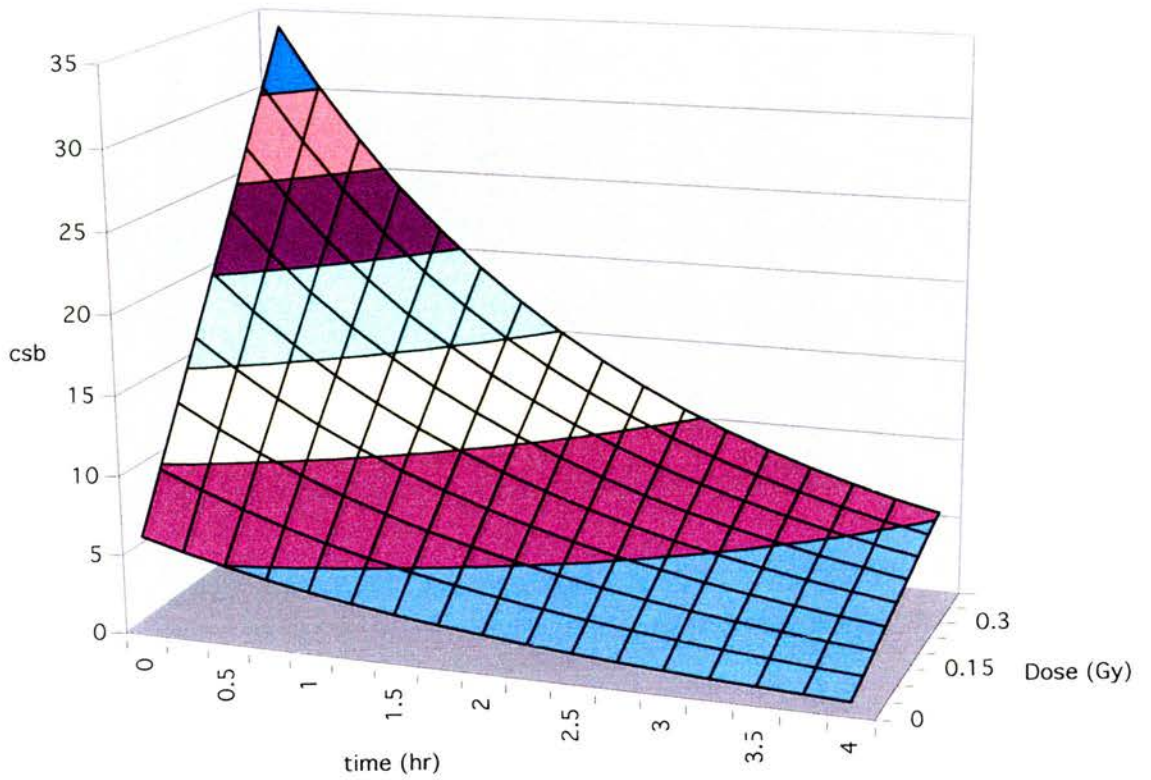


Figure 3.8. Three-dimensional plot of colour switch break surface for the G₂ phase of the cell cycle (4 hr) showing time vs. dose vs. colour switch breaks per 100 cells for a normal lymphoblastoid cell line. Data points were calculated using equation (3.21) as described in the text.

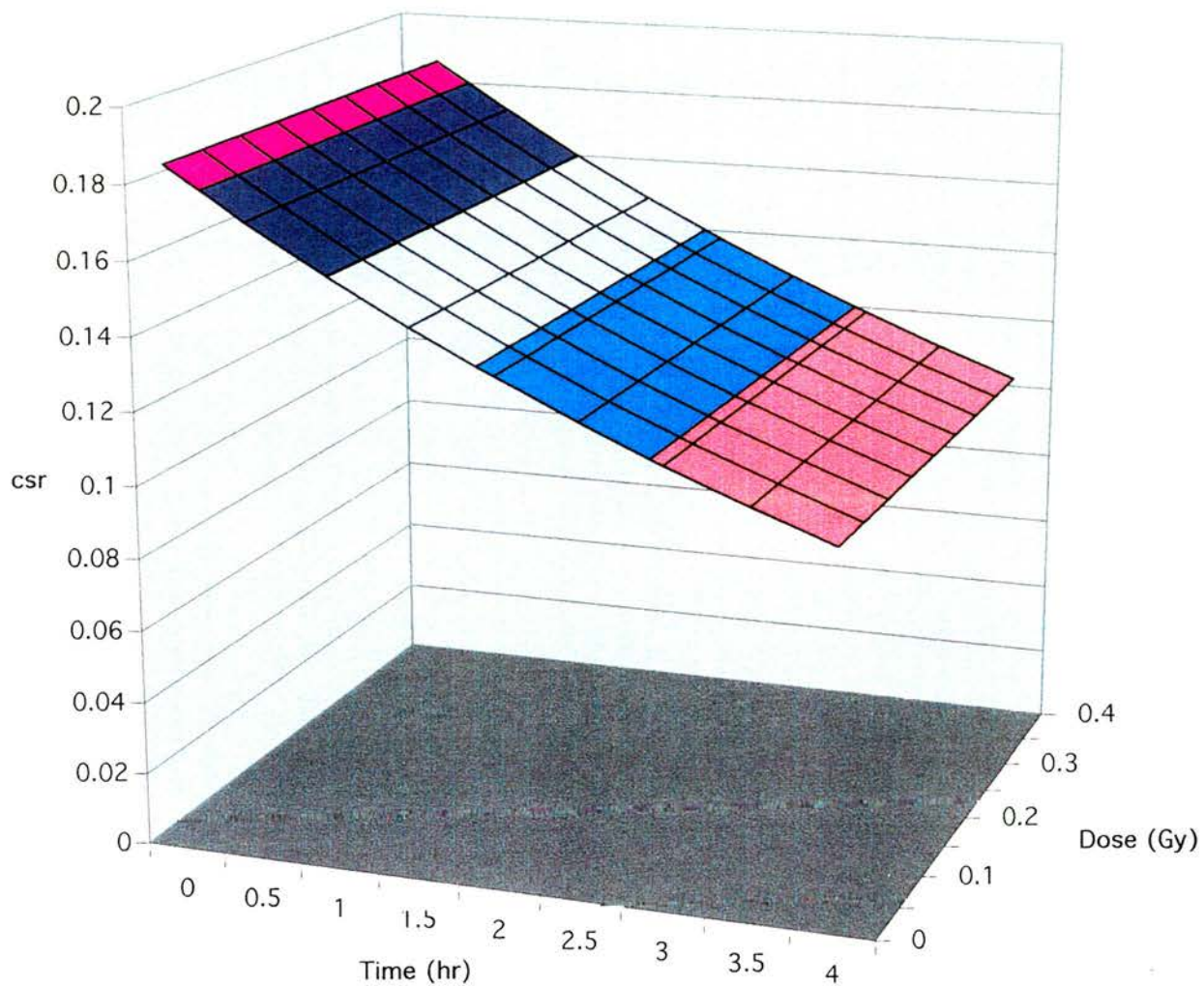


Figure 3.9. Three-dimensional plot of the colour switch ratio (csr) surface for the G₂ phase of the cell cycle (4 hr) showing time vs. dose vs. csr for a normal lymphoblastoid cell line. Data points were calculated using equation (3.20) and (3.21) using $(csr) = csb/Tb$.

From the foregoing analysis the general equations representing the breakage surface for any specific cell type can be written (e.g. combining equations (3.5) and (3.18)):

$$T_b = (m_{10} D + c_{10}) \exp (-k_1 t) \quad (3.22)$$

$$c_{sb} = (m_{20} D + c_{20}) \exp (-k_2 t) \quad (3.23)$$

$$n_{csb} = (m_{30} D + c_{30}) \exp (-k_3 t) \quad (3.24)$$

where the subscripts zero represent the values at sample time $t = 0$ at the start of the slow phase of rejoining within G_2 .

The predicted chromatid break frequencies for $t = 1.5$ hr and $t = 3$ hr at $D = 0.2$ Gy calculated using equations (3.20) and (3.21) are compared with the observed chromatid break frequencies shown in Table 3.2. Most of the predicted values in Table 3.2 fall within the 95% confidence limits (i.e. $\pm SE \times 1.96$) for the observed values.

3.3.6. Rejoining characteristics of ATM and NBS cells.

It has been shown in Appendix B that the exponential decay constants (k_1 , k_2 and k_3) are constant and independent of dose. In order to determine if the chromatid break rejoining characteristics for ATM and NBS lymphoblastoid cells are similar to those obtained for a normal lymphoblastoid cell line it is necessary to determine the k values for these disease syndrome cell lines. If the chromatid break rejoining characteristics are the same for all three cell lines then the values for k_1 , k_2 and k_3 would be the same. When measuring the rejoining characteristics of the ATM and NBS cell lines an irradiation value of

Table 3.2. Predicted and observed values for chromatid break rejoining in normal lymphoblastoid cells for total, non-colour switch and colour switch breaks. A radiation dose of 0.2 Gy and a sample times of 1.5 and 3 hr were used. The observed data values for $t = 1.5$ hr are from Table 2.2. The 95% confidence interval is shown in brackets.

Time (hr)	Total breaks (Tb)	Non-colour switch breaks (ncsb)	Colour switch breaks (csb)
t = 1.5 hr; predicted:	64	55	8
t = 1.5 hr; observed:	60.8 (± 2.47)	52.8 (± 2.16)	8.0 (± 1.96)
t = 3 hr predicted:	39	35	3.9
t = 3 hr observed:	37.6 (± 10.78)	33.7 (± 9.4)	3.96 (± 1.67)

0.2 Gy was used. This not only gives chromatid break rejoining data to determine the k values for direct comparison with those obtained for the normal cell line but also allows the resulting exponential equations to be used to predict chromatid break frequencies for $t = 1.5$ hr. These values can then be compared with the experimental values obtained for this sample time in Chapter 2 (Table 2.4). This approach also provides a measure of how consistent the scoring of breaks is within the entire investigation.

Tables 3.3 and 3.4 show the frequencies, as a function of sample time, total chromatid breaks, non-colour switch breaks (ncsb) and colour switch breaks

Table 3.3 (a) Frequencies of chromatid breaks per 100 cells in ATM (ATAR) cells treated with 0.2 Gy ionising radiation and incubated for up to 4 hours, inclusive of 1 hour in the presence of colcemid. 200 metaphases scored per sample.

Time after irradiation (hr)	Total no. damaged cells	Breaks in dark strand*	Breaks in light strand*	Colour switch breaks	Total breaks	Colour switch ratio (%)
1	72	60.0	54.0	9.5	123.5	7.69
2	77.5	49.0	66.0	10.5	125.5	8.37
3	67.5	37.5	56.0	7.5	101.0	7.43
4	64.0	36.5	47.0	8.0	91.5	8.74

Table 3.3 (b) Mean frequencies of chromatid breaks per 100 cells in ATM cells subjected to 0.2 Gy ionising radiation and incubated for 1.5 hours, from Table 2.4. 400 metaphases scored per sample.

Time after irradiation (hr)	Total no. damaged cells	Breaks in dark strand*	Breaks in light strand*	Colour switch breaks	Total breaks	Colour switch ratio (%)
1.5	73 ± 6.3	69 ± 8.9	55 ± 8.1	11 ± 2.6	135 ± 18.9	8.6

* Non-colour switch breaks are the sum of the dark and light strand breaks.

Table 3.4 (a) Frequencies of chromatid breaks per 100 cells in NBS (94P112) cells subjected to 0.2 Gy ionising radiation and incubated for up to 4 hours, inclusive of 1 hour in the presence of colcemid. 200 metaphases scored per sample.

Time after irradiation (hr)	Total no. damaged cells	Breaks in dark strand*	Breaks in light strand*	Colour switch breaks	Total breaks	Colour switch ratio (%)
1	73.4	57.0	54.0	8.0	119.0	6.73
2	76.0	55.0	62.0	11.5	128.5	8.95
3	72.0	44.0	47.0	7.5	98.5	7.61
4	66.0	44.5	41.5	9.5	95.5	9.95

Table 3.4 (b) Mean frequencies of chromatid breaks per 100 cells in NBS cells subjected to 0.2 Gy ionising radiation and incubated for 1.5 hours, from Table 2.4. 400 metaphases scored per sample.

Time after irradiation (hr)	Total no. damaged cells	Breaks in dark strand*	Breaks in light strand*	Colour switch breaks	Total breaks	Colour switch ratio (%)
1.5	67 ± 16.9	87 ± 45	31 ± 4.7	4 ± 1.7	122 ± 48	3.3

* Non-colour switch breaks are the sum of the dark and light strand breaks.

(csb) in Ataxia telangiectasia (AT) and Nijmegen Breakage (NBS) lymphoblastoid cells respectively, subjected to 0.2 Gy irradiation. Cells were incubated for between one and four hours, inclusive of one hour in the presence of colcemid. Mean data values for total breaks, non-colour switch breaks and colour switch breaks for $t = 1.5$ hr are also included (from Table 2.4). The mean values were used rather than the individual data points for the ATAR and 94P112 cell lines (Table 2.4) as this takes into account the scatter of data values expected, as described in Chapter 2. Sister chromatid exchange (SCE) frequencies were similar to those presented in Table 2.5 for these cell lines (ATAR and 94P112).

As described for normal lymphoblastoid cell lines, the data for the AT and NBS cell lines can also be represented graphically using non-linear regression analysis as shown in Figures 3.10 and 3.11 for AT and NBS cells respectively. Comparing the equations for the best fit curves of Figure 3.10 and 3.11 with the theory presented here (3.3.2) the initial frequency of total chromatid breaks (Tb_0), colour switch breaks (csb_0) and non-colour switch breaks ($ncsb_0$) can be determined together with their respective rate constants (k_1 , k_2 and k_3). Thus for the AT cells subjected to 0.2 Gy:

$$\begin{array}{lll} Tb_0 = 143.0 & csb_0 = 10.9 & ncsb_0 = 132.2 \\ k_1 = 0.107 & k_2 = 0.083 & k_3 = 0.108 \end{array}$$

and for NBS cells:

$$\begin{array}{lll} Tb_0 = 137.7 & csb_0 = 9.0 & ncsb_0 = 129.0 \\ k_1 = 0.089 & k_2 = 0.0053 & k_3 = 0.097 \end{array}$$

These values can be compared to the predicted values calculated for the normal

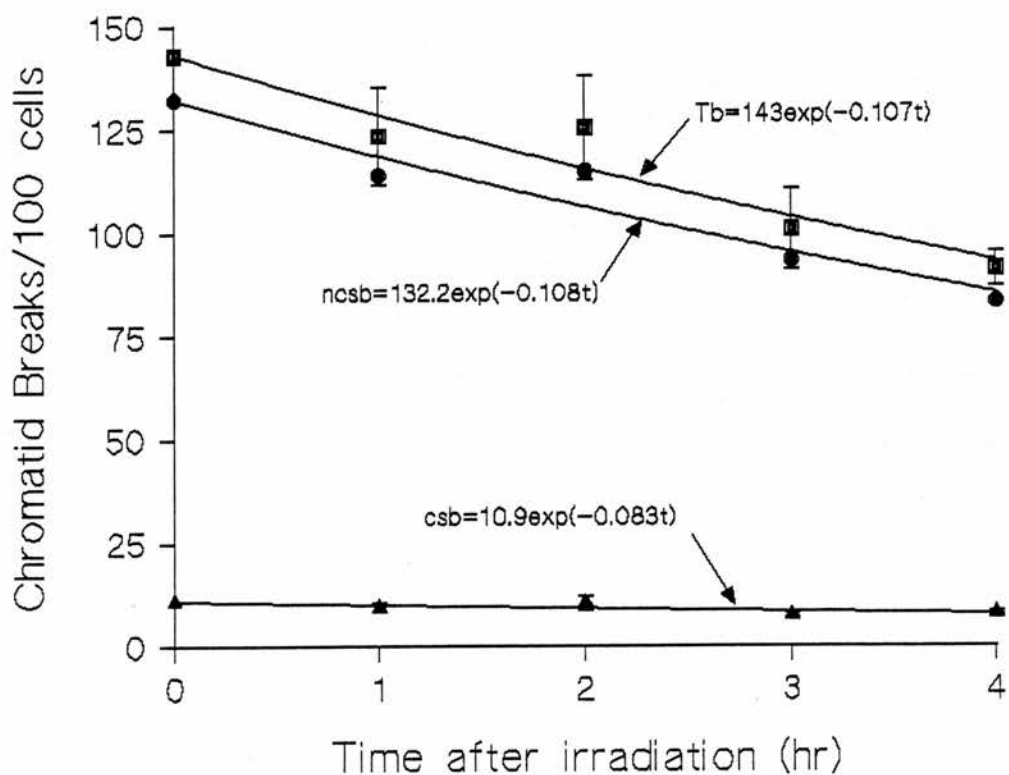


Figure 3.10. Graph of time after irradiation (0.2 Gy) vs. exponential decay in the frequency of chromatid breaks per 100 cells for ATM lymphoblastoid cells from Table 3.2. 200 metaphases were scored in total and results obtained from three independent experiments. Equations describing the exponential decay of total chromatid break (Tb), non-colour switch break (ncsb) and colour switch break (csb) frequencies are shown. Error bars represent standard error of the mean. $r^2(\text{Tb}) = 92.0\%$; $r^2(\text{csb}) = 67.5\%$; $r^2(\text{ncsb}) = 95.0\%$.

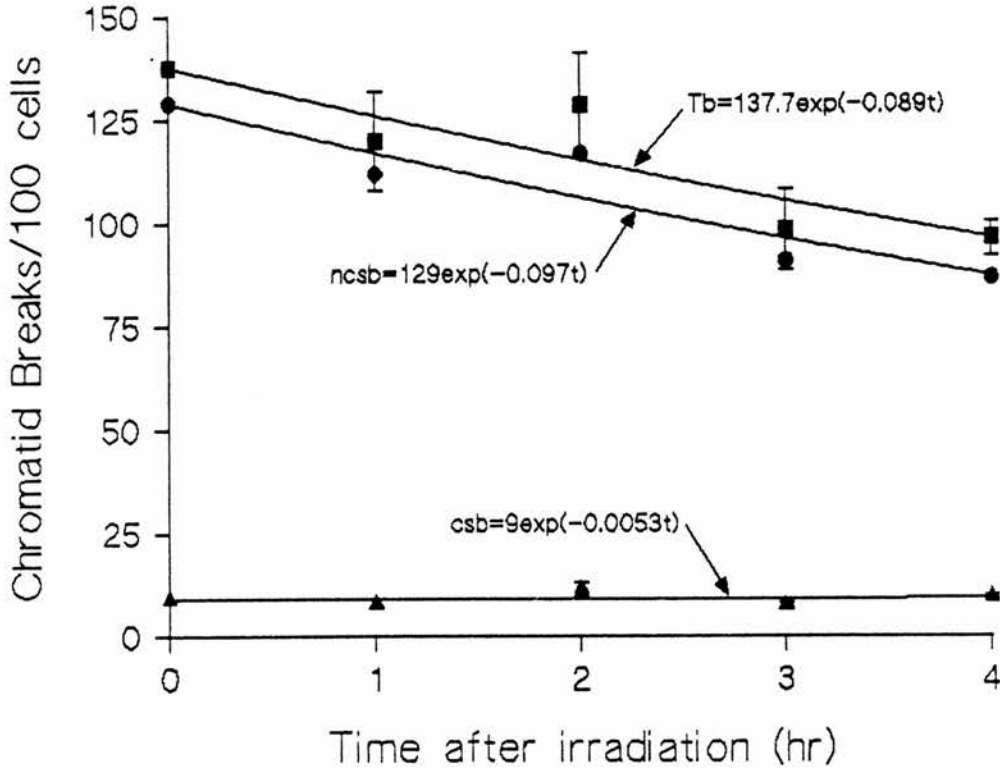


Figure 3.11. Graph of time after irradiation (0.2 Gy) vs. exponential decay in the frequency of chromatid breaks per 100 cells for NBS lymphoblastoid cells from Table 3.3. 200 metaphases were scored in total and results obtained from three independent experiments. Equations describing the exponential decay of total chromatid break (Tb), non-colour switch break (ncsb) and colour switch break (csb) frequencies are shown. Error bars represent standard error of the mean. $r^2(Tb) = 80.5\%$; $r^2(ncsb) = 86.5\%$. There is no r^2 value for csb as there is no exponential decay, the frequency of csb remains sensibly constant.

lymphoblastoid cell line subjected to 0.2 Gy using equations (3.20) and (3.21):

$$\begin{array}{lll} \text{Tb}_0 = 103 & \text{csb}_0 = 16.2 & \text{ncsb}_0 = 86.8 \\ k_1 = 0.32 & k_2 = 0.47 & k_3 = 0.3 \end{array}$$

As expected the total number of chromatid breaks (Tb_0) is higher for ATM and NBS than for normal cell lines. However, the above data show that rates of rejoining (k_1 , k_2 and k_3) for ATM and NBS cell lines are much lower than for normal lymphoblastoid cells. The lower frequency of observed colour switch breaks in the ATM cell line (Table 3.3) and NBS cell line (Table 3.4) compared to the normal lymphoblastoid cell line (Table 3.1) is in agreement with the results presented in Chapter 2 (Tables 2.2 and 2.4).

From the best fit curves obtained for ATM cells (Figure 3.10) the following equations can be determined:

$$\text{Tb} = 143 \exp(-0.107 t) \quad (3.25)$$

$$\text{csb} = 10.9 \exp(-0.083 t) \quad (3.26)$$

$$\text{ncsb} = 132.2 \exp(-108 t) \quad (3.27)$$

Similar equations can be written for the NBS cell lines as shown in Figure 3.11. The predicted chromatid break frequencies for ATM and NBS lymphoblastoid cell lines at $t = 1.5$ hr calculated using the equations shown in Figures 3.10 and 3.11 are shown in Table 3.5 together with the observed chromatid break frequencies.

For comparison with half time values for normal lymphoblastoid cells (section 3.3.3) half time values for total breaks for ATM and NBS cells are $t_{1/2} = 6.5$ hr and $t_{1/2} = 7.8$ hr respectively. This reflects the slow rate of chromatid break rejoining in these disease syndrome cell lines compared to normal lymphoblastoid cells. Due to the small variations in csb frequencies and therefore small time decay constants calculated $t_{1/2}$ values for csb are inappropriate.

Table 3.5. Predicted and observed values for chromatid break rejoining in ATM and NBS lymphoblastoid cells. The observed data values for $t = 1.5$ hr are the mean irradiated values for ATM and NBS lymphoblastoid cell lines from Table 2.4. The 95% confidence interval is shown in brackets.

Cell type	Total breaks (Tb)	Non-colour switch breaks (ncsb)	Colour switch breaks (csb)
ATM: t = 1.5 hr; predicted:	122	112.4	9.6
ATM: t = 1.5 hr; observed:	135 (± 18.9)	124 (± 8.5)	11 (± 2.6)
NBS: t = 1.5 hr predicted:	120.5	111.5	9
NBS: t = 1.5 hr observed:	122 (± 48)	118 (± 24.8)	4 (± 1.7)

Most of the predicted values in Table 3.5 fall within the 95% confidence limits (i.e. $\pm SE \times 1.96$) for the observed values. A cursory glance at Figures 3.10 and 3.11 shows that the observed chromatid break frequencies listed in Table 3.5 at $t = 1.5$ hr lie in the correct region of the respective exponential decay curves.

The colour switch ratio (csr) for ATM cells can be found using equation (3.8):

$$\text{i.e.} \quad \text{csr} = \text{csr}_0 \exp((k_1 - k_2)t) \quad (3.8)$$

Thus for the ATM cell line:

$$\text{csr (ATM)} = (10.9/143.0) \exp((0.107 - 0.083) t)$$

$$\text{csr (ATM)} = 0.076 \exp(0.024t) \quad (3.28)$$

The csr calculated from equation (3.28) is shown as a function of rejoining time in Figure 3.12 and shows an increase in csr with time in contrast to the decline in csr with rejoining time observed for normal lymphoblastoid cells (Figure 3.3).

Carrying out the same method of analysis to the best fit curves for NBS cells (Figure 3.11), the colour switch ratio (csr) for these cells is found to be:

$$\text{csr (NBS)} = 0.065 \exp(0.0837 t) \quad (3.29)$$

The variation of csr as a function of rejoining time for NBS cells is also shown in Figure 3.12. This diagram shows that the increase in csr for the NBS is even more rapid than the ATM cells again contrasting with the decline in csr with rejoining time for normal lymphoblastoid cells (Figure 3.3).

Figures 3.10 and 3.11. show that there is very little change in the csb values after irradiation and consequently the mono-exponential regression curves are poor representations of the measured data. However the resulting variations in csr values illustrated by Figure 3.12 show a trend which the csr values listed in

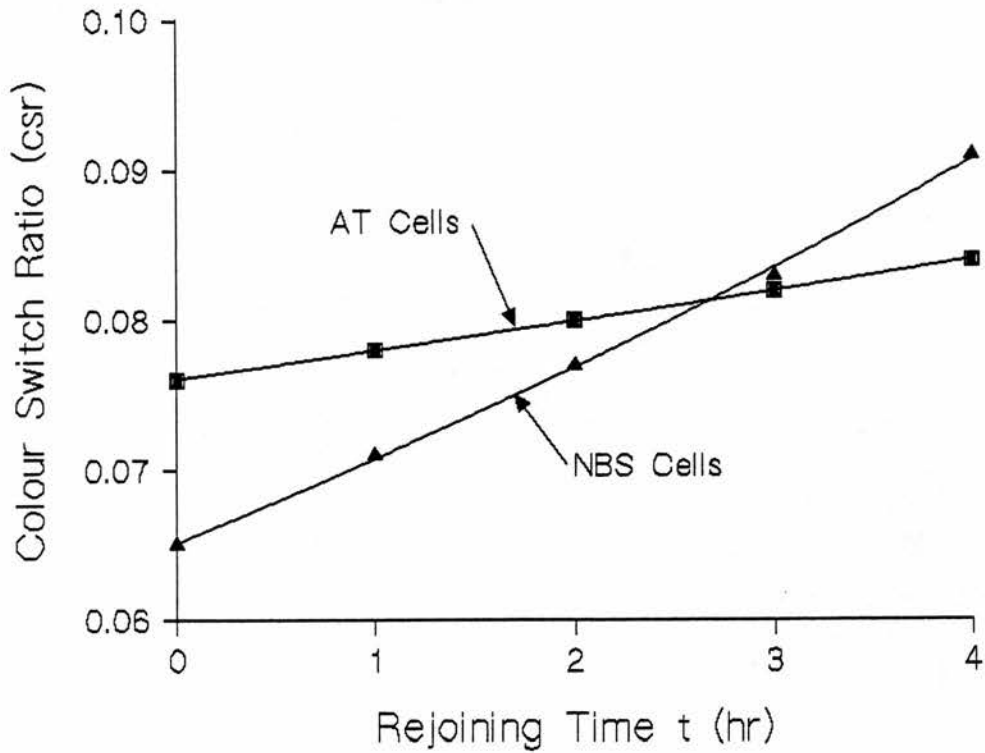


Figure 3.12. Graph of rejoining time for chromatid breaks per 100 cells vs. colour switch ratio (csr) value for ATM and NBS lymphoblastoid cells subjected to 0.2 Gy irradiation. The csr values are obtained using equations (3.28) and (3.29). The curves show an increase in csr with rejoining time, in contrast to the decline in csr rejoining time for normal lymphoblastoid cells as shown in Figure 3.3.

Tables 3.3 and 3.4 tend to obscure. In Table 3.3 the mean csr for ATM cells is 8.6% (SD = 0.6) and the corresponding values for NBS cells in Table 3.4 show a mean csr of 8.31% (SD = 1.4). The mean csr and standard deviation values calculated from the data in Tables 3.3 and 3.4 agree well with the curves derived from equations (3.28) and (3.29) in Figure 3.12.

The equations shown in Figures 3.10 and 3.11 can be used to determine the rejoining of chromatid breaks using equations (3.9), (3.10) and (3.11). The results of these calculations are shown plotted in Figure 3.13 and 3.14 for ATM and NBS cells respectively. The rejoining of colour switch breaks (csb) for ATM (Figure 3.13) is lower than that observed for normal lymphoblastoid cells (Figure 3.4) and there is almost no rejoining of colour switch breaks for NBS cells (Figure 3.14).

Further calculations using the theory described in section 3.3.2 have been used to determine the ratio of rejoining colour switch breaks (csb) to non-colour switch breaks (ncsb) using equation (3.15) together with equations (3.28) and (3.29). This ratio is plotted in Figure 3.15 for the ATM and NBS cells and compared with the values for normal cells already presented in Figure 3.6. The rejoining ratio R^* is much lower for the ATM and NBS cells compared to the normal lymphoblastoid cells, the lowest ratio being that obtained for the NBS cells. This factor is caused by the very low rate of rejoining of csb for these disease syndrome cells.

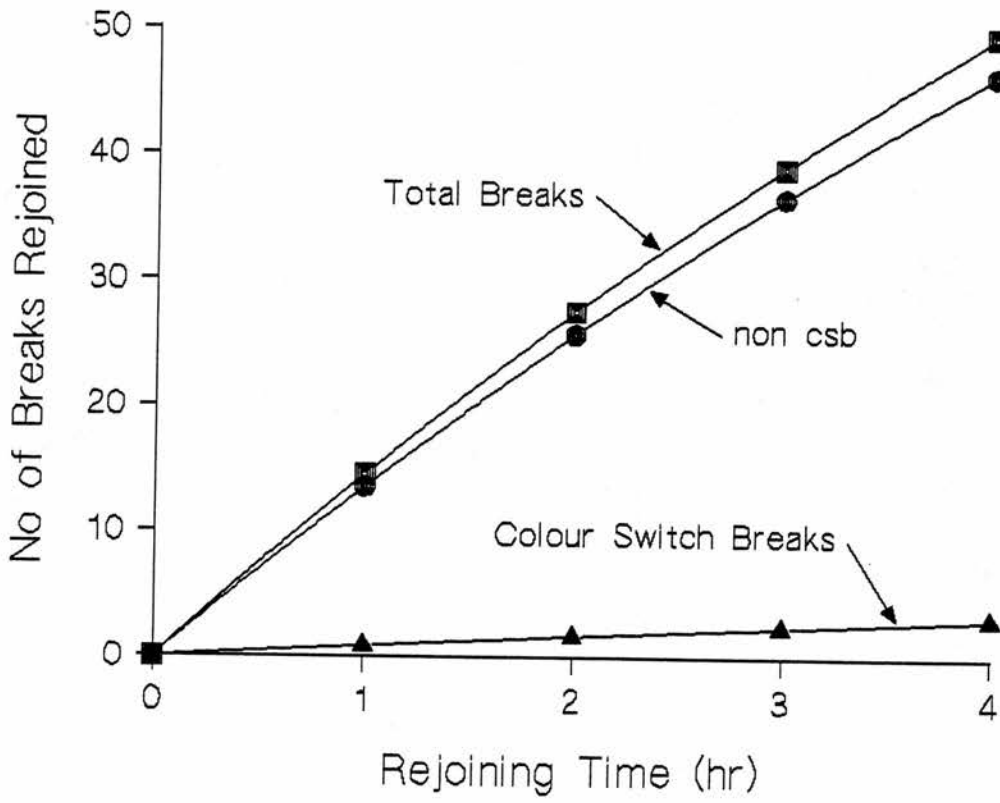


Figure 3.13. Graph of rejoining time vs. number of chromatid breaks rejoined per 100 cells for ATM cells subjected to 0.2 Gy irradiation. The curves were obtained using equations (3.9) - (3.11).

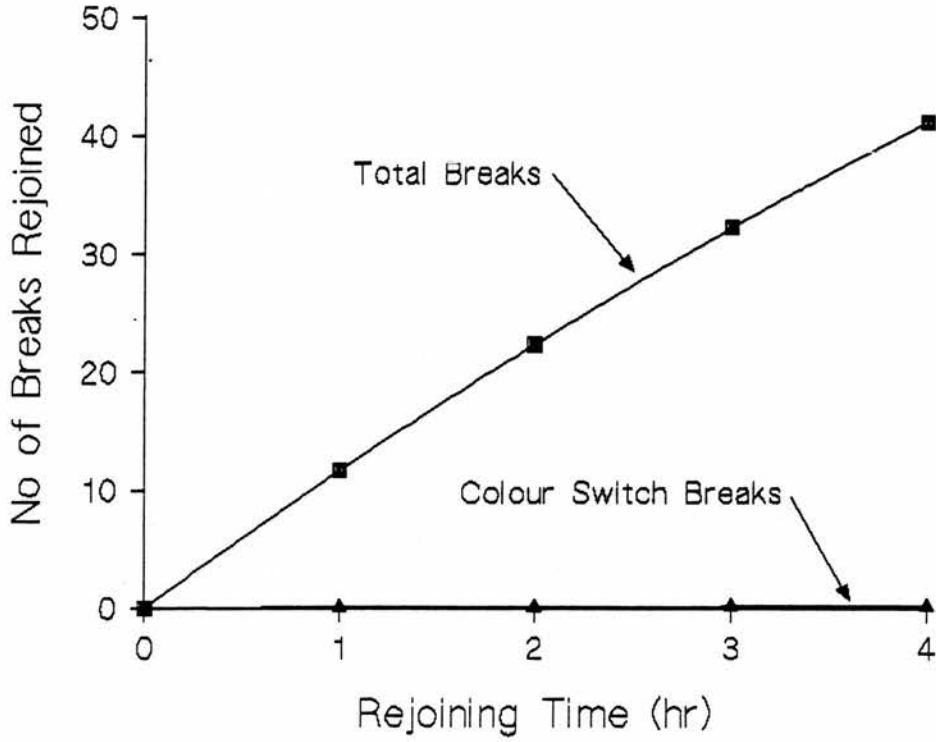


Figure 3.14. Graph of rejoining time vs. number of chromatid breaks rejoined per 100 cells for NBS cells subjected to 0.2 Gy irradiation. The curves were obtained using equations (3.9) - (3.11). Non-colour switch break data points are not shown as they have almost the same numerical values as total breaks data points.

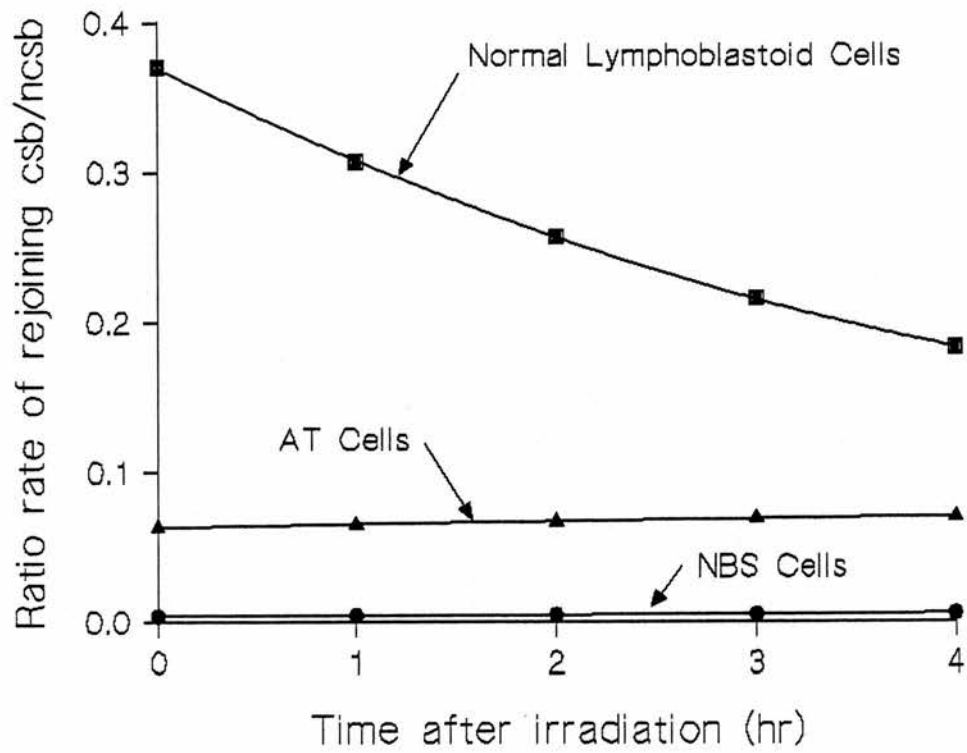


Figure 3.15. Graph of time after irradiation vs. ratio of rate of rejoining of colour switch breaks (csb) to non-colour switch breaks (ncsb) for normal, ATM and NBS lymphoblastoid cell lines. Data points were calculated using equation (3.15) as described in the text.

3.4 Discussion

The results presented here support the previously reported findings that an exponential decay in chromatid break frequency occurs during the G₂ phase of the cell cycle. The scope of this investigation has been widened to examine the relative rejoining characteristics of chromatid break subtypes: colour switch and non-colour switch breaks. These findings suggest that the rejoining kinetics of colour and non-colour switch breaks in a normal lymphoblastoid cell line are different and thus the colour switch ratio is not constant with time. It has been shown by calculating the ratio of the rate of rejoining of colour switch breaks (csb) to non-colour switch breaks (ncsb) that ncsb rejoin at a faster rate than csb leading to a decline in the value for the colour switch ratio (csr) with time after irradiation for normal lymphoblastoid cells.

Furthermore the chromatid break rejoining characteristics of Ataxia telangiectasia (AT) and Nijmegen Breakage Syndrome lymphoblastoid cell lines differ from those observed for the normal lymphoblastoid cell line. This raises implications for the involvement of these gene products in the repair and processing of chromatid breaks and by implication the repair of the double strand breaks that if unrepaired, give rise to observed chromatid aberrations.

3.4.1. Rejoining characteristics of normal lymphoblastoid cells.

The decrease in chromatid break frequency observed in the normal lymphoblastoid cells (Table 3.1 and Figures 3.1 and 3.2) are in broad agreement with previously reported findings (Bryant *et al* , 1998; MacLeod and Bryant, 1992). However these previous investigations only analysed data logarithmically and did not consider the exponential decay equations which

represent the slow phase of rejoining. Previous work was also limited to rejoining of total breaks and did not consider the subdivision of chromatid break types. The availability of computer software enabling non-linear regression analysis to be performed has made the comparison of exponential decay curves possible and highlights possible subtle differences in results obtained from experimental procedures. It is also of interest to investigate potential differences in chromatid break rejoining characteristics as this may shed light on whether chromatid aberration subtypes persist in the genome as a result of DNA damaging events. If some chromatid break subtypes are more persistent within the genome these may subsequently give rise to long term changes such as an increase in genomic instability which may confer an elevated risk of cancer predisposition.

Previous work considering the colour switch ratio (csr) has assumed a constant csr regardless of radiation dose, restriction enzyme concentration or sampling time (Harvey and Savage, 1997; Bryant, 1998). The conditions defining the constancy of the csr with radiation dose are considered in Chapter 2 and the effect of restriction enzyme concentration on csr in Chapter 4. Possible changes in csr as a direct function of time has not previously been investigated. The foregoing Section 3.3.2 outlines the conditions necessary for the csr to remain constant with time throughout the G₂ phase of the cell cycle. The critical criterion to be met to ensure a constant csr with time is the condition $k_1 = k_2$, where k_1 and k_2 are the time constants for the exponential decay for total and colour switch breaks respectively (see equation (3.8)). The results presented here using non-linear regression analysis demonstrate that the k_1 and k_2 values for the exponential decay of total breaks (Tb) and colour switch breaks (csb) respectively for normal lymphoblastoid cells are not equal ($k_1 = 0.32$, $k_2 = 0.47$). Consequently the csr obtained in this investigation is not constant over the G₂ time phase, the csr value calculated using equation (3.16) in fact declines as a

function of time (Figure 3.3).

It has been shown mathematically in Appendix B that if a linear relationship exists between chromatid breaks and radiation dose at differing sample times throughout G₂ (as demonstrated in Chapter 2), then the exponential decay constant describing break rejoining must be constant and independent of the initial radiation dose. This conclusion is supported by measurements published by Gotoh *et al*, (1999), where double-strand break (dsb) and chromatid break rejoining kinetics were investigated using premature chromosome condensation (PCC). In this work the rejoining of dsb chromatid breaks was found to be a two component first order kinetic event of the type similar to that described by Loucas and Geard (1994):

$$Y = Ae^{-k_i t} + Be^{-k_{ii} t} + C \quad (3.2)$$

where Y = yield of prematurely condensed chromosomes and fragments at time t; A = the fraction of fragments which rejoin with fast kinetics; B = the fraction of fragments which rejoin with slow kinetics; k_i = rejoining rate constant of the fast component; k_{ii} = rejoining rate constant of the slow component and C = sum of chromosomes.

The fast component measured using PCC, which is analogous to the (Ae^{-k_it}) component of equation (3.2), corresponded to the rejoining kinetics for dsb whereas the second slower component (Be^{-k_{ii}t}) corresponded to the rejoining kinetics for chromatid breaks resulting from unrepaired dsb. The exponential decay of chromatid breaks presented here can be considered to be analogous to the slow component of repair described by Gotoh *et al*, (1999). It would be of interest to couple the dsb repair kinetics for this cell system in order to

determine the complete dsb/chromatid breaks rejoining characteristics for this model cell system for the whole of the G2 phase of the cell cycle.

As described in 3.3.5. and Appendix B it is possible to generate a three-dimensional surface representing the relationship between radiation dose, sample time and either total chromatid breaks or colour switch breaks throughout G2.

The time-dependent nature of the csr for this cell system suggested that it may be informative to investigate the relative rates of rejoining of colour and non-colour switch breaks. The difference in rejoining of chromatid break subtypes with time (Figure 3.4) can be more clearly seen if the rate of break rejoining is considered (Figure 3.5) where the non-parallel nature of the curves produced support the conclusion that the proportion of csb in the total number of chromatid breaks is not constant. When the ratio of the rates of rejoining (csb to ncsb) is considered (Figure 3.6) it can be clearly seen that $R^* \ll 1$ and therefore the non-colour switch breaks (ncsb) are rejoining approximately 3-4 times more quickly than the colour switch breaks (csb) in these normal lymphoblastoid cells. The reasons for this slower rejoining of csb compared to ncsb is not known, but this may be due to different DNA repair pathways being used to rejoin different break types. It is possible that different repair or rejoining pathways, which may be competing to rejoin chromatid break subtypes, would operate with different kinetics. Alternatively the structural nature of the chromatin around the csb site may differ from that found around the ncsb site. Such differences in chromatin structure may preclude the involvement of repair complex subsets which are not able to access the break site. The involvement of different repair complexes with different kinetics in the resolution of chromatid breaks may be determined by the ability to access break sites.

3.4.2. Rejoining characteristics of chromatid breaks in syndrome cell lines

Analysis of chromatid break frequencies for ataxia telangiectasia (ATM) (Table 3.3 and Figure 3.10) and Nijmegen Breakage Syndrome (NBS) (Table 3.4 and Figure 3.11) show a much slower reduction in the number of rejoined chromatid breaks for both syndrome cell lines when compared with a normal lymphoblastoid cell line (Table 3.1 and Figure 3.1). Comparison of the k values for these three cell types confirms the decline in chromatid break rejoining kinetics for total breaks and hence chromatid break subtypes. The most dramatic decline in rejoining kinetics is seen for colour switch breaks with k_2 values of 0.47, 0.083 and 0.0053 for normal, ATM and NBS cell lines respectively. This is further illustrated by the number of chromatid breaks rejoined with time; Figure 3.13 demonstrates the small number of csb rejoined in ATM cells compared to the frequency of rejoined csb in normal lymphoblastoid cells (Figure 3.4). The rejoining frequency for csb in NBS cells (Figure 3.14) is almost zero, indicating no measurable rejoining of csb in this cell line.

The association of NBS and ATM proteins in signalling complexes associated with repair has been demonstrated (see Chapter 2) and together with the results presented in Chapter 2 where ATM and NBS were found to have significantly low csr values at a sample time of 1.5 hr, suggests that these gene products are involved in both formation and resolution of colour switch breaks (csb) but not non-colour switch breaks (ncsb). This supports the hypothesis that ATM and NBS (and other repair proteins which associated with them) are involved in the formation and rejoining of recombinational events arising as a result of dsb which, if incomplete at metaphase, results in a colour switch break. They do not however appear to be involved in the formation and resolution of dsb-induced recombinational events which can give rise to non-

colour switch breaks. These results are therefore supportive of the signal model as the disappearance of chromatid breaks with time is interpreted as the completion of the recombinogenic rearrangements and do not reflect dsb repair capability in cells. ATM cells have been shown to have normal dsb rejoining ability but an increase in the formation of chromatid breaks and other chromosomal aberrations compared with normal cells. The results presented here suggest that both ATM and NBS cells undertake recombinational events giving rise to Revell type 1a and 2a chromatid aberrations (referred to as colour switch breaks in the signal model) at a lower rate compared to normal cells to give a lower csr (Figure 2.14). These results also suggest that if such recombinational events are initiated ATM and NBS cells are either unable to adequately process these rearrangements or do so with much slower kinetics compared to normal cells. However it would appear that although the frequency of ncsb formation in ATM and NBS cells is normal (Figure 2.16) the rate of rejoining of ncsb (Revell types 2a, 2b, 3a, and 3b) is slower in ATM and NBS compared to normal lymphoblastoid cells. This also suggests that the recombinogenic pathway(s) involved in both the formation and resolution of ncsb and to a greater extent csb is impaired in ATM and NBS lymphoblastoid cell lines leading to a significantly different csr throughout the G₂ phase of the cell cycle.

The ratio of the rate of rejoining of csb to ncsb indicates that ncsb are rejoined 20 times and 200 times faster than csb in ATM and NBS cells respectively (Figure 3.15). These ratios are significantly lower than that calculated for the normal lymphoblastoid cell line, in which ncsb are rejoined 3-4 times faster than csb. This observation supports the conclusion that ATM and NBS are principally deficient in csb rejoining and ncsb rejoining is slower but less affected by the absence of the ATM or NBS protein than csb kinetics. Published observations suggesting that ATM cells have different chromatin conformation

would support the conclusions presented here (Hittelman and Pandita, 1994).

The absence or abrogation of a G₂/M restriction point in ATM and NBS cells must be considered when comparing the rejoining characteristics of these cells with normal lymphoblastoid cell lines.

As described in Chapter 2 (2.2.4.1) AT cells display radioresistant DNA synthesis and radiation-induced chromosomal damage (Morgan *et al*, 1997) as well as a correlation between radiosensitivity and the amount of ATM protein present in cells (Lavin and Khanna, 1999a; 1999b). Although the repair of chromatid breaks in ATM cells has been measured as normal (Mozdarani and Bryant, 1989) there is also evidence of faster initial double-strand break (dsb) rejoining (Foray *et al*, 1997) followed by a slow dsb rejoining phase (Coquerelle *et al*, 1987). This results in a higher residual number of dsb (approximately 10%) compared to normal cells (approximately 1%) (Foray *et al*, 1997; Dahm-Daphi and Dikomey, 1996). This elevated level of unrepaired dsb is then thought to be the cause of the observed increased incidence of chromosome and chromatid breaks in ATM cells (Mozdarani and Bryant, 1987; Liu and Bryant, 1994; Pandita and Hittelman, 1992). The results presented here are in agreement with these previous observations of higher residual dsb, leading to increased numbers of chromatid breaks and slower rejoining characteristics. Studies of dsb repair in ATM cells suggests that they are unable to repair camptothecin (CPT) induced dsb in replicating DNA (Johnson *et al*, 1999) giving rise to higher frequencies of chromatid exchanges in G₂. It is possible that this subset of unrepaired dsb may give rise to the csb which are shown here to persist in these cells over the time period being considered.

It is possible that ATM cells are unable to rejoin subsets of breaks within the time period considered here either because of slower rejoining kinetics or

because of abrogation of signal transduction pathways necessary for the rejoining pathways to proceed.

The AT protein is a member of the PI-3 kinase superfamily (Ventikaraman *et al*, 1999) and is associated with a pathways involved in recognition of DNA damage, repair initiation and cell cycle checkpoint activation. ATM is known to interact with p53, ATM cells having a reduced p53 response following radiation-induced damage (Khanna *et al*, 1998), though a p53 response is still possible via AT-related (ATR) protein in AT cells (Tibbetts *et al*, 1999). ATM also plays a more general role in activation of cytoplasmic signalling cascades including intracellular calcium release following ionising radiation (Yan *et al*, 2000) and activation of the c-abl tyrosine kinase pathway (Baskaran *et al*, 1997; Shafman *et al*, 1997). Changes in the kinetics of these pathways could lead to slower rejoining of chromatid breaks.

Radioresistant DNA synthesis, a characteristic of ATM cells, is due to an inability to inhibit cyclin A-cdk2 and cyclin B-cdc2 or cdk1, due to a lack of increase in cdk-associated p21 expression. This results in a reduced time delay at the G₂/M checkpoint point. The G₂ replication block is also ATM-dependent as ATM is required to phosphorylate Chk2 (Matsuoka *et al*, 2000; Chaturvedi *et al*, 1999). The ATM-dependent phosphorylation of Brca1 following ionising radiation (Scully *et al*, 1997b) is further support for the postulated association of ATM with resolution of dsb (Cortez *et al*, 1999) and repair functions in general as the ATM-dependent phosphorylation of Brca1 links these proteins with the repair functions of Brca2.

Nijmegen Breakage Syndrome (NBS), considered in more detail in 2.2.4.3, forms part of the Mre11/Rad50/p95 complex localised to the nucleus and forming ionising radiation-induced foci (IRIF) in response to ionising radiation-

induced damage (Maser *et al*, 1997; Nelms *et al*, 1998). IRIF formation localises repair complexes to the DNA damage site. The NBS protein may also be necessary to allow hyperphosphorylation of Mre11, a precursor to IRIF formation, though the necessity for the presence of AT for IRIF formation to proceed is less clear (Dong *et al*, 1999). The phenotype of NBS cells is similar to that of Ataxia telangiectasia (ATM) and includes increased chromosomal breakage, radioresistant DNA synthesis, defective cell cycle checkpoints and reduced p53 response to damaging events (Shiloh, 1997; Digweed *et al*, 1999). Double-strand break (dsb) repair has been described as wild type (Kraakman-Van der Zwet *et al*, 1999) and impaired (Huo *et al*, 1994; Hanawalt and Painter, 1985) but it is possible that as for AT, NBS cells are only able to repair certain subsets of chromatid breaks normally with some types such as colour switch breaks (csb) either not being repaired at all or with very slow kinetics such that they appear to be unrepaired within the time frame considered here.

The ability of NBS to function in both an ATM-dependent (Lim *et al*, 2000; Zhao *et al* 2000) and an ATM-independent manner (Matsuura *et al*, 1998) suggests it has a central role in the formation and activation of repair complexes for the resolution of chromatid breaks. This, coupled with evidence that the DNA-PK pathway operates independently of ATM and NBS supports the speculation that colour switch breaks are primarily resolved by the ATM/NBS dependent pathways, probably by homologous recombination and by NHEJ via a RAG--dependent pathway. Non-colour switch breaks (ncsb) are rejoined via ATM/NBS independent pathways such as the DNA-PK non-homologous end-joining pathway. The lower incidence of induced csb in ATM and NBS cells coupled with the inability of these cells to resolve csb within the time frame of these investigations suggests a structural basis for the formation and resolution of csb. Access of repair complexes is determined by the ability of the DNA duplex to unwind; the ATM protein has been associated in changes

in chromatin conformation and the NBS protein is required for ATP-dependent cleavage and unwinding of DNA to allow repair and ligation to proceed (Paull and Gellert, 1999).

The absence or reduction of a G₂/M restriction point in both ATM and NBS cells (Tables 3.2 and 3.3) is probably responsible for the observed initial increase in chromatid breaks compared to normal lymphoblastoid cells (Table 3.1). The characteristic of radio-resistant DNA synthesis in these cell types would allow damaged cells to proceed to mitosis, which would not occur in normal cells. However it would still be expected that if chromatid break rejoining were normal in ATM and NBS cells then the k values would be similar for all three cell types, which is not the case. The low level of rejoining of colour switch breaks (csb) in ATM cells and the absence of csb rejoining in NBS cells gives rise to the increase in colour switch ratio for these cell types (Figure 3.12) due to the persistence of csb while non-colour switch breaks (ncsb) are successfully rejoined, albeit more slowly than measured for normal cells. This is the opposite of the trend observed in csr values for normal cells, where the csr declines throughout the time course of this investigation (Figure 3.3) due to the decay constant for csb (k_1) being significantly greater than that for Tb (k_2).

It would be of interest to further investigate this hypothesis that different types of chromatid breaks are formed as a result of the interaction of distinct classes of DNA damage recognition and repair complexes. Accessibility of dsb due to chromatin structure in the vicinity of the damage site may be determined by proteins such as ATM and NBS, determining what types of chromatid breaks might occur.

3.4.3. Summary and conclusions

- (1) Rejoining of chromatid breaks in normal lymphoblastoid cells during the slow phase of rejoining can be accurately represented by a mono-exponential decay equation where the regression best-fit curves have an accuracy quantified by r^2 values greater than 90%.
- (2) The time decay constant for total breaks (Tb) k_1 is significantly different from the decay constant k_2 for colour switch breaks (csb) and consequently the csr for normal lymphoblastoid cells varies with time throughout the G₂ phase of the cell cycle.
- (3) Rejoining rates for normal lymphoblastoid cells after irradiation is much greater for ncsb than for csb.
- (4) Frequency of chromatid breaks in irradiated cells during rejoining can be quantified using a 3-D diagram where the horizontal plane represents the dose-sample time values and the vertical ordinates represents the breaks at a specific dose and time.
- (5) The exponential time decay constant for a specific chromatid breakage surface is independent of the initial radiation dose (see Appendix B).
- (6) Rejoining rates for ATM and NBS cells after irradiation are much lower than the corresponding values for normal lymphoblastoid cells. Almost no rejoining of csb occurs in the disease syndrome cells.
- (7) Quantifying the rejoining of chromatid breaks in G₂ using a half life time value $t_{1/2}$ is not very informative and can lead to erroneous conclusions.

(8) The reduced rate of rejoining of csb leading to different csr characteristics for ATM and NBS throughout G₂ is supportive evidence in favour of the involvement of both the AT and NBS gene products in the recombinogenic pathway(s) leading to both the formation and resolution of csb. These results, together with those in Chapter 2 thus suggest that both ATM and NBS are possible candidates for the signalling molecule(s) predicted to be involved in the signal model mechanism for the formation of chromatid breaks.

3.5 Future Work

It would be interesting and informative to determine the rejoining characteristics for chromatid breaks for a synchronised cell population. This would then indicate if the G₂ cell cycle delay following irradiation affected the observation described here and if so, in what way. It may also be informative to characterise the exponential decay for other cell lines known to be deficient in genes associated with ATM and NBS in repair complexes. It would also be informative to characterise those cell lines known to be involved in alternative repair pathways, such as DNA-PK and as in Chapter 2, cell lines with two defective genes.

If the first part of the two-component first order kinetics describing the rejoining of double-strand breaks (dsb) and chromatid breaks described by Gotoh *et al*, (1999) (equation 3.2) were determined for a population of normal cell lines it would be possible to produce a complete picture for dsb/chromatid break rejoining characteristics throughout G₂ and compare the results with other published data. By extension it may be possible to determine dsb/break repair characteristics for the whole of the cell cycle and thus identify times within the cell cycle when dsb repair and break rejoining is less efficient. This information, coupled with a knowledge of dynamic changes in chromatin through the cell cycle may lead to a better understanding of when particular repair pathways are operating and if DNA damage at particular times within the phases of the cell cycle may give rise to lesions which are more critical for the long-term stability of the genome than others.

It is possible to combine equation (3.20) for the slow phase with the fast component of the rejoining kinetics defined by equation (3.2) and hence

speculate what type of breakage surface would arise for the whole of the G₂ phase of the cell cycle.

If it assumed that $k_j = 15k_{ji}$ as indicated by the measurements of Gotoh *et al*, (1999) Table 2, then using the value $k_{ji} = 0.32$ found by experiment for the lymphoblastoid cells gives a fast component decay constant $k_j = 0.32 \times 15 = 5$. The speculative equations for the chromatid breakage surface for the whole of G₂ would therefore be:

for the fast component:

$$T_b = (m_{10}D + c_{10}) \exp(-5t) \quad t < t_0$$

for the slow component:

$$T_b = (419D + 14) \exp(-0.32(t - t_0)) \quad t \geq t_0$$

where t_0 is the sample time when the change in the rate of kinetic rejoining takes place.

If this change is assumed to occur at a time $t_0 = 12\text{m} = 0.2 \text{ hr}$ then the value of the T_b surface must be the same at this time. Equating the above the expressions at $t = t_0 = 0.2$ gives:

$$(m_{10}D + c_{10}) \exp(-5 \times 0.2) = 419D + 14$$

Consequently the linear relationship at $t = 0$ at the start of the fast component is:

$$Tb_0 = m_{10}D + c_{10} = (419D + 14)/0.37$$

$$Tb_0 = 1132D + 38$$

and the speculative equations for the chromatid breakage surface are therefore:

$$Tb = (1132D + 38) \exp(-5t) \quad t < t_0 = 0.2$$

$$Tb = (419D + 14) \exp(-0.32(t - t_0)) \quad t \geq t_0 = 0.2$$

The speculative chromatid breakage surface based on these expressions is shown in Figure 3.16.

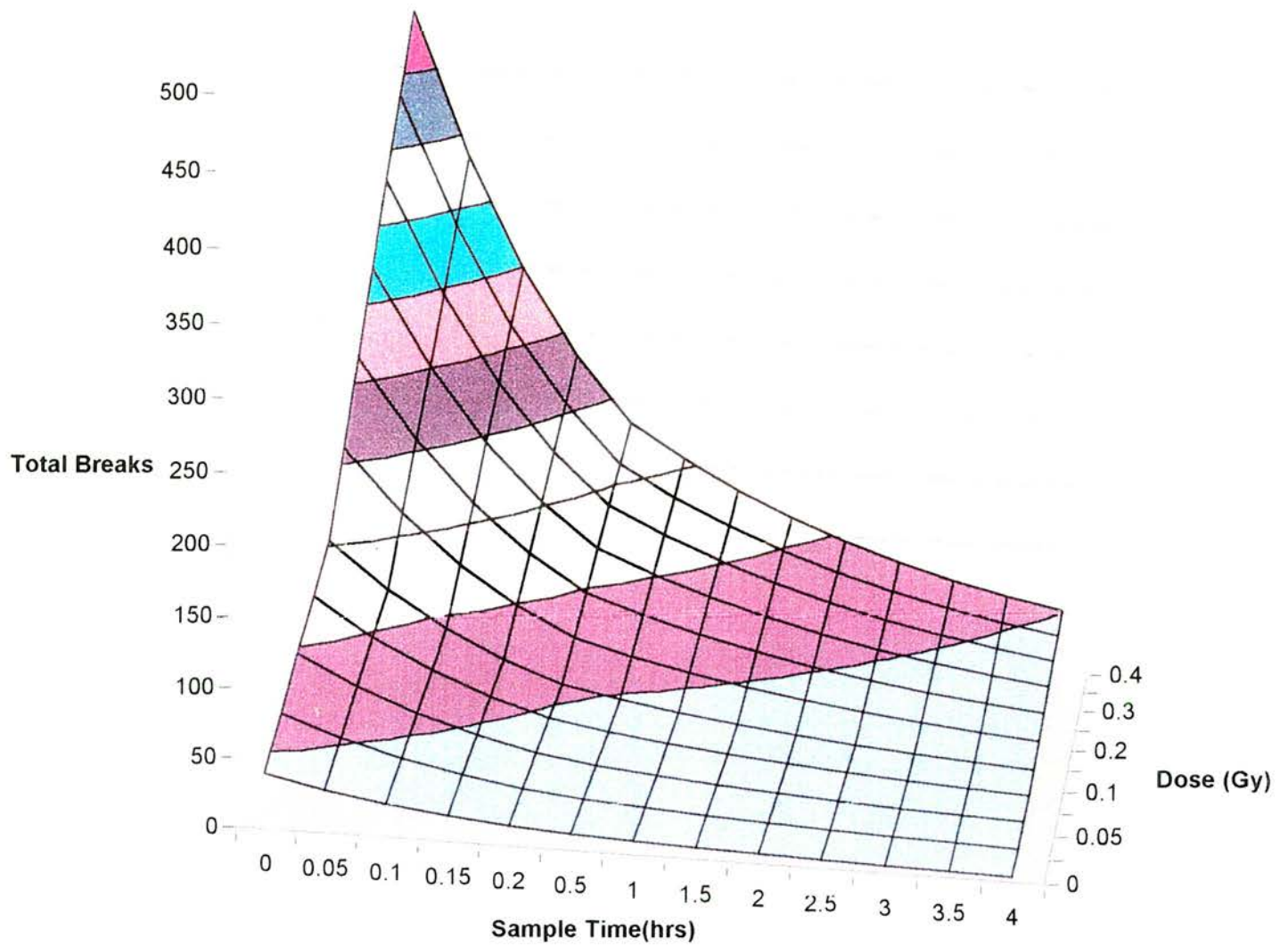


Figure 3.16. A hypothetical complete breakage surface for the whole of the G₂ phase of the cell cycle. The surface is generated by expanding equation (3.19) to include the fast component of the rejoining kinetics defined by equation (3.2) as described in the text. It is assumed that $k_j = 15 k_{jj}$ as indicated by the measurements of Gotoh (1999).

Chapter 4

Induction of chromatid breaks by a single dsb

Contents	Page No.
4.1. Introduction	195
4.1.1. Group I introns	196
4.1.2. The I-SceI system	199
4.1.3. The XRCC gene family	201
4.2. Materials and methods	203
4.2.1. Cell culture and BrdU treatment	203
4.2.2. Cell poration and endonuclease treatment of GS1943, V79 and irs1 cells	203
4.2.3. Treatment of control cells	205
4.2.4. Irradiation of cells	205
4.2.5. Harvesting	206
4.2.6. Assay of G ₁ chromosome aberrations in GS1943 cells	206
4.2.7. Preparation of slides	206
4.2.8. Fluorescence plus giemsa (FPG) staining	207
4.2.9. Scoring and analysis	207
4.3. Results	208
4.3.1. Treatment of GS1943 cells with I-SceI endonuclease	208
4.3.2. Control treatments	217
4.3.3. Assay of G ₁ chromosome aberrations	218
4.3.4. Radiation exposure	222
4.3.5. Results of V79 and irs1 transfected cell lines	222
4.3.6. Comparison of GS1943, V79 and irs1 results	227
4.4. Discussion	230
4.4.1. GS1943 transfected cell line	230
4.4.2. V79 and irs1 transfected cell lines	233
4.5. Future Work	235
4.5.1. Using the I-SceI model system to investigate translocations	235
4.5.2. Using the I-SceI model system to investigate inversion characteristics	237

4.1. Introduction

The exposure of G₂ phase cells to low doses of ionising radiation leads to the induction of chromatid breaks; these are thought to result from the production by radiation of double-strand breaks (dsb) in the DNA of cells (Natarajan *et al* 1980; Bryant, 1984; Natarajan and Obe, 1984; Bryant, 1997) as described in Chapter 1. Interest in the mechanism of chromatid breakage has increased following the report that 42% of a group of breast cancer cases studied showed elevated lymphocyte chromatid radiosensitivity compared with only 9% of a group of normal controls (Scott, 1994; Scott *et al*, 1999). It is also known that elevated frequencies of chromatid aberrations are found in individuals with cancer predisposing syndromes such as AT (Sanford *et al*, 1989). The induction of dsb using restriction endonucleases (RE) is a model system which activates cellular signalling responses thought to be similar to those involved in response to ionising radiation (Thacker, 1994; Natarajan and Obe, 1984). Additional weight has been added to these findings by reports of the heritability of elevated chromosomal radiosensitivity (Helszouer *et al*, 1996; Parshad, 1996; Patel *et al*, 1997; Scott, 1999). The molecular mechanism of conversion of dsb into chromatid breaks is not understood; however the recently proposed signal model (Bryant, 1998), described in the general introduction, suggests a mechanism for this process.

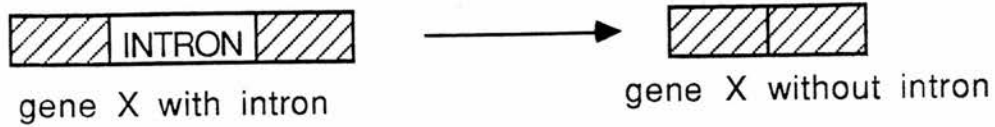
It is implicit in the signal model mechanism that a single dsb is sufficient to induce a recombinational exchange resulting in a chromatid break in G₂ cells. To test this hypothesis a Chinese hamster cell line has been used which is genetically engineered to contain a unique yeast I-Sce I endonuclease recognition site in which it is possible to generate a single dsb in the absence of any other damage to the cellular genome. Using I-Sce I endonuclease (Meganuclease), derived from a *Saccharomyces cerevisiae* Group I intron, these genetically engineered cells were treated with the I-Sce I endonuclease and resulting metaphases scored for chromatid breaks. If chromatid breaks involving recombinational exchanges (i.e. colour-switch breaks) could be detected in these cells after

treatment with meganuclease, this could be interpreted as evidence supporting an aspect of the signal model. In the Chinese hamster cell line (GS 19-43) the I-Sce I endonuclease recognition site is inserted within the hemizygous *APRT* gene locus (Sargent *et al*, 1997). A single dsb, or at higher enzyme concentrations 2 dsb at the concordant I-SceI loci in sister chromatids, were induced within the genome of this cell line by introduction of the I-Sce I endonuclease in the presence of streptolysin-O (Bryant, 1992), into cells that had been labelled through two cycles with bromodeoxyuridine (BrdU). Experiments were also carried out on two other hamster fibroblast cell lines V79 and *irs1*, both transfected with the I-Sce I endonuclease recognition site in a similar manner to the GS1943 line described below. The cells were subjected to a single enzyme dose to determine if they respond to enzyme treatment in a similar way.

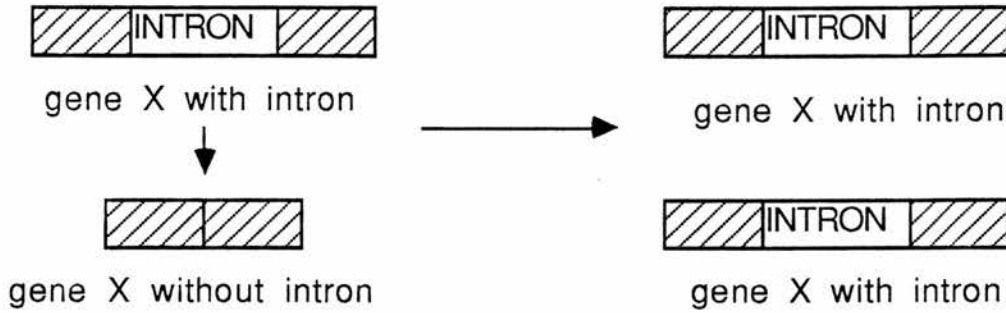
4.1.1. Group I introns.

Group I introns are found in fungi, plants, prokaryotes and bacteriophages. Although also found in mitochondria and chloroplasts they are otherwise absent from metazoans (Dujon, 1989). They are characterised by the ability of the intronic RNA sequences to fold into characteristic secondary structures to form active sites for splicing. Like Group II introns, Group I introns generally occur where transcription and translation are not physically separated, i.e. in mitochondria, chloroplasts and prokaryotic cells (the exception being introns in nuclear rRNA genes). Most Group I introns have long internal open reading frames (ORF) which points to the theory that intronic RNA needs to be translated by ribosomes.

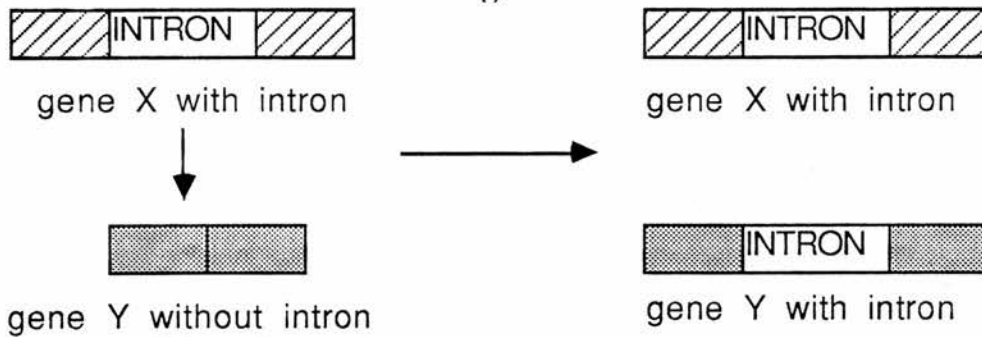
The principle characteristics of Group I introns is their ability to self-splice *in vitro* (Dujon, 1989) and their ability to propagate themselves by insertion at pre-determined positions into intron-less genes. They encode a double-strand endonuclease that cleaves



(i) **Intron loss:** the precise deletion of the intron sequence from a gene to leave a functional intron-less gene.

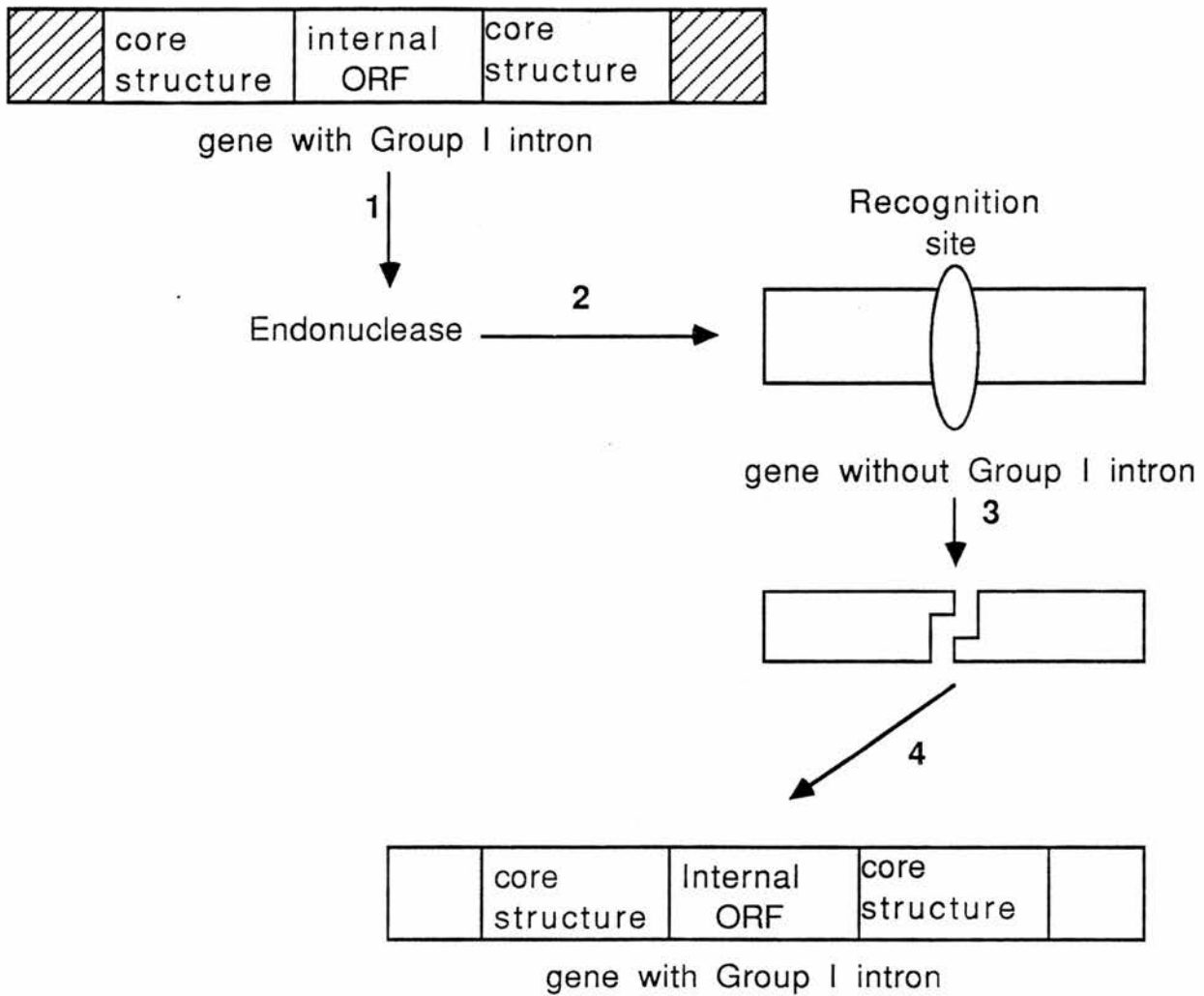


(ii) **Intron homing:** addition of an intron DNA sequence at a specific site into an intron-less gene.



(iii) **Intron transposition:** the addition of an intron sequence at a specific site into an intron-less gene, the intron sequence originating from another gene or another position of the same gene.

Figure 4.1 (a) Simplified mechanisms of intron mobility. Adapted from Dujon (1989).



Step 1: The ORF is expressed to produce the I-endonuclease.

Step 2: The I-endonuclease recognises the appropriate sequence in a copy of the same gene lacking this intron and binds to it.

Step 3: The I-endonuclease generates a 4bp 3' overhang within the recognition sequence.

Step 4: The dsb is repaired by using uncleaved sequences of the intron-plus copies of the same gene as a template, i.e. by inserting a copy of the intron. The repair mechanism can extend over flanking region. Once inserted the new intron can copy itself to produce copies of the endonuclease.

Figure 4.1 (b) Simplified mechanism for intron homing. Adapted from Dujon (1989).

intron-less genes in a sequence-specific manner. This phenomenon was originally discovered in the *omega* system of *Saccharomyces cerevisiae* (Dujon, 1989).

The mobility of the Group I introns can be categorised into intron loss, intron homing and intron transposition. Intron loss involves the precise deletion of the intron DNA sequence to leave a functional intron-less gene. Intron homing is associated with the addition of an intron DNA sequence at a specific site into an intron-less gene, the sequence arising from the same position of an intron-containing variant of that gene. Intron transposition is the addition of an intron into an intron-less gene, the sequence originating from another gene or another position of the same gene. These processes are shown in figure 4.1. All require the generation of a dsb within the recognition sequence itself.

4.1.2. The I-SceI system.

The r1 intron of the mitochondrial 21S rRNA (or LSU) gene of *S. cerevisiae* and other related yeasts contains a 235 codon ORF encoding the endonuclease I-Sce I (Monteilhet *et al*, 1990). This gene was previously known as the *omega* transposase as it has the property of propagating itself during crosses between intron-plus (*omega*⁺) and intron-minus (*omega*⁻) yeast strains, producing a transient dsb at or near the recipient site of the *omega*⁻ strain (Colleaux *et al*, 1988). The I-Sce I recognition site generates a cut with a 3'OH 4 bp overhang similar to those produced by Class II restriction endonucleases (Colleaux *et al* 1988). The recognition site is a non-symmetrical 18 bp sequence which is centred around the cleavage site:

5' - TAGGG ATAA/CAGGGTAAT - 3'

3' - ATCCC/TATT GTCCCATTA - 5'

On a random DNA sequence with 50% GC content it has been calculated that the probability of an I-Sce I site occurring by chance is 4×10^{-11} , i.e. a single cleavage site would be expected in a DNA length sixty times the size of the human genome (6000 Mbp) (Thierry and Dujon, 1992). Colleaux *et al*, (1988) engineered the r1 ORF to allow the protein to be expressed in plasmid vectors for transfection into cells of interest. They also proposed a mechanism for I-Sce I-induced dsb generation in *Escherichia coli*.

The I-Sce I protein is a monomeric globular protein which requires Mg^{2+} ions for enzymatic activity (Monteilhet *et al*, 1990) but is unstable in the presence of these ions and is also highly temperature dependent in its activity. The ability to generate a single dsb within a cellular genome using this unique site has been exploited as an investigative tool in many areas of interest including homologous and illegitimate recombination in hamster cell lines (Sargent *et al*, 1997), gene replacement in mouse embryonic stem cells (Cohen-Tannoudji *et al*, 1998), characterisation of transposition patterns of *Ac* elements in *Arabidopsis thaliana* (Machida *et al* 1997). The I-SceI endonuclease has also been used to study recombinational repair of dsb (Rouet *et al* 1994a; 1994b) and to investigate the coupling of recombination and replication in a embryonic stem cell system (Akgun *et at*, 1997, Donoho *et al*, 1998; Richardson *et al*, 1998). This model system has also been used to investigate the ability of mutant hamster cell lines XRCC2 and XRCC3 to undergo homologous recombination (Brenneman *et al*, 2000).

In the present investigation the hamster cell line GS1943 containing the I-Sce I recognition site within the APRT gene locus has been used, the cell line being hemizygous for the APRT locus (Sargent *et al*, 1997). A single dsb was induced within the genome by introduction of I-Sce I endonuclease. This was achieved by treating the cells with Streptolysin-O after they had been labelled through two cell cycles with BrdU.

A comparison was also undertaken between the V79 fibroblast-derived hamster cell line and the XRCC2- deficient *irs1* CHO-derived cell line, both transfected with a single copy of the unique *I-Sce I* endonuclease recognition site. This was done to investigate if it was possible to generate chromatid breaks and gaps in these other transfected cell lines in a similar manner to the CHO-derived GS19-43. All three cell lines were also subjected to 0.4 Gy gamma radiation to compare induced damage characteristics.

4.1.3. The XRCC gene family

The XRCC (or X-ray repair cross-complementing) gene family is a group of genes originally identified by their ability to complement hamster cell lines which display hypersensitivity to ionizing radiation and other DNA damaging agents. Several of these genes have subsequently been found to be involved in the repair of dsb in the non-homologous end-joining pathway (Jeggo, 1997).

The XRCC4 gene encodes a nuclear phosphoprotein and co-precipitates with DNA ligase IV (Grawunder *et al*, 1998; Bryans *et al*, 1999), the two proteins interacting via the two tandem BRCT repeats in the carboxy terminal domain of DNA ligase IV (Critchlow *et al*, 1997). The interaction of these two components of dsb processing is critical for lymphogenesis and neurogenesis in murine embryonic development (Gao *et al*, 1998) and is required to stabilise intermediates of the end-joining pathway in V(D)J recombination (Kabotyanski *et al*, 1998, Li *et al*, 1995). Other integral members of this pathway are Ku80, Ku70 and DNA-PK_{CS}, encoded by XRCC5, XRCC6 and XRCC7 respectively (Jeggo, 1997).

The XRCC2 and XRCC3 genes form a subset within this family, the cells display only moderate hypersensitivity to ionizing radiation compared to XRCC5 - 7 previously mentioned, displaying normal levels of dsb rejoining and V(D)J recombination (Brenneman *et al*, 2000). The hamster cell lines *irs1* and *irs1SF* are respectively deficient

in the *XRCC2* and *XRCC3* genes. These two genes have been cloned and sequenced (Cartwright *et al*, 1998; Liu *et al*, 1998) and are now considered to be members of the *Rad51* gene family associated with repair pathways utilising homologous recombination and their presence in the cell is required for repair of dsb via homologous recombination to occur (Johnson *et al*, 1999a). Rad51 has been shown to aggregate into discrete nuclear foci in a similar manner to Rad 50 (and associated proteins) and to be required for DNA damage repair in yeast and mammals (Haaf *et al*, 1995). The *XRCC2* and *XRCC3* gene products are also necessary to maintain chromosomal stability (Cui *et al*, 1999; Tebbs *et al*, 1995).

In this investigation the *irs1* cell line, transfected with the *I-Sce I* endonuclease recognition site, will be treated with the *I-Sce I* endonuclease to determine if there is any difference in the type and frequency of chromatid breaks and gaps induced by the induction of a single dsb and the spectrum of breaks induced by ionising radiation compared to the *I-SceI* transfected CHO GS1943 cell line (Sargent *et al*, 1997; Rogers-Bald *et al*, 2000).

4.2. Materials and methods

An outline of the protocol used in this investigation is shown in Figure 4.2.

4.2.1. Cell Culture and BrdU treatment.

The GS 19-43 cell line (Sargent *et al* 1997), V79, *irs1* and CHOK1 cells (laboratory stocks) were grown in Eagle's Minimal Essential Medium with Earle's salts (MEM Gibco), 50 IU/ml Penicillin, 50µg/ml streptomycin (Gibco) supplemented with 2mM L-glutamine and 10% foetal calf serum (Gibco) at 37°C and routinely passaged to maintain a sub-confluent state. Following trypsinization cells were set up at a concentration of 5×10^5 cells ml⁻¹ and after 24 hours 5-bromo-2'-deoxyuridine (BrdU) was added to a final concentration of 10 µM and the cells allowed to grow through a further 24 hours (two cell cycles) before treatment.

4.2.2. Cell poration and endonuclease treatment of GS19-43, V79 and *irs1* cells.

To introduce the *I-SceI* endonuclease into the cells, the medium was first removed from the GS19-43, V79 and *irs1* cells and the cell layer rinsed *in situ* with Hank's balanced salt solution (HBSS) without calcium, magnesium or phenol red (Gibco BRL). The GS1943 cell layer was then flooded with 1 ml of HBSS containing streptolysin SLO (Murex Diagnostics) at a concentration of 0.3 units ml⁻¹ together with varying concentrations (0, 25, 50, 100, 150, 200 units ml⁻¹) of the *I-SceI* endonuclease (Meganuclease, Boehringer Mannheim). The V79 and *irs1* cell layers were flooded with 1 ml of HBSS containing streptolysin SLO (Murex Diagnostics) at a concentration of 0.6 units ml⁻¹ together with 50 units ml⁻¹) of the *I-SceI* endonuclease. During incubation with the endonucleases the flasks were continually tilted backwards and forwards to ensure the entire cell layer was evenly treated. After 5 minutes the SLO/*I-SceI* endonuclease solution was aspirated and

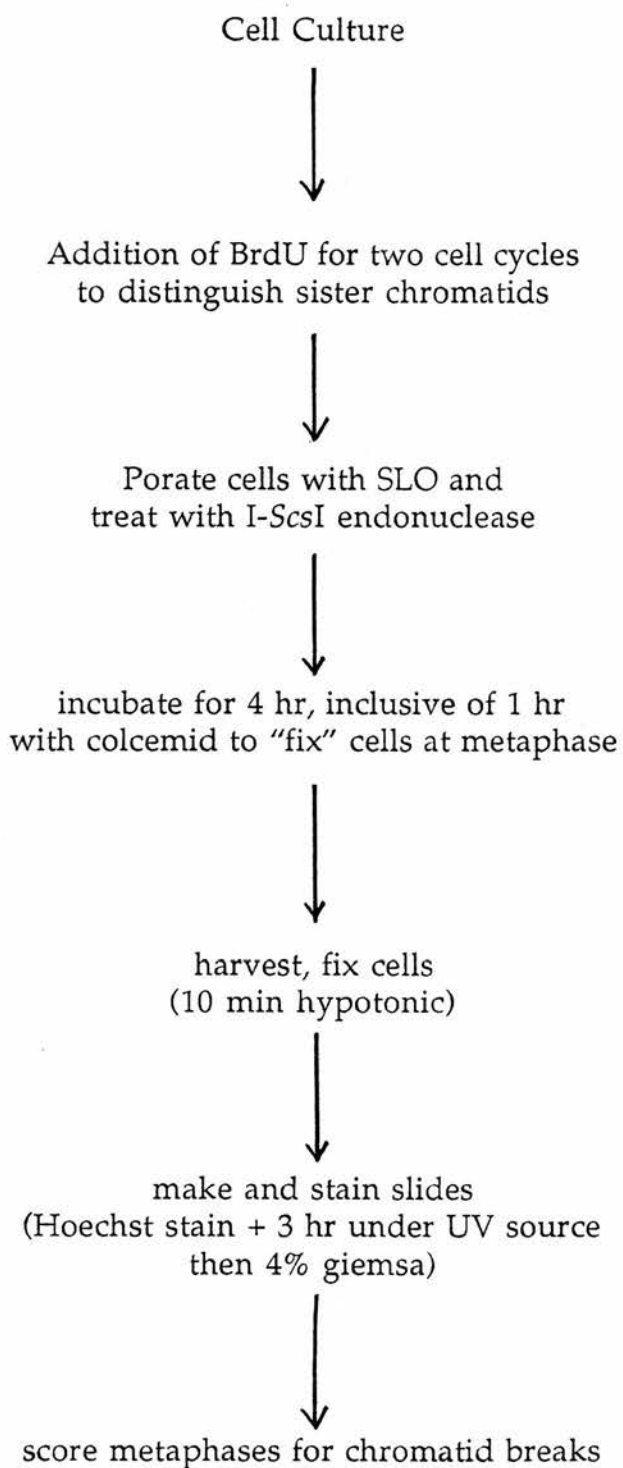


Figure 4.2. General experimental protocol.

the cell layer rinsed twice with fresh MEM + FCS; then 10 ml fresh MEM + FCS containing $0.1 \mu\text{gml}^{-1}$ colcemid (Sigma) was added and the cells were incubated for 4 hours at 37°C .

4.2.3. Treatment of control cells.

Control flasks were similarly treated with reduced SLO, at 0.3 IUml^{-1} in HBSS or incubated with SLO plus the I-*Sce* I endonuclease storage buffer. As a further control CHO cells (not containing the I-*Sce* I recognition site) were treated with SLO alone or with $100 \text{ units ml}^{-1}$ I-*Sce* I endonuclease in the presence of SLO. An additional control flask of GS1943 cells was treated with 100 units of Pst I (Sigma), a type II restriction endonuclease recognising a 6bp site and generating a 3'OH 4bp overhang similar to that produced by the I-*Sce* I endonuclease at the sequence. V79 and *irs1* cells were treated with HBSS alone, reduced SLO at 0.6 IUml^{-1} in HBSS or with 50 IUml^{-1} I-*Sce* I endonuclease in the presence of SLO at 0.6 IUml^{-1} . V79 and *irs1* cells were treated in normal light conditions of the laboratory or in the dark (flask completely enclosed in foil) to determine any breaks produced were light-induced. Additionally V79 and *irs1* cells were also treated without BrdU under normal light conditions to determine if the presence of BrdU itself induced breaks.

4.2.4 Irradiation of cells.

GS19-43, V79 and *irs1* cells were irradiated *in situ* with 0.2 Gy from a ^{137}Cs gamma source (CIS Biointernational IBL437C gamma-irradiator) at a dose rate of 7.7 cGysec^{-1} . The flasks were returned to the incubator for 30 min following irradiation before being treated with $100 \mu\text{l}$ colcemid (Sigma) and incubated for a total of 4 hours at 37°C prior to harvesting.

4.2.5. Harvesting.

After incubation the medium was removed and reserved and the cells trypsinised for 6 min at 37°C. The resulting suspension including original medium and trypsin washes was centrifuged (Hereaus Laborfuge 400R) at 1200 rpm (~ 200 g) for 10 min at 4°C. The supernatant was aspirated, the cell pellet resuspended in ice-cold hypotonic solution (0.075M KCl) and held on ice for 10 minutes before centrifuging at 1200 rpm for 10 min. The supernatant was removed, the pellet loosened and fixative (75% methanol, 25% glacial acetic acid v/v) was added very slowly to prevent clumping of cells. The resulting suspension was washed at least three more times in fixative. Finally the cell pellet was resuspended in a small volume of fresh fixative and kept at 4°C.

4.2.6. Assay of G₁ chromosome aberrations in GS1943 cells.

In the G₁ assay GS1943 cells were not pre-treated with BrdU. Flasks of cells were set up at 5×10^5 cells flask⁻¹, incubated for 24 hours and treated with SLO and 100 IUml⁻¹ of I-Sce I endonuclease as described above. After treatment the cells were incubated at 37°C for approximately 18 hours including 2 hours in colcemid before harvesting as described above. Metaphase preparations of G₁ cells incubated for 18 hours after treatment were spread and solid stained with 4% Giemsa.

4.2.7. Preparation of slides.

The microscope slides were first cooled in ice-cold distilled water for 30 min. The ice-cold slides were briefly wiped with the edge of a filter paper and flooded with ice-cold 50% glacial acetic acid solution before a single drop of cell suspension was placed on the slide and dried on a warm-plate at approximately 50°C.

4.2.8. Fluorescence plus giemsa (FPG) staining

Once dry the slides were placed in a solution of Hoechst 33258 (bis-Benzamide solution; Sigma) at $0.2 \mu\text{g ml}^{-1}$ in distilled water in the dark for 10 min and then blotted dry on filter papers. The slides were then covered with 2xSSC (0.3 M sodium chloride, 0.03 M sodium citrate, Analab) and placed under a UV-A (Philips TLD 18W/08) source for 3 hours. They were then rinsed three times in distilled water, 5 min each time, and blotted dry. Once dry the slides were then stained in 4% Giemsa for 10 min and rinsed in distilled water containing a few drops of ammonia per litre prior to blotting dry.

4.2.9. Scoring and analysis

Slides were examined under a light microscope (Zeiss, with a planapochromat 1.4 aperture \times 63 objective) and 400 metaphases scored in each sample for chromatid breaks (including gaps) and isochromatid breaks. The frequencies of breaks occurring in the light or dark stained chromatids was noted as well as the number of breaks with associated colour-switches ("colour-switch breaks"). The sister chromatid exchange frequency was also determined using the formula described in section 2.3.5. G_1 metaphases (which were solid-stained) were scored for chromosome breaks and exchanges. 400 metaphases were also scored in each sample for chromosome breaks, dicentrics and rings. Chi-square tests (Appendix I), Michaelis-Menten and linear regression analysis were used to analyse chromatid break characteristics.

4.3. Results .

A paper published in the International Journal of Radiation Biology (Rogers-Bald *et al*, 2000) was based on the results for the GS1943 cell line presented in this chapter (see appended reprint in Appendix D). Further analysis has been carried out on the data since submission for publication. The graphs presented in the results section therefore differ somewhat from those in the research paper (Appendix D) though the same data values have been used throughout.

4.3.1 Treatment of GS1943 cells with I-Sce I endonuclease.

The results of chromatid break frequencies for both control conditions and I-SceI endonuclease treatment with increasing concentrations of endonuclease are presented in Table 4.1. There was an increase in both chromatid and isochromatid breaks with increasing concentration of endonuclease. The isochromatid breaks are included in the total breaks as they are considered to contribute to induced chromatid breaks produced at concordant recognition sites on the sister chromatids. Although a single 18 bp I-SceI endonuclease recognition site was incorporated into this engineered cell line (Sargent *et al*, 1997) there are two sites present within the genome as the cells have passed through the S phase of the cell cycle and are sampled in G₂. Increasing endonuclease concentration increases the probability of both available recognition sites being cut by the introduced endonuclease. Thus with increasing endonuclease concentration the frequency of isochromatid breaks increase from 1.3 for the SLO control to 24.3 per 100 metaphases for the 200 IUml⁻¹ I-SceI endonuclease concentration (Table 4.1). Overall there was an increase in the total amount of damage sustained by the cells up to approximately 150 units ml⁻¹ of I-Sce I endonuclease after which there appeared to be saturation in the frequency of breaks induced (Figure 4.3). Only one break per cell was observed in metaphase spreads and the break always occurred in one of the larger

Table 4.1. Frequencies of chromatid breaks and exchanges per 100 cells in GS1943 cells treated with various concentrations of I-SceI endonuclease in the presence of streptolysin-O and incubated for 4 hr. 400 metaphases were scored per sample. Only one break per cell was observed except in Pst I and irradiated cells.

Treatment	Number of damaged cells	Breaks in light strand*	Breaks in dark strand*	Colour-switch breaks	Total breaks	Colour-switch ratio (%)	Isochromatid breaks	Exchanges
Control (untreated)	8	1.5	3.5	1.8	6.8	26.5	1.3	0
Storage buffer	11.3	4.0	4.8	0.8	9.6	8.3	1.8	0
Pst I (100 IU)	38.8	6.2	6.3	2.3	14.8	12.5	24.5	20.0
SL0	9	2.4	3.3	2	7.7	26.0	1.3	0
I-SceI 25 IU	25	9.7	9.8	1.5	21.0	7.1	4	0
I-SceI 50 IU	31.3	8.3	8.2	2.8	19.3	14.5	11.5	0
I-SceI 100 IU	36.4	9.0	13.8	3.8	26.6	14.3	9.8	0
I-SceI 150 IU	38.0	13.8	13.3	4.5	31.6	14.6	20.5	0
I-SceI 200 IU	32.2	12.0	12.0	5.8	25.0	23.2	24.3	0
0.4Gy irradiation	64.0	40.0	38.0	12.3	90.3	13.62	1.0	9.3

*non-colour switch breaks are the sum of the light and dark strand breaks

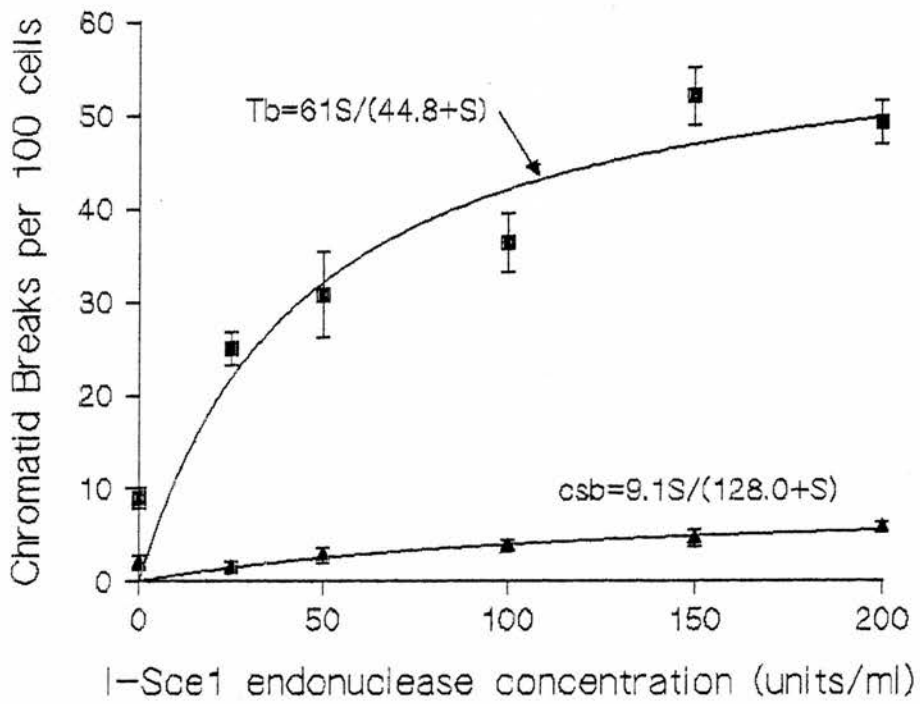


Figure 4.3. Graph of chromatid breaks per 100 cells as a function of I-SceI endonuclease concentration for GS1943 cells. Regression analysis using a Michaelis-Menten type hyperbolic curve-fit was used. Frequency of total chromatid breaks (Tb) and colour switch breaks (csb) are shown together with the best fit equations. 400 metaphases scored per data point. Error bars are standard error of the mean. r^2 (Tb) = 88.9%; r^2 (csb) = 97.2%.

chromosomes as would be expected since there should only be one recognition site within the diploid genome of this cell line. Figure 4.4 shows typical metaphase spreads of GS1943 cells. Karyotyping using a single arm FISH paint analysis suggests that the break site is on the X chromosome at or near the fragile site (Bryant, unpublished observations). The *APRT* gene in non-transformed hamster cells is located on chromosome 3 (Wang *et al.*, 1997), so the new position of this gene is presumably due to the occurrence of a translocation event in the immortalization of this cell line. CHO-derived cell lines are difficult to karyotype due to extensive chromosomal rearrangements associated with transformation (Balajee *et al.* 1995). No chromatid exchanges were observed. Assuming a lack of concentration dependence of colour switch ratio (csr), the mean ratio can be calculated from the data in Table 4.1 as 15.68% (SD = 6.60).

The experimental values for total breaks inclusive of isochromatid breaks are plotted against increasing *I-SceI* endonuclease concentration in Figure 4.3. If the isochromatid breaks are not included in the graphical analysis the resulting best fit curves give very poor r^2 values. The values for total breaks in particular show a tendency towards a saturation effect in break frequency with increasing endonuclease concentration. This suggests that any best-fit curve fitted to this data should satisfy the Michaelis-Menten type equations which forces the breaks through the origin at zero concentration and then tends to a constant value as the concentration increases.

In general terms the breaks B are related to the concentration S by the equation:

$$B = B_{\max} [S/(S + K_m)] \quad (4.1)$$

where K_m is the Michaelis constant and represents the affinity of an enzyme for its substrate and is effectively equal to the substrate concentration when the reaction is proceeding at half its maximum rate ($1/2V_{\max}$) (Woolf, 1993).



Figure 4.4 (a) Typical metaphase spread of a GS1943 cell treated with 100 IU I-*SceI* endonuclease showing a chromatid break at the endonuclease site.



Figure 4.4 (b) Typical metaphase spread of a GS1943 cell treated with 25 IU I-*SceI* endonuclease showing a colour switch break at the endonuclease site.



Figure 4.4 (c) Typical metaphase spread of an *irs1* cell treated with SLO only.

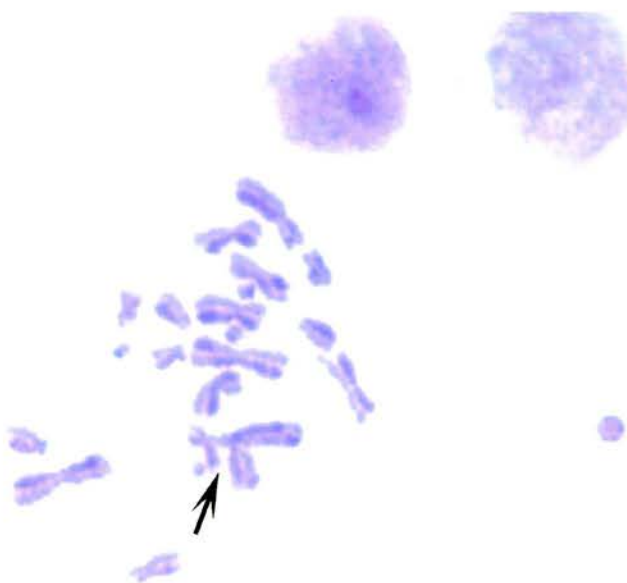


Figure 4.4 (d) Typical metaphase spread of an *irs1* cell irradiated with 0.4 Gy showing an exchange.

Applying computer regression analysis to the data of Figure 4.3 shows that the Michaelis-Menten type equations in this case are:

$$Tb = 61S/(44.8 + S) \quad (4.2)$$

$$csb = 9.1S/(128.0 + S) \quad (4.3)$$

where $r^2 = 88.9\%$ and 97.2% for total breaks (Tb) and colour switch breaks (csb) respectively. In line with the definitions given in Chapter 2 (section 2.4.2) the colour switch ratio (csr) for the action of I-SceI endonuclease on GS1943 cells using equation (4.2) and (4.3) is:

$$csr = csb/Tb = \frac{9.1S}{(128 + S)} \frac{(44.8 + S)}{61S}$$

i.e.
$$csr = 0.15 (44.8 + S) / (128 + S) \quad (4.4)$$

The csr represented by equation (4.4) is plotted in Figure 4.5 which shows that as the concentration (S) increases the csr tends to an asymptotic value of 0.15.

As described by Woolf, (1993) equations of the type (4.1) can be linearised by plotting the inverse values $1/B$ vs. $1/S$ to obtain the constants K_m and B_{max} . However with the software now available it is no longer necessary to follow this procedure to obtain these constants from experimental data as shown in Figure 4.3.

Figure 4.6 shows the experimental total chromatid break data of Table 4.1 plotted against the natural logarithm of the enzyme concentration S. Linear regression analysis applied to the data of Figure 4.6 produces the following expressions:

$$Tb = 30.1 (\log S) - 18.8 \quad (4.5)$$

$$csb = 4.43 (\log S) - 4.8 \quad (4.6)$$

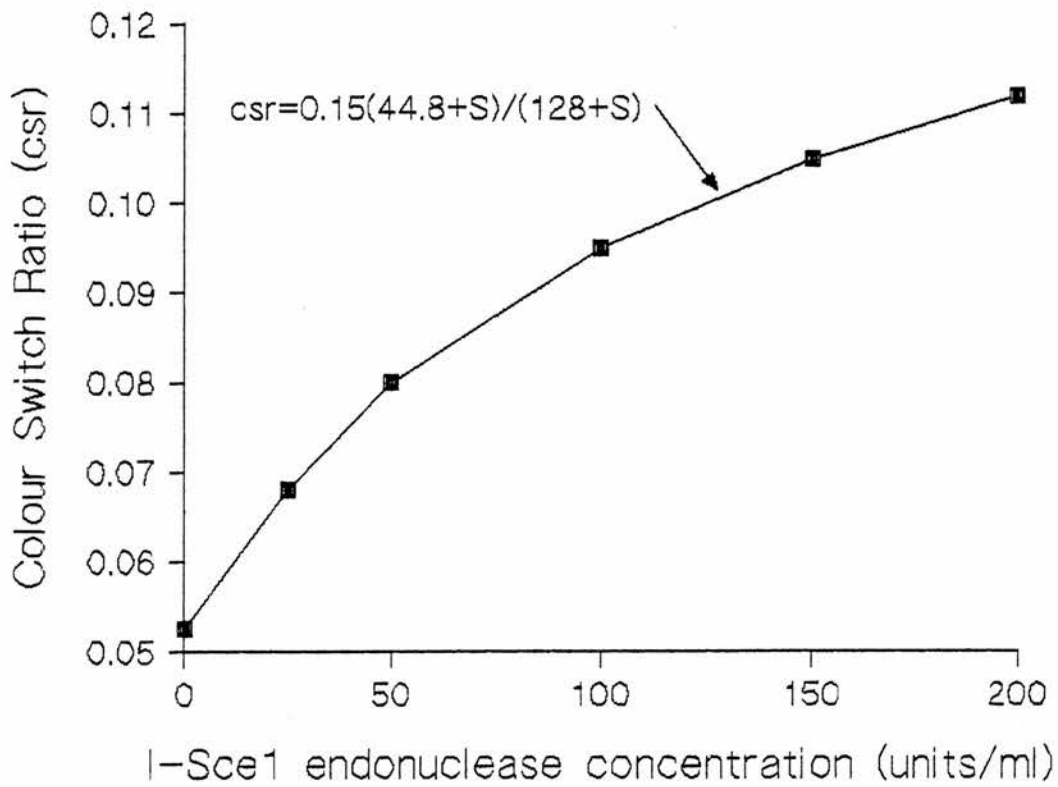


Figure 4.5. Graph of colour switch ratio (csr) values as a function of I-SceI endonuclease concentration for GS1943 cells. The csr values were calculated using equation (4.4). As the I-SceI endonuclease concentration increases the csr asymptotically approaches a value of 0.15 (15%).

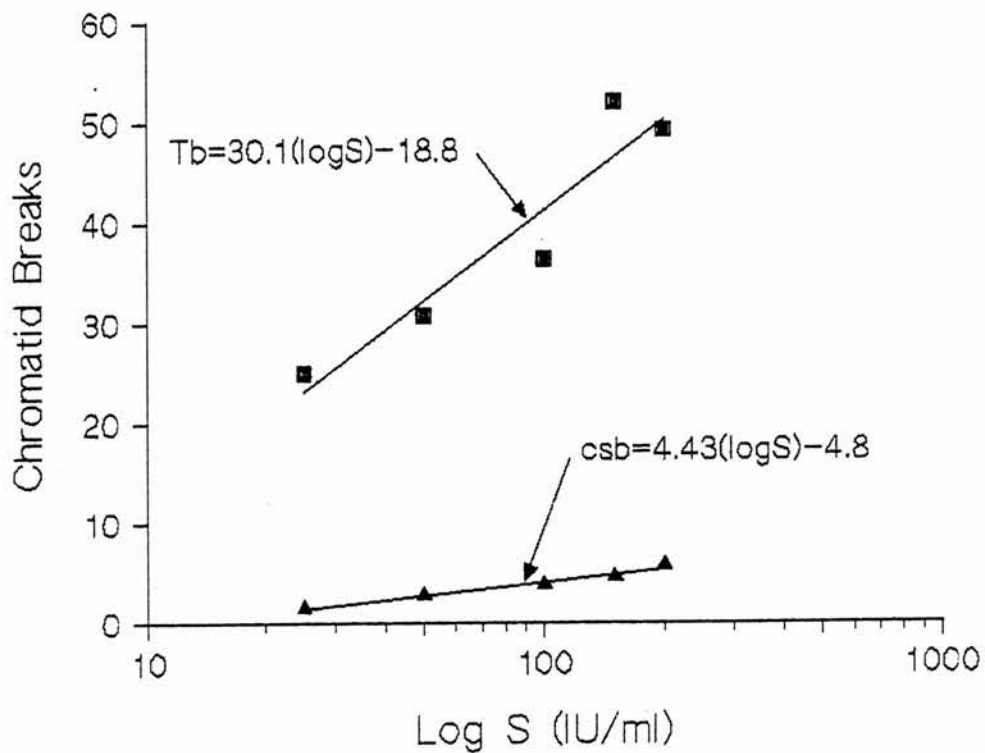


Figure 4.6. Graph of total chromatid breaks (Tb) and colour switch breaks (csb) data from Table 4.1 vs. log of I-SceI endonuclease concentration (S) for GS1943 cells. 400 metaphases scored per data point. From these linear equations it is possible to determine the csr in the same way as in equation (2.4) giving a csr value of 0.147 (14.7%) close to the value obtained from Figure 4.3. r^2 (Tb) = 88.9%; r^2 (csb) = 97.2%.

Comparing equations (4.5) and (4.6) with the general equations (2.1) and (2.2) of chapter 2, (i.e. $T_b = m_1D + c_1$, (2.1) and $csb = m_2D + c_2$, (2.2)) it is apparent that they are of the same form with the dose D replaced by $\log S$ in this case. The linear slopes for this I-SceI endonuclease reaction are therefore $m_1 = 30.1$, $m_2 = 4.43$ and consequently using equation (2.4):

$$csr = m_2/m_1 = 4.43/30.3 = 0.147 \quad (4.7)$$

This csr value of 0.147 (14.7%) agrees with the asymptotic value suggested by equation (4.4) and Figure 4.5.

4.3.2. Control treatments.

To determine if the damage recorded was due to the I-Sce I endonuclease treatment alone, G_2 assays were undertaken in which the GS1943 cells were treated with only SLO or I-Sce I endonuclease storage buffer or without any treatment at all. Storage buffer and SLO treated cells showed similar numbers of total breaks, indicating that neither the SLO or the presence of the storage buffer affected dsb formation (Table 4.1). The restriction endonuclease (PstI) was also used to treat GS1943 cells to confirm that cell poration had occurred. PstI induced similar numbers of dsb to treatment with 50 IUml^{-1} I-Sce I endonuclease (Table 4.1), a Chi square test (Appendix A) showing no significant difference in induced chromatid break frequencies based on $p < 0.01$ ($\chi^2 = 2.56$ (Yates corection), 2.88 (Woolf correction)). Assuming cell poration is equally effective in all experiments, more exchanges were induced in PstI than I-SceI treated cells, due to the large number of recognition sites for this restriction enzyme which recognises a 6bp site and creates a 4 bp 3' overhang similar to that produced by the I-Sce I endonuclease. Overall, the proportion of control cells with damage was lower than those recorded for

Table 4.2. Frequencies of chromatid aberrations per 100 cells in CHOK1 cells treated with I-SceI endonuclease in the presence of streptolysin-O and incubated for 4 hr. 400 metaphases scored per sample.

Treatment	Number of damaged cells	Breaks in light strand	Breaks in dark strand	Colour-switch breaks	Total breaks	Colour switch ratio (%)	Isochromatid break	Exchanges
Control (untreated)	3.3	1.0	1.3	0.25	2.55	9.8	0.8	0
SLO	4.6	0.8	2.0	0.8	3.6	22.2	1.0	0
100 IU	6.8	1.3	3.0	0.5	4.8	10.4	2.0	0

* Non-colour switch breaks are the sum of light and dark strand breaks.

Table 4.3. Frequencies of chromosome aberrations per 100 cells in GS1943 cells treated with I-SceI endonuclease in the presence of streptolysin-O and incubated for 18 and 22 hours. 400 metaphases were scored per sample. Only one break per cell was observed.

Treatment	Number of damaged cells	Breaks	Rings	Dicentrics
Control (no treatment)	6.3	4.3	0.5	1.5
18 hr incubation: SLO only	5.3	0.5	0.8	4.0
25 IU	32.5	32.3	0	0.2
50 IU	38.9	38.5	0.3	0.3
100 IU	11.5	11.1	0.2	0.2
22 hr incubation: SLO only	4.8	4.0	0	0.8
25 IU	18.3	17.5	0	0.8
50 IU	24.75	24.2	0	0.6
100 IU	33.5	33.1	0.2	0.2

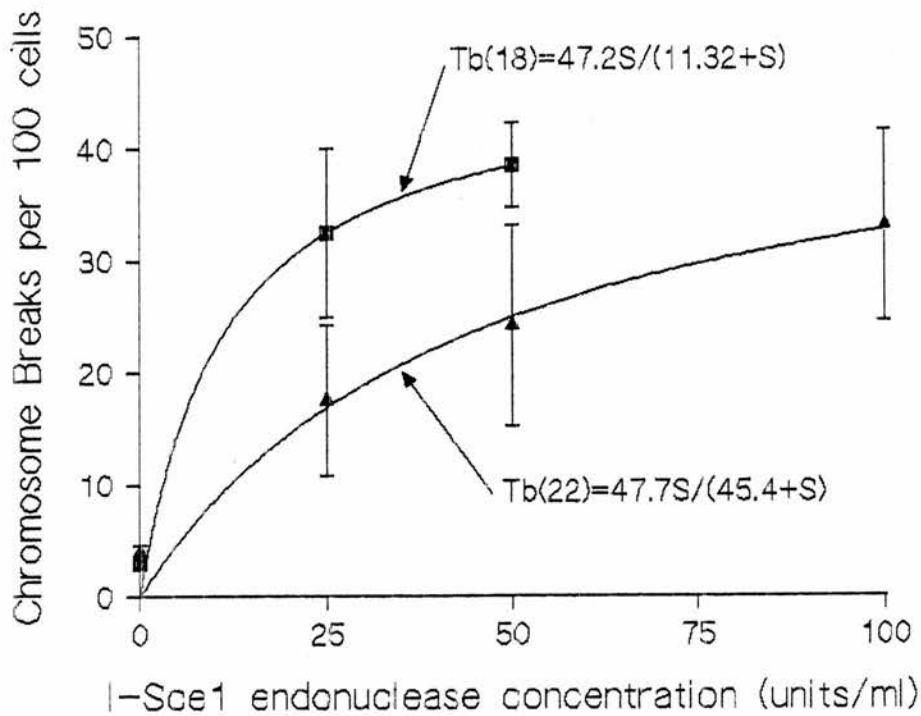


Figure 4.7. Graph of chromosome breaks per 100 cells as a function of I-SceI endonuclease concentration for GS1943 cells. Regression analysis using a Michaelis-Menten type hyperbolic curve-fit was used. Frequency of total chromosome breaks for 18 (Tb 18) and 22 (Tb 22) hour incubation periods are shown together with the best fit equations. 400 metaphases scored per data point. Error bars are standard error of the mean. r^2 (Tb 18) = 88.9%; r^2 (Tb 22) = 97.2%.

the endonuclease to interact with the *I-Sce I* endonuclease recognition site as the same batch was used for the 22 h incubation.

Although treatment with the *I-Sce I* endonuclease increased the overall number of chromosome breaks, there was no significant increase in the frequency of ring or dicentric formation. Results of treatment of CHOK1 cells with *I-SceI* endonuclease and sampled at 18 h are shown in Table 4.4 and show a decrease in the number of damaged cells and aberrations compared to 4 h incubation break frequencies (Table 4.2), but this decrease is not significant based on $p < 0.01$ ($X^2 = 2.57$ (Yates correction), 3.15 (Woolf correction)).

In contrast to *I-Sce I* endonuclease -induced breaks in the GS1943 cells, the few breaks observed in CHOK1 cells showed no particular pattern, they occurred at random within the genome and not always on the same chromosome.

4.3.4 Radiation exposure

The results for exposure of GS1943 cells to 0.4 Gy gamma radiation are also shown in Table 4.1. Although a greater number of breaks were induced compared to either the *I-Sce I*- endonuclease or the Pst 1 treatment, the csr value of 0.136 (13.62%) is well within the range of csr values obtained for these treatments. Fewer isochromatid breaks were induced in the irradiated cells and approximately half the number of exchanges induced in the irradiated compared to the Pst1 treated cells.

4.3.5 Results of V79 and *irs1* transfected cell lines.

Results of control, SLO only and *I-Sce I* endonuclease treatment for V79 and *irs1* cell lines are shown in Tables 4.5 and 4.6 respectively. The V79 cell line sustained less

Table 4.4. Frequencies of chromosome aberrations per 100 cells in CHOK1 cells treated with I-SceI endonuclease in the presence of streptolysin O and incubated for 18 hr. 400 metaphases were scored per sample.

Treatment	Number of damaged cells	Breaks	Rings	Dicentrics
Control (untreated)	7.8	6.5	0	1.3
SLO	6.8	6.5	0	0.3
100 IU	4.5	3.8	0	0.8

Table 4.5. Frequencies of chromatid aberrations per 100 cells in V79 cells containing the I-SceI recognition site. Cells were treated with 50 IU I-SceI endonuclease in the presence of streptolysin-O and incubated for 4 hr. 400 metaphases scored per sample

Treatment	Number of damaged cells	Breaks in light strand*	Breaks in dark strand*	Colour-switch breaks	Total breaks	Colour switch ratio (%)	Isochrom- atid break	Exchanges
V79 cells:								
Control no BrdU	1.8				1.8		0	0
Control BrdU in dark	2.6	3.3	3.5	0.5	7.3	6.90	0	0
Control BrdU in light	6.3	2.8	3.0	0.5	6.3	8.0	0	0
SLO	14.3	9.5	4.5	1.3	15.3	8.20	2.0	1.8
50 IU	26.0	22.0	10.8	4.8	37.6	12.67	6.0	5.3
0.4 Gy irradiation	34.5	18.5	18.8	5.0	42.3	11.82	0.5	0.5

* non-colour switch breaks are the sum of the light and dark strand breaks.

Table 4.6. Frequencies of chromatid aberrations per 100 cells in *irs1* cells containing the I-SceI recognition site. Cells were treated with 50 IU I-SceI endonuclease in the presence of streptolysin-O and incubated for 4 hr. 400 metaphases scored per sample.

Treatment	Number of damaged cells	Breaks in light strand*	Breaks in dark strand*	Colour-switch breaks	Total breaks	Colour switch ratio (%)	Isochrom- atid break	Exchanges
<i>irs1</i> cells								
Control no BrdU	29				32.3		1.0	2.0
Control BrdU in dark	38.8	22.5	21.5	4.8	54.8	8.76	0.0	1.5
Control BrdU in light	50	57.8	17.3	7.3	82.4	8.86	0.25	9.8
SLO	66.6	47.8	17.0	5.8	70.6	8.22	0.8	10.5
50 IU	59.8	60.0	29.5	10.8	100.3	10.76	0.25	17.3
0.4 Gy irradiation	59.0	56.8	35.0	12.3	104.1	11.82	0.25	11.5

*Non-colour switch breaks are the sum of the light and dark strand breaks.

damage for all treatments compared to the *irs1* cells. The *irs1* cell line sustained more light strand breaks than dark strand as well as high numbers of exchanges compared to the V79 cells when the effect of light exclusion on both cell lines was investigated. There was no increase in the total number of breaks in V79 cells due to light-induced breakage in the presence of BrdU (Table 4.5). V79 cells do however appear to be sensitive to SLO treatment (Table 4.5). There were no exchanges or isochromatid breaks in any V79 control samples. This is in contrast to the *irs1* cells (Table 4.6) which showed a marked increase in both number of damaged cells and in all types of break in light conditions. *irs1* cells kept in the dark had a lower frequency of total chromatid breaks compared to those in the light for all treatment conditions (Table 4.6).

The degree of background damage in the *irs1* cells, either control (untreated) or with SLO alone is much higher than that observed for the V79 cells, but the number of breaks induced by the *I-Sce I* endonuclease treatment is not significantly different. The difference between the 50 IU-treated cells and the SLO-treated control cells for V79 and *irs1* is 22.25 and 29.75 chromatid breaks per 100 cells respectively. Chi square analysis (Appendix A) shows no significant difference between these values based on $p < 0.01$ ($X^2 = 5.46$ (Yates correction), 5.86 (Woolf correction)). There is however a significant difference in numbers of induced chromatid breaks for GS1943 cells based on $p < 0.01$ ($X^2 = 21.7$ (Yates correction), 23.2 (Woolf correction)) when the SLO and 50 IU ml⁻¹ breaks frequencies are compared. When chromatid break frequencies for 50- IU ml⁻¹ are compared for these three cell lines, there is no significant difference in induced breaks in GS1943 and V79 cells based on $p < 0.01$ ($X^2 = 0.92$ (Yates correction), 1.1 (Woolf correction)). There was a significant difference in induced breaks in GS1943 and *irs1* cells treated with 50 IU ml⁻¹ *I-SceI* endonuclease based on $p < 0.01$ ($X^2 = 11.35$ (Yates correction), 12.0 (Woolf correction)). The GS1943 and *irs 1* cell lines derive from different parental strains; the GS1943 is a CHO line, the *irs 1* is a fibroblast line. Although the endonuclease recognition site is the same in both cell lines the difference in cell type may account for part of the significant difference observed in chromatid break induction in

these cell lines. It should also be noted that the V79 and irs1 cells were porated with a higher SLO concentration than the GS1943 cells (0.6 IUml^{-1} for V79 and irs1 compared to 0.3 IUml^{-1} for GS1943) and that this may account for any significant differences in overall chromatid break frequencies. Generally more isochromatid breaks and exchanges were observed in all irs1 cells for all conditions compared to V79 and GS1943 cells.

4.3.6. Comparison of GS1943, V79 and irs1 results.

It is possible to directly compare the csr value for the V79 and irs1 data values and hence csr with GS1943 in the same manner that disease cell line values were compared to the csr value for a normal lymphoblastoid cell population described in chapter 2. Figure 4.8 shows a plot of total breaks vs. colour switch breaks per 100 cells for GS1943 cells, where the slope of the line obtained by reduced major axis regression analysis is the colour switch ratio (csr) for this system. 95% confidence limits have been added to take into account the spread of experimental data values, but since there are fewer data points than those obtained for the comparable lymphoblastoid plot, additional confidence limits are not justified.

Figure 4.8 shows that the data points obtained for V79 cells (Table 4.5) treated with SLO alone or with 50 IU *I-Sce* I endonuclease fall well within the 95% confidence limits for GS1943 cells. The V79 total chromatid breaks data points plotted on Figure 4.8 include the isochromatid breaks for the same reasons described in 4.3.1. The irs1 values for the same enzyme concentration (Table 4.6) fall well outside the range of values obtained for V79 and GS1943 and are not shown on Figure 4.8 as the data values are so large compared to those obtained for GS1943 and V79 (Tables 4.1, 4.5 and 4.6). It was decided not to extrapolate the regression line to compare plotted irs1 values on the same graph as there are insufficient data points to justify this. However the mean csr for irs 1 cells obtained from Table 4.6 for SLO (control) and 50 IUml^{-1} *I-Sce* I endonuclease treatment is 9.49%

(SD = 1.27). This value is close to that obtained by the reduced major axis regression analysis of the GS1943 cells of 8.8% (Figure 4.8).

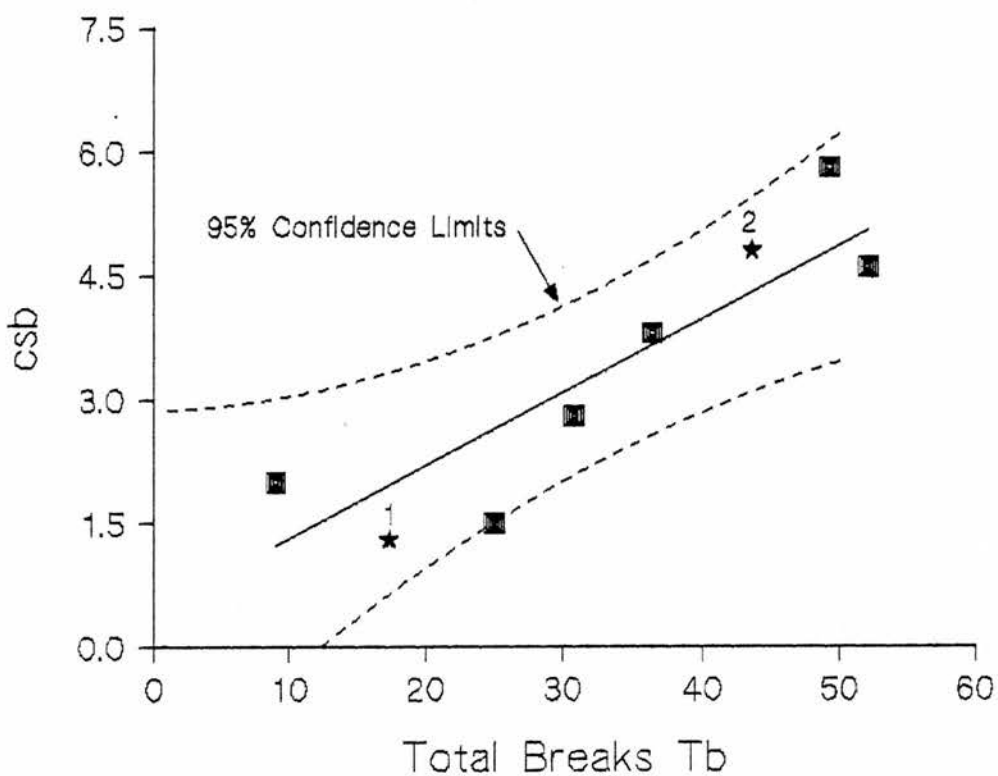


Figure 4.8 Graph of colour switch breaks (csb) vs. total chromatid breaks (Tb) per 100 cells for GS1943 and V79 cells. Total chromatid break values are inclusive of isochromatid breaks. The slope of the reduced major axis regression line represents the csr and is thus analogous to Figures 2.13 and 2.14. The equation for the resulting line is $csb = 0.088 Tb + 0.43$, giving a csr value of 8.8%. 95% confidence limits have been included to take into account the scatter of data. Star data points are V79 data values. $r^2 = 75.5\%$.

Key for numbered data points lying inside 95% confidence limits:

1. V79, SLO only;
2. V79 50 IUml⁻¹ I-SceI endonuclease.

4.4. Discussion.

The results presented here support three main conclusions. Firstly, that a chromatid break results from a single isolated double-strand break (dsb) as predicted by the signal model. Secondly, that differential mechanisms are likely to exist for the production of breaks and exchanges in G₂ cells, and thirdly that the induction of chromatid breaks by a single dsb due to transfection of the *I-SceI* endonuclease site is not a unique characteristic of the CHO transfected cell line GS1943 itself but is similarly observed in V79 and *irs 1* transfected cells lines.

4.4.1 GS1943 transfected cell line

As explained previously (Bryant, 1998) the production of a chromatid break of a width equivalent to some 5 - 40 Mbp would require the interaction of at least two dsb, an extremely unlikely event at low doses of radiation (<0.2 Gy) where chromatid breaks are frequently observed. Also, as explained earlier the resultant intervening (interstitial) fragment would most likely remain with the unaffected chromatid and not be lost. Furthermore, chromatid breaks associated with colour-switches in FPG stained cells are observed in control (untreated) cells supporting the recombinational exchange origin of these breaks (Table 4.1 and Harvey and Savage, 1997). Thus, the results presented here support the signal model which proposes that chromatid breaks arise via a recombinational exchange mechanism involving large loops of chromatin. Some of these (10-20%; Table 4.1) arise by inter-chromatid exchanges and thus exhibit a colour-switch at the break-point. It is assumed the rest occur via intra-chromatid rearrangement. No more than one aberration occurred per cell in *I-SceI* treated cells and the breaks produced were invariably in the same chromosome (preliminary assigned to derivative chromosome 7). This conforms to the expectation for a single recognition site within GS1943 cells. Chromatid exchanges (interchromosomal) were not observed in *I-*

SceI endonuclease treated GS1943 cells in contrast to *Pst* I treated and irradiated cells, indicating that formation of this type of aberration requires a dsb in more than one chromosome, i.e. they are probably formed as a result of illegitimate dsb rejoining. Thus it is concluded that the formation of chromatid (and possibly also isochromatid breaks) appear to result from an entirely different mechanism to that of exchange (interchromosomal) aberration types.

A marked increase in isochromatid breaks was observed as I-*SceI* endonuclease concentration increased (Table 4.1), presumably as a result of the increased probability of incision by the endonuclease at concordant sites in the chromatids. If the isochromatid breaks are considered to be independent breaks occurring at concordant sites within the genome of these cells then the mechanism of chromatid break formation here is the same as for chromatid breaks occurring at only one I-*Sce* I endonuclease recognition site. In this case the increase in isochromatid breaks is due solely to an increase in I-*Sce* I endonuclease concentration increasing the probability of both sites being cut during the poration/endonuclease treatment. However the possibility of interaction between the two dsb created within these cells where both I-*Sce* I endonuclease recognition sites are cut cannot be ruled out and a recombination process of the type proposed by Revell (1959) remains a possibility. However, if this were the case isochromatid breaks would appear as sister chromatid unions and this was not observed.

Treatment of GS1943 cells with I-*SceI* endonuclease in the G₁ part of the cell cycle (Table 4.3) produced exclusively chromosome breaks (acentric and corresponding centric fragments). No inter- or intra-chromosome exchanges were observed indicating that formation of dicentrics and rings requires the interaction of two dsb, confirming the conclusion reached by Bedford and Cornforth, (1983).

Figure 4.5 suggests a concentration dependency of colour switch ratio (csr). This may be due to the increase in I-*Sce* I endonuclease concentration leading to an increase in the

absolute numbers of all types of chromatid breaks and hence the csr tends asymptotically to the maximum value possible and hence the true csr value for this particular experimental system. It is expected that total break frequencies and thus resultant csr will be a function of both *I-Sce I* endonuclease and SLO concentration since both of these affect the amount of enzyme which has access to the *I-Sce I* endonuclease recognition sites.

The concentration-dependent increase in the frequency of colour switch breaks (Table 4.1) with *I-Sce I* endonuclease concentration provides supportive evidence for the signal model since such breaks are interpreted to be the failure of the cell to complete a recombination exchange event triggered by the initially induced single dsb. However if the isochromatid breaks are included in the total break frequencies then the csr value is 15 % (Figure 4.5). The mean csr excluding isochromatid breaks is 15.68 (Table 4.1), close to the value for CHO cells (16%) found by Harvey and Savage, (1997) using X-rays and data using gamma-rays (Bryant, 1998). This value is also similar to that obtained from the regression analysis for GS1943 (Figure 4.5) which gives a csr value of 15%. This supports the inclusion of isochromatid breaks in the analysis of chromatid breaks frequencies. It is also supportive evidence in favour of isochromatid breaks being the result of two independent breakage events rather than two *I-Sce I* endonuclease-induced dsb interacting to give a different break type.

The large size of the *I-Sce I* endonuclease recognition site ensures a very low probability of a second site occurring by chance in the genomic DNA as demonstrated by the CHOK1 control results (Tables 4.2 and 4.4). However it has been demonstrated that the chromatin of this cell line is still sensitive to attack from other restriction endonucleases with more frequently occurring recognition sites as demonstrated by the damage induced by *PstI* which recognises a 6bp recognition site (Table 4.1). The probability of a *Pst I* site occurring at random in a genome with 50% GC content is 9.8×10^{-4} compared with a

probability of 4×10^{-11} for the *I-Sce I* endonuclease recognition site (Thierry and Dujon, 1992).

4.4.2. V79 and *irs1* transfected cell lines.

The induction of significantly different numbers of chromatid breaks in V79 and *irs1* compared to GS1943 cells transfected with the *I-SceI* recognition site (Tables 4.1, 4.5 and 4.6) suggests that both cell poration and hence enzyme efficiency differed between these cell lines. These differences may also due to differential sensitivity of CHO and V79 cells to the endonuclease used in this investigation. Interestingly chromatid exchanges were observed in *irs 1* but not V79 (or GS1943) cells, both in endonuclease treated and irradiated cells and to a lesser extent in control cells (Table 4.6). The *irs 1* cell line is defective in *XRCC2*, a gene which participates in the homologous recombination dsb repair pathway. The exchanges observed in these cells may be due to the *I-SceI* endonuclease-induced site interacting with spontaneous breaks which arise in this cell type. An alternative possibility is that more than one endonuclease site has been incorporated into the genome of these cells, leading to an increase in exchange frequency. The significant difference in chromatid break frequency may also be due the higher SLO concentration used for V79 and *irs1* cells (0.6 IUml^{-1}) compared to GS1943 cells (0.3 IUml^{-1}), indicating that the SLO concentration is an important consideration when comparing results involving SLO-induced cell poration. It is of interest to note that although *irs1* cells sustain a high level of apparently spontaneous damage events (Table 4.5) the number of dsb induced by the single break site is very similar to that observed for the other two cell lines. Since these cells are known to be deficient in a member of the *Rad51* gene family (Cartwright *et a*, 1998; Lui *et al*, 1998) associated with dsb repair via homologous recombination (Johnson *et al*, 1999), it is likely that the observed elevated frequency of spontaneous and radiation-induced aberrations is due to the dysfunction of this pathway. There is however a lack of any observable net increase in aberrations

induced by a single dsb in these cells compared to V79 and GS1943 suggests that the dsb induced in this cell system may not be processed using a homologous recombination pathway.

In summary, it is found that the generation of a single dsb within the genome of the Chinese hamster GS19-43, V79 and irs1 cell lines lead to the induction of chromatid breaks as predicted by the signal model but with no exchanges (in the case of V79 and GS19-43), suggesting that the mechanism involved in the production of chromatid breaks differs from that of the formation of exchange aberrations such as rings and dicentrics.

4.5 Future Work.

It is important to fully investigate the effect of SLO concentration on chromatid break frequencies and hence csr as Figure 4.5 suggests that the colour switch ratio (csr) approaches a maximum value at large concentrations. This infers there will be a maximum number of possible breaks that can be induced for a particular I-Sce I endonuclease and SLO concentration. It is therefore necessary to determine how this affects the csr. Figure 4.5 indicates a maximum csr value of 15% for an SLO concentration of 0.3 IUml^{-1} , which suggests that data should be produced for different SLO concentrations with the same I-Sce I endonuclease concentration to see if this has any affect on the resultant csr value.

The linearity relationships between chromatid breaks and the natural logarithm of the concentration shown in Figure 4.6 can lead to further speculations in the light of the breakage conclusions of Chapter 3. If the radiation dose D of Chapter 3 is replaced by $\log S$ in any 3-dimensional plot involving rejoining time it is speculated that a similar experimental breakage surface would arise.

4.5.1. Using the I-SceI model system to investigate translocations.

It would also be of interest to investigate whether the I-SceI endonuclease-induced dsb used in this system caused translocations. Although translocations can be identified using karyotyping, the application of the fluorescence *in situ* hybridisation (FISH) technique to identify translocation events is more suitable for quantitative analysis of large sample sizes to determine which chromosomes are involved in such rearrangements. It has been shown that chromosome breaks increase homologous recombination by three orders of magnitude or more (Rouet *et al*, 1994a; Rouet *et al*, 1994b; Chouluka *et al*, 1995; Sargent *et al*, 1997; Laing *et al*, 1998). Richardson and

Colleagues, (1998) using the *I-SceI* endonuclease system in mouse embryonic stem (ES) cells showed that a single dsb can increase recombination events by at least three orders of magnitude from $<1 \times 10^{-9}$ to $>1 \times 10^{-6}$. A similar frequency has been seen with allelic recombination in ES cells (Moynahan and Jasin, 1997), gene targeting in ES cells using the *I-SceII* endonuclease (Donoho *et al*, 1998; Elliot *et al*, 1998) and repeat recombination (Laing *et al*, 1998) where a single dsb was introduced into one of two direct repeats and where homologous recombination was responsible for 30-50% of observed events in hamster cells. However Richardson *et al*, (1998) observed no corresponding increase in translocations suggesting that there is a mechanism which represses chromosomal translocations in mammalian cells or alternatively that two dsb are required for translocations to occur. More recently, an increase in translocations resulting from the interaction of two dsb in a mouse embryonic stem cell system has been reported where the frequency of translocations increases 2000-fold when two dsb were induced (Richardson *et al*, 2000). This is in contrast to the situation observed in yeast despite the similarity between mechanisms of recombinational repair in mammalian and yeast cells (Burgess and Kleckner, 1999). Homologous recombination is necessary for genomic integrity (Lim and Hasty, 1996; Laing *et al*, 1996) but if this were accompanied by translocations this could lead to destabilisation of the genome. The suppression of translocations in mammalian cells is important in maintaining the stability of the genome as illustrated by a rare example of repetitive element recombination i.e. Chronic Myelogenous Leukaemia (CML). Suppression may be due to sequence divergence in repetitive elements within the genome which can account for a large proportion of the total genome (a third of the human genome is composed of *Alu* elements). Alternatively a reduction in frequency of recombination due to spatial separation of repeats (also observed in yeast (Burgess and Kleckner, 1999)) and a suppression of crossover events when they do occur, possibly due to chromatin structure making such events difficult to achieve. When translocations do occur they do so between broken ends of nonhomologous chromosomes which are then each able to rejoin with another partner. It is possible that alteration of expression of genes that monitor genomic

integrity will allow translocations to occur without the affected cells being forced into apoptosis enabling conditions such as CML to develop.

4.5.2. Using the I-SceI model system to investigate inversion characteristics.

The Revell model (section 1.6.2) explaining the production of chromatid rearrangements following the induction of double-strand break(s) proposes different classes of recombinogenic rearrangements (Figure 1.9). Revell (1958) postulated that following DNA damage, recombination occurred at the base of the chromatin loops to give distinct rearrangements of chromatid material which can be seen in metaphase chromosomes if the recombination events have not been completed before the cell enters mitosis. The classification proposed by Revell (Figure 1.9) distinguishes between colour switch breaks (csb) (types 1a and 1b); non-colour switch breaks (ncsb) (types 2a, 2b, 3a and 3b) and isochromatid deletions (types 4a and 4b). This convention is also used to categorise chromatid break types in the signal model (Bryant, 1998). A proportion of the non-colour switch break types will be the result of inversion of part of one of the chromatids and thus not detectable using the fluorescence-plus-giemsa (FPG) staining technique (Perry and Wolff, 1974). It is not possible to determine which ncsb are the result of an inversion event or which are "simple" chromatid breaks using the FPG technique as these recombinogenic rearrangements are intra-chromatid in character.

An alternative approach is to use fluorescence *in situ* hybridisation (FISH) to determine the frequency of inversions within a cell type. The advantage of using a cell system with a single break I-SceI site such as those used in this chapter is that it would then be possible to determine the complete chromatid break characteristics for this model system.

Results presented here and elsewhere (Harvey and Savage, 1997; Bryant, 1998) demonstrate that the induction of chromatid breaks (which can be subdivided into ncsb

and csb) is linear with dose (section 2.4.2). The proportion of colour switch breaks (csb) within the total breaks (Tb) defined as the colour switch ratio (csr) has been demonstrated to be independent of radiation dose. It has also been demonstrated in this chapter that the csr is independent of \log_{10} endonuclease concentration at a specific sample time. However since the characteristics and induction of ncsb which involve an inversion event are not known, it would be informative to determine whether the induction of inversions is also linear with either radiation dose or endonuclease concentration as is the case for csb. It would also be very informative to demonstrate if the frequency of inversions is sample time dependent.

It should be possible to determine the frequency of inversions following induced damage by using FISH probes. Preliminary investigations have been undertaken using a locus specific (LSI) probe for chromosome 5q31 on a normal human lymphoblastoid cell line where an inversion could be visualised as a relative displacement of one of the probe sites on sister chromatids following exposure to ionising radiation. A general protocol for FISH together with the materials and methods used for this preliminary investigation is presented in Appendix C. Although the probe was clearly visible (Figure 4.9) it was not possible to detect inversions using the LSI probe. Although the resolution of the captured images could have been better, it is unlikely that it would be possible to detect anything but extremely large relative movements of the signal within the chromosome arm due to the small size of the probe. A more appropriate approach for determining the inversion frequency in cells in the G₂ phase of the cell cycle may be to use multiple FISH probes along one arm of a target chromosome. If an inversion occurs in this region, it would then be possible to detect such an event by a change in the relative positions of the different probes. Alternatively in the case of inversion events which involve smaller regions of the chromosome, a change in the relative size of the probe would occur compared to the corresponding chromosome arm in which there has been no inversion. Although it may be possible to visually detect such changes, an image analysis system would be a more sensitive and thus more accurate method of

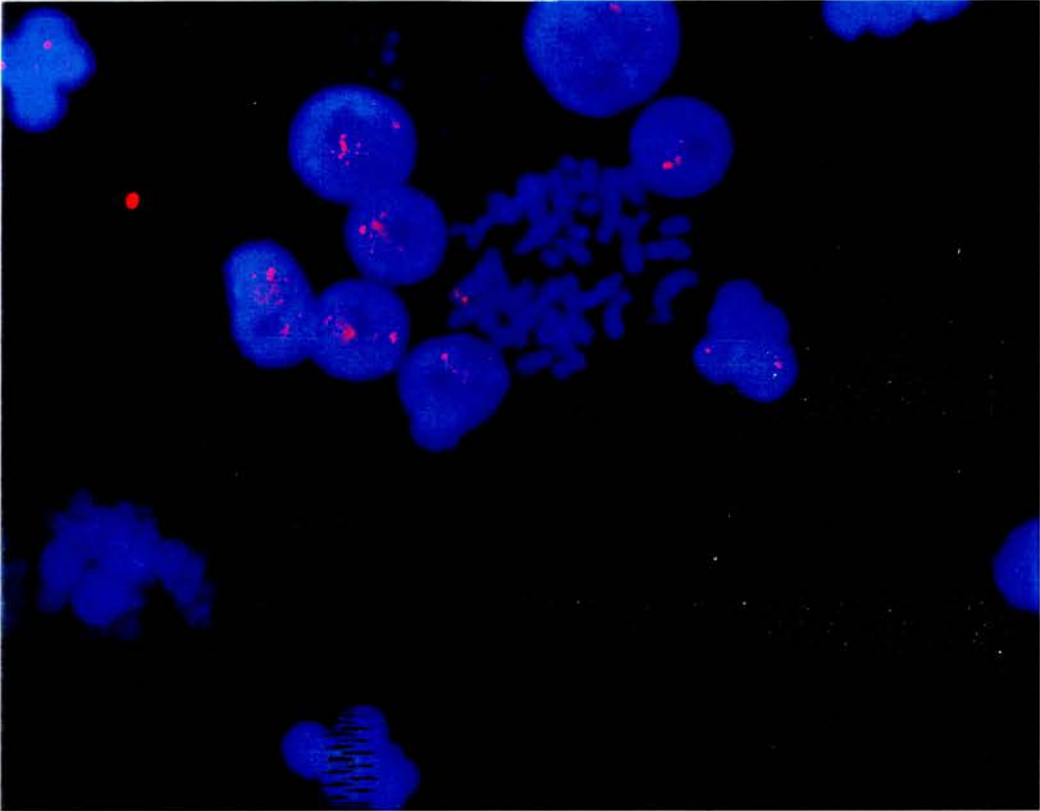


Figure 4.9 Typical metaphase spread of a normal lymphoblastoid cell irradiated with 0.2 Gy and counterstained with DAPI showing the two LSI 5q31 probe sites in both interphase nuclei and mitotic chromosomes.

analysis. This technique would be particularly suitable for the I-SceI model system under consideration here as the probes could be targeted to the endonuclease recognition site and thus determine the inversion frequency as a result of a single induced dsb.

Inversions would be visualised as either changes in the sequence of visible probes or possibly as splitting of probe sequences to give detectably smaller colour bands.

On the assumption that inversion frequencies could be determined by the approach outlined above, it would then be possible to determine the proportion of inversion-associated ncsb within the total chromatid breaks, here defined as the inversion ratio (ivr).

It has been shown in section 2.4.2 that a linear relationship exists between total breaks (Tb) and radiation dose (D), the linear expression for this is:

$$Tb = m_1D + c_1 \quad (2.1)$$

where Tb = total chromatid breaks, D = dose (Gy), m_1 = slope of line and c_1 = intercept on y axis. A similar expression was determined for the induction of colour switch breaks (csb) with dose, i.e.

$$csb = m_2D + c_2 \quad (2.2)$$

and thence to obtain a linear relationship for the csb and Tb:

$$csb = (m_2/m_1)(Tb - c_1) + c_2 \quad (2.3)$$

where the csr is the slope of the line (m_2/m_1) when csb are plotted against Tb.

If a linear relationship also exists between the inversion-associated breaks and total breaks it would therefore be possible to obtain an analogous relationship between the total breaks and inversion-associated breaks (ivb):

$$ivb = m_4 D + c_4 \quad (4.10)$$

where ivb = inversion-associated breaks, D = dose, c_4 = intercept on the y axis.

Thus:

$$ivb = (m_4/m_1)(Tb - c_1) + c_4 \quad (4.11)$$

The slope of the straight line relationship between ivb and Tb, defined here as the inversion ratio (ivr), would then be:

$$ivr = m_4/m_1 \quad (4.12)$$

From the foregoing definitions the csr and ivr are directly related by the expression:

$$ivr = (ivb/csb) \cdot csr \quad (4.13)$$

or in terms of the slopes of the lines representing the variation of ivb and csb with dose D, equation (4.13) becomes:

$$m_4 = (ivb/csb) \cdot m_2 \quad (4.14)$$

A further relationship can be derived from the foregoing definitions concerning inversion-associated breaks. If the fraction of ncsb which comprises the ivb is denoted by μ , i.e. $\mu = ivb/ncsb$ then:

$$ivb = \mu \cdot ncsb$$

i.e.

$$ivb = \mu (Tb - csb)$$

or

$$ivr = ivb/Tb = \mu (1 - csr) \quad (4.15)$$

Although the inversion ratio is postulated here on the assumption that induction of inversion-associated breaks is linear with dose, it is also possible to determine the *ivr* where the relationship is non-linear in the same manner as described in section 2.4.2 when the consequence of a non linear induction of total and colour switch chromatid breaks at higher radiation doses was considered. As described in 2.4.2, provided the equations describing the total break or inversion frequency as a function of dose are of a similar form (e.g. both quadratic) it is still possible to determine a linear relationship for the *ivr* in terms of total breaks and inversion-associated breaks. Similarly the *ivr* can also be determined for the *I-SceI* model system (and for other investigations using restriction endonucleases) where a linear relationship exists between the \log_{10} of the endonuclease concentration and the induced chromatid break frequencies.

Extending this approach discussed above, a breakage surface could be experimentally determined for *ivb* and *ivr* to cover the whole spectrum of applied radiation dose and sample time within G_2 .

Chapter 5

Determination of the colour switch ratio in different species

Contents	Page No.
5.1. Introduction	243
5.1.1. Chromosome structure in metazoans	245
5.1.2. Chromatin remodelling	249
5.1.3. Cell lines under investigation	252
5.1.3.1. <i>Potorus tridactylus</i>	253
5.1.3.2. <i>Drosophila melanogaster</i>	254
5.1.3.3. <i>Vicia faba</i>	255
5.1.3.4. Mouse CB17 cell line	256
5.2. Materials and methods	257
5.2.1. Cell culture and BrdU treatment of CB17 and <i>Potorus</i> cells	257
5.2.2. Irradiation of cells	257
5.2.3. Harvesting	257
5.2.4. Preparation of slides	258
5.2.5. Fluorescence plus giemsa (FPG) staining	258
5.2.6. Scoring and analysis	259
5.2.7. Cell culture and BrdU treatment of <i>Drosophila melanogaster</i> cells	259
5.2.8. Harvesting, slide preparation and staining of <i>Drosophila</i> cells	260
5.2.9. Culture of <i>Vicia faba</i> seeds	260
5.2.10. Irradiation of <i>Vicia faba</i> root tips	261
5.2.11. Slide preparation and staining of <i>Vicia faba</i> root tips	261
5.3. Results	
5.3.1. Chromatid break characteristics of <i>Potorus</i> and CB17 cell lines	262
5.3.2. Comparison of species with a normal human cell line	262
5.3.3. The <i>Drosophila</i> cell line	270
5.3.4. <i>Vicia faba</i>	270
5.3.5. Breakage characteristics for V79 and GS1943 cells.	270
5.4. Discussion	274
5.5. Future Work	276

5.1 Introduction.

Throughout evolution the DNA of all organisms has been damaged by endogenous (hydrolysis, methylation, oxidation) and exogenous (exposure to uv, ionising and cosmic radiation) damaging events. It is therefore not surprising that a wide range of DNA damage recognition and repair processes have evolved to deal with this problem. There is a high degree of conservation of both the structure and function of proteins involved in DNA repair processes from bacteria to mammals, for example human *RAD51* shares a 69% sequence homology with *Saccharomyces cerevisiae* (Taylor and Lehmann 1998). This infers that the large body of research into DNA repair mechanisms in yeast model systems is directly applicable to the understanding of mammalian repair pathways. However, the details of DNA damage recognition, repair and recombinational mechanisms specific to yeast systems are beyond the scope of the present investigation. The nuclear architecture and chromosome structure of metazoans is also thought to be highly conserved. Thus it may be predicted that the recognition and processing of primary DNA damage caused by ionising radiation and other clastogenic agents would also be highly conserved. It is therefore of interest to consider if the relative proportions of the different chromatid break types observed in cells using the G₂ assay will also be constant for all cell types. If this were found to be the case, it would support the hypothesis that double-strand breaks (dsb) induced in G₂ which give rise to a fixed proportion of colour switch breaks, do so as a result of the change in the chromatin configuration in the vicinity of the initiating dsb. Depending on where a dsb arises within the chromatin fibre loop system within the nucleus, a different chromatin configuration may be presented. Subsets of chromatin configurations would then be accessible to different repair complexes giving rise to the fixed proportions of colour switch breaks observed previously in this investigation and predicted by the signal model (Bryant, 1998).

The structure of chromatin is highly conserved in metazoans and it is possible that the nuclear organisation of replication and transcription complexes into "factories" (Hughes, 1995; Iborra 1996; Cook 1999) may also be highly conserved. It may therefore be postulated that the ability of repair and recombination protein complexes to access damaged regions of the DNA following a damaging event (e.g. exposure to ionising radiation) will be essentially the same in all metazoans. Access to damaged chromatin is dependent on the three-dimensional configuration of the DNA and its associated proteins. If the ability of repair and recombinational protein complexes to interact with regions of damaged DNA is determined by the conserved chromatin conformation at these damage sites then the proportion of colour switch breaks (the csr) should be similar in all metazoans, within the limits of experimental error. The signal model (Bryant, 1998) like the Revell model (1959) postulates that recombination events (which if incomplete at mitosis), lead to the formation of colour switch and non-colour switch breaks in cells grown through two cell cycles in the presence of BrdU (Perry and Wolff, 1974). The recombinational events leading to the formation of csb and ncsb take place at the base of the chromatin loops present in cells in the G₂ phase of the cell cycle. As the looping structure of the DNA is a repeating motif throughout the genome and highly conserved through evolution it may be predicted that there is a finite number of chromatin configurations which could occur, which will fall into distinct subsets recognised by different repair complexes. A fixed proportion will be recognised and interact with those recombinational repair complexes which give rise to colour switch breaks as an observable end-point and thus lead to a constant csr regardless of the number of chromosomes into which the DNA is subdivided.

The organisation of DNA into chromosomes and how this is affected by the

actions of DNA damaging agents (in particular ionising radiation) will be considered, followed by a brief description of the cell lines investigated.

5.1.1. Chromosome structure in metazoans

The image of condensed chromosomes segregating along the spindle of a dividing cell is a familiar one. Apart from the number of chromosomes and their relative size, the chromosomes of all metazoans are similar in appearance being linear and are immediately distinguishable from those of prokaryotes which have circular chromosomes. A possible reason for this conserved dichotomy may be that linear chromosomes are necessary for productive meiosis which gives rise to genetically diverse offspring and is thus a major driving force in evolution (Ishikawa and Naito, 1999). Eukaryotic genome size (C value) does not appear to correlate with either complexity or the number of functional genes within an organism (Petrov, 2001) as much of the genetic material consists of repetitive sequences, introns and other forms of non-coding "junk" DNA.

Chromatin is the macromolecular association of DNA, histones and nuclear proteins which make up chromosomes (Alberts *et al*, 1994). Metaphase chromosomes represent the most condensed form of chromatin. The average human chromosome contains approximately 130 million base pairs, which corresponds to a physical length of 45 mm. If this is compared to the length of the mitotic spindle (10 - 20 μm) it is obvious that chromosomes are massively condensed by a factor 10^4 in order for the cell to successfully complete mitosis. Chromosomes are less condensed during interphase, however the level of chromatin condensation changes throughout the cell cycle. Cell fusion studies have shown that in G₁ and S phase, chromosomes consist of very long threads, but sister chromatids are only visible in G₂ with apparently continuous

condensation from the end of S phase to the onset of mitosis (Murray and Hunt, 1993). The various levels of chromosome condensation are shown in Figure 5.1. The double helix is wrapped around histone complexes which are the major structural protein of chromosomes. Histones are small basic proteins arranged in octamers and each histone core is wound with two turns of the DNA helix to create a nucleosome with spacer regions between where histone 1 (H1) is positioned. The resulting nucleosome string is wound into a solenoidal fibre with adjacent nucleosomes forming a zig-zag pattern (Rydberg *et al*, 1998) which is in turn arranged into loops approximately 50,000 bp or 50 kbp in length (Murray and Hunt, 1993). Some disagreement exists over the precise lengths of these loops depending on the procedure used to determine their length and also the condensation status of the chromosomes (i.e. their precise position in the cell cycle) when the analysis is performed.

Viscoelastometry data (a measurement of the elastic recovery of solutions from mechanical stress) estimates the average loop size to be 1.3 Mbp in G₀/G₁ cells (Ostashevsky *et al*, 1999) but later work suggests that chromatin loops form 10-30 Mbp clusters or micelles (Ostashevsky, 2000) whereas other groups have estimated loop size to be approximately 75 kb (Laemmli *et al*, 1977) and 1.6 Mbp (Johnston *et al*, 1997). These loops are considered to be the basic unit of transcription and replication and are supported by a protein scaffold which contains lamins and topoisomerase I and II.

The major scaffold protein is topoisomerase II and DNA elements called scaffold-associated regions (SAR) may define the base of chromatin loops. SAR are rich in AT sequences, such AT-rich DNA regions (also identified as G-bands) are generally associated with gene-poor regions of the chromosome which replicate late in S phase. This is in contrast to the GC-rich regions (R-bands) which replicate early in S phase these regions being associated with highly expressed housekeeping genes. R-bands may be less tightly coiled than

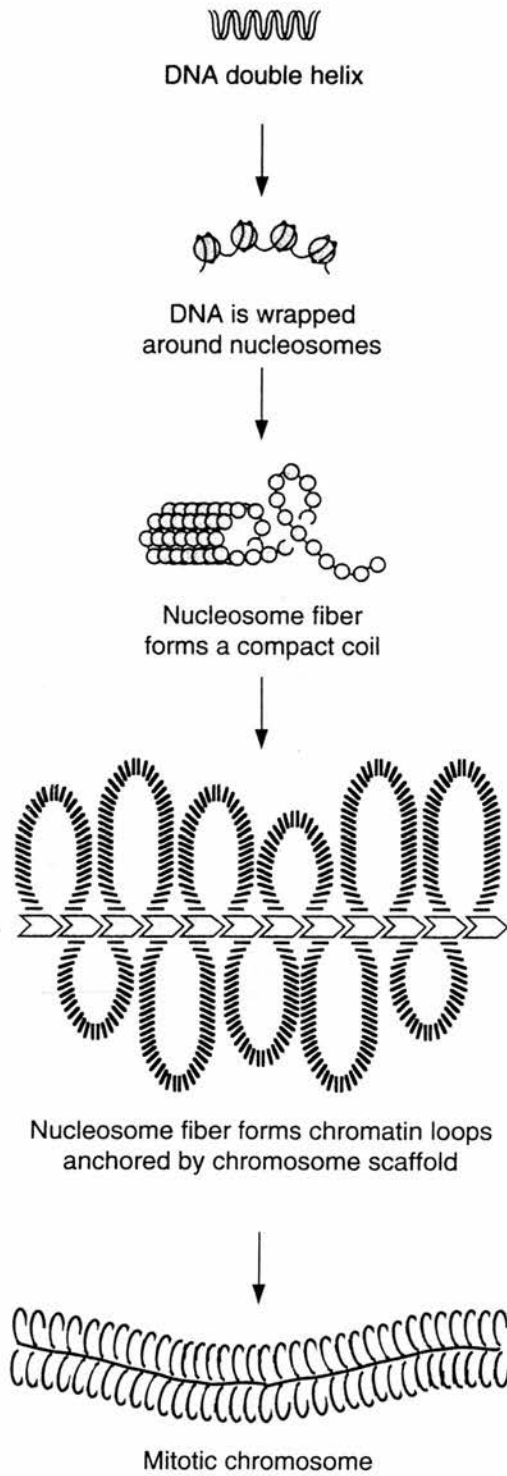


Figure 5.1 Diagram showing levels of chromatin condensation. From Murray and Hunt, 1993.

G-bands with longer chromatin loops (Saitoh and Laemmli, 1994). Bickmore and colleagues (1996) used Comparative Genomic Hybridisation (CGH) to determine average chromatin loop size and also showed that loop sizes were generally smaller in gene-rich areas (R-bands) with a greater number of scaffold attachments. Those in the gene-poor regions (G-bands) contained larger chromatin loops and hence fewer SAR. Also regions of the genome associated with high densities of RNA polymerase are preferentially associated with the nuclear skeleton but not the nuclear scaffold or matrix (Craig *et al*, 1997). These findings are also in general agreement with the work of Cook (1995) who also predicted more frequent attachments to the nuclear skeleton and hence smaller loops in R-bands compared to G-bands. Further work using fluorescence *in situ* hybridisation (FISH) showed that specific DNA sequences are associated with the axial region of metaphase chromosomes. Origins of replication are associated with the chromosome scaffold, with replication occurring as the DNA template moves through the replication factory which is itself fixed in association with the nuclear scaffold or matrix (Hozak *et al*, 1993; Bickmore and Oghene, 1996; Cook 1999). This evidence is in agreement with the generally accepted model of chromatin structure in which the basic structural elements of the chromosome are nucleosomes, chromatin loops and transcription factories situated at the base of the chromatin loops. The chromatin loops are in close association with transcription factors, RNA polymerases and repair complexes concentrated in the "factories". The remnant of these factories (chromomeres) remain in association with the loops (average length 86 kbp) during mitosis and increased adhesiveness between nucleosomes and the factories drives a "sticky-end" aggregation to form a cylinder of nucleosomes around an axial core which represents the most stable and compact structure for mitotic chromosomes (Cook, 1995; Hughes *et al*, 1995). The number of transcription and replication factories varies depending on the activity level of the cell, 2000 - 7000 being observed in HeLa cells (Iborra

et al, 1996) with each “factory site” containing many transcription units.

The mechanisms of chromosome condensation and decondensation are not yet fully understood, but it appears that the nuclear architecture and positioning of chromosomes within the interphase nucleus is not a random event and that chromosomes occupy specific domains with respect to each other within the non-dividing nucleus (Nagele *et al*, 1999). The spatial organisation of the genome appears to be established early in G₁ (Bridger *et al*, 2000). The regulation of access of genes by transcription factors is of great importance in the maintenance of cellular systems and the processing of DNA damage. DNA sequences are often masked by histones which must be moved or modified to allow access. The umbrella term for such changes in chromosome condensation and histone movement is chromatin remodelling.

5.1.2. Chromatin remodelling.

The regulated alteration of chromatin structure or chromatin remodelling (reviewed by Aalfs and Kingston, 2000) can be achieved by covalent modification to the histones themselves or by the activity of ATP-dependent remodelling complexes. The acetylation and phosphorylation status of the histone proteins is a major determinant in the accessibility of the DNA for replication, transcription, silencing and repair mechanisms to proceed. There is an increasing amount of interest in the possible role of chromatin remodelling in the onset or repression of cancer (Archer and Hodin, 1999). Possibly the best understood mechanism of chromatin remodelling regulating transcription is the interaction of the retinoblastoma (RB) protein with histones regulating their acetylation status. A repressor complex containing hypophosphorylated RB and histone deacetylase forms early in G₁. This complex interacts with E2F, a transcription factor which is bound to S phase-specific promoters. This

complex deacetylates the nucleosomes surrounding the promoter region and induces a change in chromatin conformation which effectively prohibits access to the promoter region (Brehm and Kouzarides, 1999). Other proteins, for example the DEK proto-oncogene which is associated with acute myeloid leukaemia, have also been found to alter chromatin conformation and thus the ability of DNA to replicate (Alexiadis *et al*, 2000).

The association between chromatin organisation and cellular responses to DNA damaging events is also of interest. There is evidence supporting chromatin remodelling following radiation exposure in G₀/G₁ (Figgitt and Savage, 1999). Studies have also looked at the interaction of chromosomes subjected to radiation in G₀/G₁ to test the breakage-and-reunion model by theoretically predicting the ability of individual chromosomes to interact based on large-scale chromatin geometry (Sachs *et al*, 2000). However given the difficulties encountered in attempting to produce an accurate three-dimensional model of chromatin structure *in vivo*, it is not yet possible to accurately determine chromosomal interactions by this method.

The hypothesis that components of DNA double-strand break repair is dependent on the relative position of lesions within the chromatin structure is not new. Multiple dsb in loops were found to be repaired slower than single dsb in loops (Johnston and Bryant, 1994) and that such multiple dsb are not repairable in cells deficient in V(D)J recombination in cells subjected to high doses of radiation (up to 200 Gy), measured by neutral filter elution (Johnston *et al*, 1998). Changes in supercoiling in DNA during repair of ionising-radiation induced damage have been observed (Van Rensberg *et al*, 1987) as well as an increase in the flexibility of DNA following damage and in particular base damage (Marathias *et al*, 1999). These observed changes in DNA character following damage may be due to long range effects emanating from the

original lesion such as long range oxidative damage (Nunez *et al*, 1999). They may also be due to changes in the phosphorylation status of histones H1 and H3 caused by the action of radiation-induced signal pathways, which alter the binding affinity of the histones and DNA due to changes in electrostatic attraction and enable access of DNA repair complexes. Both H1 and H3 are dephosphorylated after ionising radiation, H1 in an ATM-dependent and H3 in an ATM-independent manner (Guo *et al*, 2000). This observation is in agreement with previous speculations that the radiosensitivity of AT cells is due to an altered chromatin structure (Hittelman and Pandita, 1994). The BRCT domain of *BRCA1* has also been recently associated with chromatin remodelling. *BRCA1* has a number of regulatory roles including transcription, repair, recombination and checkpoint control (Miyake *et al*, 2000), the BRCT domain being principally involved in transcriptional activation and DNA repair. This chromatin remodelling ability is not a universal feature of proteins containing BRCT domains and may hold clues to the precise role of *BRCA1* within the cell. Yeast studies have also found evidence linking chromatin remodelling with DNA damage repair including the discovery of a motif in histone 2A, one of the octamer core histones, which is required for the completion of dsb repair by non-homologous end-joining in *Saccharomyces cerevisiae*. This implies that the histone octamer may also play a role in chromatin remodelling to facilitate DNA repair (Downs *et al*, 2000). The evidence available at present suggests that chromatin remodelling complexes may represent a subset of those complexes primarily considered as involved in different types of DNA repair (Meijer and Smerdon, 1999).

There has been some evidence to suggest that the frequency of chromosomal aberrations is not the same for all chromosomes (Cigarran *et al*, 1998; Xiao and Natarajan, 1999) but these results are generally inconclusive. It is possible that regions of DNA are differentially susceptible to radiation-induced DNA

damage during different phases of the cell cycle due to the protective effect of DNA-associated proteins (Sak *et al*, 2000). Thus not all regions of DNA are equally likely to sustain damage, but it is not clear whether the distribution of DNA among chromosomes of differing sizes is an important factor.

5.1.3. Cell lines under investigation.

A number of transformed cell lines were selected to determine the chromatid break characteristics in an attempt to cover a wide range of metazoan species. The main purpose was to determine if the processing of dsb to form chromatid breaks in G₂ is sufficiently similar to produce the same csr. If the csr is the same in a wide range of species this would provide important evidence supporting the dual role of protein complexes in both DNA repair and recombination and in chromatin structure maintenance and remodelling. A mouse fibroblast cell line (CB17), a marsupial cell line derived from *Potorus tridactylus*, a *Drosophila* cell line (C18+) derived from *Drosophila melanogaster* and non-transformed root tips from the broad bean *Vicia faba* have been investigated at a specific sample time of 1.5 hr. Chapter 3 has highlighted the importance of using a specific sample time within G₂ to investigate chromatid damage. These results have been compared to the human lymphoblastoid population characterised in Chapter 2 to determine if the csr varies significantly in different species. Chromatid break characteristics for hamster fibroblast V79 and CHO-derived GS1943 cells (Chapter 4) are also used to determine the csr for a sample time of 1.5 hr on the assumption that the presence of the I-SceI endonuclease site in these cells would not significantly affect the chromatin structure.

It was not possible to produce sufficiently good scorable metaphases for either

Drosophila or *Vicia faba* as described later. It was however decided to include the materials and methods for these two cell types for completeness.

5.1.3.1. *Potorus tridactylus*.

The *Potorus tridactylus* or potoroo is also known as the long-nosed rat-kangaroo is a marsupial native to Tasmania. It is thought to be the descendent of *Potorus longpipes* from which it is thought to have evolved as a separate species by chromosomal fusion as *Potorus tridactylus*, has half the number of chromosomes of *Potorus longpipes* ($2n = 24$) (Johnston *et al* 1984). *P. tridactylus* ($2n = 12$ in females, $2n = 13$ in males) and has been successfully used a laboratory animal for some time (Ullmann and Brown 1983). Cell lines have been established to investigate the effect of UV light on SCE formation (Kato 1974, Liang and Berns 1983, Ishizaki and Takabee 1985, Ishizaki *et al* 1980), to determine kinetochore structure (McEwen *et al* 1998) and to test Revell's exchange hypothesis by Heddle *et al* (1970).

Discussed in more detail in 1.5.2, Revell's exchange model predicted that 2/5 or 40% of all chromatid exchanges would involve an exchange between sister chromatids (which could be visualised as a colour switch break in cells grown through two cell cycles in the presence of BrdU). Heddle and co-workers (1970) tested this prediction with cell grown in a medium containing tritiated thymidine (3HTdr) which, like BrdU, is incorporated into the newly synthesised strand of actively dividing cells enabling the sister chromatids to be distinguishable autoradiographically (Taylor *et al* 1956). They reported an exchange frequency associated with terminal deletions (termed colour switch breaks (csb) in this investigation) of 38%, close to that predicted by Revell's hypothesis. This was based on a small sample size (14/37 breaks) and indicated

problems in scoring breaks and gaps where the chromatid ends at the gap or break sites were not displaced. It is therefore of interest to repeat the experiment but with *Potorus* cells grown in the presence of BrdU rather than tritiated thymidine to see if the same csb frequency is found.

5.1.3.2. *Drosophila melanogaster*

Drosophila melanogaster is an excellent and extensively used model system for the study of the genetics of development due to its short life-cycle, easily seen mutable characteristics (eye colour, wing shape etc) and the ease with which large numbers can be maintained within a laboratory environment. *Drosophila melanogaster* has 4 pairs of chromosomes in total, an XX (female) a XY (male) pair and three somatic chromosome pairs, named 2, 3 and 4, but the smallest chromosome pair (4) cannot be scored for aberrations (Ashburner, 1989).

One of the many aspects of cellular and genetic regulation investigated in this model system is the formation of sister chromatid exchanges (SCE). There is some inconsistency between published results as to whether SCE occur spontaneously in *Drosophila*. Gatti *et al*, (1978) could not detect spontaneous SCE in neural ganglia of third instar larvae, but a consistently higher rate of SCE induction was observed in females compared to males and also a clustering of SCE at the junctions of euchromatin and heterochromatin. This is in contrast to Tsuji (1982) who detected spontaneous SCE and equal frequency of formation in both sexes. These differences may be due in part to differences in scoring methods and BrdU concentrations. There is some evidence for different frequencies in sex chromosomes compared to autosomes (Dolfini, 1978; Tsuji, 1981).

Investigations into chromatid break characteristics in larval neuroblast cells of *Drosophila* carrying recombination and repair defective mutations suggested that chromatid, isochromatid breaks, SCE and chromatid interchanges all arise via different pathways (Gatti, 1979; Gatti *et al*, 1980).

In this investigation into chromatid break characteristics, an insect cell line (Cl8+) derived from the third instar wing imaginal disc (Cottam and Milner, 1997) was used to determine chromatid break characteristics and csr.

5.1.3.3. *Vicia faba*

The mechanisms of dsb repair in plants are similar to those found in animals and include mechanisms for homologous recombination and non-homologous end joining (Gorbunova and Levy, 1999). The existence of a mechanism for dsb repair in plants was reported by Barbara McClintock in 1931, when she showed that X-ray-induced chromosome breaks resulted in various aberrations formed as a result of the fusion of broken ends of chromosomes. The major dsb repair pathway in plants is the more error-prone non-homologous end joining rather than the high fidelity homologous recombination mechanism. This pathway, being associated in plants with genetic rearrangements which include deletions and insertions, is believed to be an important force in plant evolution (Gorbuna and Levy, 1999).

The broad bean, *Vicia faba*, has been extensively used in a number of areas of research. Revell used this plant species to investigate chromatid break characteristics in the elucidation of his Exchange Hypothesis (Revell, 1959). Early studies of sister chromatid exchange (SCE) formation used this species as a model system (Kilhman and Anderson, 1982) for investigation into the

formation chromatid aberrations (Kilhman *et al*, 1978). Frequency of SCEs in *Vicia faba* have also been used as an inexpensive and easy method to detect mutagens and carcinogens in food preservatives, pesticides and similar chemical agents (Xing and Zhang, 1990). The effects of arsenic contamination of drinking water has also been investigated using this plant as a model system (Gomez-Arroyo *et al*, 1997) as has the possible deleterious effect of alterations of dNTP levels induced by physical and chemical mutagens (Xing, 1997). Transformation studies of *Vicia faba* have produced ploidy levels ranging from $2n$ to $9n$. The broad bean variety used in the present studies (Suttons) involve root tips grown from seeds and are thus non-transformed and have a chromosome complement $2n = 6$.

5.1.3.4. Mouse CB17 cell line.

The CB17 mouse cell line ($2n = 40$) used in the present investigation is a transformed fibroblast cell line which has been previously used as a model system to investigate chromatid break characteristics following restriction endonuclease treatment or exposure to ionising radiation (Bryant *et al*, 1998).

5.2. Materials and methods.

The experimental protocol used was the same as shown in Figure 2.3.

5.2.1. Cell Culture and BrdU treatment of CB17 and *Potorus* cells.

The CB17 cells were grown in Waymouth's Medium with Earle's salts (MEM Gibco), 50 IU/ml Penicillin, 50 $\mu\text{g ml}^{-1}$ streptomycin (Gibco) supplemented with 2mM L-glutamine and 10% foetal calf serum (Gibco). The *Potorus* cells were grown in Eagle's Minimal Essential Medium with Earle's salts (MEM Gibco), 50 IU ml^{-1} Penicillin, 50 $\mu\text{g ml}^{-1}$ streptomycin (Gibco) supplemented with 2mM L-glutamine and 10% foetal calf serum (Gibco) and 1 mM sodium pyruvate at 37°C. Both cell types were routinely passaged to maintain a sub-confluent state. Following trypsinization cells were set up at a concentration of 5×10^5 cells ml^{-1} and after 24 hours 10 μM 5-bromo-2'-de-oxymidine (BrdU) was added and the cells allowed to grow through a further 24 hours (two cell cycles) before treatment.

5.2.2. Irradiation of cells.

Cells were irradiated *in situ* with 0.2 or 0.4 Gy from a ^{137}Cs gamma source (CIS Biointernational IBL437C gamma-irradiator) at a dose rate of 7.7 cGysec^{-1} . The flasks were returned to the incubator for 30 min following irradiation before being treated with 0.1 $\mu\text{g ml}^{-1}$ colcemid (Sigma) and incubated for a total of 1.5 hours at 37°C prior to harvesting.

5.2.3. Harvesting.

After incubation the medium was removed and reserved and the cells trypsinised for 6 min at 37°C. The resulting suspension including original

medium and trypsin washes was centrifuged (1200 rpm for 10 minutes) at 4°C. The supernatant was aspirated, the cell pellet resuspended in ice-cold hypotonic solution (0.075M KCl) and held on ice for 10 minutes before centrifuging (Hereaus Laborfuge 400R) at 1200 rpm (~ 200g) for 10 min. The supernatant was removed, the pellet loosened and fixative (75% methanol, 25% glacial acetic acid v/v) was added very slowly to prevent clumping of cells. The resulting suspension was washed at least three more times. Finally the cell pellet was resuspended in a small volume of fresh fixative and kept at 4°C.

5.2.4. Preparation of slides.

The microscope slides were first cooled in ice-cold distilled water for 30 min. The ice-cold slides were briefly wiped with the edge of a filter paper and flooded with ice-cold 50% glacial acetic acid solution before a single drop of cell suspension was placed on the slide and dried on a warm-plate at approximately 50°C.

5.2.5. Fluorescence plus giemsa (FPG) staining

Once dry the slides were placed in a solution of Hoechst 33258 (bis-Benzamide solution; Sigma) at $0.2 \mu\text{g ml}^{-1}$ in distilled water in the dark for 10 min and then blotted dry on filter papers. The slides were then covered with 2xSSC (0.3 M sodium chloride, 0.03 M sodium citrate, Analar) and placed under a UV-A (Philips TLD 18W/08) source for 3 hours. They were then rinsed three times in distilled water, 5 min each time, and blotted dry. Once dry the slides were then stained in 4% Giemsa for 10 min and rinsed in distilled water containing a few drops of ammonia per litre prior to blotting dry.

5.2.6. Scoring and analysis

Slides were examined under a light microscope (Zeiss, with a planapochromat 1.4 aperture x 63 objective) and 400 metaphases scored in each sample for chromatid breaks (including gaps). A scorable chromatid was determined to be where there was clear discontinuity in the chromatid material either in the light or dark strand or in both. The frequencies of breaks occurring in the light or dark stained chromatids were noted as well as the number of breaks with associated colour-switches ("colour-switch breaks"). The sister chromatid exchange frequency was also determined using the formula described in section 2.3.5.

5.2.7. Cell culture and BrdU treatment of *Drosophila melanogaster* cells.

Cl8+ (clone 8) cells are grown in 5cm³ dishes in complete supplemented medium (CSM) containing 200 ml SS3 basal medium pH 6.73, 2 ml insulin solution, 5 ml FE2 (fly extract - haemolymph), 4 ml 2% FCS (raw or inactivated) filtered through a 0.22 µm filter. Dishes of cells typically at 4 days passage were selected which have a dense lawn of cells and are just beginning to form aggregates.

Cells were washed off the substrate using a pasteur pipette and transferred to a V-tube. After centrifugation at 1100 rpm for 5 min, cells were set up in 10 cm³ dishes at a density of 3×10^6 cells/dish in 5 ml CSM.

The next day 10 µM BrdU was added to the dishes and the cells left to grow for two cell cycles (48 hrs). 0.1 µg ml⁻¹ colcemid was added to each dish and the cells incubated for at 4 hrs.

5.2.8. Harvesting, slide preparation and staining of *Drosophila* cells.

The cells were washed off the dishes as before and transferred to centrifuge tubes and spun at 1000 rpm for 4 mins. The supernatant was removed and 2 ml of 1% Na citrate added to the resuspended cells and left for 12 min at room temperature before being centrifuged again at 1000 rpm for 4 min.

The supernatant was removed and the pellet resuspended in 0.25 ml of 1% Na citrate 4 ml ice-cold fixative (75% methanol, 25% glacial acetic acid v/v) was slowly added, continuously mixing on whirlmixer.

The fixed cell suspension was centrifuged at 1000 rpm for 4 min, the supernatant removed and the cells resuspended in enough fixative to make very slightly cloudy suspension, which was dropped onto ice-cold slides (straight from the freezer) while the film of condensation is still on the slides. The slides were dried flat and then put in drying cabinet overnight.

Next day, cells were stained with Hoechst 33258 for 10 min and then placed under the UV lamp in 2 × SSC (0.3 M sodium chloride, 0.03 M sodium citrate, Analar) for 3 hours. Slides were then stained with 5% giemsa in phosphate buffer (pH 6.8) for 10 min.

5.2.9. Culture of *Vicia faba* seeds

The protocol used was based on that used by Xing *et al*, (1997).

Seeds of *Vicia faba* were germinated in 9 cm petri dishes on filter paper in tap

water in the dark. Once the root tips were approximately 0.5 cm long the seed were transferred to new petri dishes on filter paper and grown in 10 cm³ of a 10⁻⁴ M solution of BrdU for a total of 17 hr in the dark at room temperature (approx. 25°C). The root tips were removed and placed in a fresh 10 cm³ solution of 10⁻⁴M BrdU and colcemid (Sigma) to give a final concentration of 0.1 µg ml⁻¹ for 1 hr prior to harvesting.

The root tips were placed in a solution of 3% pectinase (Sigma) and 3% cellulase (Sigma) at 25°C for 2 hr in a 75 cm³ centrifuge tube in a water bath to digest the cell wall. After rinsing in tap water the last 2-3 mm of root tip were removed and ground to a paste with a few drops of fresh fixative (75% methanol, 25% glacial acetic acid v/v) to produce a slightly cloudy suspension. This suspension was then dropped onto the moisture film formed on dry slides which had been kept in the freezer overnight and removed for use.

5.2.10. Irradiation of *Vicia faba* root tips

The root tips were irradiated before being removed from the seeds. They were returned to the dark for 30 min prior to the root tips being removed and incubated on new 9 cm petri dishes with new filter papers in a fresh solution of 10⁻⁴ M BrdU and colcemid to give a final concentration of 0.1 µg ml⁻¹ as described above (5.2.9).

5.2.11. Slide preparation and staining of *Vicia faba* root tips.

The slides were stained using the FPG staining method previously outlined in 5.2.5. and scored as described in 5.2.6.

5.3. Results

5.3.1. Chromatid break characteristics of CB17 and *Potorus* cell lines.

Chromatid break frequencies and colour switch ratio (csr) for the *Potorus tridactylus* and CB17 cell lines for a sample time of 1.5 hr are shown in Table 5.1. The induction of total, colour and non-colour switch breaks with dose is linear for both cell lines as shown in Figures 5.2 and 5.3, where linear regression analysis has been used to determine the csr as described in 2.4.2. The csr calculated from the linear regression line for *Potorus* by taking the ratio of the slopes of the colour switch break and total break lines (Figure 5.2) is 0.1921 (19.21%). This value is close to that calculated from the mean values of Table 5.1 of 19.39% (SD = 3.77). The linear regression value lies well within the 95% confidence limits for the mean tabulated value ($19.39\% \pm 4.27$). The csr value obtained from the linear regression analysis of Figure 5.3 for CB17 cells is 0.1544 (15.44%). Comparison with the mean csr value from Table 5.1 (13.37%, SD = 1.22) shows that the linear regression csr value lies just outside the 95% confidence limits for the tabulated mean value ($13.37\% \pm 1.38\%$). There was no significant differences in SCE frequencies in the species considered here (Table 5.2) although SCE values were higher than those obtained for lymphoblastoid cells (Table 2.5). Examples of metaphase spreads of both *Potorus tridactylus* and CB17 cells are presented in Figure 5.4.

5.3.2. Comparison of species with a normal human cell line.

In order to determine if there is a significant difference in the overall csr values between species the chromatid breakage data and csr values obtained for a population of 12 normal lymphoblastoid cells described in Chapter 2 has been used to compare this data with csr values in other species.

Table 5.1. Frequency of chromatid breaks per 100 cells lines of different species.

Cell line	No. damaged cells	Breaks in light strand*	Breaks in dark strand*	Colour-switch breaks	Total breaks	Colour switch ratio (%)
<i>Potorus tridactylus</i> cell line:						
non-irradiated:	23.5	7.5	12.0	6.3	25.8	24.42
0.2 Gy irradiation:	50.0	22.0	31.1	9.5	62.8	15.13
0.4 Gy irradiation:	59.0	29.8	41.3	18.5	89.6	20.67
Mouse CB17 fibroblast line:						
non-irradiated:	18.8	13.5	11.0	3.5	28.0	17.07
0.2 Gy irradiation:	46.8	20.0	40.3	9.0	69.3	12.98
0.4 Gy irradiation:	59.8	31.8	53.0	14.5	99.3	14.60

Frequencies of chromatid breaks per 100 cells lines of different species for a sample time of 1.5 hr. 400 metaphases scored per sample. Results obtained from at least two independent experiments.

*non-colour switch breaks are the sum of the light and dark strand breaks.

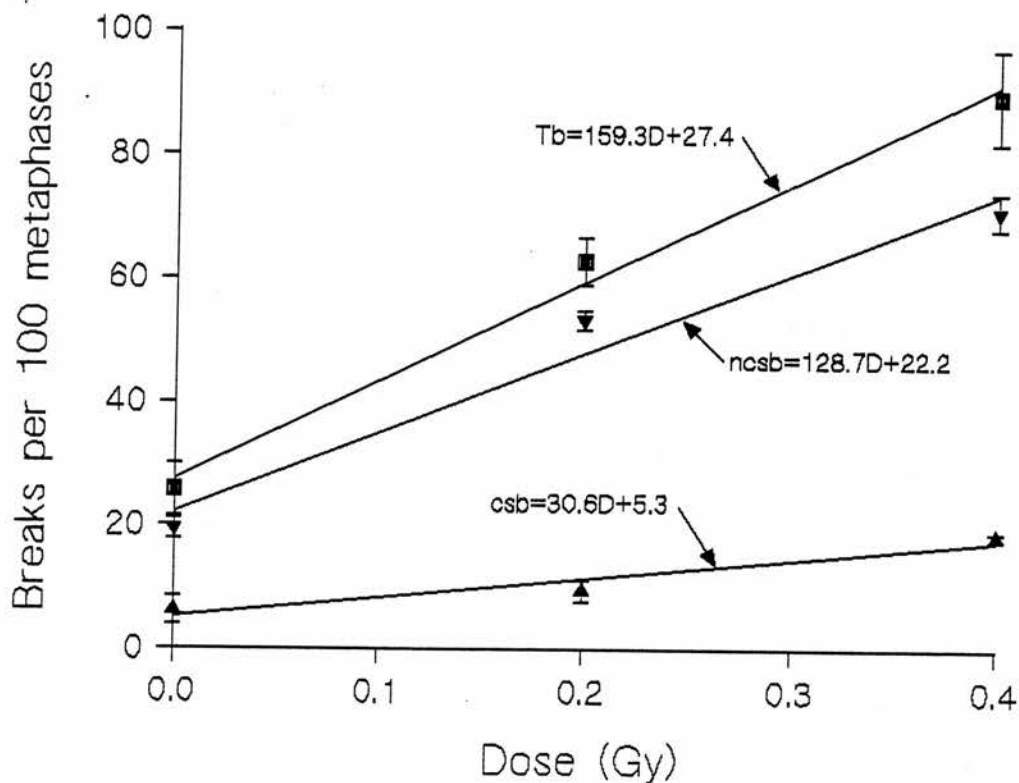


Figure 5.2. Graph showing experimental results of chromatid breaks per 100 metaphases vs. dose for *Potorus tridactylus* cell line showing total breaks (Tb), colour switch breaks (csb) and non-colour switch breaks (ncsb) with the appropriate linear regression equation. 400 metaphases scored per point. Data pooled from at least three independent experiments. Error bars represent standard error of the mean. $r^2(Tb) = 99.1\%$; $r^2(csb) = 93.1\%$; $r^2(ncsb) = 96.9\%$.

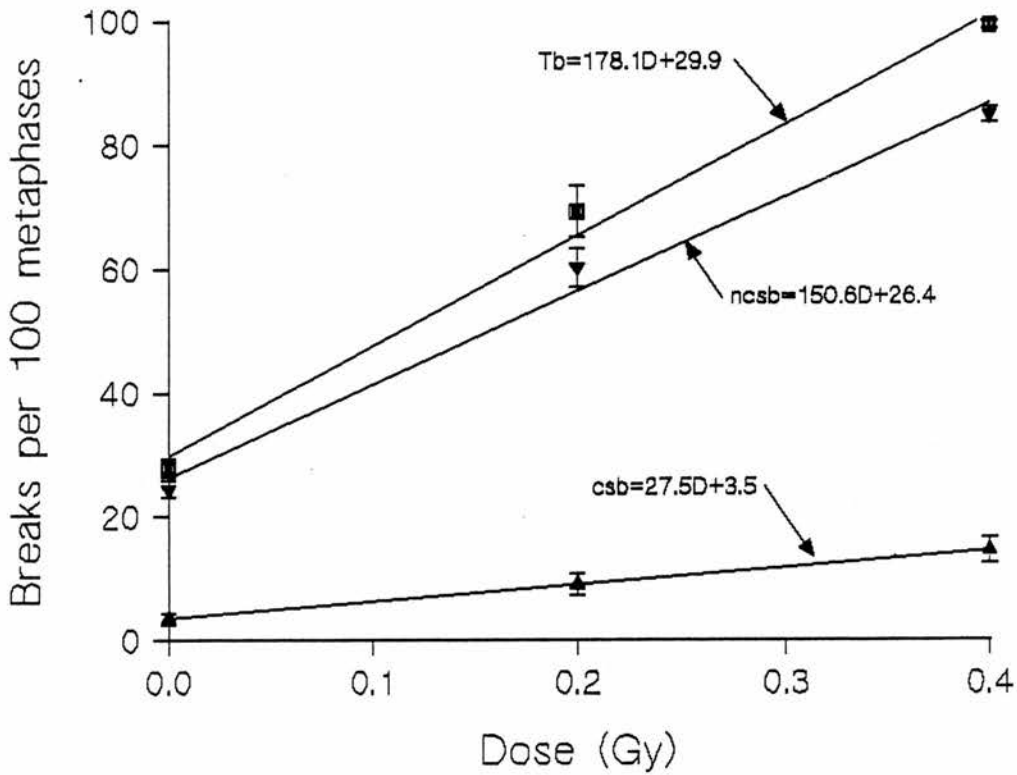


Figure 5.3. Graph showing experimental results of chromatid breaks per 100 metaphases vs. dose for a mouse fibroblast cell line CB17 showing total breaks (Tb), colour switch breaks (csb) and non-colour switch breaks (ncsb) with the appropriate linear regression equation. 400 metaphases scored per point. Data pooled from at least three independent experiments. Error bars represent standard error of the mean. $r^2(Tb) = 99.2\%$; $r^2(csb) = 100\%$; $r^2(ncsb) = 98.8\%$.

In Chapter 2, the experimental data, together with the 95% confidence limits and adjusted confidence limits for normal lymphoblastoid cells were used to compare this data with the csr values for cell lines derived from patients with different disease syndromes. In a similar manner it is possible to directly compare csr characteristics of different species with this normal lymphoblastoid population, at the same sample time ($t = 1.5$ hr) in order to test the postulation that all cells derived from species with a wild-type genotype will have similar csr.

Figure 5.5 shows this comparison for the different species considered in this investigation with the exception of the *Drosophila cell* line. It can be seen from Figure 5.5 that all the CB17 and *Potorus* csr data points lie well within the 95% confidence limits with the exception of the 0.4 Gy value for *Potorus*.

Species	SCE/cell
<i>Potorus tridactylus:</i>	
non-irradiated:	6.2
0.2 Gy irradiation:	4.3
0.4 Gy irradiation:	3.1
Mouse CB17:	
non-irradiated:	14.7
0.2 Gy irradiation:	16.2
0.4 Gy irradiation:	15.4

Table 5.2. Frequencies of sister chromatid exchanges (SCE) in different species grown in $10 \mu\text{g ml}^{-1}$ BrdU for two cell cycles. 25 cells scored per sample.

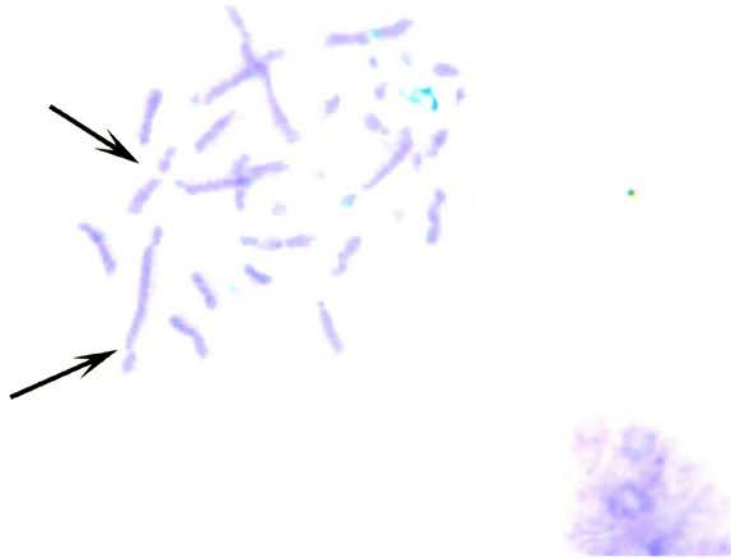


Figure 5.4 (a) Typical metaphase spread of a *Potorus tridactylus* cell irradiated with 0.4 Gy showing dark strand breaks and a colour switch break.

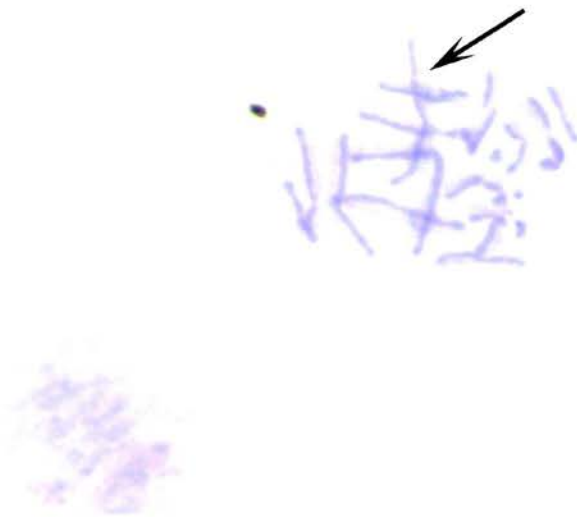


Figure 5.4 (b) Typical metaphase spread of a *Potorus tridactylus* cell irradiated with 0.4 Gy showing a light strand break.

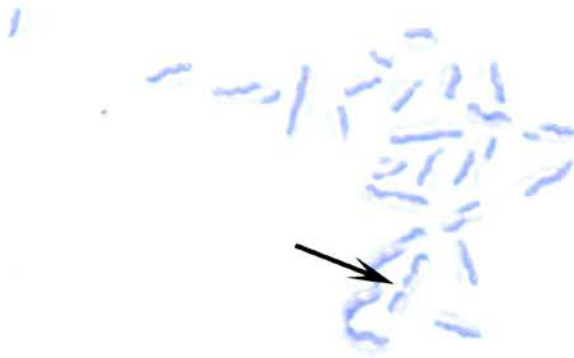


Figure 5.4 (c) Partial metaphase spread of a mouse CB17 fibroblast cell irradiated with 0.4 Gy showing a dark strand break.

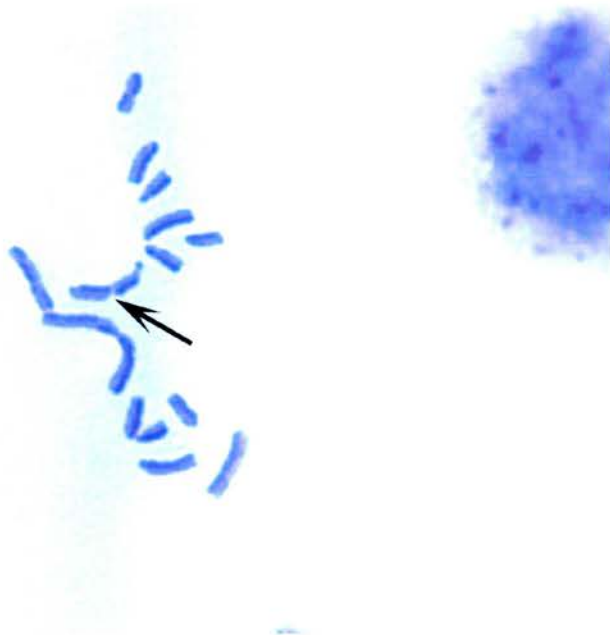


Figure 5.4 (d) Partial metaphase spread of a mouse CB17 fibroblast cell irradiated with 0.4 Gy showing a colour switch break.

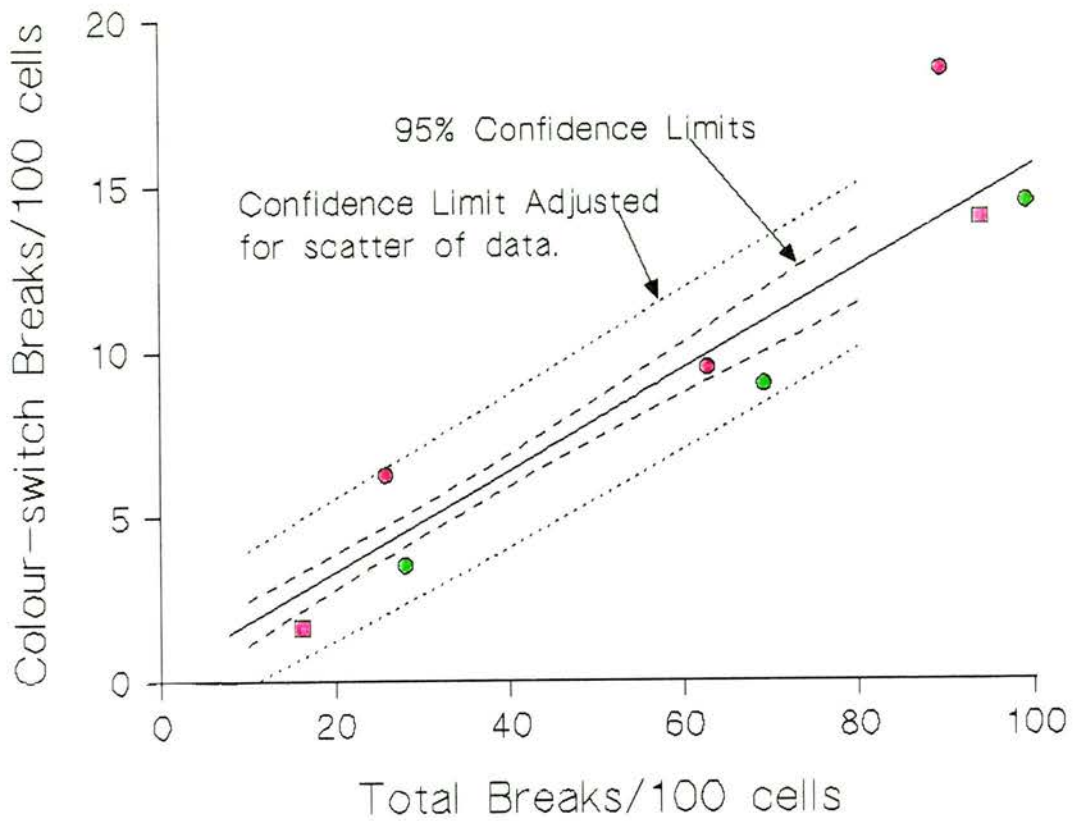


Figure 5.5 Graph comparing experimental values for different species with total chromatid breaks vs. colour switch breaks for normal lymphoblastoid cells per 100 cells showing 95% confidence limits (dashed line) and confidence limit adjusted for the scatter of data (dotted line) from Figure 2.12.

Key for species data points:

Red circles: *Potorus tridactylus*; Green circles: mouse CB17 fibroblast.
Red squares: hamster V79 fibroblast.

5.3.3. The *Drosophila* cell line.

It was not possible to obtain good metaphases for the *Drosophila* cells despite repeated efforts. This was due in part to the very low mitotic index of these cells which appeared to be depressed still further by the presence of BrdU in the growth medium. In addition the only protocols available were those obtained from past papers which were evidently incomplete. It is possible that using a wing imaginal disc cell line for this procedure may have been a factor when all the available published protocols used neural cells.

5.3.4. *Vicia Faba*.

Attempts to obtain good metaphase spreads of *Vicia faba* chromosomes were not successful. Although isolated chromosomes were clearly visible which showed dual staining, no complete metaphases were observed. It was also very difficult to get clean preparations which were free of cellular material.

5.3.5. Breakage characteristics for V79 and GS1943 cells.

Table 4.5 of Chapter 4 shows the results for total breaks (Tb) and colour switch breaks (csb) at a sample time of 4 hr for V79 cells for both control and for cells subjected to 0.4 Gy irradiation. This limited data can be used to illustrate the strength of the Chromatid Breakage Surface model (discussed in sections 3.3.4. and 3.3.5) for reaching quantitative results from limited data of this kind.

Assuming a straight line relationship between breaks and dose at a sample time of $t = 4$ hr, and using the values of Table 4.5 for Tb and csb the slopes of these

lines are given by:

$$m_1 = (42.3 - 6.3) / 0.4 = 90 \text{ breaks/Gy}$$

$$m_2 = (5 - 0.5) / 0.4 = 11.25 \text{ breaks/Gy}$$

thus at $t = 4$ hr, the $\text{csr} = m_2/m_1 = 0.125$.

If it is assumed that the time decay constants k_1 and k_2 for V79 cells are the same as for the lymphoblastoid cells (see section 3.3.3) then:

at a dose $D = 0.4$ Gy

$$Tb = Tb_0 \exp(-k_1 t)$$

$$42.3 = Tb_0 \exp(-0.32 \times 4)$$

$$Tb_0 = 152.1$$

hence at $t = 1.5$ hr

$$Tb = 152.1 \exp(-0.32 \times 1.5)$$

$$Tb = 94.1$$

Applying the same approach to the csb values of Table 4.5 using the value $k_2 = 0.47$,

then at $t = 1.5$ hr

$$\text{csb} = 16.2$$

In a similar manner using the values of Table 4.5 for the controls ($D = 0$) then for the total breaks again using $k_1 = 0.32$:

$$6.3 = T_{b0} \exp(-0.32 \times 4)$$

$$T_{b0} = 22.6$$

hence, at $t = 1.5$ hr,

$$T_b = 22.6 \exp(-0.32 \times 1.5)$$

$$T_b = 14.0$$

Again using $k_2 = 0.47$ for the csb values for the controls of Table 4.5

$$csb = 1.62$$

The foregoing values for total breaks and csb for both the control (non-irradiated) and irradiated V79 cells at a sample time of 1.5 hr are plotted on Figure 5.5.

The slope of the straight line relationships between chromatid breaks and dose at a sample time $t = 1.5$ hr can also be estimated from this data using:

$$m_1 = (94.1 - 16.2)/0.4 = 194.75 \text{ breaks/Gy}$$

$$m_2 = (14 - 1.62)/0.4 = 30.95 \text{ breaks/Gy}$$

and at $t = 1.5$ hr:

$$csr = m_2/m_1 = 0.16$$

The same approach was used to determine the chromatid break characteristics for GS1943 cells from the data obtained in Chapter 4 for these cells subjected to zero and 0.4 Gy irradiation for a sample time of 4 hr (Table 4.1).

At $t = 4$ hr, the $csr = 0.126$

Also at $t = 1.5$ hr for the irradiated GS1943 cells ($D = 0.4$ Gy):

$$Tb = 201 \qquad csb = 39.8$$

and for the control (non-irradiated) cells at $t = 1.5$ hr:

$$Tb = 15.1 \qquad csb = 4$$

It is possible using the approach described above for V79 cells to arrive at a csr for this cell line at $t = 1.5$ hr:

$$csr = 0.192$$

The values for total breaks and colour switch breaks for the GS1943 cells are not shown on Figure 5.5 as the total break frequency is high compared to the other data points plotted and therefore inclusion of the GS1943 data would make the graph less clear. The values for total and colour switch breaks for the control cells is however well within the 95 % confidence limits determined for a normal lymphoblastoid cell population (Figure 5.5).

5.4 Discussion

The architecture of chromosome and chromatin structure are highly conserved in metazoans as are the structure and function of proteins associated with DNA damage recognition and repair processes (Taylor and Lehmann, 1998). The postulate outlined here (5.1) is that this conservation of chromatin structure would give rise to fixed proportions of *csb* within the total chromatid break frequency and hence the same *csr* value. This is supported by the results presented here for wild type cells. Although the number of chromosomes in each of these species is different, the *csr* values fall largely within the 95% confidence limits calculated for a normal human lymphoblastoid cell population. The outlying data value (Figure 5.5) is probably due to the inherent variability in the scoring method used and it would be expected that a larger number of scored metaphases would clarify whether this point is in fact significantly different. It may be indicative of a greater inherent variability in these cell types compared to the others investigated here. This is despite the fact that the *Potorus* and CB17 are both fibroblast cell lines. The experimental results for *Potorus* differ from those published previously by Heddle *et al.*, (1970) where a *csr* of 38% was found. This was based on a smaller sample size, Heddle and co-workers scored a total of only 37 breaks, a much smaller sample size than that used here (Table 5.1), also the investigation undertaken by Heddle *et al.* used cells labelled with tritiated thymidine which may give more ambiguous results than those obtained using BrdU. It is possible however that the difference in labelling technique has in some way contributed to the disagreement in results obtained between the present work and Heddle *et al.* The results presented here are in line with the rest of the findings in this investigation in that they do not show significantly different induction of chromatid breaks (Table 5.1, Figures 5.2 - 5.3) or SCE (Table 5.2) and are in agreement with the hypothesis being tested.

The chromatid break characteristics for V79 hamster fibroblast cells derived from the experimental data presented in Chapter 4 (Tables 4.1 and 4.5) also fall within the 95% confidence limits for a normal lymphoblastoid cell population (Figure 5.5). The GS1943 show a similar trend although the number of total breaks for irradiated CHO-derived GS1943 cells is higher than that obtained for V79, indicating that this cell type is more radiosensitive than V79. Previously published csr values for CHO cell lines of 16% (Harvey and Savage, 1997) are similar to those determined in this investigation, supporting the assumption that the presence of a transfected I-SceI site within the genome does not significantly alter the chromatin structure within these cells.

Data based on previous studies of Muntjac cells (n = 6 (female); n = 7 (male)) (Wurster and Benischke, 1970) indicates a mean csr value of approximately 11% for this cell type (H. Mendoza, 1999) which would also indicate that the csr for this species would also lie within the 95% confidence limits on Figure 5.5.

It was unfortunate that it was not possible to obtain csr values for *Drosophila* and *Vicia faba* cells. Other cell types may yield better results, particularly transformed cell lines where cell populations can be grown under more controlled conditions, although care must be taken to determine the stable ploidy level in transformed plant cell lines (Ramsey and Kumar, 1990; Pearce *et al.*, 1996).

5.5. Future Work

It would be of interest to determine the chromatid break characteristics of other species, particularly those which come from different evolutionary lineages, for example reptiles, birds, invertebrates and other plant groups. The most reliable approach may be to use transformed cell lines, for example *Agrobacterium*-transformed *Vicia faba* cell lines (Ramsey and Kumar, 1990; Pearce *et al*, 1996) or transformed frog cell lines developed to investigate SCE frequency (Rosenstein, 1984; Chao *et al*, 1985). Alternatively embryo-derived cell lines such as that produced from the yellow-bellied turtle, *T. scripta* to study translocations (Ulsh *et al*, 2001). It would also be useful to attempt to gain a csr value for *Drosophila*, perhaps using a neural cell type to further test the validity of the previously published protocols.

Given the close correlation between the different species investigated here, it would be of great interest to attempt to further elucidate the chromatin structure within the nucleus, particularly in G₂ to attempt to understand the structural reason for a fixed csr. The dynamic nature of chromatin condensation, particularly in G₂ as the cell nears the end of interphase and approaches mitosis poses particular challenges when trying to elucidate the accessibility of DNA to damaging agents. The accessibility of the DNA duplex to external agents such as ionising radiation and also the ability of DNA damage recognition and recombination repair complexes to gain access to the damaged regions of DNA needs to be more fully understood before such questions can be answered satisfactorily. A possible way forward is the development of computer models based on the current knowledge of chromatin structure and chromatid aberration characteristics. Such a computational approach would allow predictions to be made and tested theoretically before comparing such theoretical results with experimental data

to further refine the model.

Chapter 6

Overall conclusions

Contents	Page No.
6. Overall conclusions	278
6.1. Development of a quantitative model	278
6.2. Chromatid break characteristics and type of induced damage	280
6.3. Chromatid break induction with a single dsb	281
6.4. Chromatid break rejoining characteristics	282
6.5. Constancy of csr in different cell types	283
6.6. Candidates for the signalling molecule(s)	284
6.7. Inversion frequency in chromatids	286
6.8. General conclusions	286

6. Overall conclusions.

The principle aim of this investigation was to theoretically and experimentally test the predictions and assumptions of the signal model (Bryant, 1998). A summary of the results obtained for each of the major areas of investigation set out in section 1.8 is presented here together with a consideration of the success of the adopted experimental approach and suggestions for future work to extend these investigations.

6.1. Development of a quantitative model.

Aim:

- To attempt to produce a more mathematically based model to investigate the nature of chromatid break induction, which can be used to quantitatively predict and analyse the relationship between different types of chromatid (colour and non-colour switch) breaks and the effect of DNA damaging agents on the formation and rate of rejoining of these chromatid break types with time.

The signal model and those models preceding it proposed a qualitative explanation for the formation of chromosome and in particular chromatid breaks in G₂. Although useful as a starting point this approach does not address the challenge of determining relative frequencies of chromatid break types simultaneously as a function of radiation dose (or restriction endonuclease concentration) and sample time. It is therefore proposed in this thesis to achieve this by using a more rigorous and quantitative analysis.

The three-dimensional breakage surface model presented here (section 3.3.5) allows all three variables to be simultaneously considered for both total

chromatid breaks and chromatid break subtypes. Using this model it is possible to develop a complete theoretical model for the formation and rejoining of chromatid breaks which can then be tested experimentally. The two main principles on which this three-dimensional surface is based are summarised in the following two statements:

(1) It has been shown that a basic algebraic linear relationship exists between chromatid break frequency and radiation dose when cells are subjected to low doses of ionising radiation. If a linear relationship exists between total breaks (T_b) and radiation dose and some different linear relationship exists between colour switch breaks (csb) and dose then the ratio csb/T_b known as the colour switch ratio (csr) must be constant and equal to m_2/m_1 where m_2 is the slope of the csb line and m_1 is the slope of the T_b line. Furthermore this basic relationship must also exist for the non-colour switch breaks (ncsb) (section 2.4.2).

(2) It has been shown mathematically in Appendix B that if a linear relationship exists between chromatid breaks and dose at different sample times within the G_2 phase of the cell cycle, then the exponential decay constant during break rejoining must be constant and independent of the initial dose. This conclusion is justified by measurements of Gotoh *et al* (1999) (section 3.3.5).

This approach allows comparison of complete chromatid breakage characteristics for different cell types to be undertaken, this may be particularly informative when considering disease syndromes which are associated with chromosomal instability and cancer predisposition. Results presented here suggest that different chromatid break subtypes are formed in different proportions and rejoined with different kinetics in AT and NBS cell lines compared to normal lymphoblastoid cell lines.

6.2. Chromatid break characteristics and type of induced damage.

Aim:

- To investigate the nature of chromatid breaks in relation to radiation dose and restriction enzyme concentration. Are the frequencies of colour switch breaks (csb) and non-colour switch breaks (ncsb) induced in similar proportions regardless of the type of damage sustained by the DNA?
- Is the proportion of csb and ncsb (i.e. the colour switch ratio, (csr) and the non-colour switch ratio (ncsr) of the total chromatid breaks the same regardless of the type of damage sustained by the DNA?

The relationship between dose and total chromatid break frequency is linear in the same way as are the relationships between radiation dose and non-colour and colour switch breaks. As stated in statement (1) of section 6.1 and 2.4.2 a consequence of this relationship is that the csr must be constant and furthermore will remain constant even at higher radiation doses when the break-dose relationship is non-linear providing the two variables can be described by similar functions. This suggests that csb are induced in cells as a constant proportion even at higher levels of damage but the overall increase in damage together with the decreased mitotic index at higher radiation exposure would make this prediction difficult to verify experimentally using current techniques.

The chromatid break-dose relationship for a given sample time developed here allows a reduced major axis regression analysis to be performed on chromatid

break data, where the csr is the slope of the resultant line (section 2.4.6). This approach is more rigorous than the t score analysis also presented here (section 2.4.7) since it allows the csr for any cell population to be determined and directly compared with the csr for any other cell type. This approach was used to compare csr values for a number of disease syndrome cell lines against healthy cells when investigating the role of possible signalling molecules (section 6.6 and Figures 2.14 and 2.15) and for comparison of the csr for different species (section 6.5) and different single break model systems (section 6.3 and Figure 4.8).

6.3. Chromatid break induction with a single dsb.

Aim:

- Is one double-strand break (dsb) sufficient to induce chromatid aberrations as predicted by the signal model? If so, are the csr and ncsr the same as those observed for damage where numerous dsb are induced either by radiation ("dirty" breaks) or by restriction endonucleases ("clean" breaks) with numerous cut sites within the DNA?

One of the major differences between the signal model (Bryant, 1998) and previous explanations for the formation of chromatid breaks (with the exception of Chadwick and Leenhouts) is that a single dsb is sufficient to induce chromatid breaks since the initiating dsb is not itself directly involved in the recombinogenic process leading to the formation of chromatid breaks.

In this investigation the I-SceI model system was used to produce a single dsb in the DNA of cell transfected with the unique 18bp I-Sce-I recognition site to

determine if it is possible to produce chromatid aberrations within the genome with a single dsb (Sargent *et al*, 1997). This model system successfully induced chromatid breaks within cell subjected to a range of I-SceI endonuclease doses (Rogers-Bald *et al*, 2000). The results presented here support three main conclusions. Firstly, that a chromatid break may result from a single isolated double-strand break (dsb) as predicted by the signal model. Secondly, that differential mechanisms are likely to exist for the production of breaks and exchanges in G₂ cells, and thirdly that the induction of chromatid breaks by a single dsb due to transfection of the I-SceI endonuclease site is not a unique characteristic of the CHO transfected cell line GS1943 itself but is similarly observed in V79 and *irs1* transfected cells lines.

When considering the chromatid breakage surface for endonuclease concentration the log₁₀ of the endonuclease dose is analogous to the radiation dose and can thus be used to generate a predictive three-dimensional breakage surface for this experimental system.

6.4. Chromatid break rejoining characteristics.

Aim:

- To investigate the nature of repair of csb and ncsb to determine if the rate of repair of these break types differs by measuring the proportion of each breaks type remaining over a period of time.

Statement (2) of section 6.1 (and section 3.3.5) above together with the theoretical considerations presented in Chapter 3 show that in order for the *csr* to be constant within the G₂ phase of the cell cycle the rate of rejoining of total and colour switch chromatid breaks must be equivalent i.e. $k_1 = k_2$. Results

presented in Chapter 3 (section 3.3.3) demonstrate that this is not the case and that the rate of total break rejoining (k_1) is not equal to the rate of rejoining of csb (k_2). The ratio of the rate of rejoining demonstrated that the nscb rejoined approximately 3-4 times faster than the csb for normal lymphoblastoid cells. This gives rise to a slow decline in csr over the period of time investigated. In contrast the ratio of the rate of rejoining of nscb to csb for AT and NBS cells is 20 and 200 times greater for AT and NBS cells respectively (section 3.3.6). This gives rise to an increase in csr over the time period under investigation. The almost constant csb value within AT and NBS cells suggests a role for non-rejoined csb in the phenotype of chromosomal instability observed in these cell types. Although csb frequencies are small in AT and NBS cells, and thus it is difficult to draw extensive conclusions from these results, they suggest that the AT and NBS gene products are involved in recombination pathways associated with the formation and rejoining of csb but not nscb, which is indicative of different mechanisms operating in the formation of these chromatid break subtypes. This may be due to either different chromatin conformation in these cell types or in an inability to recognise and process signals indicating DNA damage has occurred.

6.5. Constancy of csr in different cell types.

Aim:

- Are the csr and ncsr the same regardless of cell type, i.e. is the csr/ncsr an intrinsic property of a particular cell line or do all eukaryotic cell types produce a similar proportion of csb for the same amount of exposure to DNA damaging events such as ionising radiation?
- Is the production of csb a conserved mechanism in all eukaryote cell

types? The structure of DNA is highly conserved in eukaryotes so a similar csr in widely evolutionary diverse species may indicate that there are structural considerations in the formation of csb in the observed proportions.

Chromatin structure is highly conserved in metazoans. If, as suggested by the signal model, a dsb initiates a recombinogenic process within the DNA at the base of the chromatin loops then it is possible that the relative number of csb and ncsb formed as the result of this process will be approximately the same since they formed as a result of the structural characteristics of the chromatin. Data presented from mammalian and marsupial investigations suggest the same csr for wild-type cell lines within the inherent variability of the results. This suggests that the csr is essentially the same in all these cell types and by extension, may also be the same for all metazoans (section 5.3.2 and Figure 5.5). Further experiments to determine the csr for *Drosophila* and *Vicia faba* were unsuccessful and further work needs to be undertaken to test this hypothesis. Also it is important to relate these and future results to the physical changes occurring throughout G₂ in terms of chromatin condensation as the cell approaches mitosis.

6.6. Candidates for the signalling molecule(s).

Aim:

- What signalling molecules may be involved in the proposed recombinogenic mechanism leading to csb? If this is a fundamental mechanism for processing dsb in the genome, it may be possible to detect a significantly different csr in cell lines derived from disease conditions known to be associated with defective dsb processing and

repair and predisposition to tumourgenesis.

Lymphoblastoid cell lines derived from patients with Down Syndrome, Blooms Syndrome, Omenn Syndrome, AT homozygotes, NBS, BRCA1 and BRCA2 heterozygotes and members of families associated with familial breast cancer but with unknown mutations (i.e. wild type BRCA1) were compared to a normal population of lymphoblastoid cells using reduced major axis regression analysis to determine if the csr was significantly different (section 2.4.7). It was important to compare these individual disease syndrome and mutant cell lines with a normal population in order to take into account the inherent variability of chromatid break characteristics within a cell population type. Of the cell lines investigated only the AT, NBS, Omenn and BRCA2 cell lines showed a correlation of both increased radiosensitivity (as measured by the rdi) (section 2.4.8) and significantly low csr. This is supportive evidence in favour of a role for all of these proteins in a signalling pathway leading to the formation and resolution of chromatid breaks within G₂, probably via a homologous recombination pathway. The reduction but not abolition of the formation of csb suggests that there are several parallel pathways operating to give csb as an endpoint. The Omenn Syndrome cell line also showed a low csr but normal levels of radiosensitivity, suggesting a number of recombinogenic pathways exist within the cell to give the same endpoint (csb formation) when analysed by counting chromatid aberrations in metaphase spread. It is thus possible there are different subtypes of csb produced by different pathways but more sophisticated analysis would be required to determine if this is the case, possibly using sequence analysis.

6.7. Inversion frequency in chromatids.

Aim:

- Can the frequency of inversions in cells in the G₂ phase of the cell cycle be determined? The inversion of chromosomal material cannot be detected in BrdU-incorporated cells, but this may be possible using fluorescence *in situ* hybridisation (FISH). It would then be possible to determine the relative frequency of both inter- and intra-chromatid recombinational events in a cell type.

As described in section 4.5 the single break model system could be used to investigate inversion characteristics. Preliminary experiments were not successful, but using multiple FISH probes as described in section 4.5 may make it possible to produce inversion frequency (ivb) data and thus determine an inversion ratio (ivr) as theoretically presented in section 4.5.2. The proposed relationship between csr and ivr could also be experimentally tested and a three-dimensional surface also generated for inversions in the G₂ phase of the cell cycle.

6.8. General conclusions.

The aim of this investigation was to test experimentally the assumptions and predictions arising from the signal model (Bryant, 1998). The predictions that a single dsb is sufficient to induced chromatid breaks, that the csr is independent of dose are upheld. However the constancy of the csr with radiation dose (and restriction endonuclease concentration) is a consequence of the linear relationship itself as shown by statement (1) of section 6.1 (and 2.4.2). The assumption that the csr is independent of sample time is not upheld, the csr in

normal cells declines throughout G₂ and the reverse is true for AT and NBS cells (sections 3.3.3 and 3.3.6). The csr is not found to be an inherent characteristic of a particular cell line but more likely to be an inherent characteristic of the chromatin conformation within the cell nucleus and within the parameters of experimental variability is the same for all metazoans (section 5.3.2 and Figure 5.5).

As outlined in Section 6.1 above, the development of a more predictive and more rigorous quantitative model where the three principle variables within this experimental system can be considered simultaneously allows the complete chromatid breakage characteristics for the G₂ phase of the cell cycle to be predicted and experimentally tested.

References

Aalfs JD and Kingston RE (2000) What does 'chromatin remodelling' mean? *Trends in Biochem.* **25**, pp 548-555.

Agkun E, Zahn J, Baumes S, Brown G, Liang F, Romanienko PJ, Lewis S and Jasin (1997) Palindrome resolution and recombination in the mammalian germ line. *Mol and Cell Biol.* **17**, pp 5559-5570.

Alberts B, Bray D, Lewis J, Raff M, Roberts K and Watson JD (1994) *Molecular biology of the cell*. 3rd ed. Garland Pub. New York.

Alexiadis V, Waldmann T, Andersen J, Mann M, Knippers R and Gruss C (2000) The protein encoded by the proto-oncogene DEK changes the topology of chromatin and reduces the efficiency of DNA replication in a chromatin-specific manner. *Genes & Dev.* **14**, pp 1308-1312.

Agami R, Blandino G, Oren M and Shaul Y (1999) Interaction of c-abl and p73 and their collaboration to induce apoptosis. *Nature* **399**, pp 809-813.

Aggarwal AK (1995) Structure and function of restriction endonucleases. *Curr. Opin. Struct. Biol.* **5**, pp 11-19.

Antoccia A, Stumm M, Saar K, Ricordy R, Maraschio P and Tanzarella C (1999) Impaired p53-mediated DNA damage response, cell cycle disturbance and chromosomal aberrations in Nijmegen breakage syndrome lymphoblastoid cell lines. *Int. J. Radiat. Biol.* **75**, pp 583-591.

Archer SY and Hodin RA (1999) Histone acetylation and cancer. *Curr. Opin. Genetics & Dev.* **9**, pp 171-174.

Ashburner M (1989) *Drosophila* A laboratory Manual. Cold Spring Harbor Laboratory Press.

Balajee AS, Dominguez I and Natarajan AT (1995) Construction of chinese hamster chromosome specific DNA libraries and their use in the analysis of spontaneous chromosome rearrangements in different cell lines. *Cytogenet. Cell Genet.* **70**, pp 95-101.

Banin S, Moyal L, Shieh S-Y, Taya Y, Andreson CW, Chessa L, Smorodinsky NI, Prives C, Reiss Y, Shiloh Y and Ziv Y (1998) Enhanced phosphorylation of p53 by ATM in response to DNA damage. *Science* **281**, pp 1674-1679.

Baskaran R, Wood LD, Whitaker LL, Canman CE, Morgan SE, Xu Y, Barlow C, Baltimore D, Wynshaw-Boris A, Kastan MB and Wang YJY (1997) Ataxia telangiectasia mutant protein activates c-Abl tyrosine kinase in response to ionizing radiation. *Nature* **387**, pp 516-519.

Bassing CH, Alt FW, Hughes MM, D'Auteuil M, Wehrly T, Woodman BB, Gartner F, White JM, Davidson L and Sleckman BP (2000) Recombination signal sequences restrict chromosomal recombination beyond the 12/23 rule. *Nature* **405**, pp 583-586.

Bell DW, Varley JM, Szydlo TE, Kang DH, Wahrer DCR, Shannon KE,

Lubratovich M, Versalis SJ, Isselbacher KJ, Fraumeni JF, Birch JM, Li FP, Garber JE and Haber DA (1999) Heterozygous germ line *hCHK2* mutations in Li-Fraumeni syndrome. *Science* **86**, pp 2528-2531.

Bender MA, Griggs HG and Bedford JS (1974) Mechanisms of chromosomal aberration production III: Chemicals and ionising radiation. *Mut. Res.* **23**, pp 197-212.

Bennet CB, Lewis AL, Baldwin KK and Resnik MA (1993) Lethality induced by a site-specific double-strand break in a dispensable yeast plasmid. *Proc. Natl. Acad. Sci. USA* **90**, pp 5613-5617.

Bhattacharyya A, Ear US, Kollerm BH, Weichselbaum RR and Bishop DK (2000) The breast cancer susceptibility gene *BRCA1* is required for subnuclear assembly of Rad 51 and survival following treatment with the DNA cross-linking agent cisplatin. *Jnl. Biol. Chem.* **275**, pp 23889-23903.

Bickmore WA and Oghene K (1996) Visualising the spatial relationships between defined DNA sequences and the axial region of extracted metaphase chromosomes. *Cell* **84**, pp 95-104.

Blocher (1990) In CHEF electrophoresis a linear induction of dsb corresponds to a nonlinear fraction of DNA with dose. *Int. Jnl. Radiat. Biol.* **57**, pp 7-12. cited in Foray *et al*, 1999.

Blunt T, Finnie NJ, Taccioli GE, Smith GCM, Demengeot J, Gottlieb TM, Mizuta R, Varghese AJ, Alt FW, Jeggo PA and Jackson SP (1995) Defective DNA-dependent protein kinase activity is linked to V(D)J recombination and DNA repair defects associated with the murine *scid* mutation. *Cell*, **80**, pp 813-823.

Bochar DA, Wang L, Beniya H, Kinev A, Xue Y, Lane WS, Wang W, Kashanchi F and Shiekhattar R (2000) BRCA1 is associated with a human SWI/SNF-related complex: linking chromatin remodelling to breast cancer. *Cell* **102**, pp 257-265.

Bogue M and Roth DB (1996) Mechanisms of V(D)J recombination. *Curr. Biol.* **8**, pp 175-180.

Bork P, Hofmann K, Bucher P, Neuwald AF, Altschul SF and Koonin EV (1997) A superfamily of conserved domains in DNA-damaging responsive cell cycle checkpoint proteins. *FASEB J.* **11**, pp 68-76.

Bosma GC (1983) A severe combined immunodeficiency mutation in the mouse. *Nature* **301**, pp 527-530.

Boudaiffa B, Cloutier P, Hunting D, Huels MA and Sanche L (2000) Resonant formation of DNA strand breaks by low-energy (3 to 20 eV) electrons. *Science* **287**, pp 1658-1660.

Boulton SJ and Jackson SP (1996a) Identification of a *Saccharomyces cerevisiae* Ku80 homologue: roles in DNA double-strand rejoining and in telomeric maintenance. *Nucleic Acids. Res.* **24**, pp 4639-4648.

Boulton SJ and Jackson SP (1996b) *Saccharomyces cerevisiae* Ku70 potentiates illegitimate DNA double-strand break repair and serves as a barrier to error-prone DNA repair pathways. *EMBO* **15**, pp 5093-5103.

Boulton SJ and Jackson SP (1998) Components of the Ku-dependent non-homologous end-joining pathway are involved in telomeric length maintenance and telomeric silencing. *EMBO*. **17**, pp 1819-1828.

Brehm A and Kouzarides T (1999) Retinoblastoma protein meets chromatin. *Trends in Biochem. Sci.* **24**, pp 142-145.

Brenneman MA, Weiss AE, Nickoloff JA and Chen DJ (2000) XRCC3 is required for efficient repair of chromosome breaks by homologous recombination. *Mut. Res.* **459**, pp 89-97.

Brenner DJ, Hlatky LR, Hahnfeldt PJ, Huang Y and Sachs RK (1998) The linear-quadratic model and most other common radiobiological models result in similar predictions of time-dose relationships. *Rad. Res.* **150**, pp 83-91.

Bridger JM, Boyle S, Kill IR and Bickmore WA (2000) Re-modelling of nuclear architecture in quiescent and senescent human fibroblasts. *Current Biol.* **10**, pp 149-152.

Brooks EG, Filipovich AH, Padgett JW, Mamlock R and Goldblum RM (1999) T-cell receptor analysis in Omenn's Syndrome: evidence for defects in gene rearrangement and assembly. *Blood* **93**, pp 242-250.

Bryans M, Valenzano MC and Stamato TD (1999) Absence of DNA ligase IV protein in XR-1 cells: evidence for stabilization by XRCC4. *Mut. Res.* **443**, pp 53-58.

Bryant PE (1984) Enzymatic restriction of mammalian-cell DNA using Pvu II and Bam HI: Evidence for the double-strand break origin of chromosomal aberrations. *Int. J. Radiat. Biol.* **46**, pp 57-65.

Bryant PE (1985) Enzymatic restriction of mammalian cell DNA: Evidence for double strand breaks as potentially lethal lesions. *Int. J. Radiat. Biol.* **48**, pp 55-60.

Bryant PE (1988) Use of Restriction endonucleases to study relationships Between DNA double-strand breaks, chromosomal aberrations and other end points in mammalian cells. *Int. J. Radiat. Biol.* **54**, pp 869-890.

Bryant PE (1989) Restriction endonuclease- and radiation-induced DNA double-strand breaks and chromosomal aberrations: Similarities and differences. *Chromosomal Aberrations, Basic and Applied Aspects*. Ed. G. Obe and AT Natarajan. Springer-Verlag 1989 Berlin.

Bryant PE (1997) DNA Damage, repair and chromosomal damage. *Int. J. Radiat. Biol.* **71**, pp 675-680.

Bryant PE (1998a) The Signal Model: A possible explanation for the conversion of DNA double Strand-breaks into chromatid breaks. *Int. J. Radiat. Biol.* **73**, pp 243-251.

Bryant PE (1998b) Mechanisms of radiation-induced chromatid breaks. *Mut. Res.* **404**, pp 107-111.

Bryant PE and Blocher D (1982) The effects of 9- β -D-arabinofuranosyladenine on the repair of DNA double-strand breaks in X-irradiated Ehrlich ascites tumour cells. *Int. Jnl. Radiat. Biol.* **42**, pp 385-394.

Bryant PE, Birch DA and Jeggo PA (1987) High chromosomal sensitivity of chinese hamster xrs 5 cells to restriction endonuclease induced DNA double-stranded breaks. *Int. J. Radiat. Biol.* **52**, pp 537-554.

Bryant PE and Christie AF (1989) Induction of chromosomal aberrations in CHO cells by restriction endonucleases: Effects of blunt- and cohesive-ended double-strand breaks in cells treated by "Pellet" Methods. *Mut. Res.* **213**, pp 233-241.

Bryant PE, Finnegan CE, Swaffield L and Mozdarani H (1998) G2 chromatid breaks in murine SCID cells. *Mutagenesis* **13**, pp 481-485.

Bryant PE and Slijepcevic P (1993) G2 Chromatid aberrations: Kinetics and possible mechanisms. *Env. and Molecular Mutagenesis* **22**, pp 250-256.

Buchwald M and Moustacchi E (1998) Is Fanconi anaemia caused by a defect in the processing of DNA damage? *Mut. Res.* **408**, pp 75-90.

Burgess SM and Kleckner N (1999) Collisions between yeast and chromosomal loci are governed by three layers of organization. *Genes & Dev.* **13**, pp 1871-1883.

Carey RB, Peterson SR, Wang J, Bear DG, Bradbury EM, Chen DJ (1997) DNA Looping by Ku and the DNA-dependent protein kinase. *Proc. Natl. Acad. Sci. USA* **94**, pp 4267-4272.

Carnero A, Hudson JD, Price CM and Beach DH (2000) p16^{INK4A} and p19^{ARF} act in overlapping pathways in cellular immortalization. *Nature Cell Biol.* **2**, pp 148-155.

Carney JP (1999) Chromosomal breakage syndromes. *Curr. Opin. Immunology* **11**, pp 443-447.

Carney JP, Maser RS, Olivares H, Davis EM, Le Beau M, Yates III JR, Hays L, Morgan WF and Petrini JH (1998) The hMre11/Rad50 protein complex and Nijmegen Breakage Syndrome: Linkage of double-strand break repair to the cellular DNA damage response. *Cell* **93**, pp 477-486.

Carr AM and Hoekstra MF (1995) The cellular responses to DNA damage. *Trends in Cell Biol.* **5**, pp 32-39.

Cartwright R, Tambini CE, Simpson PJ and Thacker J (1998) The XRCC2 DNA repair gene from human and mouse encodes a novel member of the *recA/RAD51* family. *Nuc. Acids Res.* **26**, pp 3084-3089.

Chadwick KH and Leenhouts HP (1978) The rejoining of DNA double-strand breaks and a model for the formation of chromosomal rearrangements. *Int. J. Radiat. Biol.* **33**, pp 517-529.

Chadwick KH and Leenhouts HP (1994) On the linearity of the dose-effect relationship of DNA double-strand breaks. *Int. J. Radiat. Biol.* **66**, pp 549-552.

Chan TA, Hermeking H, Lengauer C, Kinzler KW and Vogelstein B (1999) 14-3-3 σ is required to prevent mitotic catastrophe after DNA damage. *Nature* **401**, pp 616-620.

Chao CCK, Rosenstein RB and Rosenstein BS (1985) Induction of sister-chromatid exchanges in ICR 2A frog cells exposed to 265-313 nm monochromatic ultraviolet wavelengths and photoreactivating light. *Mut. Res.* **149**, pp 443-450.

Chapman MS and Verma IM (1996) Transcriptional activation of BRCA1. *Nature* **382**, pp 678-679.

Chaturvedi P, Eng WK, Zhu Y, Mattern MR, Mishra R, Hurle MR, Zhang X, Lu Q, Faucette LF, Scott GF, Li X, Johnson RK, Winkler JD and Zhou B-BS (1999) Mammalian Chk2 is a downstream effector of the ATM-dependent DNA damage checkpoint pathway. *Oncogene* cited in Lavin and Khanna (1999).

Chen C and Kolodner RD (1999) Gross chromosomal rearrangements in *Saccharomyces cerevisiae* replication and recombination defective mutants. *Nature Genet.* **23**, pp 81-85. cited in Pfeiffer *et al*, 2000.

Chen P-L, Chen C-F, Chen Y, Xiao J, Sharp ZD and Lee W-H (1998a) The BRC repeats in BRCA2 are critical for RAD51 binding and resistance to methylsulfonate treatment. *Proc. Natl. Acad. Sci. USA* **95**, pp 5287-5292.

Chen G and Lee EYHP (1996) The product of the ATM gene is a 370kDa nuclear phosphoprotein. *Jnl. Biol. and Chem.* **271**, pp 33693-33697.

Chen AM, Lucas JN, Hill FS, Brenner DJ and Sachs RK (1996) Proximity effects for chromosome aberrations measured by FISH. *Int. J. Radiat. Biol.* **69**, pp 411-420.

Chen J, Silver DP, Walpita D, Canotr SB, Gazdar AF, Tomlinson G, Couch FJ, Weber BL, Ashley T, Livingston DM, Scully R (1998b) Stable interaction between the products of the *BRCA1* and *BRCA2* tumor supressor genes in mitotic and meiotic cells. *Mol. Cell* **2**, pp 317-328.

Chen X, Yang L, Udar N, Liang T, Uhrhammer N, Xu S, Bay J-O, Wang X, Dandakar S, Chiplunkar S, Klisak I, Telatar M, Yang H, Concannon P and Gatti R (1997) *CAND3* A ubiquitously expressed gene immediately adjacent and in opposite transcriptional orientation to the *ATM* gene at 11q23.1. *Mammalian*

Genome **8**, pp 129-133. cited in Lavin Khanna (1999).

Chester N, Kuo F, Kozak C, O'Hara CD and Leder P (1998) Stage-specific apoptosis, developmental delay, and embryonic lethality in mice homozygous for a targeted disruption in the murine Bloom's syndrome gene. *Genes & Dev.* **12**, pp 3382-3393.

Choulika A, Perrin A, Dujon B, Nicholas JF (1995) Induction of homologous recombination in mammalian chromosomes by using the I-Sce I system of *Saccharomyces cerevisiae*. *Mol. Cell. Biol.* **15**, pp 1968-1973.

Cigarran S, Barrios L, Barquinero JF, Caballin MR, Ribas M and Egozcue J (1998) Relationship between the DNA content of human chromosomes and their involvement in radiation-induced structural aberrations analysed by painting. *Int. J. Radiat. Biol.* **74**, pp 449-455.

Cohen-Tannoudji M, Robine S, Choulika A, Pinto D, El Marjou F, Babinet C, Louvard D and Jaissier F (1998) I-Sce I-induced gene replacement at a natural locus in embryonic stem cells. *Mol. Cell. Biol.* **18**, pp 1444-1448.

Colleaux L, D'Auriol L, Galibert F and Dujon B (1988) Recognition and cleavage site of the intron-encoded *Omega* Transposase. *PNAS USA* **85**, pp 6022-6026.

Connor F, Bertwhistle D, Mee PJ, Ross GM, Swift S, Grigorieva E, Tybulewicz VLJ and Ashworth A (1997) Tumorigenesis and a DNA repair defect in mice with a truncating *Brca2* mutation. *Nature Genetics* **17**, pp 423-430.

Cook PR (1999) The organization of replication and transcription. *Science* **284**, pp 1790-1795.

Cook PR (1995) A chromomeric model for nuclear and chromosome structure. *Jnl. Cell Sci.* **108**, pp 2927-2935.

Cook PR and Brazell IA (1975) Supercoils in human DNA. *J. Cell Sci.* **19**, pp 261-279.

Coquerelle TM, Weibezahn KF and Lucke-Huhle C (1987) Rejoining of double-strand breaks in normal human and ataxia-telangiectasia after exposure to ⁶⁰Co gamma-rays, ²⁴¹Am alpha-particles or bleomycin. *Int. Jnl. Radiat. Biol.* **51**, pp 209-218.

Cornforth MN and Bedford JS (1983) X-ray induced breakage and rejoining of human interphase chromosomes. *Science* **222**, pp 1141-1143.

Cornforth MN and Bedford JS (1985) On the nature of a defect in cells from individuals with Ataxia-telangiectasia. *Science* **227**, pp 1589-1591.

Cortez D, Wang Y, Qin J and Elledge SJ (1999) Requirement for ATM-dependent phosphorylation of Brca1 in the DNA damage response to double-strand breaks. *Science* **286**, pp 1162-1166.

Cottam DM and Milner M (1997) Effect of age on the growth and response of a

Drosophila cell line to moulting hormone. *Tissue & Cell* **29**, pp727-732.

Countryman PI, Heddle JA and Crwaford E (1977) The repair of X-ray induced chromosomal damage in trisomy 21 and normal diploid lymphocytes. *Cancer Res.* **37**, pp 52-58.

Craig JM, Boyle S, Perry P and Bickmore WA (1997) Scaffold attachments in the human genome. *Jnl. Cell Sci.* **110**, pp 2673-2682.

Critchlow SE, Bowater RP and Jackson SP (1997) Mammalian DNA double-strand break repair protein XRCC4 interacts with DNA ligase IV. *Curr. Biol.* **7**, pp 588-598.

Critchlow SE and Jackson SP (1998) DNA end-joining: from yeast to man. *Trends in Biochem. Sci.* **23** pp 394-398.

Cui X, Brenneman M, Meyne J, Oshimura M, Goodwin EH, Chen DJ (1999) The *XRCC2* and *XRCC3* repair genes are required for chromosomal stability in mammalian cells. *Mut. Res.* **434**, pp 75-88.

Dahm-Daphi J and Dikomey E (1996) Rejoining of DNA double-strand breaks in X-Irradiated CHO Cells studied by constant- and graded-field gel electrophoresis. *Int. J. Radiat. Biol.* **69**, pp 615-621.

de Alarcon P, Patil S, Golberg J, Allen JB and Shaw S (1987) Use of cytogenetic studies and *in vitro* colony assay for granulocyte progenitor to distinguish acute nonlymphocytic leukemia from a transient myeloproliferative disorder. *Cancer* **60**, pp 987-993.

Debrauwere H, Buard J, Tessier J, Aubert D, Vergnaud G, Nicolas A (1999) Meiotic instability of human minisatellite CEB1 in yeast requires DNA double strand breaks. *Nature Genet.* **23**, pp 367-371. cited in Pfeiffer *et al*, 2000.

Deng C-H and Brodie SG (2000) Roles of Brca1 and its interacting proteins. *BioEssays* **22**, pp 728-737.

Digweed M, Reis A and Sperling K (1999) Nijmegen Breakage Syndrome: consequences of defective DNA double strand break repair. *BioEssays* **21**, pp 649-656.

Dikomey E, Dahm-Daphi J, Brammer I, Martensen R, Kaina B (1998) Correlation between cellular radiosensitivity and non-repaired double-strand breaks studied in nine mammalian cell lines. *Int. J. Radiat. Biol.* **73**, pp 269-278.

Dolfini SF (1978) Sister chromatid exchanges in *Drosophila melanogaster* cell lines *in vitro*. *Chromosoma* **69**, pp 339-347.

Dolganov GM, Maser RS, Novikov A, Tosto L, Chong S, Bressan DA and Petrini JHJ (1996) Human Rad50 is physically associated with human Mre11: Identification of a conserved multiprotein complex implicated in recombinational DNA repair. *Mol. Cell Biol.* **16**, pp 4832-4841.

- Dong Z, Zhong Q and Chen P-L (1999) The Nijmegen breakage syndrome protein is essential for Mre11 phosphorylation upon DNA damage. *Jnl. Biol. Chem.* **274**, pp 19513-19516.
- Donoho G, Jasin M and Berg P (1998) Analysis of gene targeting and intrachromosomal homologous recombination stimulated by genomic double-strand breaks in mouse embryonic stem cells. *Mol. and Cell. Biol.* **18**, pp 4070-4078.
- Downs JA and Lowndes NF and Jackson SP (2000) A role for *Saccharomyces cerevisiae* histone H2A in DNA repair. *Nature* **408**, pp 1001-1004.
- Dujon B (1989) Group I introns as mobile elements: facts and mechanistic speculations - a review. *Gene* **82**, pp 91-114.
- Elliott B, Richardson C, Winderbaum J, Nickoloff JA and Jasin M (1998) Gene conversion tracts from double-strand break repair in mammalian cells. *Mol. Cell Biol.* **18**, pp 93-101.
- Ellis NA (1997) DNA helicases in inherited human disorders. *Curr. Opin. Genetics & Dev.* **7**, pp 354-363.
- Ellis NA, Groden J, Ye TZ, Straughen J, Lennon DJ, Ciocci S, Proytcheva M and German J (1995) The Bloom's Syndrome gene product is homologous to RecQ helicases. *Cell* **83**, pp 655-666.
- Escarceller M, Buchwald M, Singleton BK, Jeggo PA, Jackson SP, Moustacchi E and Papadopoulo D (1998) Fanconi Anemia C gene product plays a role in the fidelity of blunt DNA end-joining. *Jnl. Mol. Biol.* **279**, pp 375-385.
- Famulski KS and Paterson MC (1999) Defective regulation of Ca²⁺/calmodulin-dependent protein kinase II in gamma-irradiated ataxia telangiectasia fibroblasts. *FEBS Letters* **453**, pp 183-186.
- Featherstone C and Jackson SP (1999) DNA repair: Ku, a DNA repair protein with multiple cellular functions? *Mut. Res.* **434**, pp 3-15.
- Feldmann E, Schiemann V, Goedecke W, Reichenberger S And Pfeiffer P (2000) DNA double-strand break repair in cell-free extracts from Ku80-deficient cells: implications for Ku serving as an alignment factor in nonhomologous DNA joining. *Nuc. Acids. Res.* **28**, pp 2585-2596.
- Figgitt M and Savage JRK (1999) Interphase chromosome domain reorganization following irradiation. *Int. J. Radiat. Biol.* **75**, pp 811-817.
- Foray N, Arlett CF and Malaise EP (1999) Underestimation of the small residual damage when measuring DNA double-strand breaks (DSB): is the repair of radiation-induced DSB complete? *Int. J. Radiat. Biol.* **75**, pp 1589-1595.
- Foray N, Randrianarison V, Marot D, Perricaudet M and Lenoir G (1999a) Gamma-rays-induced death of human cells carrying mutations of *BRCA1* or *BRCA2*. *Oncogene* **18**, pp 7334-7342.

Foray N, Badie C, Alsbeih G, Fertil B and Malaise EP (1996) A new model describing the curves for repair of both DNA double-strand breaks and chromosome damage. *Rad. Res.* **146**, pp 53-60.

Foray N, Priestly A, Alsbeih G, Badie C, Capulas EP, Arlett CF and Malaise EP (1997) Hypersensitivity of ataxia-telangiectasia fibroblasts to ionizing radiation is associated with a repair deficiency of DNA double strand breaks. *Int. Jnl. Radiat. Biol.* **72**, pp 271-283.

Fowler J and Cohen L (1990) *Practical statistics for field biology*. John Wiley and Sons, Chichester, UK.

Frankenberg-Schwager M and Frankenberg D (1990) DNA double-strand breaks: their repair and relationship to cell killing in yeast. *Int. Jnl. Radiat. Biol.* **58**, pp 569-575.

Fukuchi K, Martin GM and Monnat RJ (1989) Mutator phenotype of Werner Syndrome is characterized by extensive deletions. *Proc. Natl. Acad. Sci. USA* **86**, pp 5893-5897.

Futamura M, Arakawa H, Matsuda K, Katagari T, Saji S, Miki Y and Nakamura Y (2000) Potential role of BRCA2 in a mitotic checkpoint after phosphorylation by hBUBR1. *Cancer Res.* **60**, pp 1531-1535.

Gao Y, Ferguson DO, Xie W, Manis JP, Sekiguchi JA, Frank KM, Chaudhuri J, Horner J, DePinho RA and Alt FW (2000) Interplay of p53 and DNA-repair protein XRCC4 in tumourgenesis, genomic stability and development. *Nature* **404**, pp 897-900.

Gao Y, Sun Y, Frank KM, Dikkes P, Fujiwara Y, Seidl KJ, Sekiguchi JM, Rathburn GA, Swat W, Wang J, Bronson RT, Malynn BA, Bryans M, Zhu C, Chaudhuri J, Davidson L, FerrininR, Stamato T, Orkin SH, Greenberg ME and Alt FW (1998) A critical role for DNA end-joining proteins in both lymphogenesis and neurogenesis. *Cell* **95**, pp 891-902.

Gatti M (1979) Genetic control of chromosomal breakage and rejoining in *Drosophila melanogaster*: spontaneous aberrations in X-linked mutants defective in DNA metabolism. *Proc. Natl. Acad. USA* **76**, pp 1377-1381.

Gatti M, Pimpinelli S and Baker BS (1980) Relationships among chromatid interchanges, sister chromatid exchanges and meiotic recombination in *Drosophila melanogaster*:. *Proc. Natl. Acad. USA* **77**, pp 1575-1579.

Gatti M, Santini G, Pimpinelli S and Olivieri G (1978) Lack of spontaneous sister chromatid exchanges in somatic cells of *Drosophila mealnogaster*:. *Genetics* **91**, pp 255-274.

Gatti RM, Berkel I, Boder E, Braedt G, Charmley P, Concannon P, Ersoy F, Foround T, Jaspers NGJ, Lange K, Lathrop GM, Leppert M, Nakamura Y, O'Connell P, Paterson M, Salser W, Sanal O, Silver J, Sparkes RS, Susi E, Weeks DE, Wei S, White R and Yoder F (1988) Localization of an ataxia-telangiectasia

gene to chromosome 11q22-23. *Nature* **336**, pp 577-580.

Gianelli F, Benson PF, Pawsey SA and Polani PE (1977) Ultraviolet light sensitivity and delayed DNA-chain maturation in Bloom's syndrome fibroblasts. *Nature* **265**, pp 466-469.

Girard PM, Foray N, Stumm M, Waugh A, Riballo E, Maser RS, Phillips WP, Petrini J, Arlett CF and Jeggo PA (2000) Radiosensitivity in Nijmegen breakage syndrome cells is attributable to a repair defect and not cell cycle checkpoint defects. *Cancer Res.* **60**, pp 4881-4888.

Glasunov AV, Frankenberg-Schwager M and Frankenberg D. (1995) Different repair kinetics for short and long DNA double-strand gaps in *Saccharomyces cerevisiae*. *Int. J. Radiat. Biol.* **68**, pp 421-428.

Gomez-Arroyo S, Armienta MA, Cortes-Eslava J and Villalobos-Pietrini R (2000) Sister chromatid exchanges in *Vicia faba* induced by arsenic-contaminated drinking water from Zimapan, Hidalgo, Mexico. *Mut. Res. Gen. Toxicol. & Env. Mutagen.* **394**, pp 1-7.

Gong JG, Costanzo A, Yang HQ, Melino G, Kaelin Jr WG, Levrero M and Wang JYJ (1999) The tyrosine kinase c-abl regulates p73 in apoptotic response to cisplatin-induced DNA damage. *Nature* **399**, pp 806-809.

Gotoh E, Kawata T and Durante M (1999) Chromatid break rejoining and exchange aberration formation following y-ray exposure: analysis in G₂ human fibroblasts by chemically induced premature chromosome condensation. *Int. J. Radiat. Biol.* **75**, pp 1129-1135.

Grawunder U, West RB and Lieber MR (1998) Antigen receptor gene rearrangement. *Curr. Biol.* **10** pp 172-180.

Griffin CS, Harvey AN and Savage JRK (1994). Chromatid damage induced by ²³⁸Pu α-particles in G₂ and S phase of chinese hamster V79 cells. *Int. J. Radiat. Biol.* **66**, pp 85-98.

Guo CY, Mizzen C, Wang Y and Larner JM (2000) Histone H1 and H3 dephosphorylation are differentially regulated by radiation-induced signal transduction pathways. *Cancer Res.* **60**, pp 5667-5672.

Haaf T, Golub EI, Reddy G, Radding C and Ward DC (1995) Nuclear foci of mammalian Rad51 recombination protein in somatic cells after DNA damage and its localisation in synaptonemal complexes. *Proc. Natl. Acad. Sci USA* **92**, pp 2298-2302.

Haber JE (1999) Gatekeepers of recombination. *Nature N&V* **398**, pp 665-666.

Haber JE (1999a) DNA recombination: the replication connection. *Trends Biochem. Sci.* **24**, pp271-275. cited in Pfeiffer *et al*, 2000.

Haber JE (1998) The many interfaces of Mre11. *Cell* **95**, pp 583-586.

Hanawalt P and Painter R (1985) On the nature of a DNA-processing defect in ataxia telangiectasia. In Gatti RA editors *Ataxia telangiectasia: genetics, neuropathology and immunology of a neurodegenerative disease of childhood*. New York, Alan R Liss Inc pp 67-71. cited in Digweed *et al* (1999).

Hand R and German J (1975) A retarded rate of DNA chain growth in Blooms syndrome. *Proc. Natl. Acad. Sci. USA* **72**, pp 758-762.

Harfst E, Cooper S, Neubauer S, Distel L and Grawunder U (2000) Normal V(D)J recombination in cells from patients with Nijmegen breakage syndrome. *Mol. Immunol.* **37**, pp 915-929.

Harvey AN and Savage JRK (1997) Investigating the nature of chromatid breaks produced by restriction endonucleases. *Int. J. Radiat. Biol.* **71**, pp 21-28.

Heartlein MW, Tsuji H and Latt SA (1987) 5-bromodeoxyuridine-dependent increase in sister-chromatid exchange formation in Bloom's Syndrome is associated with reduction in topoisomerase II activity. *Exp. Cell Res.* **169**, pp 245-254.

Heddle JA and Bodycote DJ (1970) On the formation of chromosomal aberrations. *Mut. Res.* **9**, pp 117-126.

Heddle JA, Whissell D and Bodycote DJ (1969) Changes in chromosome structure induced by radiations: A test of the two chief hypotheses. *Nature* **221**, pp 1158-1160.

Helzlsouer KJ, Harris EL, Parshad R, Perry HR, Price FM and Sandford KK (1996) DNA repair proficiency: Potential susceptibility factor for breast cancer. *J. Nat. Cancer Inst.* **88**, pp 754-755.

Hirao A, Kong YY, Matsuoka S, Wakeham A, Ruland J, Yoshida H, Liu D, Elledge SJ and Mak TW (2000) DNA damage-induced activation of p53 by the checkpoint kinase Chk2. *Science* **287**, pp 1824-1827.

Hittelman WN and Pandita TK (1994) Possible role of chromatin formation in the radiosensitivity of ataxia-telangiectasia. *Int. Jnl. Radiat. Biol.* **66**, pp S109-S113.

Hollstein MD, Sidransky B, Vogelstein B and Harris CC (1991) p53 mutations in human cancers. *Science* **253**, pp 49-53. cited in Kaelin (1999).

Hozak P, Hassan AB, Jackson DA and Cook PR (1993) Visualisation of replication factories attached to a nucleoskeleton. *Cell* **73**, pp 361-373.

Hughes TA, Pombo A, McManus J, Hozak P, Jackson DA and Cook PR (1995) On the structure of replication and transcription factories. *Jnl. Cell Sci.* **19**, pp 59-65.

Huo YK, Wang Z, Hong JH, Chessa L, McBride WH, Periman SL and Gatti RA (1994) X-linked agammaglobulinemia and related syndromes use a modified colony assay. *Cancer Res.* **54**, pp 2544-2547. cited in Digweed *et al* (1999).

Huttley GA, Eastal S, Southey MC, Tesoriero A, Giles GG, McCredue MRE, Hopper JL, Venter DJ and the Australian Breast Cancer Family Study (2000). Adaptive evolution of the tumour suppressor *BRCA1* in humans and chimpanzees. *Nature Genetics* **25**, pp 410-413.

Huyton T, Bates PA, Zhang X, Sternberg MJE and Freemont PS (2000) The *Brcal* C-terminal domain: structure and function. *Mut. Res.* **460**, pp 319-332.

Iborra FJ, Pombo A, Jackson DA and Cook PR (1996) Active RNA polymerases are localized within discrete transcription "Factories" in human nuclei. *J. Cell Sci.* **109**, pp 1427-1436.

Imai T, Yamauchi M, Seki N, Sugawara T, Saito T, Matsuda Y, Ito H, Nagase T, Nomura N and Hori TA (1996) Identification and characterization of a new gene physically linked to the ATM gene. *Genome Res.* **6**, pp 439-447. cited in Lavin and Khanna (1999)

Ishikawa F and Naito T (1999) Why do we have linear chromosomes? A matter of Adam and Eve. *Mut. Res.* **434**, pp 99-107.

Ishizaki K, Nikaido O and Takebe H (1980) Photoreactivation of ultraviolet light-induced sister chromatid exchanges in potprus cells. *Photochem. and Photobiol.* **31**, pp 277-279.

Ishizaki K and Takebe H (1985) Comparative studies on photoreactivation of ultraviolet light-induced T4 endonuclease susceptible sites and sister chromatid exchanges in Potorus cells. *Mut. Res.* **150**, pp 91-97.

Jeggo PA (1990) Studies on mammlaian mutants defective in rejoining double-strand breaks in DNA. *Mut. Res.* **239**, pp 1-16. cited in Pfeiffer *et al*, 2000.

Jeggo PA (1997) DNA-PK: At the cross-roads of biochemistry and genetics. *Mut. Res.* **384**, pp 1-14.

Jeggo PA, Guillermo E, Taccioli and Jackson SP (1995) Menage a trois: Double strand break repair, V(D)J recombination and DNA-PK. *BioEssays*, **17**, pp949-957.

Johnson MA, Bryant PE and Jones NJ (2000) Isolation of camptothecin-sensitive chinese hamster cell mutants: phenotypic heterogeneity within the ataxia telangiectasia-like XRCC8 complementation group. *Mutagenesis* **15**, pp 367-374.

Johnson RD, Liu N and Jasin M (1999) Mammalian XRCC2 promotes the repair of DNA double-strand breaks by homologous recombination. *Nature* **401**, pp 397-399.

Johnson RT, Gotoh E, Mullinger AM, Ryan AJ, Shiloh Y, Ziv Y and Squires S (1999) Targeting double-strand breaks to replicating DNA identifies a subpathway of DSB repair that is defective in Ataxia-telangiectasia cells. *Biochem. and Biophys. Res. Com.* **261**, pp 317-325.

Johnson RT and Rao PN (1970) Mammalian cell fusion: Induction of premature chromosome condensation in interphase nuclei. *Nature*, **266**, pp 717

Johnston PG, Davey RJ and Seebeck JH (1984) Chromosome homologies in *Potorus tridactylus* and *Potorus longpipes* (Marsupialia: Macropodidae) based on G-banding patterns. *Aust. Jnl. Zool.* **32**, pp 319-324.

Johnston PJ and Bryant PE (1994) A component of DNA double-strand break repair is dependent on the spatial orientation on the lesions within the higher-order structures of chromatin. *Int. J. Radiat. Biol.* **66**, pp 531-536.

Johnston PJ, MacPhail SH, Stamato TD, Kirchgessner CU and Olive PL (1998) Higher-order chromatin structure-dependent repair of DNA double-strand breaks: Involvement of the V(D)J recombination double-strand break repair pathway. *Rad. Res.* **149** pp 455-462.

Johnston PJ, Olive PL and Bryant PE (1997) Higher-order chromatin structure-dependent repair of DNA double-strand breaks: Modelling the elution of DNA from nucleoids. *Rad. Res.* **148**, pp 561-567.

Jongmans W, Vuillaume M, Chrzanowska K, Smeets D, Sperling K and Hall J (1997) Nijmegen Breakage Syndrome cells fail to induce the p53-mediated DNA damage response following exposure to ionizing radiation. *Mol. Cell Biol.* **17**, pp 5016-5022.

Jorgensen TJ and Shiloh Y (1996) Review: The ATM gene and the radiobiology of Ataxia-telangiectasia. *Int. J. Radiat. Biol.* **69**, pp 527-537.

Kabotyanski EB, Gomelsky L, Han JO, Stamato TD and Roth DB (1998) Double-strand break repair in Ku86- and XRCC4-deficient cells. *Nuc. Acids. Res.* **26**, pp 5333-5342.

Kaelin WG Jr (1999) The emerging p53 gene family. *Jnl. of the Natl. Cancer Inst.* **91**, pp 594-598.

Kanaar R, Hoeijmakers JHJ and van Gent DC (1998) Molecular mechanisms of DNA double-strand break repair. *Trends in Cell Biol.* **8**, pp 483-489.

Kastan MB, Zhan Q, Wafik S, El-Deiry S, Carrier F, Jacks T, Walsh WV, Plunkett BS, Vogelstein B, Fornace Jr, AJ (1992) A mammalian cell cycle checkpoint pathway utilizing p53 and GADD45 is defective in Ataxia-telangiectasia. *Cell* **71**, pp 587-597.

Kato H (1974) Photoreactivation of sister chromatid exchanges induced by ultraviolet irradiation. *Nature* **249**, pp 552-553.

Kato H (1974) Induction of sister chromatid exchanges by chemical mutagens and its possible relevance to DNA repair. *Exp. Cell Res.* **85**, pp 239-247.

Kedizora J, Lukaszewicz R, Sibinska E and Jeske J (1985) Down syndrome: decreased oxygen enhancement ratio in lymphocytes' DNA. *Hereditas* **102**, pp 301-303.

Keegan KS, Holtzman DA, Plug AW, Christenson ER, Brainerd EE, Flaggs G, Bentley NJ, Taylor EM, Meyn MS, Moss SB, Carr AM, Ashley T and Hoekstra MF (1996) The Atr and Atm protein kinases associate with different sites along meiotically pairing chromosomes. *Genes & Dev.* **10**, pp 2423-2437.

Kemp LM, Sedgwick SG and Jeggo (1984) X-Ray sensitive mutants of chinese hamster ovary cells defective in double-strand break rejoining. *Mut. Res.* **132**, pp 189-196.

Khanna KK, Keating KE, Kozlov KE, Scott S, Gatei M, Hobson K, Taya Y, Gabrielli B, Chan D, Lees-Miller SP and Lavin MF (1998) ATM associates with and phosphorylates p53: mapping the region of interaction. *Nature Genetics* **20**, pp 398-400.

Khanna KK and Lavin MF (1993) Ionizing radiation and UV induction of p53 by different pathways in ataxia-telangiectasia. *Oncogene* **8**, pp 3307-3312.

Khanna KK, Yan J, Watters D, Hobson K, Beamish H, Spring K, Shiloh Y, Gatti RA and Lavin MF (1997) Defective signalling through the B cell antigen receptor in Epstein-Barr-transformed Ataxia telangiectasia cells. *mJnl. Biol. Chem.* **272**, pp 9489-9495.

Kharbanda S, Pandey P, Shengfang J, Inoue S, Bharti A, Yuan ZM, Weichselbaum R, Weaver D and Kufe D (1997) Functional interaction between DNA-PK and c-abl in response to DNA damage. *Nature* **386**, pp 732-735.

Kharbanda S, Ren R, Pandey P, Shafman TD, Feller SM, Weichselbaum RR, Kufe DW (1999) Activation of the c-abl tyrosine kinase in the stress response to DNA damaging agents. *Nature* **376**, pp 785-788.

Kilham BA and Andersson HC (1982) Sister chromatid exchanges in plants from Sister Chromatid Exchange, Chapter 9 pp 243-265, ed Sheldon Wolff, John Wiley & Sons, 1982.

Kilham BA, Natarajan AT and Andersson HC (1978) Use of the 5-bromodeoxyuridine-labelling technique for exploring mechanisms involved in the formation of chromosomal aberrations. *Mut. Res.* **52**, pp 181-98.

Kinzler KW and Vogelstein B (1997) Gatekeepers and caretakers. *Nature N&V* **386**, pp 761-763.

Kinzler KW and Vogelstein B (1996) Lessons from Hereditary colorectal cancer. *Cell* **87**, pp 159-170.

Kraakman-van der Zwet M, Overkamp WJI, Friedl AA, Klein B, Verhaegh GWCT, Jaspers NGJ, Midro AT, Eckardt-Schupp F, Lohman PHM and Zdienicka MZ (1999) Immortalization and characterisation of Nijmegen breakage syndrome fibroblasts. *Mut. Res.* **434**, pp 17-27.

Kramer KM, Brock JA, Bloom K, Moore JK and Haber JE (1994) Two different

types of double-strand breaks in *Saccharomyces cerevisiae* are repaired by similar RAD52-independent, nonhomologous recombination events. *Mol. and Cell. Biol.* **14**, pp 1293-1301.

Knudson AG (1993) Antioncogenes and human cancer. *Proc. Natl. Acad. USA* **90**, pp 10914-10921.

Kuby J (1991) *Immunology* 2nd ed. W.H. Freeman & Co. New York. Chapter 8.

Laemmli UK, Cheng SM, Adolph KW, Paulson JR, Brown JA and Baumbach WR (1977) Metaphase chromosome structure: the role of nonhistone proteins. *Cold Spring Harbor Symp.* **42**, pp 351-360. Cited in Saitoh and Laemmli (1994).

Lakin ND, Weber P, Stankovic T, Rottinghaus ST, Taylor AM and Jackson SP (1996) Analysis of the ATM protein in wild-type and ataxia telangiectasia cells. *Oncogene* **13**, pp 2707-2716.

Landenburger EM, Fackelmeyer FO, Hameister H and Knippers R (1997) MCM4 and PRKDC, human genes encoding proteins MCM4 and DNA-PK_{CS}, are close neighbours on chromosome 8q12-q13. *Cytogenetics Cell Genetics* **77**, pp 268-270. cited in Lavin and Khanna (1999)

Lambert PF, Kashanchi F, Radonovich MF, Shiekhattar R and Brady JN (1998) Phosphorylation of p53 serine 15 increases its interaction with CBP. *Jnl. Biol. Chem.* **273**, pp 33048-33053.

Lange CS, Mayer PJ and Reddy NMS (1997) Tests of the double-strand break, lethal-potentially lethal and repair-misrepair models for mammalian cell survival using data for survival as a function of delayed palting interval for log-pahse chinese hamster V79 cells. *Rad. Res.* **148**, pp 285-292.

Latt SA (1973) Microfluorometric detection of deoxyribonucleic acid replication in human metaphase chromosomes. *Proc. Nat. Acad. Sci. USA* **70**, pp 3395-3399.

Lavin MF and Khanna KK (1999) Review: ATM: the protein encoded by the gene mutated in the radiosensitive syndrome ataxia-telangiectasia. *Int. J. Raidat. Biol.* **75**, pp 1201-1214.

Lavin MF, Khanna KK, Beamish H, Spring K and Watters D (1995) Relationship of the ataxia-telangiectasia protein ATM to phosphoinositide3-kinase. *Trends in Biochem.* **20**, pp 382-383.

Lavin MF, Khanna KK, Watters D, Spring K, Scott S, Keating K, Gatei M, Kaneko H and Kozlov S (1999) Sensing damage in DNA: ATM and cellular signalling. *Proceedings of 11th Int. Congress of Rad. Res. Vol 2*, pp 348-351.

Lea DE (1946) *Actions of radiations on living cells.* 1st. ed. Cambridge Uni. Press.

Leach FS, Tokino T, Meltzer P, Oliner JD and Smith S (1993) p53 mutation and MDM2 mutation in human soft tissue sarcomas. *Cancer Res.* **53** (10 Suupl) pp 2231-2234. cited in Kaelin (1999).

Lee SE, Moore JK, Holmes A, Umezu K, Klodner RD, Haber JE (1998) *Saccharomyces* Ku70, Mre11/Rad50, and RPA proteins regulate adaptation to G₂/M arrest after DNA damage. *Cell* **94**, pp 399-409.

Lehmann AR and Stevens S (1977) The production and repair of double-strand DNA breaks in cells from normal humans and from patients with ataxia telangiectasia. *Biochimica et Biophysica Acta*. **474**, pp 49-60.

Leonard JC and Merz T (1987) Chromosomal aberrations in irradiated Down's syndrome fibroblasts. *Mut Res.* **180**, pp 223-230.

Leonard JC and Merz T (1983) The influence of cell cycle kinetics on the radiosensitivity of Down's syndrome lymphocytes. *Mut Res.* **109**, pp 111-121.

Li NX, Banin S, Quyang HH, Li GC, Courtois G, Shiloh Y and Karin M (2001) ATM is required for I kappa B kinase (IKK) activation in response to DNA double strand breaks. *Jnl. Biol. Chem.* **276**, pp 8898-8903.

Li S, Ting NSY, Zheng L, Chen P-L, Ziv Y, Shiloh Y, Lee EY-HP, Lee W-H (2000) Functional link of Brca1 and ataxia telangiectasia gene product in DNA damage response. *Nature* **406**, pp 210-215.

Li Z, Otevrel T, Gao Y, Cheng H, Seed B, Stamato TD, Taccioli GE and Alt FW (1995) The XRCC4 gene encodes a novel protein involved in DNA double-strand break repair and V(D)J recombination. *Cell* **83**, pp 1079-1089.

Liang H and Burns MW (1983) Establishment of nucleolar deficient sublines of Ptk2 (*Potorus tridactylus*) by ultraviolet laser. *Exp. Cell Res.* **144**, pp 234-240.

Liang F and Jasin M (1996) ku-80 deficient cells exhibit excessive degradation of extrachromosomal DNA. *Jnl. Biol. Chem.* **271**, pp 14405-14411. cited in Pfeiffer *et al*, 2000.

Liang F, Han M, Romanienko PJ and Jasin M (1998) Homology-directed repair is a major double-strand break repair pathway in mammalian cells. *Proc. Natl. Acad. Sci. USA* **95**, pp 5172-5177.

Liao S, Graham J and Yan H (2000) The function of *Xenopus* Bloom's Syndrome protein homolog (xBLM) in DNA replication. *Genes & Dev.* **14**, pp 2570-2575.

Lieber MR (1997a) The FEN-1 family of structure-specific nucleases in eukaryotic DNA replication, recombination and repair. *BioEssays* **15**, pp 233-240. cited in Pfeiffer *et al*, 2000.

Lieber MR, Grawunder U, Wu X and Yaneva M (1997b) Tying loose ends: Roles of Ku and DNA-dependent protein kinase in the repair of double-strand breaks. *Curr. Opin. Gen. Dev.* **7** pp 99-104.

Lim DS and Hasty P (1996) A mutation in mouse *rad51* results in an early embryonic lethal that is suppressed by a mutation in *p53*. *Mol. Cell Biol.* **16**, pp 7133-7143.

- Lim DA, Kirsch DG, Canman CE, Ahn JH, Ziv Y, Newman LS, Darnell RB, Shiloh Y and Kastan MB (1998) ATM binds to β -adaptin in cytoplasmic vesicles. *Proc. Natl. Acad. Sci.* **95**, pp 10146-10151.
- Lim DS, Kim ST, Xu B, Maser RS, Lin J, Petrini JHJ and Kastan MB (2000) ATM phosphorylates p95/nbs1 in an S-phase checkpoint pathway. *Nature* **404**, pp 613-617.
- Lin MS and Wertelecki W (1982) Evidence that sister chromatid exchanges and chromatid breaks are two independent events. *Chromosoma* **85**, pp 413-419.
- Liu N and Bryant PE (1994) Enhanced chromosomal response of ataxia-telangiectasia cells to specific types of DNA double-strand breaks. *Int. J. Radiat. Biol.* **66**, pp S115-S121.
- Liu N, Lamerdin JE, Tebbs RS, Schild D, Tucker JD, Shen MR, Brookman KW, Siciliano MJ, Walter CA, Fan W, Narayana LS, Zhou Z, Adamsom AW, Sorensen KJ, Chen DJ, Jones NJ and Thompson LH (1998) XRCC2 and XRCC3, new human Rad51-family members, promote chromosome stability and protect against DNA cross-links and other DNA damages. *Mol. Cell* **1**, pp 1-20.
- Liu N, Lmaerdin JE, Tucker JD, Zhou ZQ, Walter CA, Albala JS, Busch DB and Thompson LH (1997) The Human XRCC9 gene corrects chromosomal instability and mutagen sensitivities in CHO UV40 cells. *Proc. Natl. Acad. USA* **94**, pp 9232-9237.
- Lloyd AC (2000) p53: only ARF the story. *Nature N&V* **405**, pp E48-50.
- Loechelt BJ, Shapiro RS, Jyonouchi H and Flipovich AH (1995) Mismatched bone marrow transplantation for Omenn syndrome: a variant of severe combined immunodeficiency. *Bone Marrow Transplantation* **16**, pp 381-385.
- Lohrum MAE and Vousden KH (2000) Regulation and function of the p53-related proteins: same family, different rules. *Trends in Cell Biol.* **10**, pp 197-202.
- Lonn U, Lonn S, Nylen U, Winblad G and German J (1990) An abnormal profile of DNA replication intermediates in Bloom's Syndrome. *Cancer Res.* **50**, pp 3141-3145.
- Loucas BD and Geard CR (1994) Kinetics of chromosome rejoining in normal human fibroblasts after exposure to low- and high-LET radiations. *Rad. Res.* **138**, pp 352-360.
- Lozano G and Elledge SJ p53 sends nucleotides to repair DNA. *Nature N&V* **404**, pp 24-25.
- Lukaszewicz R, Sibinska E and Kedizora J (1981) Down's Syndrome: decreased radiosensitivity of lymphocytes' DNA. *Hereditas* **97**, pp 155-156.
- Ludwig T, Chapman DL, Papioannou VE, Efstradiadis A (1996) Targeted

mutations of breast cancer susceptibility genes in mice: lethal phenotypes of *Brca1*, *Brca2*, *Brca1/Brca2*, *Brca1/p53*, and *Brca2/p53* nullizygous embryos. *Genes & Dev.* **10**, pp 1226-1241.

Luo G, Yao MS, Bender CF, Mills M, Bladl AR, Bradley A and Petrini JHJ (1999) Disruption of *mRad50* causes embryonic stem cell lethality, abnormal embryonic development and sensitivity to ionizing radiation. *Proc. Natl. Acad. Sci. USA* **96**, pp 7376-7381.

McBlane JF, van Gent DC, Ramsden DA, Romeo C, Cuomo CA, Gellert M, Oettinger MA (1995) Cleavage at a V(D)J recombination signal requires only RAG1 and RAG2 proteins and occurs in two steps. *Cell* **63**, pp 387-395.

McDaniels LD and Schultz RA (1992) Elevated sister chromatid exchange phenotype of Blooms syndrome cells is complemented by human chromosome 15. *Proc. Natl. Acad. Sci.* **89**, pp 7968-7972.

McEwen BF, Hseih C-E, Matteyses AL and Rieder CL (1998) A new look at kinetochore structure in vertebrate somatic cells using high-pressure freezing and freeze substitution. *Chromosoma* **107**, pp 366-375.

McMillan TJ and Peacock JH (1994) Molecular determinants of radiosensitivity in mammalian cells. *Int. Jnl. Radiat. Biol.* **65**, pp 49-55.

Machida C, Onouchi H, Hamada S, Seimarti E, Torikai S and Machida Y (1997) Characterization of the transposition pattern of the *Ac* element in *Arabidopsis thaliana* using the endonuclease I-*Sce* I. *Proc. Natl. Acad. Sci. USA* **94**, pp 8675-8680.

MacLeod RAF and Bryant PE (1992) Effects of adenine arabinoside and conformycin on the kinetics of G₂ aberrations in X-irradiated human lymphocytes. *Mutagenesis* **7**, pp 285-290.

Manfredi MJ and Prives C (1994) The transforming activity of simian virus 40 large tumour antigen. *Biochem. et Biophys. Acta* **1198**, pp65-83.

Marathias VM, Jerkovic B and Bolton PH (1999) Damage increases the flexibility of duplex DNA. *Nucleic Acids Res.* **27**, pp 1854-1658.

Marder BA and Morgan WF (1993) Delayed chromosomal instability induced by DNA damage. *Mol. Cell Biol.* **13** pp 6667-6677.

Marians KJ (2000) Replication and recombination intersect. *Curr. Opin. Gen. & Dev.* **10**, pp 151-156.

Marin MC, Jost CA, Brooks LA, Irwin MS, O'Nions J, Tidy JA, James N, McGregor JM, Harwood CA, Yulug IG, Vousden KH, Allday MJ, Gusterson B, Ikawa S, Hinds PW, Crook T and Kaelin Jr WG (2000) A common polymorphism acts as an intragenic modifier of mutant p53 behaviour. *Nature genetics* **25**, pp 47-54.

Maser RS, Monsen KJ, Helms BE and Petrini JH (1997) hMre11 and Rad50

nuclear foci are induced during the normal cellular response to DNA double-strand breaks. *Mol. Cell Biol.* **17**, pp 6087-6096.

Maser RS, Zinkel R and Petrini JHJ (2001) An alternative mode of translation permits production of a variant NBS1 protein from the common Nijmegen breakage syndrome allele. *Nature Genet.* **27**, pp 417-412.

Mateos S, Slijepcevic P, MacLeod RAF and Bryant PE (1994) DNA double-strand break rejoining in *xrs5* Cells is more rapid in the G2 phase of the cell cycle. *Mut. Res.* **315**, pp 181-187.

Matsuoka S, Rotman G, Ogawa A, Shiloh Y, Tamai K and Elledge SJ (2000) Ataxia telangiectasia-mutated phosphorylated Chk2 *in vivo* and *in vitro*. *Proc. Natl. Acad. Sci.* **97**, pp 10389-10394.

Matsuura K, Balmukhanov T, Tauchi H, Weemaes C, Smeets D, Chrzanowska K, Endou S, Matsuura S and Komatsu K (1998) Radiation induction of p53 in cells from Nijmegen Breakage Syndrome is defective but not similar to Ataxia-telangiectasia. *Biochem, and Biophys, Res. Comm.* **242**, pp 602-607.

Meijer M and Smerdon MJ (1999) Accessing DNA damage in chromatin: insights from transcription. *BioEssays* **21**, pp 596-603.

Mendoza H (1999) Irradiation of the D Muntjac cell line, testing the predictions of the signal model and a comparison to other cell lines. Internal report, University of St. Andrews.

Meselson MM and Radding CM (1975) A general model for genetic recombination. *Proc. Natl. Acad. Sci. USA* **72**, pp 358-361. cited in Pfeiffer *et al*, 2000.

Meyne J, Goodwin EH and Moyzis RK (1994) Chromosome localisation and orientation of the simple sequence repeat of human satellite I DNA. *Chromosoma* **103**, pp 99-103.

Milne GT, Jin S, Shannon KB and Weaver DT (1996) Mutations in two Ku homologs define a DNA end-joining repair pathway in *Saccharomyces cerevisiae*. *Mol. Cell. Biol.* **16**, pp 4189-4198.

Milner J, Ponder B, Hughes-Davies L, Seltsmann M and Kouzarides T (1997) Transcriptional activation functions of Brca2. *Nature* **386**, pp 772-773.

Mitchell ELD and Scott D (1997) G₂ Chromosomal radiosensitivity in fibroblasts of Ataxia telangiectasia heterozygotes and a Li-Fraumeni Syndrome patient with radioresistant cells. *Int. J. Radiat. Biol.* **72**, pp 435-438.

Miyaka T, Hu Y-F, Yu DS and Li R (2000) A functional comparison of BRCA1 C-terminal domains in transcription activation and chromatin remodelling. *Jnl. Biol. Chem.* **275**, pp 40169-40173.

Mizuta R, LaSalle JM, Cheng H-L, Shinohara A, Ogawa H, Copelands N, Jenkins NA, Lalande M and Alt FW (1997) RAB22 and RAB163/mouse BRCA2:

Proteins that specifically interact with the RAD51 protein. Proc. Natl. Acad. Sci. USA (1997) **94**, pp 6927-6932.

Monteilhet C, Perrin A, Tiery A, Colleaux L and Dujon B (1990) Purification and characterization of the *in vitro* activity of I-Sce I, a novel and highly specific endonuclease encoded by a group I intron. Nuc. Acids Res. **18**, pp 1407-1413.

Moore JK and Haber JE (1996) Cell cycle and genetic requirements of two pathways of nonhomologous end-joining repair and double-strand breaks in *Saccharomyces cerevisiae*. Mol. and Cell. Biol. **16**, pp 2164-2173.

Morgan SE, Lovly C, Pandita TK, Shiloh Y and Kastan M (1997) Fragments of ATM which have dominant-negative or complementing activity. Mol. & Cell. Biol. **17**, pp 2020-2029.

Morgan WF, Day JP, Kaplan MI, McGhee EM, Limoli CL (1996) Genomic instability induced by ionizing radiation. Rad. Res. **146** pp 247-258.

Moroney MJ (1951) Facts from Figures. Penguin Books Ltd, Harmondsworth, Middx.

Moynahan ME and Jasin M (1997) Loss of heterozygosity induced by a chromosomal double-strand break. Proc. Natl. Acad. Sci. USA **94**, pp 8988-8993.

Mozdarani H and Bryant PE (1989) Kinetics of chromatid aberrations in G2 ataxia-telangiectasia cells exposed to X-rays and ara A. Int. J. Radiat. Biol. **55**, pp 71-84.

Mozdarani H and Bryant PE (1987) The effect of 9- β -D-arabinofuranosyladenine on the formation of X-ray induced chromatid aberrations in X-irradiated G2 human cells. Mutagenesis **2**, pp 371-374.

Murray A (1998) How to compact DNA. Nature **282**, pp pp 425-427.

Murray A and Hunt T (1993) The Cell Cycle an Introduction. Chapter 5, Mitosis. Oxford University Press, Oxford.

Nagele RG, Freeman T, McMorrow L, Thomson Z, Kitson-Wind K and Lee H (1999) Chromosomes exhibit preferential positioning in nuclei of quiescent human cells. Jnl. Cell Sci. **112**, pp 525-535.

Nakamura Y (1998) ATM: the p53 booster. Nature Med. **4**, pp 1231-1232.

Natarajan A, Obe G, Van Zeeland AA, Palitti F, Meijers M and Verdegaal-Immerzeel EAM (1980) Molecular mechanisms involved in the production of chromosomal aberrations II: Utilization of neurospore endonuclease for the study of aberration production by X-rays in G₁ and G₂ stages of the cell cycle. Mut. Res. **69**, pp 293-305.

Natarajan A and Obe G (1984) Molecular mechanisms involved in the production of chromosomal aberrations III. Restriction endonucleases. Chromosoma **90**, pp 120-127.

Nelms BE, Maser RS, MacKay JF, Lagally MG and Petrini JHJ (1998) In situ visualisation of DNA double-strand break repair in human fibroblasts. *Science* **280**, pp 590-592.

Ninio J (2000) Illusory defects and mismatches: why must DNA repair always be error-prone? *BioEssays* **22**, pp 396-401.

Notorangelo LD, Villa A and Schwarz K (1999) RAG and RAG defects. *Curr. Opin. Immunology* **11**, pp 435-442.

Nunez ME, Hall DB and Barton JK (1999) Long-range oxidative damage to DNA: effects of distance and sequence. *Chemistry and Biology* **6**, pp 85-97.

Nunez MI, Villalobos M, Olea N, Valenzuela MT, Pedraza V, McMillan TJ and Ruiz de Almodovar JM (1995) Radiation-induced DNA double-strand break rejoining in human tumour cells. *Brit. J. Cancer* **71**, pp 311-316.

Oettinger MA, Schatz DG, Gorka C and Baltimore D (1990) RAG-1 and RAG-2, adjacent genes that synergistically activate V(D)J recombination. *Science* **248**, pp 1517-1523.

Oliner JD, Kinzler KW, Meltzer PS, George DL and Vogelstein B (1992) Amplification of a gene encoding a p53-associated protein in human sarcomas. *Nature* **358**, pp 80-83. cited in Kaelin (1999)

Oliner JD, Pietenpol JA, Thiagalingam S, Gyuris J, Kinzler KW and Vogelstein B (1993) Oncoprotein MDM2 conceals the activation domain of tumour suppressor p53. *Nature* **362**, pp 857-860. cited in Kaelin (1999).

Ostashevsky JY (1992) Cellular recovery and postirradiation treatments. *Int. Jnl. Radiat. Biol.* **62**, pp 337-351.

Ostashevsky JY, Reichman B and Lange CS (1999) Higher order structure of mammalian chromatin deduced from viscoelastrometry data. *Jnl. Biomolecular structure & dynamics* **17**, pp 567-580.

Paques F and Haber JE (1999) Multiple pathways of recombination induced by double-strand breaks in *Saccharomyces cerevisiae*. *Microbiol. and Mol. Biol. Revs.* **63**, pp 349-404.

Pandita TK and Hittelman WN (1992) Initial chromosome damage but not DNA damage is greater in ataxia telangiectasia cells. *Rad. Res.* **130**, pp 94-103.

Parshad R, Price FM, Bohr VA, Cowans KH, Zujewski JA and Sanford KK (1996) Deficient DNA repair capacity, a predisposing factor in breast cancer. *Brit. Jnl. Cancer* **74**, pp 1-5.

Parshad R and Sanford KK (2001) Radiation-induced breaks and deficient DNA repair in cancer predisposition. *Crit. Rev. in Oncol. Haematol.* **37**, pp 87-96.

Patel RK, Trivedi AH, Arora DC, Bhatadekar JM and Patel DD (1997) DNA

repair proficiency in breast cancer patients and their first-degree relatives. *Int. Jnl. Cancer* **73**, pp 20-24.

Paul (2000) A critical role for histone H2AX in recruitment of repair factors to nuclear foci after DNA damage. *Curr. Biol.* **10**, pp 886-895. cited in Scully and Livingstone, 2000.

Paull TT and Gellert M (1998) The 3' to 5' exonuclease activity of Mre11 facilitates repair of DNA double strand breaks. *Mol. Cell* **1**, pp 969-979.

Paull TT and Gellert M (1999) Nbs1 potentiates ATP-driven DNA unwinding and endonuclease cleavage by the Mre11/Rad50 complex. *Genes & Dev.* **13**, pp 1276-1288.

Paulovich AG, Toczyski DP and Hartwell LH (1977) When checkpoints fail. *Cell* **88**, pp 315-321.

Peng CY, Graves PR, Thoma RS, Wu Z, Shaw AS, Piwnicka-Worms H (1997) Mitotic and G2 checkpoint control: regulation of 14-3-3 protein binding by phosphorylation of Cdc25C on serine 216. *Science* **277**, pp 1501-1505. cited in Kaelin (1999).

Perry PE and Evans HJ (1975) Cytological detection of mutagen-carcinogen exposure by sister chromatid exchange. *Nature* **258**, pp 121-125.

Perry PE and Wolff S (1974) New giemsa method for the differential staining of sister chromatids. *Nature* **251**, pp 156-158.

Petrov DA (2000) Evolution of genome size: new approaches to an old problem. *Trends in Genetics* **17**, pp 23-28.

Pfeiffer P, Goedecke W and Obe G (2000) Mechanisms of DNA double-strand break repair and their potential to induce chromosomal aberrations. *Mutagenesis* **15**, pp 289-302.

Pfeiffer P and Vielmetter W (1988) Joining of nonhomologous DNA double-strand breaks *in vitro*. *Nuc. Acids. Res.* **16**, pp 907-923. cited in Pfeiffer *et al*, 2000.

Porter IH and Paul B (1974) Chromosomal anomalies and malignancy. *Birt Defects: Original Articles X*, pp 54-59.

Preston RJ (1981) X-ray induced chromosom aberrations in Down lymphocytes: An explanation of their increased sensitivity. *Environ. Mutagen.* **3**, pp85-89.

Radvoyevitch T, Hoel DG, Hahnfeldt PJ, Rydberg B and Sachs RK (1998) recent data obtained by pulsed-field gel electrophoresis suggest two types of double-strand breaks. *Rad. Res.* **149**, pp 52-58.

Ramsay G and Kumar A (1990) Transformation of *Vicia faba* cotyledon and stem tissues by *Agrobacterium rhizogenes*: Infectivity and cytological studies. *Jnl. Exp. Botany* **41**, pp 841-847.

Ramsden DA, Paull TT and Gellert M (1997) Cell-free V(D)J recombination. *Nature* **388**, pp 488-491.

Reddy NM, Myaer PJ, Nori D and Lange CS (1995) Chinese hamster V79 cells harbor potentially lethal damage which is neither fixed nor repaired for long times after attaining maximal survival under growth conditions. *Rad. Res.* **141**, pp 252-258.

Resnick MA (1976) The repair of double-strand breaks in DNA: A model involving recombination. *J. Theor. Biol.* **59**, pp 97-106.

Revell MA (1955) A new hypothesis for "chromatid" changes. In *Radiobiology Symposium*, ed. SH Bacq and P Alexander, London, Butterworth, pp 243-253.

Revell SH (1958) A new hypothesis for the interpretation of chromatid aberrations and its relevance to theories for the mode of action of chemical agents. *Ann. New York Acad. Sci.* **68**, pp 802-807.

Revell SH (1959) Some implications of a new interpretation of chromatid aberrations induced by ionising radiations and chemical agents. *Chemische Mutagenese Erwin-Bauer-Gedachtnisvorlesungen* **1**, 45-46.

Revell SH (1959a) The accurate estimation of chromatid breakage, and its relevance to a new interpretation of chromatid aberrations by ionizing radiation. *Proc. of the Royal Soc. of London B*, **150**, pp 563-589.

Revell SH (1974) The Breakage and Reunion Theory and the Exchange Theory for chromosomal aberrations induced by ionising radiations: A short history. *Adv. in Rad. Bio.* **4**, pp 367-416.

Richardson C and Jasin M (2000) Frequent chromosomal translocations induced by DNA strand breaks. *Nature* **405**, pp 697-700.

Richardson C, Moynahan ME and Jasin M (1998) Double-strand break repair by interchromosomal recombination: suppression of chromosomal translocation. *Genes & Development* **12**, pp 3831-3842.

Rogers-Bald M, Sargent RG and Bryant PE (2000) Production of chromatid breaks by single dsb: evidence supporting the signal model. *Int. Jn. Radiat. Biol.* **76**, pp 23-29.

Rosenstein BS (1984) Mitotic inhibition of ICR 2A frog cells exposed to 265-313 nm monochromatic ultraviolet wavelengths and photoreactivating light. *Int. J. Radiat. Biol.* **45**, pp 85-91.

Roth DB and Wilson JH (1985) Relative rates of homologous and nonhomologous recombination in transfected DNA. *Proc. Natl. Acad. Sci. USA* **82**, pp 3355-3359.

Roth DB and Wilson JH (1988) Illegitimate recombination in mammalian cells. In Kucherlalapti R and Smith G (eds) *Genetic Recombination*. ASM Press,

Washington DC, pp 621-653. cited in Pfeiffer *et al*, 2000.

Rouet P, Smih F and Jasin M (1994a) Expression of a site-specific endonuclease stimulates homologous recombination in mammalian cells. *Proc. Natl. Acad. Sci. USA* **91**, pp 6064-6068.

Rouet P, Smih F and Jasin M (1994b) Introduction of double-strand breaks into the genome of mouse cells by expression of a rare-cutting endonuclease. *Mol. Cell Biol.* **14**, pp 8096-8106.

Ruffner H, Jiang W, Craig AG, Hunter T and Verma IM (1999) Brca1 is phosphorylated at serine 1497 in vivo at a cyclin-dependent kinase 2 phosphorylation site. *Mol. Cell Biol.* **19**, pp 4843-4854.

Ruiz de Almdovar JM, Nunez MI, McMillan TJ, Olea N, Mort C, Villalobos M, Pedraza V and Steel GG (1994) Initial radiation-induced DNA damage in human tumours cell lines: a correlation with intrinsic cellular radiosensitivity. *Br. Jnl. Cancer* **69**, pp 457-462.

Runger TM and Kraemer KH (1989) Joining of linear plasmid DNA is reduced and error-prone in Bloom's syndrome cells. *EMBO* **8**, pp 1419 -1425.

Rydberg B, Holley WR, Mian IS and Chatterjee A (1998) Chromatin conformation in living cells: support for a zig-zag model of the 30 nm chromatin fiber. *J. Mol. Biol.* **284**, pp 71-84.

Sachs RK, Brenner DJ, Hahnfeldt PJ and HlatkysLR (1998) A formalism for analysing large-scale clustering of radiation induced breaks along chromosomes. *Int. J. Radiat. Biol.* **74**, pp 185-206.

Sachs RK, Levy D, Chen AM, Simpson PJ, Cornforth MN, Ingerman EA, Hahnfield P and Klatky LR (2000) Random breakage and reunion chromosome aberration formation model; an interaction-distance version based on chromatin geometry. *Int. Jnl. Radiat. Biol.* **76**, pp 1579-1588.

Saito T, Matsuda Y, Watanabe F, Mori M, Hayashi A, Araki R, Fujimore A, Fukumura R, Morimyo M, Tatsumi K, Hori T-A and Abe M (1998) Mouse *Cdc21* only 0.5kb upstream from *DNA-PK_{CS}* in a head-to-head organization: an implication of co-evolution of ATM members and cell cycle regulating genes. *Mammalian Genetics* **9**, pp 769-772. cited in Lavin and Khanna (1999).

Saitoh Y and Laemmli UK (1994) Metaphase chromosome structure: bands arise from a differential folding path of the highly AT-rich scaffold. *Cell* **76**, pp 609-622.

Sak A, Stuschke, Wurm R and Budach V (2000) Protection of DNA from radiation-induced double-strand breaks: influence of replication and nuclear proteins. *Int. Jnl. Radiat. Biol.* **76**, pp 749-746.

Saitoh Y and Laemmli UK (1994) Metaphase chromosome structure: bands arise from a differential folding path of the highly A-T rich scaffold. *Cell* **76**, pp 609-622.

Sanchez Y, Bachant J, Wang H, Hu F, Liu D, Tetzlaff M and Elledge SJ (1999) Control of the DNA damage checkpoint by Chk1 and Rad53 protein kinase through distinct mechanisms. *Science* **286**, pp 1166-1171.

Sanford KK, Parshad R, Gantt R, Tarone RE, Jones GM and Price FM (1989) Factors affecting and significance of G₂ chromatin radiosensitivity in predisposition to cancer. *Int. Jnl. Radiat. Biol.* **55**, pp 963-981.

Sargent RG, Brenneman MA and Wilson JH (1997) Repair of site specific double-strand breaks in a mammalian chromosome by homologous and illegitimate recombination. *Mol. Cell Biol.* **17**, pp 267-277.

Sasaki MS and Tonomura A (1969) Chromosomal radiosensitivity in Down's syndrome. *Jap. J. Human Genet.* **14**, pp81-92.

Savage JRK (1993) Update on Target Theory as applied to chromosomal aberrations. *Env. and Molecular Mutagenesis* **22**, pp 198-207.

Savage JRK and Harvey AN (1991) Revell revisited. *Mut. Res.* **250**, pp 307-317.

Savage JRK, Preston RJ and Neary GJ (1968) Chromatid aberrations in *Tradescantia bracteata* and a further test of Revell's hypothesis. *Mut. Res.* **5**, pp 47-56.

Savitsky K, Bar-Shira A, Gilad S, Rotman G, Ziv Y, Vanagaite L, Tagle DA, Smith S, Uziel T, Sfez S, Askenazi M, Pecker I, Frydman M, Harnik R, Patanjali SR, Simmons A, Clines GA, Sartiel A, Gatti RA, Chessa L, Sanal O, Lavin MF, Jaspers NGJ, Malcolm A, Taylor R, Arlett CF, Miki T, Weissman SM, Lovett M, Collins FS and Shiloh Y (1995) A single Ataxia Telangiectasia gene with a product similar to PI-3 kinase. *Science* **268**, pp 1749-1753.

Sax K (1940) An analysis of X-ray induced chromosome aberrations in *Tradescantia*. *Genetics* **25**, pp 41-68.

Scott D (1994) Genetic predisposition in breast cancer. *The Lancet* **344**, p 1444.

Scott D, Spreadborough AR, Jones LA, Roberts SA and Moore CJ (1996) Chromosomal radiosensitivity in G₂-phase lymphocytes as an indicator of cancer predisposition. *Rad. Res.* **145**, pp 3-16.

Scott D, Barber JBP, Spreadborough AR, Burrill W and Roberts SA (1999) Increased chromosomal radiosensitivity in breast cancer patients: a comparison of two assays. *Int. Jnl. Radiat. Biol.* **75**, pp 1-10.

Scully R, Chen J, Ochs RL, Keegan K, Hoekstra M, Feunteun J and Livingston DM (1997a) Dynamic changes of Brca1 subnuclear location and phosphorylation state are initiated by DNA damage. *Cell* **90**, pp 425-435.

Scully R, Chen J, Plug A, Xiao Y, Weaver D, Feunteun J, Ashley T and Livingston DM (1997b) Association of BRCA1 with Rad51 in mitotic and meiotic cells. *Cell* **88**, pp 265-275.

Scully R and Livingston DM (2000) In search of the tumour-suppressor functions of Brca1 and Brca2. *Nature* **408**, pp 429-432.

Shafik HM, Au WW and Legator MS (1988) Chromosomal sensitivity of Down syndrome lymphocytes at different stages of the cell cycle. *Hum. Genet.* **78**, pp 71-75.

Shafman T, Khanna KK, Kedar P, Spring K, Kozlov S, Yen T, Hobson K, Gatel M, Zhang N, Watters D, Egerton M, Shiloh Y, Kharbanda S, Kufe D and Lavin MF (1997) Interaction between ATM protein and c-abl in response to DNA damage. *Nature* **387**, pp 520-523.

Sharan SK, Morimatsu M, Albrecht U, Lim DS, Regel E, Dinh C, Sands A, Eichele G, Hasty P and Bradley A (1997) Embryonic lethality and radiation hypersensitivity mediated by Rad51 in mice lacking *Brca2*. *Nature* **386**, pp 804-810.

Shaughnessy Jnr J, Tian E, Sawyer J, Bumm K, Landos R, Badros A, Morris C, Trocit G, Epstein J and Barlogie B (2000) High incidence of chromosome 13 deletion in multiple myeloma detected by multiprobe interphase FISH. *Blood* **96**, pp 1505-1511.

Shen JC and Loeb LA (2000) The Werner Syndrome gene; the molecular basis of RecQ helicase deficiency diseases. *Trends in Genetics* **16**, pp 213-220.

Shepherd NS, Pfrogner BD, Coulby JN, Ackerman SL, Vaidyanathan G, Sauer RH, Balkenhol TC and Sternberg N (1994) Preparation and screening of an arrayed human genomic library generated with the P1 cloning system. *Proc. Natl. Acad. Sci. USA* **91**, pp 2629-2633.

Shiloh Y (1997) Ataxia Telangiectasia and the Nijmegen Breakage Syndrome: Related disorders but genes apart. *Ann. Rev. Genet.* **31**, pp 635-662.

Simpson PJ, Papworth DG and Savage JRK (1999) X-ray-induced simple, pseudosimple and complex exchanges involving two distinctly painted chromosomes. *Int. Jnl. Radiat. Biol.* **75**, pp 11-18.

Simpson PJ and Savage JRK (1996) Dose-response curves for simple and complex chromosome aberrations induced by X-rays and detected using fluorescence *in situ* hybridization. *Int. J. Radiat. Biol.* **69**, pp 429-436.

Sipi P, Lindholm C and Saloma S (2000) Kinetics of formation of exchanges and rejoining of breaks in human G0 and G2 lymphocytes after low-LET radiation. *Int. Jnl. Radiat. Biol.* **76**, pp 823-830.

Smeets (1993) Radiation-induced DNA damage and repair in radiosensitive and radioresistant human tumour cells measured by field inversion gel electrophoresis. *Int. Jnl. Radiat. Biol.* **63**, pp 57-60.

Steiner ME and Woods WG (1982) Normal formation and repair of radiation-induced single and double strand breaks in Down syndrome fibroblasts. *Mut.*

Res. **95**, pp 515-523.

Sternberg NL (1992) Cloning high molecular weight DNA fragments by the bacteriophage P1 system. *TIG* **8**, pp 11-16.

Stewart GS, Maser RS, Stankovic T, Bressan DA, Kaplan MI, Jaspers NGJ, Raams A, Byrd PJ, Petrini JHJ, Taylor AMR (1999) The DNA double-strand break repair gene *hMRE11* is mutated in individuals with an Ataxia-telangiectasia-like disorder. *Cell* **99**, pp 577-587.

Szekely L, Pokrovskaja K, Jiang W-Q, Selinova G, Lowbeer M, Ringertz N, Wiman KG and Klein G (1995) Resting B-cells, EBV infected B-blasts and established lymphoblastoid cell lines differ in their Rb, p53 and EBNA-5 expression patterns. *Oncogene* **10**, pp 1869-1874.

Szekely L, Selivanova G, Magnusson KP, Klein G and Wiman KG (1993) EBNA-5, an Epstein-Barr virus-encoded nuclear antigen, binds to the retinoblastoma and p53 proteins. *Proc. Natl. Acad. Sci. USA* **90**, pp 5455-5459.

Szostak JW, Orr-Weaver TL and Rothstein RJ (1983) The double-strand-break repair model for recombination. *Cell*, **33**, pp 25-35.

Takata (1998) Homologous recombination and non-homologous end-joining pathways of DNA double-strand break repair have overlapping roles in the maintenance of chromosomal integrity in vertebrate cells. *EMBO* **17**, pp 5497-5508

Tanaka H, Arakawa H, Yamaguchi T, Shiraishi K, Fukuda S, Matsui K, Takei Y and Nakamura Y (2000) A ribonucleotide reductase gene involved in a p53-dependent cell-cycle checkpoint for DNA damage. *Nature* **404**, pp 42-49.

Taylor EM and Lehmann AR (1998) Review: Conservation of eukaryotic DNA repair mechanisms. *Int. J. Radiat. Biol.* **74**, pp 277-286.

Taylor JH, Woods PS and Hughes WL (1956) The organisation and duplication of chromosomes as revealed by autoradiographic studies using tritium-labelled thymidine. *Biochem.* **43** pp 122-127.

Terzoudi GI, Jung T, Hain J, Vrouvas J, Magaritis K, Donta-Bakoyianni C, Makropoulos V, Angelakis PH and Pantelias GE (2000) Increased G2 chromosomal radiosensitivity in cancer patients: the role of cdk1/cyclin-B activity level in the mechanisms involved. *Int. Jnl. Radiat. Biol.* **76**, pp 607-615.

Thacker J (1989) Inherited sensitivity to X-rays in Man. *BioEssays* **11**, pp 58-61.

Thacker J (1994) The study of responses to 'model' DNA breaks induced by restriction endonucleases in cells and cell-free systems: achievements and difficulties. *Int. Jnl. Radiat. Biol.* **66**, pp 591-596.

Thacker J (1999) Repair of ionizing radiation damage in mammalian cells. Alternative pathways and their fidelity. *C.R. Acad. Sci. Paris, Sciences de la vie.* **322**, pp 103-108.

Thierry A and Dujon B (1992) Nested chromosomal fragmentation in yeast using the meganuclease I-Sce I: a new method for physical mapping of eukaryotic genomes. *Nuc. Acids. Res.* **20**, pp 5625-5631.

Thode S, Scafer A, Pfeifer P, Vielmetter W (1990) A novel pathway of DNA end-to-end joining. *Cell* **60**, pp 921-928.

Tibbetts RS, Brumbaugh KM, Williams JM, Sarkaria JN, Cliby WA, Shieh S-Y, Taya Y, Prives C and Abraham RT (1999) A role for ATR in the DNA damage-induced phosphorylation of p53. *Genes & Dev*, **13**, pp 152-157.

Tishkoff DX, Filosi N, Gaisa GM and Kolodner RD (1997) A novel mutation avoidance mechanism dependent on *S. cerevisiae* RAD27 is distinct from DNA mismatch repair. *Cell* **88**, pp 253-263. cited in Pfeiffer *et al*, 2000.

Trujillo KM, Yuan SF, Lee EYP and Sung P (1998) Nuclease activities in a complex of human recombination and DNA repair factors RAD50, Mre11 and p95. *J. Biol. Chem.* **273**, pp 21447-21450.

Tsubouchi H and Ogawa H (1998) A novel *mre11* mutation impairs processing of double strand breaks of DNA during both mitosis and meiosis. *Mol Cell Biol.* **18**, pp 260-268. cited in Usui *et al* (1998).

Tsuji H (1981) Presence of base line level of sister chromatid exchanges in somatic cells of *Drosophila melanogaster* *in vivo* and *in vitro*. *Genetics* **100**, pp 259-278.

Tubiana M, Dutreix J, Wambersie A (1990) Introduction to Radiobiology. Taylor & Francis, London.

Ullmann SL and Brown R (1983) Further observations on the potoroo (*Potorus tridactylus*) *Lab. Animals*, **17**, pp 133-137.

Ulsh BA, Whicker FW, Hinton TG, Congdon JD and Bedford JS (2001) Chromosome translocations in *T. scripta*: the dose-rate effect and *in vivo* lymphocyte radiation response. *Rad. Res.* **155**, pp 63-73.

Usui T, Ohta T, Oshiumi H, Tomizawa J, Ogawa H and Ogawa T (1998) Complex formation and functional versatility of Mre11 of budding yeast in recombination. *Cell* **95**, pp 705-716.

Van Dyck E, Stasiak AZ, Stasiak A and West SC (1999) Binding of double-strand breaks in DNA by human Rad52 protein. *Nature* **398**, pp 728-731.

Van Etten RA (1999) Cycling, stressed-out and nervous: cellular functions of c-Abl. *Trends in Cell Biol.* **9**, pp 179-186.

Van Gent DC, Ramsden DA and Gellert M (1996) The RAG1 and RAG2 proteins establish the 12/23 rule in V(D)J recombination. *Cell* **85**, pp 107-113.

Van Rensburg EJ, Louw WKA and Van der Merwes KJ (1987) Changes in DNA

supercoiling during repair of gamma-radiation-induced damage. *Int. Jnl. Raidat. Biol.* **52**, pp 693-703.

Varon R, Vissinga C, Platzer M, Cerosaletti KM, Chrzanowska KH, Saar K, Beckmann G, Seemanova E, Cooper PR, Nowak N, Stmm M, Weemaes CMR, Gatti RA, Wilson RK, Digweed M, Rosenthal A, Sperling K, Comcannon P and Reis A. (1998) Nibrin, A novel DNA double-strand break repair protein, is mutated in Nijmegen Breakage Syndrome. *Cell* **93**, pp 467-476.

Venkitaraman AR (1999) Breast cancer genes and DNA repair. *Science* **286**, pp 1100-1102.

Villa A, Santagata S, Bozzi F, Giliani S, Frattini A, Imberti L, Gatta LB, Ochs HD, Schwarz K, Notarangelo LD, Vezzone P and Spanopoulou E (1998) Partial V(D)J recombination leads to Omenn Syndrome. *Cell* **93**, pp 885-896.

Villa A, Santagata S, Bozzi F, Imberti L and Notarangelo LD, (1999) Omenn Syndrome: A disorder of Rag1 and Rag2 genes. *Jnl. Clinical Immunol.* **19**, pp 87-97.

Wang JC (1996) DNA topoisomerases. *Ann. Rev. Biochem.* **65**, pp 635-692. cited in Pfeiffer *et al*, 2000.

Wang JYJ (1998) Cellular responses to DNA damage. *Trends in Cell Biol.* **5**, pp 240-247.

Wang JYJ (2000) New link in a web of human genes. *Nature N&V* **405**, pp 404-405.

Wang P, Zhou RH, Zou Y, Jackson-Cook C and Povirk LF (1997) Highly conservative reciprocal translocatins formed by apparent joining of exchanged DNA double-strand break ends. *Proc. Natl. Acad. Sci. USA* **94**, pp 12018-12023.

Waterman MJF, Starridi ES, Waterman JLF and Halzonetis TD(1998) ATM-dependent activation of p53 involves dephosphorylation and association with 14-3-3- proteins. *Nature Genet.* **19**, pp 175-178.

Weaver DT (1996) Regulation and repair of double-strand DNA breaks. *Crit. Revs. in Eukaryotic Gene Expression* **6**, pp 345-375.

Weinert TA and Hartwell LH (1988) The *RAD9* gene controls the cell cycle response to DNA damage in *S. cerevisiae*.. *Science* **241**, pp 317-322.

Welsch PL, Owens KN and King M-C (2000) Insights into the functions of BRCA1 and BRCA2. *Trends in Genetics* **16**, pp 69-74.

Winegar RA, Phillips JW, Youngblom JH and Morgan WF (1989) Cell electroporation is a highly efficient method for introducing restriction endonucleases into cells. *Mut. Res.* **225**, pp 49-53.

Winegar RA and Preston RJ (1988) The induction of chromosome aberations by restriction endonucleases that produce blunt end or cohesive breaks. *Mut. Res.*

198, pp 141-149.

Winkler FK (1992) Structure and function of restriction endonucleases. *Curr. Biol.* **2**, pp 93-99.

Wolfe SL (1993) *Molecular and Cellular Biology*. Supplement 3-1, pp 105-106 Wadsworth Pub. Co. California.

Wolff S, Bodycote J and Painter RB (1974) Sister chromatid exchanges induced in chinese hamster cells by uv irradiation of different stages of the cell cycle: the necessity for cells to pass through S. *Mut. Res.* **25**, pp 73-81.

Wong AKC, Pero R, Ormonde PA, Tavtigian SV and Bartel PL (1997) RAD51 interacts with the evolutionary conserved BRC motifs in the human breast cancer susceptibility gene *brca2*. *Jnl. Biol. Chem.* **272**, pp 31941-31944.

Woo RA, Mclure KG, Lees-Miller SP, Rancourt DE and Lee PWK (1998) DNA-dependent protein kinase acts upstream of p53 in response to DNA damage. *Nature* **394**, pp 700-704.

Woolf B (1957) *Ann. Human Genet. London* **21**, pp397- 409.

Wooster R, Neuhausen SL, Mangion J, Quirk Y, Ford D, Collins N, Nguyen K, Seal S, Tran T, Averill D, Fields P, Marshall G, Narod S, Lenoir GM, Lynch H, Feunreun J, Devilee S, Cornelisse CJ, Menko FH, Daly PA, Ormiston W, McManus R, Pye C, Lewis CM, Cannon-Albright LA, Peto J, Ponder BAJ, Skolnick MH, Easton DF, Goldgar DE and Stratton MR (1994) Localization of a breast cancer susceptibility gene, *BRCA2*, to chromosome 13q12-13. *Science* **265**, pp 2088-2090.

Wu X, Ranganathan V, Weisman DS, Heine WF, Ciccone DN, O'Neill TB, Crick KE, Pierce KA, Lane WS, Rathbun G, Livingston DM and Weaver DT (2000) ATM phosphorylation of Nijmegen breakage syndrome protein is required in a DNA damage response. *Nature* **405**, pp477-482.

Xiao Y and Weaver (1997) Conditional gene targeted deletion by Cre recombinase demonstrates the requirement for the double-strand break repair Mre11 protein in Murine embryonic stem cells. *Nuc. Acids Res.* **25**, pp 2985-2991.

Xing W (1997) Effects of dNTPs on the SCE frequency in plant root tip cells. *Mut. Res. Fundamental and Molecular Mechs. of Mutagenesis* **379**, pp 117-119.

Xing W and Zhang Z (1990) A comparison of SCE test in human lymphocytes and *Vicia faba*: a hopeful technique using plants to detect mutagens and carcinogens. *Mut. Res.* **241**, pp 109-113.

Xu Y and Baltimore D (1996) Dual roles of ATM in the cellular response to radiation and in cell growth control. *Genes & Dev.* **10**, pp 2401-2410.

Yang A, Walker N, Bronson R, Kaghad M, Oosterwegel M, Bonnin J, Vagner C, Bonnet H, Dikkes P, Sharpe A, McKeon F and Caput D (2000) p73-deficient

mice have neurological phermonal and inflammatory defects but lack spontaneous tumours. *Nature* **404**, pp 99-103.

Yan J, Khanna KK and Lavin MF (2000) Defective signal transduction in ataxia-telangiectasia cells. *Int. Jnl. Radiat. Biol.* **76**, pp 1025-1035.

Yu W, Misulovin Z, Suh H, Hardy RR, Jankovic M, Yannoutsos N and Nussenweig MC (1999a) Coordinate regulation of *RAG1* and *RAG2* by cell type-specific DNA elements 5' of *RAG2*. *Science* **285**, pp 1080-1084.

Yu L and Morse RH (1999b) Chromatin opening and transactivator potentiation by RAP1 in *Saccharomyces cerevisiae*. *Mol. and Cell. Biol.* **19**, pp 5279-5288.

Yu VPCC, Koehler M, Steinlein C, Schmid M, Hanakahi LA, van Gool AJ, West SC and Ventikaramann AR (2000) Gross chromosomal rearrangements and genetic exchanges between nonhomologous chromosomes following *BRCA2* inactivation. *Genes & Dev.* **14**, pp 1400-1406.

Yuan ZM, Huang Y, Ishiko T, Kharbanda S, Weichselbaum R and Kufe D (1997) Regulation of DNA damage-induced apoptosis by the c-abl tyrosine kinase. *Proc. Natl. Acad. Sci. USA* **94**, pp 1437-1440.

Zakian VA (1995) ATM-related genes: what do they tell us about functions of the human gene? *Cell* **82**, pp 685-687.

Zhang H, Tombine G and Weber BL (1998) *BRCA1*, *BRCA2* and DNA damage response: Collision or collusion? *Cell* **92**, pp 433-436.

Zhao J, Dynlacht B, Imai T, Hori T-A and Harlow (1998) Expression of NPAT, a novel substrate of cyclin E-dck2 promotes S phase entry. *Genes and Dev.* **12**, pp 456-461.

Zhao S, Weng YC, Yuan SSF, Lin YT, Hsu HC, Lin SC, Gerbino E, Song M, Zdzienicka MZ, Gatti RA, Shay JW, Ziv Y, Shiloh Y and Lee EY (2000) Functional link between ataxia telangiectasia and Nijmegen breakage syndrome gene products. *Nature* **405**, pp 473-477.

Zhong Q, Chen C-F, Li S, Chen Y, Wang C-C, Xiao J, Chen P-L, Sharp ZD and Lee W-H (1999) Association of *BRCA1* with the hRad50-hMre11-p95 complex and the DNA damage response. *Science* **285**, pp 747-750.

Zhou B-BS and Elledge SJ (2000) The DNA damage response: putting checkpoints in perspective. *Nature* **408**, pp 433-439.

Appendix A

Summary of statistical methods used in
analysing experimental data.

Summary of statistical methods used in analysing experimental data.

(i) Chi-square (X^2) tests.

X^2 tests have been used in the text to determine whether or not significant differences occur in comparing the experimental results of treated and untreated cells.

In these cases we are dealing with a 2×2 array having 1 degree of freedom (1 df) as shown below where a, b, c and d are the number or frequency of occurrence in each category:

	Damaged	Undamaged	Total
Control	a	c	a + c
Treated	b	d	b + d
Total	a + b	c + d	m

$$\text{where } m = a + b + c + d \quad (\text{A.1})$$

Woolf's method

In cases where the sample size is quite large (e.g. $a + c = 400$ in many cases scored) a calculation procedure developed by Woolf (Woolf, 1957) is a convenient method:

$$X^2 = g(a) + g(c) - g(a + c) + g(b) + g(d) - g(b + d) - g(a + b) - g(c + d) + g(m) \quad (\text{A.2})$$

where $g(x) = 2 \times \ln x$.

Yates method

For a 2×2 contingency table having 1 df and small sample numbers the following equation which incorporates the Yates correction (Moroney, 1951) can be used:

$$\chi^2 = \frac{m[ad - bc - m/2]^2}{(a + c)(b + d)(a + b)(c + d)} \quad (\text{A.3})$$

The Yates correction involves increasing or decreasing the values for a, b, c and d in the above table by 1/2, consequently the correction is negligibly small for large sample sizes. The above equations for χ^2 for both Woolf and Yates methods have been programmed in QBASIC which runs on IBM compatible PCs. For the 1 degree of freedom system used in the above analysis and a level of significance of 0.01, the Null hypothesis is satisfied where $\chi^2 < 6.63$.

(ii) The Student t test

The frequency distribution of colour switch ratio (csr) for both normal and irradiated lymphoblastoid cell lines were calculated from the experimental data. A total of 12 different cell lines were investigated in this part of the research programme.

In order to test the means and standard deviations of these irradiated and non-irradiated cells the t-test was used for the appropriate degrees of freedom (Fowler and Cohen, 1990). This test is valid provided the number of observations is less than 30 (in this case 12 cell lines were used).

The first condition to be satisfied for the t-test is to show that the frequency

distribution for the lymphoblastoid cell lines is normal. This is satisfied provided 70% of the observations in each case falls within the interval $\bar{x} \pm s$ where \bar{x} is the mean and s the standard deviation for the cell lines tested.

The second requirement for the t-test is to use the so-called F-test to check that the differences between the two sample variances is small:

$$\text{i.e.} \quad F = s_1^2 / s_2^2 = \text{greater variance/lesser variance} \quad (\text{A.4})$$

where the degrees of freedom are $(n_1 - 1)$ and $(n_2 - 1)$.

For the case of the lymphoblastoid cells $n_1 = n_2 = 12$ and hence $df = 11$ for both irradiated and non-irradiated cells. From the table for the F-distribution and a 0.05 level of significance $F = 3.48$.

Provided the calculated value for $F < 3.48$ we can accept that the non-irradiated and irradiated samples come from populations with similar variance. If the above two requirements are satisfied for the lymphoblastoid cell lines the sample means \bar{x}_1 and \bar{x}_2 can be compared using the following expression (Fowler and Cohen, 1990):

$$t = \frac{(\bar{x}_1 - \bar{x}_2)}{\sqrt{\left[\frac{(n_1 - 1) s_1^2 + (n_2 - 1) s_2^2}{(n_1 + n_2 - 2)} \right] \left(\frac{n_1 + n_2}{n_1 \cdot n_2} \right)}} \quad (\text{A.5})$$

where the degrees of freedom are $df = (n_1 + n_2) - 2$.

For the experiments on the lymphoblastoid cells where $n_1 = n_2 = n = 12$ the above equation simplifies to:

$$t = \frac{(\bar{x}_1 - \bar{x}_2)}{\sqrt{1/n [s_1^2 + s_2^2]}} \quad (\text{A.6})$$

having $df = 22$.

From statistical table for $df = 22$ and a significance level of 0.05 we find $t_{0.05} = 2.074$. If the calculated value for $t < 2.074$ we can conclude that there is no significant difference between the means of the irradiated and non-irradiated lymphoblastoid cell lines.

(iii) t-score.

To compare a particular syndrome cell line with the csr frequency distribution of the lymphoblastoid cells, two approaches are possible, namely the z-score and the t-score. However since we are comparing a diseased cell line with a small lymphoblastoid sample ($n = 12$), the t distribution and the calculated value for the t-score must be used (Fowler and Cohen, 1990). This is given by:

$$\text{t-score} = (|x - \bar{x}|/s) \quad (\text{A.7})$$

for $(n - 1)$ df.

Using the experimental value of csr frequency for the diseased cells as x in the equation and the known values for \bar{x} and s for the lymphoblastoid cells, the t-score for $(n - 1) = 12 - 1 = 11$ df can be calculated.

From statistical tables for $df = 11$ and a significance level of 0.05 the value

$t = 2.2$ is found. If the calculated t -score for a diseased cell line is less than this value (t -score < 2.2) we conclude that there is no significant difference in csr values between the particular syndrome cell line and the lymphoblastoid cell population.

(iv) Regression Analysis and the determination of the mean colour switch ratio (csr).

In the literature concerned with chromatid breaks and as discussed in Chapter 2, the ratio of the colour switch breaks (csb) and the total number of chromatid breaks (Tb) generally known as the colour switch ratio (csr), which is usually quoted as a percentage. It has also been shown in geometrical terms that the csr is equivalent to the slope of the straight line relationship between Tb and csb . Thus the results of a series of experiments would result in a number of data points which can best be analysed by applying the methods of Regression Analysis.

It is important when applying this technique to the results of experiments to ascertain whether or not the sets of data are random variables. In Figure 2.5 the y -axis represents the chromatid breaks which are random or dependent variables and are not fixed by the observer, whereas the x -axis represents the applied radiation dose which is set by the observer and is therefore a non-random or independent variable. It is therefore valid in this case to apply the method of Linear Regression Analysis to the data points to obtain the best-fit straight lines.

Following the approach fully discussed in Fowler and Cohen, (1990) a least squares fit of experimental data points on the yox plane can be represented by the straight line equation:

$$y = a + bx \quad (\text{A.8})$$

where b is the slope of the line and a is the intercept on the y axis.

For a total of n data points each having a co-ordinate (x,y) a least squares fit analysis shows that the values for a and b are given by:

$$b = \frac{n \sum xy - \sum x \sum y}{n \sum x^2 - (\sum x)^2} \quad (\text{A.9})$$

$$a = (\sum y - b \sum x) / n \quad (\text{A.10})$$

If the experimental data is corrected to ensure that the least squares fit line equation (A.8) passes through the origin then a = 0 and equation (A.10) gives:

$$b = \sum y / \sum x \quad (\text{A.11})$$

The value of b given by equation (A.9) or (A.11) produces the values for the slopes m_1 , m_2 , m_3 listed in Figure 2.4 when Linear Regression is applied to the experimental data for breaks vs. dose. As discussed in Chapter 2 the ratio of the slopes m_2/m_1 gives the true value for the csr for this data.

In examining the experimental data of Chapter 2, Tables 2.1 and 2.2 it was shown that a convenient approach for summarising the data was to plot the colour switch breaks (csb) on the y-axis and the total breaks (Tb) on the x-axis (see Figure 2.8). However since both the csb and Tb are random variables it is

no longer valid to apply Linear Regression Analysis to this type of data. According to Fowler and Cohen (1990, page 161) the simplest alternative is to apply the technique known as reduced major axis regression (RMAR). In accordance with the RMAR approach the slope of the best-fit line when plotting the data for csb vs. Tb is given by:

$$b = csr = (\text{standard deviation of } csb) / (\text{standard deviation of } Tb)$$

or
$$b = [\sum (y - \bar{y})^2 / \sum (x - \bar{x})^2]^{1/2} \quad (A.12)$$

and the intercept of this line with the vertical y -axis is

$$a = \bar{y} - b\bar{x} \quad (A.13)$$

If the Linear Regression method applied to Figure 2.5 for the lymphoblastoid cells produces a $csr = m_2/m_1$, then comparing this value to the one obtained for Figure 2.8 using equation (A.12), it is found that the respective csr values are 0.154 and 0.161.

In many instances in the literature the recorded experimental data tabulates the csr for each specific case (y/x) and calculates the overall mean csr for these n tabulated values using the arithmetic mean.

i.e.
$$csr = (1/n) \sum (y/x) \quad (A.14)$$

Equation (A.14) is equivalent to taking each of the n data points in the yoX plane and assuming that the csr for this point is the slope of the line from this

point to the origin. The overall csr in this case is then assumed to be the mean of all these lines irrespective of whether or not the true line passes through the origin.

COMPUTER PROGRAMME FOR CALCULATION OF X²

```

1 REM CHI SQUARE TESTS USING YATES AND WOOLFS METHODS
5 OPEN "CHISQ.DAT" FOR OUTPUT AS #1
10 PRINT #1, "RESULT OF CHI SQUARE TEST ON DNA CELL BREAKAGE"
12 M=0
15 N=100
20 REM CONTROL SAMPLE SIZE N= A+C
   REM A=NUMBER OF DAMAGED CELLS IN CONTROL SAMPLE
25 A=9
30 C=N-A
   K=100
35 REM TREATED SAMPLE SIZE K=B+D
   REM B=NUMBER OF DAMAGED CELLS IN TREATED SAMPLE
40 B=19
45 D=K-B
47 REM YATES METHOD FOR SMALL SAMPLES
50 CHISQ=(N+K) * (ABS((A*D) - (B*C)) - 0.5*(N+K)) ^2
55 CHISQ=CHISQ/((A+C)*(B+D)*(A+B)*(C+D))
60 PRINT #1, "CHI SQUARE VALUE(YATES METHOD)= ";CHISQ
65 REM USE PROBABILITY OF 0.01 FOR 1 DEG OF FREEDOM
70 CHISQ1=6.635
80 TEST=CHISQ-CHISQ1
85 IF TEST>0 THEN 100
90 PRINT #1, "NO DIFFERENCE EXISTS BETWEEN CONTROL AND TREATED CELLS"
92 PRINT #1, "NULL HYPOTHESIS IS VALID"
95 GO TO 110
100 PRINT #1, "A DIFFERENCE EXISTS BETWEEN CONTROL AND TREATED CELLS"
105 PRINT #1, "NULL HYPOTHESIS IS REJECTED"
110 IF M=1 THEN 200
115 REM WOOLF'S METHOD FOR LARGER SAMPLES
120 CHISQ=2*A*LOG(A) + 2*C*LOG(C) - 2*(A+C)*LOG(A+C)
   CHISQ=CHISQ+2*B*LOG(B) + 2*D*LOG(D) - 2*(B+D)*LOG(B+D)
   CHISQ=CHISQ-2*(A+B)*LOG(A+B) - 2*(C+D)*LOG(C+D) + 2*(N+K)*LOG(N+K)
125 M=1
130 PRINT #1, "CHI SQUARE VALUE(WOOLFS METHOD)= ";CHISQ
135 GO TO 80
140 CLOSE
145 END

```

Appendix B

Proof that the time decay constant for the repair of chromatid breaks is independent of initial dose.

This theoretical proof was kindly supplied by William Bald as a more rigorous alternative to the assumption used in Chapter 3 that the k values are independent of dose as experimentally measured by Gotoh *et al*, (1999).

Proof that the time decay constant for the repair of chromatid breaks is independent of initial dose.

The method described in section 3.3.5 for the derivation of the chromatid breakage surface for lymphoblastoid cells, assumed that the time decay constants k_1 , k_2 and k_3 appearing in equations (3.1) - (3.3) are constant and independent of the initial dose. D .

Consider the following 3-D representation showing the variation of chromatid breaks at different initial radiation dose D and sample times t (see Figure B1).

At points A and B in the above diagram at sample time t' and also for the points C and E at time t'' the chromatid breaks for the linear breaks-dose relationship coincide with the values for the exponential decays representing the rejoining curves at initial doses D_1 and D_2 .

From the linear relationship at times t' and t''

$$Tb'_1 = m' D_1 + c' \quad \text{or} \quad D_1 = (Tb'_1 - c')/m'$$

and $Tb'_2 = m' D_2 + c' \quad \text{or} \quad D_2 = (Tb'_2 - c')/m'$

hence $D_2/D_1 = (Tb'_2 - c')/(Tb'_1 - c')$ (B.1)

Similarly at sample time t'' the linear break-dose line gives:

$$D_2/D_1 = (Tb''_2 - c'')/(Tb''_1 - c'') \quad \text{(B.2)}$$

Equating equations (B.1) and (B.2) and re-arranging gives:

$$\frac{Tb'_{2} - c'}{Tb''_{2} - c''} = \frac{Tb'_{1} - c'}{Tb''_{1} - c''} \quad (B.3)$$

Substituting the exponential decay equations for initial doses D1 and D2 into equation (B.3) using the appropriate sample times t' and t'' gives:

$$\frac{Tb_{20} \exp(-k_2 t') - c'}{Tb_{20} \exp(-k_2 t'') - c''} = \frac{Tb_{10} \exp(-k_1 t') - c'}{Tb_{10} \exp(-k_1 t'') - c''} \quad (B.4)$$

If the straight line equations representing the linear regression analysis at times t' and t'' are corrected to give zero breaks at zero dose then $c' = c'' = 0$ in expression (B.4).

Thus equation (B.4) simplifies to:

$$\frac{\exp(-k_2 t')}{\exp(-k_2 t'')} = \frac{\exp(-k_1 t')}{\exp(-k_1 t'')}$$

or

$$\exp[-k_2 (t' - t'')] = \exp[-k_1 (t' - t'')] \quad (B.5)$$

Since $(t' - t'')$ is the same on both sides of the equation the equality of equation (B.5) can only be satisfied if:

$$k_2 = k_1 \quad (B.6)$$

Consequently the time decay constant for the repair surface in the case where $c' = c'' = 0$ must be independent of the initial dose.

The question now arises concerning the margin of error involved in assuming

$k_1 = k_2$ in equation (B.4) when c' and c'' are no longer zero? A measure of this error can be ascertained by using the relation $|LHS - RHS| / LHS$ of equation (B.4) expressed as a percentage (i.e. $|1 - RHS/LHS| \times 100$).

The LHS of equation (B.4) can be written in the form (remembering $k_1 = k_2 = k$) as:

$$\text{LHS} = \frac{Tb_{20} \exp(-kt') [1 - (c'/Tb_{20} \exp(-kt'))]}{Tb_{20} \exp(-kt'') [1 - (c''/Tb_{20} \exp(-kt''))]}$$

This expression can be simplified and written as:

$$\text{LHS} = [(1 - \beta_1)/(1 - \beta_2)] \exp(-k(t' - t'')) \quad (\text{B.7})$$

where $\beta_1 = c'/Tb_{20} \exp(-kt')$

and $\beta_2 = c''/Tb_{20} \exp(-kt'')$ (B.8)

Using the same approach the RHS of equation (B.4) becomes:

$$\text{RHS} = [(1 - \beta_3)/(1 - \beta_4)] \exp(-k(t' - t'')) \quad (\text{B.9})$$

where $\beta_3 = c'/Tb_{10} \exp(-kt')$

and $\beta_4 = c''/Tb_{10} \exp(-kt'')$ (B.10)

Using the relations defined by equations (B.7) - (B.10) in the error expression $|1 - RHS/LHS|$ gives:

$$\% \text{ Error} = \left| 1 - \frac{(1 - \beta_3)(1 - \beta_2)}{(1 - \beta_4)(1 - \beta_1)} \right| \times 100 \quad (\text{B.11})$$

It can be seen from equation (B.11) that if $\beta_1 = \beta_2$ and $\beta_3 = \beta_4$ the % error in assuming $k_1 = k_2$ in equation (B.4) is zero. For the numerical example discussed in Chapter 3 and using the appropriate values for $\beta_1, \beta_2, \beta_3$ and β_4 equation (B.11) gives an error of just 1% by assuming $k_1 = k_2$.

Thus it can be stated that if a linear relationship exists between chromatid breaks and dose at different sample times within the G₂ phase of the cell cycle, then the exponential decay constant during break rejoining must be constant and independent of the initial dose.

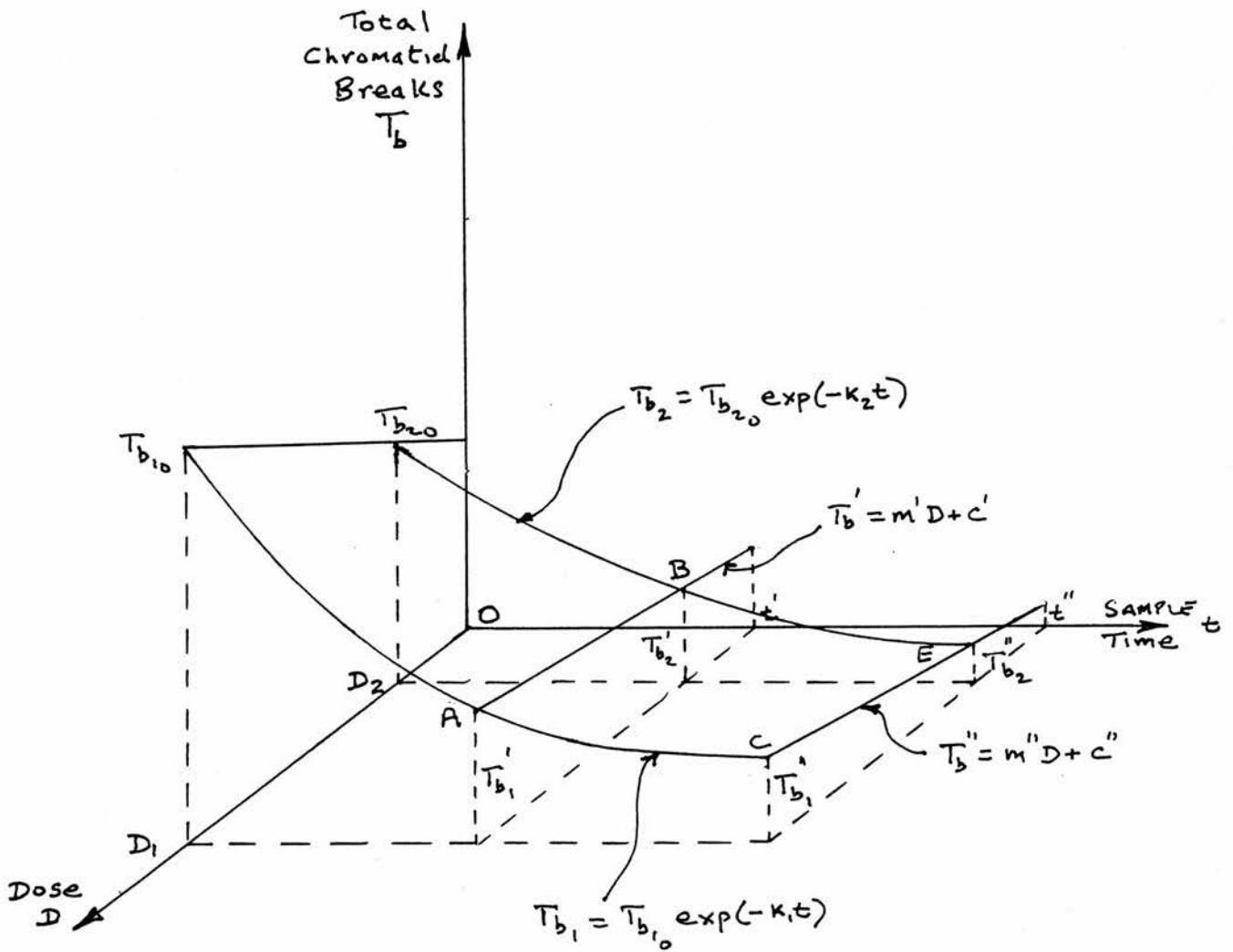


Figure B1. A three-dimensional representation of the exponential and linear variations in chromatid breaks as a function of radiation dose and sample time for a typical cell line in the G₂ phase of the cell cycle.

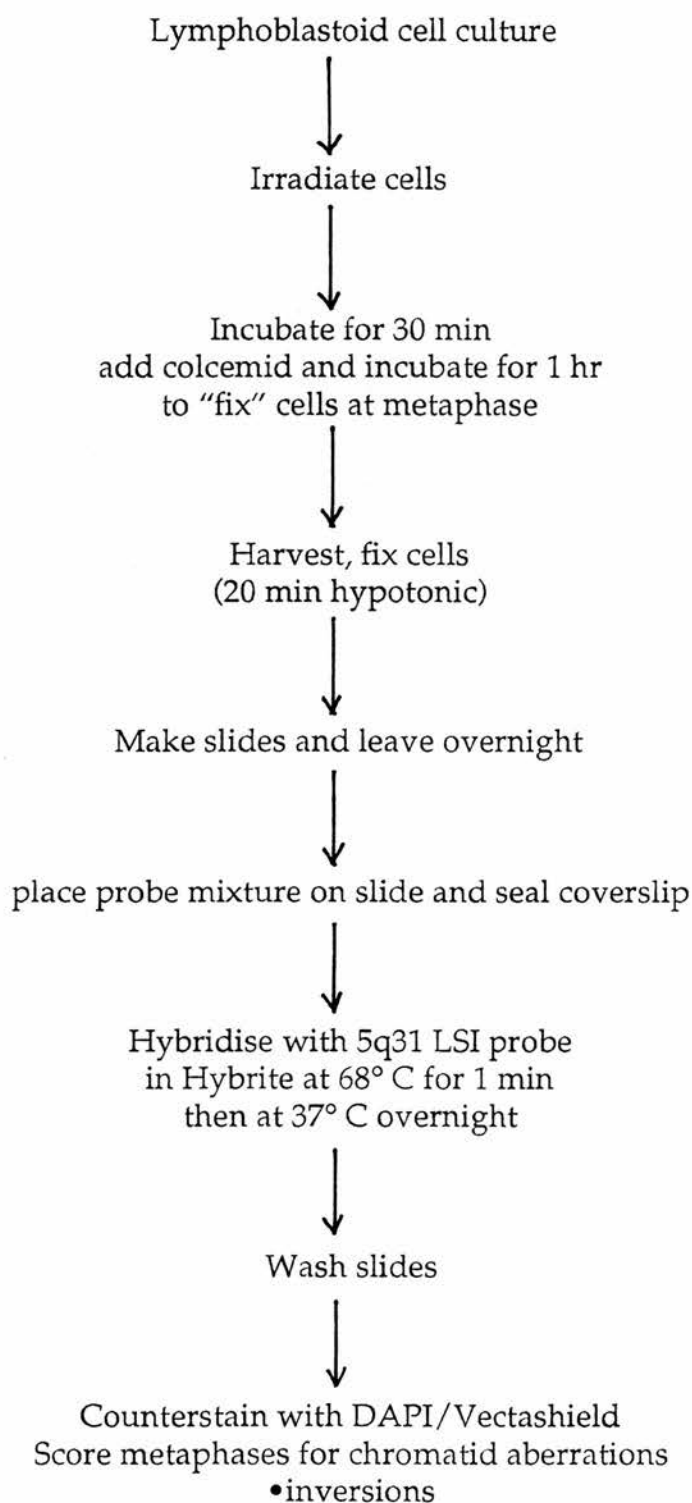
Appendix C

FISH Analysis of NC and AT
lymphoblastoid cells.

FISH Analysis of NC lymphoblastoid cells.

Materials and methods.

An outline of the protocol used in this investigation is shown below:



Cell culture

A normal lymphoblastoid cell line (NC) and an AT homozygous lymphoblastoid cell line (ATAR) were grown in RPMI 1640 as described in section 2.2.1.

Irradiation and harvesting.

Cells were irradiated *in situ* with 0.2 Gy from a ^{137}Cs gamma source (CIS Biointernational IBL437C gamma-irradiator) at a dose rate of 7.7 cGysec^{-1} . The flasks were returned to the incubator for 30 min following irradiation before treatment with 400 μl colcemid (Sigma) and incubated for 1 hour at 37°C .

After incubation the cell suspension was removed to 50 ml centrifuge tubes and chilled on ice for 10 min before centrifugation in a centrifuge (Hereaus Laborfuge 400R) at 1200 rpm ($\sim 200g$) for 10 min at 0°C . The medium was aspirated and the resulting cell pellet re suspended in ice-cold hypotonic solution (0.075M KCl) and held on ice for 20 minutes before centrifuging at 1200 rpm. The supernatant was removed, the pellet loosened and slowly resuspended in fixative (75% methanol, 25% acetic acid v/v). The resulting cell suspension was washed at least three more times in fixative. Finally the cell pellet was resuspended in a small volume of fresh fixative and kept at 4°C .

Preparation of slides.

The microscope slides were first cooled in ice-cold distilled water for 30 min. The ice-cold slides were briefly wiped with the edge of a filter paper and flooded with ice-cold 50% glacial acetic acid solution before a single drop of cell

suspension was placed on the slide. The slide was then dried on a warm-plate at approximately 50° C. The slides were left to mature for 24 hours before they were used for FISH or stored in the freezer at -20° C.

FISH procedure.

The probe used for FISH hybridisation was the LSI EGR1 (Vysis Inc) which hybridises to chromosome 5q31. A probe mixture containing 7 µl LSI hybridisation buffer, 1 µl probe and 2µl distilled water was placed on each slide, a coverslip was then placed over the target area and sealed with rubber cement. Once the cement was dry the Slides were placed in the Hybrite hybridisation system . The slides were denatured in the Hybrite at 68° C for 1 min and left at 37° C overnight (program 2). The following day the slides were removed and the rubber cement peeled off to allow the coverslips to be removed. The coverslips were washed off by agitating the slide in a coplin jar containing the first wash solution (2 × SSC (0.3 M sodium chloride, 0.03 M sodium citrate), 0.1% NP-40) at room temperature (25° C). The slides were then placed in a coplin jar in a water bath maintained at 65° C containing the second wash solution (2 × SSC (0.3 M sodium chloride, 0.03 M sodium citrate), 0.4% NP-40). The slides were agitated when first placed in the coplin jar and then left for 2 min. After 2 min the slides were returned to the first (room temperature) wash solution for 1 minute before being dried in a dark drawer. Once dry, 15 µl DAPI counterstain containing Vectashield was placed on the target area of the slide and a new coverslip placed on top. Slides were stored in the dark at 4° C until scored.

Scoring and analysis.

Metaphases were visualised using the Vysis Smart Capture software (Vysis Inc,

Illinois) and scored for any changes in the relative position of the probes on chromosome 5. A negative result was defined as the presence of both probes with no visibly detectable change in the relative intensity of the fluorescent signals or a visibly detectable change in their relative positions.

Results

Probability of chromatid break occurring within the target sequence.

The probability of finding a chromatid break at the probe site was estimated by the following reasoning: a chromatid break occurs as a result of the processing of a dsb which has not been repaired. The frequency of chromatid breaks per cell at the given radiation dose (0.2 Gy) can be determined from the data in Chapter 2 where the mean breaks per cell or rdi was determined. The size of the human genome and the size of the probe is known so the probability of a break occurring at the probe site in either of the loci can be calculated.

The human genome is 6000 Mbp (6×10^9 bp) in total and the probe size is 200 kb. The cells are at metaphase and have a probe site in each chromosome thus the total probe length within the genome is 400 kb (4×10^5 bp). From Chapter 2, (Table 2.2) the maximum calculated mean number of breaks per cell was 1.39 for normal irradiated lymphoblastoid cells and the mean number of breaks per cell for the three irradiated AT lymphoblastoid cell lines was 1.86.

Thus for normal lymphoblastoid cells, the probability of finding a chromatid break at the probe site is:

$$\frac{4 \times 10^5}{6 \times 10^9} \times 1.39 = 9.3 \times 10^{-5}$$

or an approximate 1 in 10,000 chance of success.

However, the chromatid break site will be considerably larger (~ 3 Mbp) so the probability could be correspondingly higher. It is estimated that the upper limit of probability is 1 in 1000 chance of success.

For AT lymphoblastoid cells, the probability of finding a chromatid break at the site is:

$$\frac{4 \times 10^5}{6 \times 10^9} \times 1.86 = 1.2 \times 10^{-4}$$

or again an approximate 1 in 10,000 chance of success. As described above the upper limit of probability is higher than this, also as the frequency of total number breaks in AT cells is higher than that observed for normal lymphoblastoid cells the higher limit of probability may be higher than the 1 in 1000 chance of success predicted for normal cells.

Results for normal and AT cells.

It would be expected that two double FISH probes would be detectable in each metaphase as the cell has completed S phase and there is a probe site on each sister chromatid.

Results for normal and AT lymphoblastoid cells are shown in Table C.1. A total of 100 metaphases were scored for the normal lymphoblastoid cell line, 200 metaphases for the AT line. More metaphases were scored for AT than normal lymphoblastoid cells, due to the lower mitotic index for the normal cells following exposure to radiation. Also it was not possible to score a larger sample size as there was not a large number of scorable metaphases on the target area of each slide and the FISH kit used only allowed for a limited

number of slides to be prepared. It was not possible to detect any changes in the relative positions of the probes which would correspond to inversions (i.e. a relative shift of one signal up or down the chromosome arm). This was due to the small size of the signal produced and also to the poor quality of the resolution of the metaphase spreads. This was due in part to the software used and in part to the condensation status of the chromosomes. The only detectable changes were loss of signal at one of the loci which may be due to a deletion of the probe site or more likely the result of poor hybridisation of the probe to the locus. This occurred only in the AT lymphoblastoid cells (Table C.1).

Table C.1. Total number of detectable aberrations in NC and AT cells using the 5q31 FISH probe. Cells were subjected to 0.2 Gy irradiation and a sample time of 1.5 hr was used.

Cell type	Total number of cells scored.	Frequency of loss of probe site	Number of inversions
Normal (NC)	100	0	0
AT (ATAR)	200	6	0